Fernando Jorge Fernandes Jorne

Mestre em Engenharia Civil

Injectability of hydraulic lime grouts for old masonry consolidation

Tese para obtenção do Grau de Doutor em Engenharia Civil,
Especialidade Ciências da Construção

Orientador: Fernando M.A. Henriques,
Professor Catedrático, FCT/UNL

Júri:

Presidente: Jorge Joaquim Pamies Teixeira

Arguentes: Arlindo Freitas Gonçalves

Maria Paulina Santos Forte Faria Rodrigues

Vogais: Fernando M.A. Henriques

Ana Luísa Pinheiro Lomelino Velosa

Ana Paula Ferreira Pinto França de Santana

Luís Gonçalo Correia Baltazar

Tese desenvolvida no âmbito da bolsa de doutoramento (SFRH/BD/80616/2011)
financiada pela Fundação para a Ciência e a Tecnologia (FCT)

FACULDADE DE CIÊNCIAS E TECNOLOGIA
UNIVERSIDADE NOVA DE LISBOA

Maio, 2016

Injectability of hydraulic lime grouts for masonry consolidation

Copyright © Fernando Jorge Fernandes Jorne, Faculdade de Ciências e Tecnologia, Universidade Nova de Lisboa.

A Faculdade de Ciências e Tecnologia e a Universidade Nova de Lisboa têm o direito, perpétuo e sem limites geográficos, de arquivar e publicar esta dissertação através de exemplares impressos reproduzidos em papel ou de forma digital, ou por qualquer outro meio conhecido ou que venha a ser inventado, e de a divulgar através de repositórios científicos e de admitir a sua cópia e distribuição com objectivos educacionais ou de investigação, não comerciais, desde que seja dado crédito ao autor e editor.

"Quality is never an accident; it is always the result of high intention, sincere effort, intelligent direction and skillful execution; it represents the wise choice of many alternatives"

William A. Foster

Acknowledgments

Em primeiro lugar gostaria de agradecer ao Professor Doutor Fernando Henriques, orientador científico desta tese. Agradeço a partilha do conhecimento e as valiosas contribuições que foram fundamentais para a realização deste trabalho. Destacar a disponibilidade e o apoio que o Professor sempre me deu ao longo desta caminhada.

A realização deste trabalho também não teria sido possível sem o apoio da Fundação para a Ciência e a Tecnologia (FCT/MCTES) mediante uma bolsa de doutoramento (SFRH/BD/80616/2011) durante o período de doutoramento na Faculdade de Ciências e Tecnologia da Universidade Nova de Lisboa (FCT-UNL). O trabalho desenvolvido teve também apoio do projecto "Grout optimisation for old masonry consolidation" (PTDC/ECM/104376/2008) que possibilitou a aquisição de equipamentos e a frequência de cursos e conferências.

Um agradecimento à Professora Doutora Ana Maria Ramos e ao Professor Doutor João Sotomayor do Departamento de Engenharia Química da FCT-UNL pelos conselhos relacionados com o goniómetro e superplastificantes; à Professora Doutora Maria Teresa Cidade do Departamento de Engenharia dos Materiais da FCT-UNL pelos ensinamentos e conselhos relacionados com o comportamento reológico do grout; ao Professor Carlos Galhano do Departamento de Ciências da Terra da FCT-UNL, pelos esclarecimentos na preparação das amostras a serem ensaiadas na lupa binocular; ao Professor Doutor António Urgueira do Departamento de Engenharia Mecânica e Industrial da FCT-UNL pelos conselhos relativos ao equipamento de luz estroboscópica.

Um agradecimento especial ao engenheiro Vítor Silva pela preciosa ajuda nas actividades de laboratório decorrentes durante o meu doutoramento. Quero também agradecer a colaboração dos bolseiros Ana Teresa Santos e João Matos ao longo das várias campanhas experimentais que realizei.

Aos colegas de Departamento de Engenharia Civil (DEC) pela amizade, apoio e incentivos prestados. Quero salientar o engenheiro Nuno Deusdado, o engenheiro Micael Inácio, o engenheiro Hugo Fernandes, o engenheiro André Almeida, o engenheiro Nuno Dinarte e o Professor Doutor Rui Vera Cruz.

Um agradecimento ao Departamento de Engenharia Civil da FCT/UNL pelo apoio prestado durante o período de doutoramento, em particular ao ex-presidente do departamento Professor Doutor J. Rocha de Almeida e ao actual presidente do departamento Professor Doutor António M. P. Ramos. Quero também agradecer ao professor Válter J.G. Lúcio, coordenador do programa de doutoramento em engenharia civil.

Aos funcionários do Departamento Carla Figueiredo e Maria Luz Sousa pela ajuda nas tarefas burocráticas associadas ao meu doutoramento.

O meu agradecimento à Engenheira Dina Frade da empresa Secil-Martingança e ao engenheiro Hélder Miguel da empresa BASF, pelas matérias-primas fornecidas.

Por fim, gostaria de expressar o meu enorme agradecimento à minha família, à Inês e a todos os meus amigos (em especial ao Almeida e ao Latoeiro) que me apoiaram nos últimos 4 anos.

INJECTABILITY OF HYDRAULIC LIME GROUTS FOR OLD MASONRY CONSOLIDATION

Abstract

Grout injection is a widely used technique for masonry consolidation of multi-leaf masonries, aimed at increasing the compactness and to create links between the internal and external leaves that will improve shear, flexural and compressive resistances. Grouts can be seen as mixtures of binder with water, with or without special admixtures (such as superplasticizer). To ensure an adequate flow of the grout and a correct filling of the internal voids inside the masonry, it is essential to assure good fresh grout properties. The evaluation of the performance of the grout injectability is firstly started by checking the intrinsic properties of the grout (namely fluidity, stability, water retention and rheological parameters) and then by controlling the injectability through injection tests. Besides the grout composition, the environmental temperature, resting times and injection pressure also play a significant role on the grout injectability. The lack of information about the influence of the referred parameters on the injectability of hydraulic lime grouts enhances the importance of a detailed research on the subject.

The grout specification involves the knowledge of the flow capacity within the masonry inner core and physic-chemical compatibility with the original materials present in the old masonries. Thereby, it is evaluated the injection performance of hydraulic lime based grouts as a function of the porous media to be injected. For this purpose, simplified models were created to allow injectability tests in controlled conditions. To enable the simulation of different permeabilities and internal structures of masonries, the models were created by filling plexiglass cylinders with different grain size distributions of limestone sands and crushed bricks. As these materials exhibit different water absorption coefficients, it also was possible to study the influence of water loss from grout to porous media in grout injectability. Another variable studied with influence on grout injectability was the water content of porous media. As it is not expected that masonries are always dried, the pre-wetting of some cylinders by simple injection of water is of extreme relevance to compare the results of grout injectability in the two opposite situations. The injection tests also enabled to detect different resistances to grout penetration created by the PM to the flow. The knowledge of these resistances is crucial to estimate the grout penetration in the internal voids.

The grout injection performance was analysed both in the fresh and hardened states. In order to test the effectiveness of the filling process and the bonding of the grout to the masonry materials, tomography was conducted complemented with mechanical tests. The mechanical results showed good correlation with injectability and dependence with the position of the specimen analysed on the cylinder injected, creating tensile and shear strength gradients along the height of the cylinder. In what concerns the tomography, the research demonstrated a correspondence between the characteristics of the cylinders after the injection and the information displayed in the tomograms. Thus, it is proved that tomography is a useful technique to evaluate effectiveness of the grout injections, allowing an understanding of the ability of the injections to modify the physical and mechanical properties of old masonries.

KEYWORDS:

- *multi-leaf masonry*
- *grout injection*
- *hydraulic lime*
- *superplasticizer*
- *temperature*
- *resting time*
- *mechanical tests*
- *ultrasonic tests*
- *tomography*

Resumo

A técnica de injecção de grout é frequentemente usada na consolidação de alvenarias antigas de pano múltiplo. O objectivo é aumentar a compacidade e estabelecer ligações entre o pano exterior e interior, aumentando desta forma a resistência à compressão, flexão e corte. A mistura de grout é composta normalmente por ligante e água, podendo em certos casos serem adicionados adjuvantes, como os superplastificantes. Para garantir um adequado fluxo de grout e um correcto preenchimento dos vazios internos de uma alvenaria, é essencial garantir adequadas propriedades do grout no estado fresco. A avaliação da injectabilidade do grout é iniciada pela verificação das propriedades intrínsecas do grout (nomeadamente a fluidez, estabilidade, retenção de água e os parâmetros reológicos) e seguidamente por ensaios de injecção. Além da composição do grout, a temperatura ambiente, o tempo de repouso e a pressão de injecção desempenham também um papel importante na injectabilidade do grout. A falta de informação acerca da influência dos referidos parâmetros na injectabilidade de grouts de cal hidráulica aumenta a importância de uma investigação detalhada acerca deste assunto.

A especificação do grout envolve o conhecimento da capacidade do fluxo dentro do núcleo interno da alvenaria e a compatibilidade com os materiais originais presentes nas alvenarias antigas. Assim, é avaliada a capacidade de injecção de grouts à base de cal hidráulica em função do meio poroso a ser injectado. Para este propósito, foram criados modelos simplificados para permitir a realização de ensaios de injectabilidade em condições controladas. Para permitir a simulação de diferentes permeabilidades e diferentes estruturas internas de alvenarias, os modelos criados (cilindros) foram preenchidos com diferentes distribuições granulométricas de agregado calcário e tijolo moído. Atendendo a que estes materiais exibem diferentes coeficientes de absorção, é possível estudar a influência da perda de água do grout para o meio poroso na injectabilidade do grout. Outra variável estudada foi o teor de água do meio poroso. Como não é espectável que as alvenarias se encontrem sempre secas, a pré-molhagem de alguns cilindros através de uma simples injecção de água é de extrema importância de forma a comparar os resultados da injectabilidade nestas duas situações distintas. Os ensaios de injecção também permitiram detectar diferentes resistências à penetração de grout criada pelo meio poroso ao fluxo. O conhecimento destas resistências é crucial para estimar a penetração de grout nos vazios internos do meio poroso.

A performance da injecção de grout foi analisada no estado fresco e estado endurecido. A fim de testar a eficácia do processo de preenchimento e a ligação do grout com os materiais da alvenaria, recorreu-se à tomografia complementada com os ensaios mecânicos. Os resultados mecânicos mostraram uma boa correlação com a injectabilidade e uma dependência com a posição da fatia analisada no cilindro injectado, existindo gradientes de tensão de tracção e corte ao longo da altura do cilindro. No que refere à tomografia, o estudo demonstrou a correspondência entre as características dos cilindros depois da injecção e a informação presente nos tomogramas. Assim, é provado que a tomografia é uma técnica útil para avaliar a eficácia da injecção de grout, permitindo o conhecimento da capacidade das injecções para modificar as propriedades físicas e mecânicas das alvenarias antigas.

Palavras-chave:

- alvenaria *de pano múltiplo*

- injecção de grout

- cal hidráulica

- superplastificante

- temperatura

- tempo de repouso

- ensaios mecânicos

- testes ultra-sónicos

- tomografia

Notations and symbols

Symbol	Units	Designation
A	m^2	Area
A_{tot}	m^2/g	Total specific pore area
b_{eqv}	mm	Theoretical aperture for a Bingham fluid
b_{K-C}	mm	Theoretical aperture for a Newtonian fluid
D	mm	Diameter of the void
D_{avg}	µm	Median pore diameter
F	N	Force
F_l	mm/s	Fluidity factor in Marsh cone test
I	- ; l/m^3	Injectability
I_{rate}	s^{-1}	Injectability rate
I_{tot}	mL/g	Total specific intrusion
K	m^2 ; Darcy	Permeability
L	mm	Length of channel / Length of the tube
m	kg	Injected grout mass
n	-	Porosity
p	Pa	Mercury injection pressure
P	Pa	Pressure
q	m^3/s	Water flow
q_{grout}		grout flux
Q	mm^3	Volume of cone Marsh test
R	mm	Radius
R_{Darcy}	$Pa.s/m^3$	Darcy resistance
R_{front}	$Pa.s/m^3$	Front resistance
R_{total}	$Pa.s/m^3$	Total resistance
R_s	$Pa.s/m^3$	Resistance of suspension
S	mm^2/mm^3	Specific surface
t	s	Time
t_f	s	Flow time in Marsh cone test
T	MPa	Splitting tensile strength
V	m/s	Ultrasonic velocity
V_l	mm^3	Volume of sample
Vv	m^3	Voids volume of porous medium
V_W	mm^3	Volume of decanted bleed water
WA	%	Water of absorption
W_{nom}	mm	‘‘Representative’’ diameter of channels or width of channels to be injected
α	-	Shape factor of particles of porous medium
Υ	N/m	Surface tension of mercury
$\dot{\gamma}$	s^{-1}	Shear rate
ΔP	Pa	Difference of injection pressure
θ	°	Contact angle
Ø	mm	Diameter
η_p	Pa.s	Plastic viscosity

μ	Pa.s	Dynamic viscosity of water
ρ	Kg/m^3	Density of grout
τ	Pa	Shear stress
τ_0	Pa	Yield stress
τ_{DS}	MPa	Shear bond strength

Notation	**Designation**
ASTM	American society for testing and materials
CaO	Calcium oxide
$CaCO_3$	Calcium carbonate
$Ca(OH)_2$	Calcium hydroxide
C_3A	Tricalcium aluminate
C_4AF	Tetracalcium aluminoferrite
C-S-H	Calcium-Silicate-Hydrate
CH	Portlandite
CV	Coefficient of variation
DT	Destructive test
EN	European standard
FA	Fly ash
FFT	Fluidity factor test
HL	Hydraulic lime
Mix	Mixture
PC	Polycarboxylic acid
NDT	Non-destructive test
PM	Porous media
rpm	Rotations per minute
SD	Standard deviation
SEM	Scanning electron microscopy
SF	Silica fume
SP	Superplasticizer
w/b	Water/binder ratio
XRF	X-ray florescence

Table of Contents

Contents

List of Figures

List of Tables

Publications

The development of the following papers has been produced:

Type of publication	Reference
Paper in ISI journal Published	-Jorne F, Henriques FMA, Baltazar LG (2014*) Evaluation of consolidation of grout injection with ultrasonic tomography*. Construction and Building Materials 66:494–506. doi: 10.1016/j.conbuildmat.2014.05.095
Paper in ISI journal Published	- Jorne F., Henriques F.M.A., Baltazar L.G. (2015a) *Injection capacity of hydraulic lime grouts in different porous media*. Materials and Structures 48:2211–2233. doi: 10.1617/s11527-014-0304-9
Paper in ISI journal Published	- Jorne F, Henriques FMA, Baltazar LG (2015b) *Influence of superplasticizer, temperature, resting time and injection pressure on hydraulic lime grout injectability . Correlation analysis between fresh grout parameters and grout injectability.* Journal of Building Engineering 4:140–151. doi: 10.1016/j.jobe.2015.08.007
Paper in ISI journal Published	- Jorne F, Henriques FMA, Baltazar LG (2015c) *Evaluation of consolidation of different porous media with hydraulic lime grout injection*. Journal of Cultural Heritage 16:438–451. doi: 10.1016/j.culher.2014.10.005
Paper in conference proceedings	- Jorne F., Henriques F.M.A., Baltazar L.G. (2012), "*Análise das propriedades de grout endurecido - Influência da adição de Sílica de Fumo a Grouts de Cal Hidráulica*", PATORREB 2012, Santiago de Compostela, 12-14th, Abril
Paper in conference proceedings	- Jorne F., Henriques F.M.A., Baltazar L.G. (2012), "*Grout injection in porous media with different internal structures*," in Proceedings of the 14th International Conference - Structural Faults & Repair, Scotland, 3rd –5th July, 2012
Paper in conference proceedings	- Jorne F., Henriques F.M.A., Baltazar L.G. (2012), *Avaliação da técnica de injecção de grout recorrendo ao ensaio de ultra-sons e tomografia ultra-sónica*, Actas do Congresso Construção 2012, Coimbra, Portugal, 18-20 Dezembro 2012
Paper in conference proceedings	- Jorne F., Henriques F.M.A., Baltazar L.G. (2013), *Study of hydraulic lime grout injections in different porous media – An experimental study*", Proceedings of the 13th International Conference on Studies, Repairs and Maintenance of Heritage Architecture, pp. 431–442, New Forest, UK, 25th –27th June 2013
Paper in conference proceedings	- Jorne F., Henriques F.M.A., Silva V., Rosa C. (2015), *Caracterização de alvenarias de pedra antigas - levantamento tipológico, análise das secções e caracterização dos materiais.* Actas do Congresso CONPAT 2015, Lisboa, Portugal, 8-10 Setembro 2015

Chapter 1.Introduction

1.1 Aim and scope of the research

Multi-leaf stone walls represent a masonry typology characterized by specific vulnerability, both under vertical and horizontal loads. Due to their irregular morphology (both in texture and thickness) and to the presence of voids and loose adhesive material - infill material (mainly concentrated in the internal core) they are sensitive to brittle collapse mechanism, which usually happen by the detachment of the layers and out-of-plane expulsions of material (Cotič et al., 2013; Valluzzi, 2005).

Grout injection is amongst other techniques, a powerful consolidation method to overcome masonry structural decay. In fact, the injection of grouts revealed to be an effective intervention to increase the ultimate load capacity of the walls, as well as to minimize the brittle mechanisms (since the masonry regains its monolithical behaviour) (Valluzzi, 2005). This overall improve in the mechanical resistance occurs because grout injection enables to restore the compactness, cohesion, uniformity of strength and continuity of masonry walls without altering their morphology and load-bearing system. As the grout is introduced into the masonry, it does not damage the aesthetical outlook of the building (the intervention is almost invisible) and thus preserves its authenticity, which is extremely important for the historic structures (e.g.. monuments). However, the grout injection is a non-reversible intervention (Ignoul et al., 2004). Thus, in accordance with the Venice Charter, grout injection should only be performed if the materials that are used in the grout composition are compatible with the original materials (Anzani et al., 2006; Van Gemert et al., 2015a; Van Rickstal, 2000). For this reason, one of the main criteria for the choice of the binder of the consolidation material is to minimize compatibility problems with the original walls. According some authors (Bras & Henriques, 2012; Valluzzi, 2005), hydraulic-lime binders should be used, as they present chemical composition, physical and mechanical properties very similar to the historic materials, in comparison with cement or organic polymeric binders. The choice of the binder has to be properly studied before deciding the proper type of grout, since an inappropriate type of grout can adversely affect the consolidation work and hence increase the cost of the intervention.

Research has been carried out in these last two decades have demonstrated that grout injection is an effective method for repairing seismic damage and strengthening existing masonry walls(Binda et al., 2003a, 1997; Bras & Henriques, 2012; Van Rickstal et al., 2003). In general, the aims of the technique are: (i) to fill large and small voids and cracks increasing the continuity and compactness of the masonry and hence its strength, (ii) to fill the gaps between two or more leaves of a wall, when they are badly connected. These aims can only be fulfilled by knowing with a good precision the morphology of the wall section, the composition of the materials constituting the wall in order to avoid chemical or physical incompatibility with the grout, crack distribution and size, percentage and distribution of voids (Binda et al., 2003a, 1997). Therefore, the effectiveness of a repair with grout injection depends not only on the characteristic of the mix, but also on the knowledge of wall type (Valluzzi, 2005). According to Van Rickstal (Van Rickstal et al., 2003), the permeability and moisture content of the PM are important properties in the assessment of the grout injectability. The lack of information about the performance of hydraulic lime based grouts as a function of the porous media to be injected enhances the importance of a detailed research on the subject.

The variance on the strength of the injected masonry depends mainly on the degree of filling and on the mechanical characteristics of the grout. Concerning the former, the grout injection transforms the masonry into a material with higher compactness and thus the uncertainty about the strength becomes smaller. In fact, a uniform filling of all voids leads a higher volume of grout injected and, consequently, the amount of voids that remains after grout injection is significantly reduced. In order to obtain a uniform filling of all voids it is necessary to ensure an adequate grout flow inside the masonry (porous medium - PM). To that end, the grout should be able to pass through the narrowest voids, in order to reach the maximum possible internal volume of masonry, avoiding most of possible blockages (Miltiadou-Fezans & Tassios, 2013a), which means the injection of a grout with good injectability. According to Miltiadou (Miltiadou-Fezans & Tassios, 2013a), the grout injectability is considered as the resultant of the following grout properties:

(i) Satisfactory penetrability characteristics, i.e. appropriate effective maximum grain size of the solids versus the effective lowest width of the voids of the wall, as well as appropriate grain size distribution of the solid phase of the grout;

(ii) Sufficient fluidity, i.e. the easiness of flow through the fissures and voids of the masonry, with the minimum possible pressure, throughout the entire intervention;

(iii) Satisfactory stability of the suspension, i.e. appropriately low bleeding, as well as avoidance of harmful segregation of solid grains, through the whole intervention. Actually, the segregation of solid particles or excessive bleeding should be avoided since otherwise blockage may appear and thereby the quality of the grouting intervention can be severely affected (Miltiadou-Fezans & Tassios, 2013b).

In relation to the penetrability, as aforementioned, for a suspension (such as a hydraulic grout) to be able to penetrate, the grain size distribution of its solid phase should be compatible with the characteristic dimensions of the discontinuities (voids, flaws, channels, etc.) to be injected. Thus, the grain size characteristics of the solid phase of the grout have to be selected on the basis of the ‘‘effective minimum width’’ of the voids or flaws of the wall. For such discontinuities, to be successfully penetrated by the grout, a rough estimation of the ‘‘effective maximum’’ grain size of the solid ingredients of the grout should first be made. In this work, a procedure is followed based on previous work (Eklund & Stille, 2008; Miltiadou-Fezans & Tassios, 2013a) to check if a grain size distribution of solid materials of the grout is compatible with the dimensions of the discontinuities of the porous media.

In addition to the referred fresh properties, it is also essential to ensure a good rheological behaviour and water retention in order to regulate the consolidation quality and to achieve a good injectability (Bras, 2011). Indeed, these properties provide a more homogenized behaviour of the wall due to a better filling of the voids and the cracks, ensuring a monolithical behaviour of the masonry.

Over the years, the grout injection has been developed through laboratory and in situ tests. From these studies, some general guidelines to get a good consolidation work in the masonry walls were designed by engineers, architects and researchers. However, it should be noted that each grout application is unique, and the repair procedures must be adjusted to fulfil the intervention goals. Thus, in order to analyse all of the mentioned issues, one of the main aims of this thesis is to investigate the factors that lead to a high penetration and uniform filling of internal voids in the masonry.

It seems quite logical that before any intervention it is essential to assess the masonry. The diagnosis of the masonry is most of the time a mixture of destructive and non-destructive techniques (Van Rickstal, 2000). Regarding non-destructive testing (NDT), the visual charts produced enable to locate the areas with defects/voids where grout injection should be carried out. Thus, NDT plays an essential role in the case of cultural heritage buildings with artistic value, where the structural condition should be assessed with the minimal interference. Moreover, they can shorten the evaluation process and contribute to the decision process regarding the condition of the masonry. Several NDT methods have been proposed for structural investigation of building elements (Cotič et al., 2013). Contact methods, such as ground penetrating radar (GPR), ultrasonic, sonic and impact echo are especially useful in imaging the inner structure of buildings. On masonry, such methods have been applied for detection of the morphology, localization of voids, determination of the moisture distribution, detection of severe delamination, as well as to control the effectiveness of repair by injection techniques (Anzani et al., 2006; Cotič et al., 2013; Valluzzi et al., 2009). Using the same NDT, before and after grouting, the evaluation of grout effectiveness can be made by comparing the NDT results of the initial state and after injected.

In order to test the effectiveness of the filling process and the bonding of the grout to the masonry materials, mechanical tests (splitting and shear tests) were conducted in the present work. Aiming at controlling the effect of grout injections on the compactness of masonries ultrasonic tests and tomography are also used (Zanzi et al., 2001). The combination of these techniques can be usefully applied to detect the internal morphology of the structural elements, giving qualitative information about their compactness (Porto, et al., 2003). In this way the locations in which injection it is more difficult to penetrate can be detected. For this purpose, a comparative tomography of porous media after injection is carried out. In addition, the tomographic analysis also enables to establish a relation with mechanical results (Epperson & Abrams, 1989; Miranda et al., 2010).

1.2 Research objectives

The overall goal of this research work is to understand and improve the performance of injection grouts for consolidation of old masonry walls. Old masonry buildings are one of the most common construction types in many European cities. Those masonry walls often need consolidation to improve their mechanical performance. Some buildings are historic which means that correct building intervention and philosophy of repair are needed. Injection grout is one technique for that purpose, aimed at increasing the compactness of the masonry without compromising its architectural value. Thus, to address the issue raised, some research lines were defined:

1. Study the influence of superplasticizer (SP) on fluidity, stability and water retention. In addition, rheological measurements will be made in order to better understand the flow behaviour of grouts under different environmental temperatures and resting times (i.e. the time after the grout mixing had ended). Another main goal is to evaluate the combined effect of the factors referred on grout injectability through injection tests.

2. The cylinders that resulted from injection tests of previous step are evaluated. The aim is to analyse the combined effect of the referred factors in the filling process and in the bonding of the grout with the porous media materials. Ultrasonic tomography is performed complemented with mechanical tests. Through these tests will be possible to analyse the influence of the above parameters in the bond properties of the interfaces (grout - PM particles).
3. The flow of the grout through the masonry depends on the fresh grout properties (previously mentioned), but also of the characteristics of the PM to be injected. Thus, it is studied the performance of the grout as function of a PM by controlling the grout injectability through injection tests. Masonry samples are created by filling plexiglass cylinders with a fraction of limestone sands and crushed brick. The main goal is to study the injectability of the grout in porous media with different permeabilities and internal structures. The lack of information about the performance of hydraulic lime based grouts as a function of the properties of the PM to be injected enhances the need of a detailed research on the subject.
4. Through the cylinders that resulted from injection tests of the previous step, ultrasonic tomography and mechanical tests are performed in order to test the effectiveness of the filling process and the bonding of the grout to the masonry materials. It is evaluated the correlation between the mechanical results and the ultrasonic results, as well as the importance of the bond properties of the interfaces on the mechanical results. Another aim is to check whether tomography is a useful technique to evaluate effectiveness of the grout injections, allowing an understanding of the ability of the injections to modify the physical and mechanical properties of an injected PM.
5. Study the injectability of grouts in porous media with different characteristics along the height of injection. Analyse of the different resistances to grout penetration, created by the PM to the flow during the injection test. In addition, it is evaluated the validation of Darcy's law and front resistance in grout injection tests. The main aim is the knowledge of all resistances in order to estimate the grout penetration in the internal voids of the PM.

1.3 Research structure

This thesis is organized in 11 chapters. The literature review related to grout injection is presented in chapters Chapter 2 to Chapter 4; these chapters correspond to the starting point for the research carried out throughout the work. From chapter Chapter 5 until chapter Chapter 9, the research work is presented. In general, each chapter corresponds to a global task. The descriptions of the main research lines developed during each one of these tasks are the following:

- **Task 1 (Chapter 5)** – *Influence of superplasticizer, temperature, resting time and injection pressure on hydraulic lime grout injectability*

Evaluation of the SP dosage in the injection capacity of the hydraulic lime grout. Little information is presently known regarding the effect of these products on the injectability of hydraulic lime mixtures. The evaluation of the performance of the grout injectability is firstly started by checking the intrinsic properties of the grout (namely rheological parameters, stability, water retention and fluidity) and then by controlling the injectability, through injection tests in porous media that simulate old masonries. To ensure an adequate flow of the grout and a correct filling of the internal voids inside the PM, it is essential to assure good fresh grout properties.

The other main goal of this paper is to provide indications and valuable data about the combined effect of hydraulic lime grout composition, environmental temperature, resting times and injection pressure on grout injectability, aiming at a successful injection process.

- **Task 2 (Chapter 6)** – *Combined effect of superplasticizer, temperature and resting time on hydraulic lime grout consolidation*

The evaluation of the combined effect of hydraulic lime grout composition, environmental temperature and resting times on grout injectability was firstly started in task 1 through injection tests. In the task 2, the cylinders that resulted from injection tests were evaluated. The main aim is to analyse the effect of the referred parameters in the filling process and in the bonding of the grout with the porous media materials.

Regarding the mechanical tests, two tests are performed: splitting and shear diagonal test. Through these tests will be possible to analyse the influence of the above parameters in the bond properties of the interfaces (grout - PM particles). Ultrasonic tomography is conducted complemented with mechanical tests.

- **Task 3 (Chapter 7)** – *Injection capacity of hydraulic lime grout in different porous media*

The flow of the grout through the masonry depends on the fresh grout properties (studied in the previous task) and the characteristics of the PM to be injected. Thus, it is evaluated the performance of the grout as function of a PM by controlling the grout injectability through injection tests on cylinders. Since it is difficult to reproduce a real masonry and to visualize what is happening inside the PM being injected, masonry samples were created by filling plexiglass cylinders with a fraction of limestone sands and crushed brick. These materials are sieved to obtain different grain size distributions to enable the simulation of different permeabilities and internal structures for the masonry.

- **Task 4 (Chapter 8)** – *Evaluation of consolidation of grout injection in different porous media*

The performance of grout injection in different porous media was studied in the previous task. In this task, the cylinders that resulted from injection tests were evaluated. In order to test the effectiveness of

the filling process and the bonding of the grout to the masonry materials, tomography was conducted complemented with mechanical tests. It is evaluated the correlation between the mechanical results and the ultrasonic velocities. Moreover, it is checked the importance of the bond properties of the interfaces (grout - PM particles) on the mechanical results. Regarding the tomography, the assessment of correspondence between the characteristics of the porous media after the injection and the information displayed in the tomographs is carried out. The main aim is to check whether tomography is a useful technique to evaluate effectiveness of the grout injections.

Task 5 (Chapter 9) – *Evaluation of the grout injectability and types of resistance to grout flow*

Since porosity and void size distribution are not constant within masonry, the efficiency of grouting varies along the injection. Thus, it is essential to study the injectability of grouts in porous media with different characteristics along the height of injection. To evaluate the efficiency of grout injection in this task was used 11 different porous media, in the shape of small scale cylinders. For each PM, grout injection velocity and injected mass were measured in each injection test. From these tests different resistances to grout penetration were detected, created by the PM to the flow. The knowledge of these resistances is crucial to estimate the grout penetration in the internal voids. The injection tests show that Darcy's law and front resistance are not adequate to estimate the grout injection. Therefore, an additional resistance is introduced (resistance of suspension- R_s). The performance of the grout injection was also analysed in the hardened state with ultrasonic tomography.

Conclusions and recommendations for future work are presented in Chapter 10.

Chapter 2. Overview of old masonries and their need for consolidation

2.1 Scope

Old buildings, either common of culturally relevant, represent the large majority of the construction types in most urban centres all over Europe. Due to a lack of maintenance, the masonries of old buildings are frequently in a poor state of conservation and can be characterized by their specific vulnerability, both under vertical and horizontal loads (Baronio et al., 2003; Collepardi, 1990; Valluzzi, 2005). This masonry typology present very different characteristics; some are made of a single leaf, while others have multi-leaf (Fig. 2.1 and Fig. 2.2). In the case of a multi-leaf wall, the section is composed by two resistant external leaves (with irregular texture and thickness) and an inner core filled by small stones, sand, mortar or other kind of unbounded material (Baronio et al., 2003; Vintzileou, 2011, 2006). The absence of cohesion among masonry elements, the existence of voids and cracks as well as the deficient connection between leaves lead to masonry walls with non-monolithic behaviour. This means that the wall becomes brittle, namely under vertical and horizontal loads. In order to stabilize such walls and to prevent structural failure grout injection is a current consolidate technique. In the next sections will be analysed in detail the characterization of old masonries, as well as the grout injection.

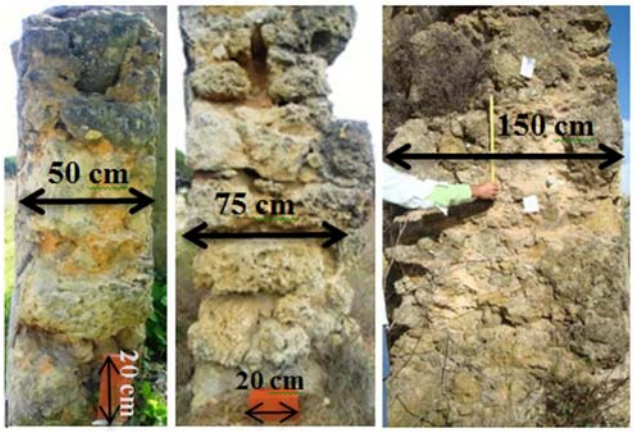

Fig. 2.1 - Masonry typology: (a) single leaf wall; (b) and (c) multi-leaf wall

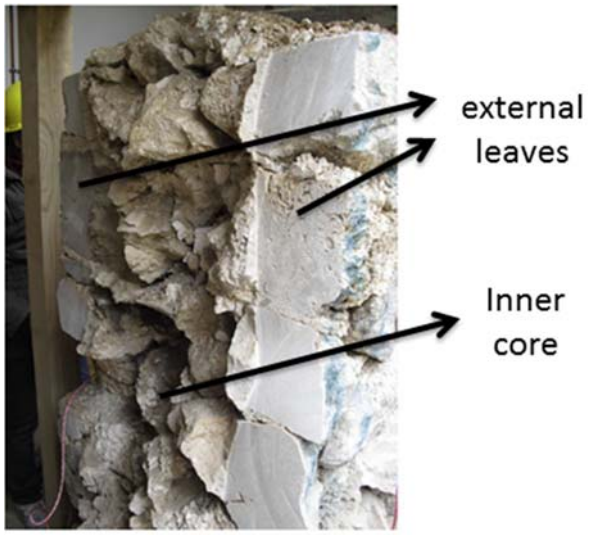

Fig. 2.2 – Cross section of a multi-leaf wall (Borri et al., 2011)

2.2 Survey and classification of the cross section of old masonry walls

The old masonry walls were built using different materials according to the local possibilities (stones, bricks, earth, various types of mortars, etc.) and different construction technologies (Binda & Saisi, 1996). Given the great number of existing cross sections and the great influence of the building technique on the mechanical behaviour, any evaluation should begin with an investigation of the different geometries and building techniques which takes into account the different layers constituting the wall and the kind of constraints which may or may not be present between the layers themselves.

Some researches were carried out in different Italian regions (Binda & Saisi, 1996; Binda et al., 2000, 1997) and in Portugal (specifically in outskirts of Almada city - Fig. 2.3) studying internal cross sections of masonry walls that can be inspected; this operation is more easily accomplished in areas where the buildings were damaged by the earthquake and have not yet been repaired. The survey consists of a graphic and photographic procedure which includes taking a photograph with a camera using a tripod which ensures the parallelism between the photograph plane and the wall plane. Through a material with known dimensions (which is placed at each cross-section before taking the photo - Fig. 2.1), it is calculated the dimension of the whole cross-section. The 2D graphic plotting (Fig. 2.3) is realized with a special care in the representation of stones, mortars, voids, etc. Consequently, the surface area occupied by the different materials is measured, which allows estimating the percentage of each material in the masonry (Fig. 2.4).

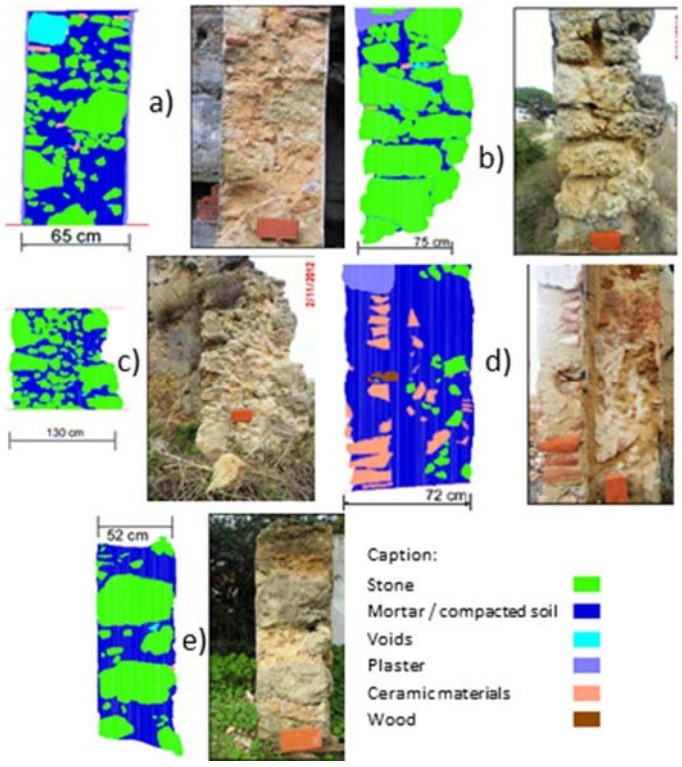

Fig. 2.3 - 2D graphic plotting where the materials presented are identified in the cross section of the masonry wall; Survey in Portugal: a) Campus FCT, b) Charneca de Caparica, c) Monte de Caparica, d) Pilotos, e) Vila Nova de Caparica (Jorne et al., 2015)

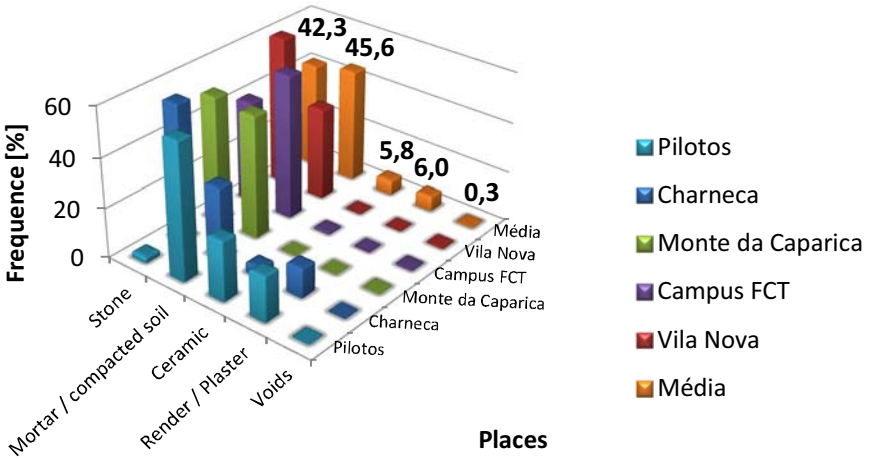

Fig. 2.4 – Percentage of materials referred to the area of the cross section of old masonry walls in various Portuguese places (Jorne et al., 2015)

Through a metric survey can be created an important database organized in tables, as shown in Fig. 2.5. In each survey to an internal section some important parameters must be analysed:

- the percentage distribution of stones, mortar, soil, ceramic material, plaster and voids;
- the dimension and distribution of voids in the cross section;
- the dimension of each cross section;
- the number of different layers and the type of constraint between them.

While the first two parameters allow the evaluation of the injectability of the wall, as subsequently described in more details (see Chapter 7), the latter two allow to formulate an important hypothesis about the mechanical behaviour of the masonry (Binda & Anzani, 1997).
According to some studies conducted by some authors (Binda & Saisi, 1996; Binda et al., 2003b, 1997; Jorne et al., 2015; Pagaimo, 2004; Pinho, 2007, 1997) in different historical regions of Portugal and Italy, the main characteristics of old masonry walls in historic buildings are the following:

- inhomogeneity, due to the presence of stones, mortars and other materials;
- lack of adhesion between external and internal leaves of the walls;
- poor adhesion between mortars and stones;
- poor cohesion of mortars in the joints and in the rubble tilling;
- high porometry of the wall system due to the presence of voids;
- high moisture content due to water penetration.

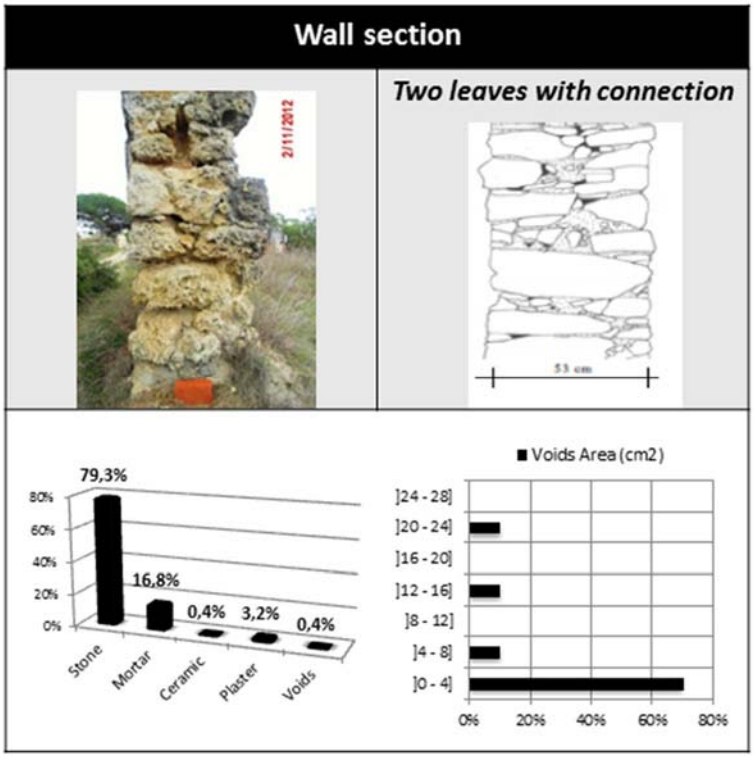

Fig. 2.5 - Form representing the wall section and the void calculation (Place: Charneca de Caparica – Portugal) (Jorne et al., 2015)

The study described above leads to a typology classification of the multiple leaf walls, based on the parameters already mentioned (Binda et al., 2000). This kind of classification (Fig. 2.6) can be an influential factor for the evaluation of the wall mechanical behaviour. Furthermore, the parameter distribution of the voids area is of utmost importance, since injection may only be used as masonry reinforcement if the distribution of the voids area is suitable. Indeed, an injection technique becomes more effective when inside the masonry there is a communication network of open porosity with a specific voids size. This issue will be detailed in Chapter 7.

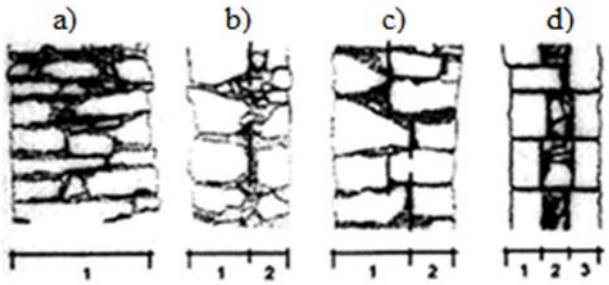

Fig. 2.6 – Classification of the cross-sections of masonry walls: a) single-leaf; b) two leaves without connection; c) two leaves with connection; d) three leaves (Binda & Saisi, 1996)

In the particular case of stone masonries more different classes of cross-sections of masonry walls can still be distinguished. There are four large classes, each one having subclasses as follows: (A) one leaf solid wall, (B) two leaves, (C) three leaves, (D) dry wall (Fig. 2.7). Each class can be further subdivided into two subclasses or even more (Binda et al., 2000). The approach for restoration should be done by classes of buildings and structures since it is frequently impossible to apply techniques of intervention equal for every building class.

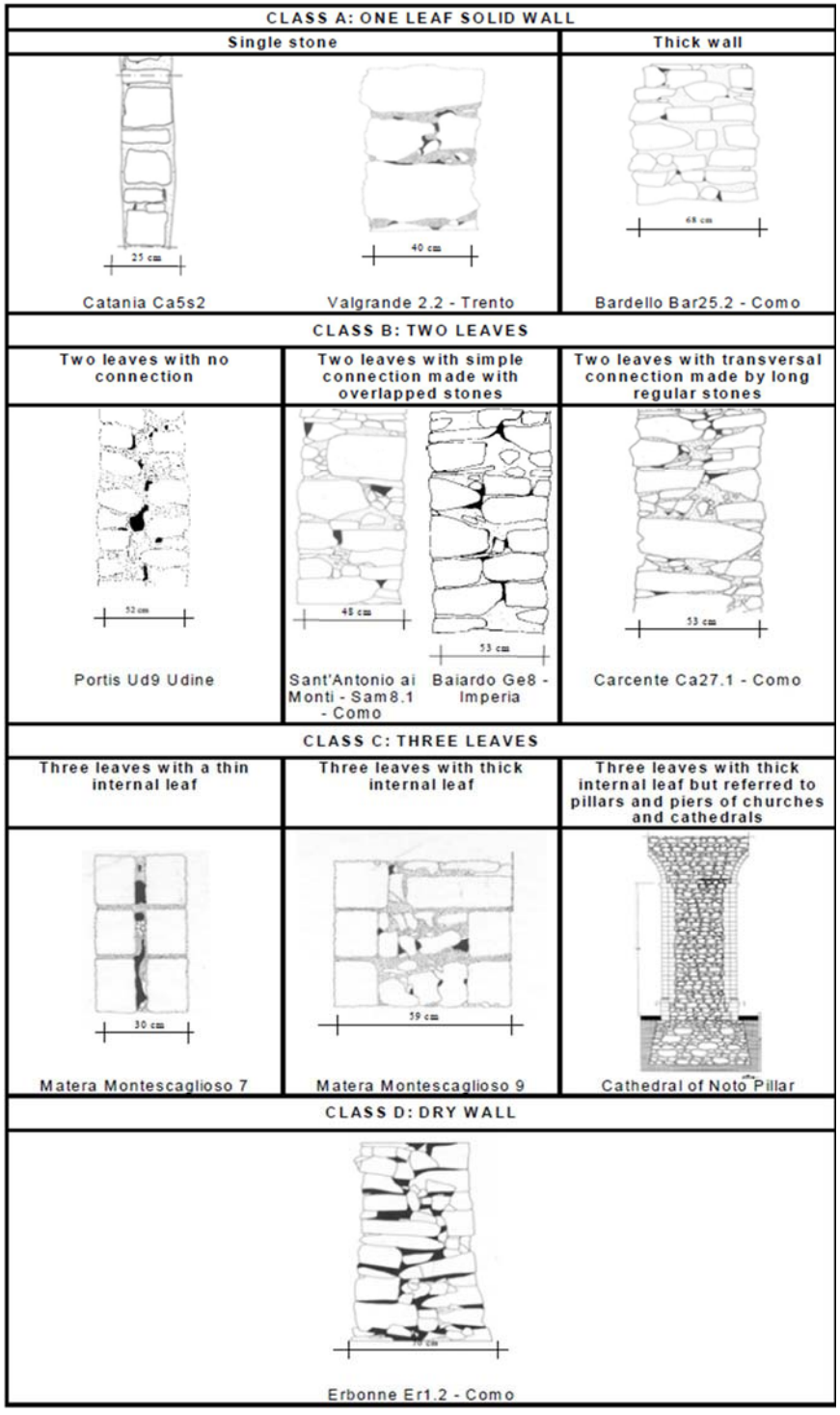

Fig. 2.7 - Example of the stonework sections (Binda et al., 2000)

The poor characteristics of old masonries may be improved to a certain extent by grouting, i.e. injecting into the voids a binder which can fill them, produce a connection between the leaves, give a better cohesion to the mortars and a better adhesion between the masonry components. Indeed, the grout increases or even re-establishes the adhesion forces between the solid constituents of the masonry, improving the general cohesion and the tensile strength of the masonry. Binda in (Binda et al., 1997) proposed as guidelines for the choice of the appropriate grout and technique of injection, the

study of the parameters mentioned above, together with the chemical, physical and mechanical properties of the materials that compose the masonry. As will be shown in Chapter 7, the effectiveness of grout injection requires a prior study of the PM (masonry) before of the injection. Indeed, it is crucial to study the grout injectability since the filling of the voids is the main basis of the mechanical improvement (Van Rickstal, 2000). The more porous the masonry, the more effective the injection will be. The importance of porosity is easily understood thinking that the main principle of grouting is to fill the inside voids. This way, a lower effectiveness in a solid stone or brick masonry can always be expected, when compared to a traditional multi-leaf masonry with a very porous rubble core. In fact, in multi-leaf masonry, besides the voids are higher, also the channels of communication between voids are much more than in the solid stone or brick masonry. Furthermore, in the case of multi-leaf masonry, a second effect is achieved. Through grout injection, the link between the two outer leaves can be established or strengthened, bonding them and thus guaranteeing monolithical behaviour. However it should be stressed that the efficiency of grouting in situ is not constant within the masonry, since the porosity varies (such issue will be studied in Chapter 9). Moreover, the rheological and mechanical properties of the grouts may not be ensured to be the same throughout the masonry.

2.3 Causes of damage to masonry

Physical and physico-chemical mechanisms

A large number of physical mechanisms are related to the presence of water inside the masonry structure. The transport of moisture is regulated by porosity, capillarity/sorptivity and permeability. As the old masonries are porous building material rain water is absorbed by capillarity. Consequently, a significant danger may arise due to frost action and crystallization phenomenon. The frost damage is associated to localized spalls, cracking and detachment of the surface due to moisture/frost back pressure (Van Rickstal, 2000). The crystallization of soluble salts can cause sufficient pressure behind of the surface material which can push off the outer masonry layer (Hinks & Cook, 1997).

Another physical mechanism that causes damage inside the masonry is thermal variations. Due to thermal cycles large stresses occur in the outer layer of masonry resulting in a map cracking (Van Rickstal, 2000).

The physical mechanisms that occur within the masonry result in a decrease of internal cohesion of the materials. Grout injection is very suitable to repair this kind of damage. The more uniform the grout to fill the voids caused by physical damage, the better the final consolidation.

Mechanical damage

The mechanical damage can happen in structural members and non-structural elements of the building. There are several types of mechanical damage: a) cracking of walls and slabs and b) aggravation of existing cracking in structural members and non-structural elements.

A mechanical damage may arise due to different actions (Table 2.1) (Van Rickstal, 2000).

Table 2.1 – Mechanical damage due to human and nature actions

Human actions:	Nature actions:
• mistakes in the original design; • poor dimensioning of structural parts; • an unexpected settlement of the soil; • modifications by man of the original structure; • a different use of the building; • vibrations induced by man;	•heavy wind; • rain or storms; • seismic action;

Most of the old masonry walls shown in 2.2 were designed to resist mainly gravity loads (Alecci et al., 2013), without any specific anti-seismic design. The recent earthquakes that in the last decades occurred in Southern Europe showed the seismic vulnerability of these walls (Mazzotti et al., 2014). Indeed, there are two possible failure mechanisms, namely in-plane shear and out-of plane bending. As regards the in-plane behaviour, there are two typical types of behaviour associated to different failure modes (Fig. 2.8): flexural behaviour (rocking with crushing) and shear behaviour (sliding shear failure and diagonal cracking) (Milosevic et al., 2013). The geometry of the walls, the boundary conditions, the mechanical characteristics of the masonry materials and the adhesion among masonry materials have influence on the type of failure mode that occurs (Kalali & Kabir, 2012).

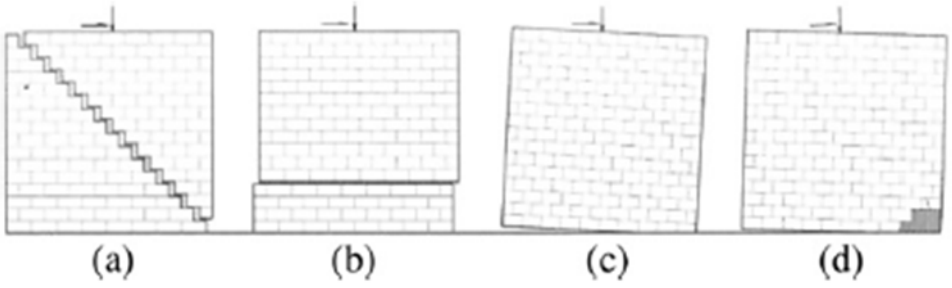

Fig. 2.8 - Failure modes of in-plane loaded masonry walls: (a) shear failure; (b) sliding failure; (c) rocking failure; and (d) toe crushing failure (Kalali & Kabir, 2012)

Another problem associated with the mechanical damage is related to the poor ductility of stone buildings (Hinks & Cook, 1997). In cases of significant differential movement (e.g. due to a settlement of the soil) there may be problems as the capacity of the stone masonry to accommodate movement. In such instances cracking of the joint and/or the stone itself can occur.

The mechanical damages can be repaired through grout injection into the masonry. This issue will be studied along of the Chapter 3.

Main defect of the three-leaf masonries

The major problem in three-leaf masonries is that they are not monolithic in the lateral direction (Fig. 2.9); this may happen for instance when the space between the two external leaves is filled with loose, low-strength material made of small pieces of stones and/or bricks and mortar (Fig. 2.1 and Fig. 2.2).

Due to weak connections between outer leaves, the predominantly irregular morphology of the walls, the presence of voids, and the low strength of the used mortar, three-leaf masonries are very vulnerable to in-plane (mainly shear) and out-of-plane actions (Uranjek & Bosiljkov, 2012). To enhance the compactness of the interior weak leaf, as well as to re-instate the links between external and internal leaves in three leaf masonry, the technique of grouting should be applied (Anzani et al., 2007). Such technique is addressed in chapter 3.1.

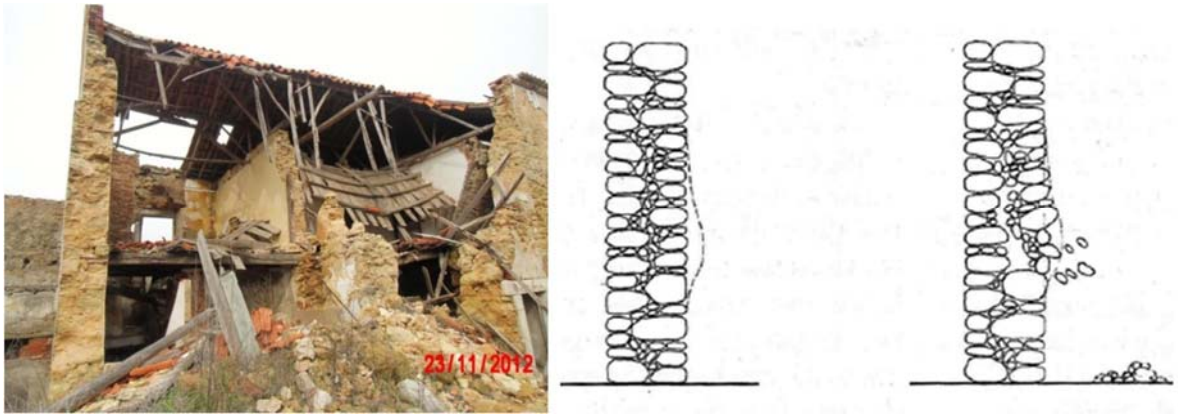

Fig. 2.9 – Deformation and failure of a two leaves wall due to non-monolithic behaviour (left picture); collapse of the outer leaf of the wall (right picture) (Binda et al., 2006)

Biological damage

Regarding the type of masonry studied, the biological damage is the type of damage with lower gravity. However, it should be noted that they produce, in combination with organic material such as rotten leafs or pigeon excrements acids which directly attack the limestone and mortar. In this way, erosion phenomena on the external surface of the masonry can arise.

Chapter 3. Grout injection as a consolidation technique for old masonry

3.1 Grout injection performance

3.1.1 Aims and procedure of grout injection

The strengthening of multi-leaf masonry is extensively performed by grout injection, which for years have been regarded as a suitable technique to restore the compactness, cohesion, uniformity of strength and continuity of masonry walls (Binda et al., 1997; Miltiadou-Fezans & Tassios, 2013b; Van Gemert et al., 2015a).

In general, the aims of the technique are:

- to fill large and small voids and cracks increasing the continuity and cohesion of the masonry and hence its strength;
- to fill the gaps (in the inner core) between two or more leaves of a wall, when they are badly connected (Valluzzi et al., 2004). The aim can be fulfilled only knowing with good precision the morphology of the wall section, the materials constituting the wall and their composition in order to avoid chemical and physical incompatibilities with the grout, the crack distribution, the size, percentage and distribution of voids (see chapter 2.2).

As the experience demonstrates the fulfilment of the above issues requires considerable investigation efforts, both in laboratory and in-situ (Binda et al., 1997). The methodology has been so far defined and implemented is substantially based on three principal steps (flowchart below): (i) survey of the wall section and sampling of the materials contained in the internal part of the wall; (ii) laboratory characterization of the materials sampled from the walls, and choice of grout suitable for injection through an injectability test and verification of the physical and chemical compatibility; (iii) injection on site of check points and control of the injection efficacy by flat-jack test and survey of the penetration and diffusion of the grout.

It should be noted that in the case of old masonry walls, due to their heterogeneity in materials and typology, there is no general method of strengthen. Thus, in each case a profound wall survey is required in order to choose the best strengthening techniques (may be more than one). The selected techniques should be experimentally studied to understand not only the best application procedure, but also their effectiveness (Borri et al., 2011).

The injectability test referred in Fig. 3.1 consists in the preparation of physical models representing the internal core of the wall to be injected. This injectability test is carried out in the laboratory (Fig. 3.2) with materials sampled from the internal part of walls. The sampled material is inserted into cylinders and then injected with different grouts. The methodology used in this work for testing the injectability of the grout is presented in Chapter 5, Chapter 7 and Chapter 9. NDT as (ultra)sonic tests can also be carried out, before and after injection in order to detect the penetration and diffusion of the grout. This issue will be further detailed in Chapter 8. Besides that, in laboratory, compressive, splitting and shear tests can be carried out on the cylinders injected after the time necessary to reach the hardening of the grout.

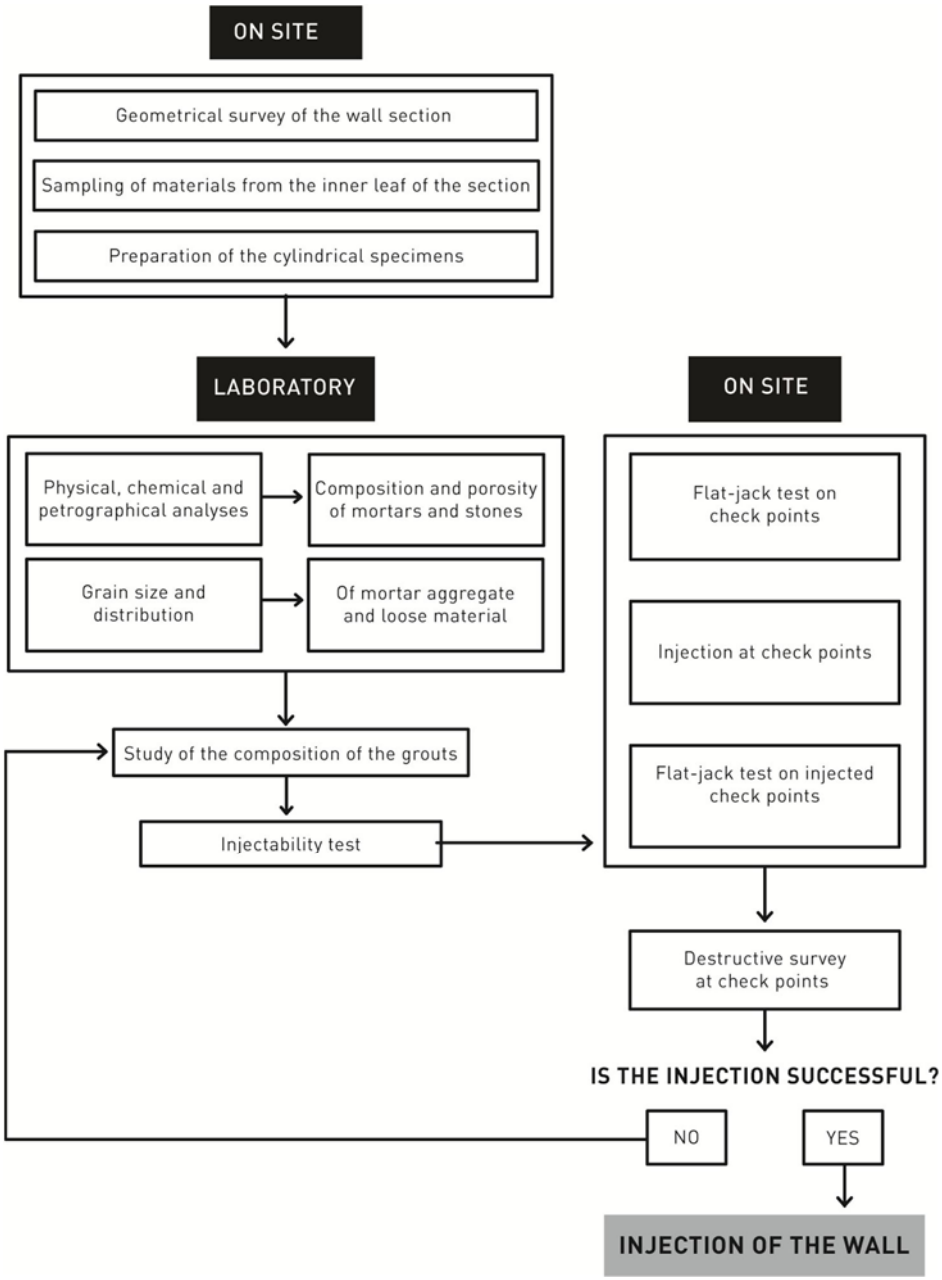

Fig. 3.1 - Procedure for selecting the grout and for detecting the efficacy of injection (Binda et al., 1997)

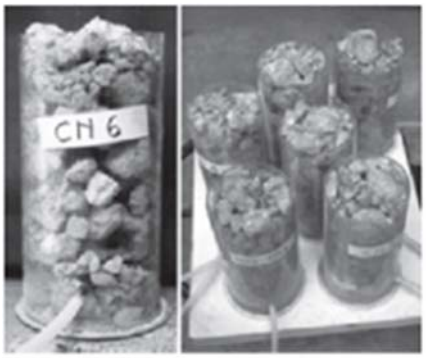

Fig. 3.2 - Cylinders are filled with the materials sampled on site in order to evaluate the masonry injectability (Binda et al., 1997)

Sometimes the effectiveness of the grout is poor in some injectability tests. The main problems related to grout injection can be summarized as follows (Binda & Saisi, 1996):

a) lack of knowledge on the size distribution of voids in the wall (must be conducted a survey as mentioned in 2.2);

b) the difficulty of the grout to penetrate into thin cracks (2-3 mm), thus the grout cannot further penetrate and fill the voids, even large voids where the grout can easily penetrate;

c) the presence in the wall, of fine and large size voids, which make difficult choosing the most suitable grain size of the grout;

d) the segregation and shrinkage of the grout due to the high rate of absorption of the material to be consolidated;

e) the need for sufficiently low injection pressure to avoid either air being trapped within the cracks and fine voids or even wall disruption.

These factors listed above show again that the effectiveness of a repair by grout injection depends not only on the characteristics of the mixture used, but also on the wall type knowledge. For instance, there are many cases of multiple leaf walls which are made with very poor mortars and stones, but at the same time have a very low percentage of voids. In certain cases, the inner core is composed with loose material, which is difficult to inject. Other strengthening techniques must be used (see 3.1.3).

3.1.2 Realization of an injection work

3.1.2.1 Injection technology

At present there are four different methods of carrying out an injection – manually, by gravity, pumped and vacuum. Pumped grouting is undoubtedly the most used technology due to its superior versatility and efficiency. It consists in supplying grout under pressure into the masonry in order to fill the voids. Due to the major importance of pumped grouting, this thesis was centred on this subject. In the next sections, the preliminary works of an injection operation, the respective design parameters and the quality control procedures are detailed. It is worth noting that these procedures should be adapted to different situations encountered with old masonries.

3.1.2.2 Preparation of masonry and holes pattern

The first step on site is to prepare the masonry to be injected. This operation must be based upon a diagnosis of the masonry to be treated/strengthened. It is important to identify the areas that need to be injected (Gil, 1994). Once the areas to inject are determined, the masonry is prepared for injection. An important part of this preparation is the sealing of surface cracks/voids of the masonry to prevent the leakage of the grout at the surface (Van Rickstal, 2000). Any suitable sealant material may be used, but it is important that the material be relatively rapid setting and must be capable of resisting injection pressure. It should be given special attention to the masonry around windows, doors, and other wall penetrations. In such cases, a general deep repointing may be required. The repointing must be fairly porous to absorb the water of the injected grout. This will improve the setting of the grout and the adhesion to the masonry.

The masonry units that show serious damage, such as extensive cracking or spalling must be replaced. Moreover, the repointing of deficient mortar joints that are unlikely to withstand injection pressures should also be done. Special attention with regard to material compatibility is needed. Thus, it is required that the mortar and the masonry units should have a composition and strength similar to existing materials. As regards the mortar, the trend is to use a mortar mixture mainly based on lime with a low percentage of cement, particularly when dealing with restoration works in historical constructions (Borri et al., 2011).

It should be noted that in a structural reinforcement of masonry, a consolidation injection is often combined with a partial or general repointing (Fig. 3.3).

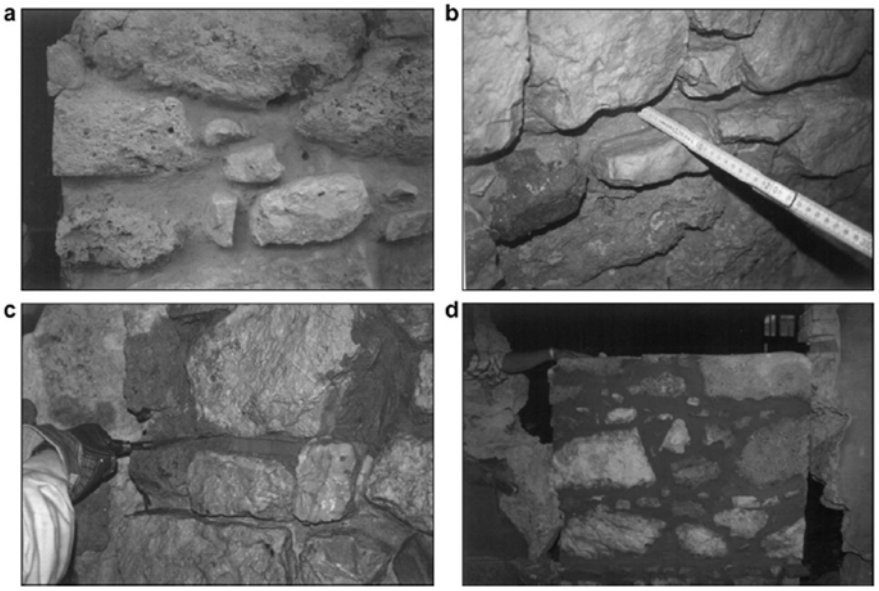

Fig. 3.3 – (a) Joint after cleaning; (b) detail of the joint depth; (c) first layer of repointing; (d) after intervention (Borri et al., 2011)

The second step starts with the preparation of the drilling of the injection holes. The diameter of the holes must be as small as possible. The holes are drilled inclined towards the bottom and, as far as possible, they are drilled in the joints (in particular the joints with cracks) to prevent chipping and damaging the masonry units. This way they will be less visible afterwards. The parameters that are related to the injection holes and the factors that influence these parameters are shown in Table 3.1.

Table 3.1 – Parameters of the injection holes; factors that influence the parameters of the injection holes

Parameters of the injection holes:	The parameters depend on the:
• pattern (position) • density or distance between two adjacent holes • depth of the holes	• type of masonry • overall condition of the masonry • rheological properties of the grout • incidence of the craks

In the case of masonries in precarious condition lower pressures must be applied and consequently the distances between holes must be reduced. On the other hand, if in certain areas of the masonry many cracks/voids are present, the grout injection will be easier and hence the pattern in these areas could be

somewhat less dense. However, for reasons of simplicity the density is often kept constant for the whole structure.

Concerning the reference number of density of holes per square metre, the values of 2 to 4 holes can be referred as a guide line (Gil, 1994). However, an experimental program conducted by (Baronio, 1992) about masonries with porometry irregularly distributed rejects these values. For this type of masonry, Baronio considers that the usual 2 to 4 injections per square metre are not enough since there are some difficulties to inject all voids. Other authors propose different values. Boineau (Boineau, 1986) proposes a maximum reference distance between holes equal to the thickness of the wall. Recently, Silva (Silva et al., 2014b) defined a triangular mesh (equilateral triangles) of 30 cm side length, in order to optimise the distribution of the injection points. Nevertheless, regardless of the existence of these reference numbers, the holes density should be set based on a diagnosis of the masonry, where the masonry characteristics must be identified. NDT (studied in Chapter 4) can function as a good feature.

Regarding the depth of the holes, it is important that their depth is at least until the middle of the wall, to ensure a uniform diffusion of the grout in a transverse section (Gil, 1994). In order to optimize the grout flow into the masonry, a staggered pattern should be adopted. Indeed, the theoretical capacity of flowing through the masonry increases around 10% from a square pattern to a staggered one, for a hole density of 4 holes/ m^2 (Fig. 3.4).

Besides all the above parameters, the grout penetration into a particular injection hole depends on the properties of the fresh grout. Indeed, the grout composition should be combined with the other parameters. This study is one of the goals of this thesis.

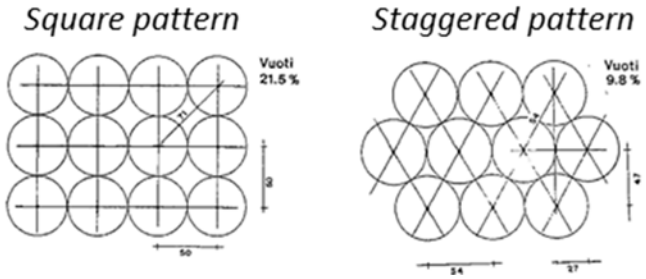

Fig. 3.4 - Theoretical flowing capacities according to the holes pattern (Gil, 1994)

3.1.2.3 Pre-wetting of masonry before injection

The advantage of pre-wetting the masonry before grout injection is something doubtful. Some authors refer that a previous water injection should be made whereas others have criticized this proceeding. According to Chaudhry (Chaudhry, 2007), pre-wetting has a positive effect depending on the nature of binder in the grout and the porometry of the wall. Eriksson *et al* (Eriksson et al., 2004) and Cachim (Cachim, 2009) noted that the pre-wetting of walls improves the grout injection capacity, increasing the diffusion of the grout. On the one hand, by flushing all injection holes with water, the dust is removed and the internal surfaces are cleaned. On the other hand, the pre-wetting allows that PM particles absorb part of the water and hence the pores are at least partly saturated. Additionally, this guarantees that particle surface is wet when the grout is injected. In this way, the presence of water on the particles surface ensures that the masonry elements with high porosity do not absorb too much

water from the grout, which could cause an inadequate hydration of the binder used. Furthermore, a large amount of grout particles will be able to penetrate into the smallest apertures of PM, thus causing a higher homogeneity injection which means a higher quality of consolidation.

In contrast, some authors argue (Bras et al., 2013b; Gil, 1994) that the pre-wetting of old masonries by water injection is an operation which always involves a certain degree of risk. First of all, it can be dangerous when the stability of the construction is doubtful. The water reduces the internal cohesion and friction and breaks existing poor links between the elements of the masonry, changing its internal arrangement. Miltiadou in (Miltiadou-Fezans, 1990) also stated that pre-wetting procedure may not be always advisable. This author studied the adhesion of cementitious grouts to a masonry support. Miltiadou stated that a saturated support is not advisable at all as it completely impedes the penetrability of the grout, weakens the stones or bricks and completely hinders the absorption of water from the grout.

As there are some doubts related to pre-wetting procedure, in particular its influence on grout penetrability and grout adhesion, this issue will be addressed in Chapter 7, Chapter 8 and Chapter 9.

3.1.2.4 The injection pressure

The injection pressure is an important parameter in the grout injection. In fact, the injection pressure is the driving force behind the penetration of the grout inside the masonry. The higher the pressure the easier and faster the grout will pass. Because the grout flows faster, the grout will loose less water by absorption and the particles will remain better in suspension (Van Rickstal, 2000).
The internal structure and the internal state of deterioration of the masonry play also an important role in the penetration of the grout. The more deteriorated the masonry is inside, the less resistance it offers to grouting. The internal porosity becomes larger and the size of pores is higher and better connected, making the diffusion of the grout easy. However, the residual strength of such masonries limits the maximum allowable pressure. Van Rickstal in (Van Rickstal, 2000) recommends the use of pressures limited to a few bars in cases of injection of a masonry with significant damages, since the internal pressure (addition of the injection pressure and the hydrostatical pressure) of the grout introduces tensile stresses that cannot be taken by the masonry. In order to avoid excessive hydrostatical pressure, a maximum injection height of 0.5 to 1 m is advisable.

Gil in (Gil, 1994) observed that the effectiveness of the grout injection is not dependent of a high pressure. Actually, in a high-pressure injection a rapid separation or filtering of solids can occur when the mixture enters a crack/void. The author argues that the pressure should be very long and constant with a reference value between one and two bars. Binda (Binda et al., 1997) also noted the importance of maintaining a constant pressure and a continuous feeding of grout to increase the effectiveness of grouting.

From several case studies, Table 3.2 shows some recommended values for the injection pressure. In accordance with these values, the range of 0.5-2 Pa was chosen for the injection tests (see Chapter 5, Chapter 7 and Chapter 9).

Table 3.2 – Injection pressure values for masonry found in literature

Reference	Pressure (bar)	Type of grout
Baltazar et al. (2014b)	1	Hydraulic lime=98% + SF=2% + SP=0.8wt% (w/b=0.5)
Binda et al. (1997)	0.2 to 0.6	Micro fine cement based grout (w/b=1.5)
Binda et al. (1997)	0.2 to 0.6	Hydraulic lime grout (w/b=0.8)
Binda et al. (1997)	0.2 to 0.6	Hydraulic lime mixed with dust bricks (w/b=?)
Bras and Henriques (2012)	1 to 2	Hydraulic lime grout (w/b=0.6-0.8)
Bras et al. (2013b)	1	NHL5 based grout and NHL5+15%FA (w/b = 0.70)
Corradi et al. (2008)	1	Hydraulic lime based grout (w/b=?)
Gil (1994)	1	Microcement based grout, SP=2wt% (w/b=1-1.2)
Kalagri et al. (2010)	0.75	NHL5+SP (w/b=0.8); NHL5 (w/b=0.8)
Valluzzi et al. (2004)	0.5	Hydraulic lime + SP=0.25wt% (w/b=0.25)
Valluzzi (2005a)	0.5	Hydraulic lime based grout (w/b=0.55)
Van Rickstal (2000)	1	CEM III/A 42.5 + SP=1.5wt%, (w/b=0.67)

* SF= silica fume; SP= superplasticizer

3.1.2.5 The operation of injection

The injection normally starts from the lowest level and progresses first sideways and then upwards in a systematic manner, to avoid trapping air in pockets (Fig. 3.5). When the injection of a certain hole is stopped, the hole is plugged and the operation is continued at an adjacent hole from which the grout has flowed. After the horizontal row is completed, the operation moves upwards (Gil, 1994).

In any hole, the grout is continuously injected until one flowing condition takes place:

- a predetermined limiting pressure is reached;

- the grout emerges freely at adjacent injection holes;

- a predetermined quantity of grout is injected in that hole.

The amount of grout inserted into each hole must always be recorded; these records can be analysed in order to check for a complete filling of the masonry, to control if no grout ran away, i.e., to check eventual grout leakages (Gil, 1994). As mentioned earlier, a good preparation of the masonry (through a repointing process) is crucial to prevent the occurrence of leakages. However, the invisible leakages cannot be sealed by means of the normal processes. In these cases it is advisable to use a fast setting grout.

Three men are the usual labour force to carry out this work. One will control the mixer and the pump and ensure the continuous flow of the mixture. The other men work in the neighbourhood of the injection hole. One of them handles the conduits and takes care of connecting the conduits to the injection hole (Fig. 3.5). The third worker helps this second man in moving the conduits and seals the occurring leakages. When the work has been completed, the injection holes need to be repointed. The

mortar used should have a colour and a composition similar to the original mortar (Borri et al., 2011; Van Rickstal, 2000).

Fig. 3.5 – Masonry structures strengthened by grout injection (photos from ZIRCOM)

3.1.2.6 Quality control in a grouting operation

General guidelines were created to ensure a standard of quality in a grouting operation (Bras, 2011; Toumbakari, 2002; Valluzzi, 2005). However, the multiplicity of different situations that emerge on-site and the heterogeneity associated to old masonry structures makes it possible to formulate recommendations only of a general character. To ensure the desired standard of quality, the masonry building must be carefully studied following the procedure mentioned in 2.2. In addition, the operation must be designed as detailed as possible according to the points mentioned in the flowchart (Fig. 3.6).

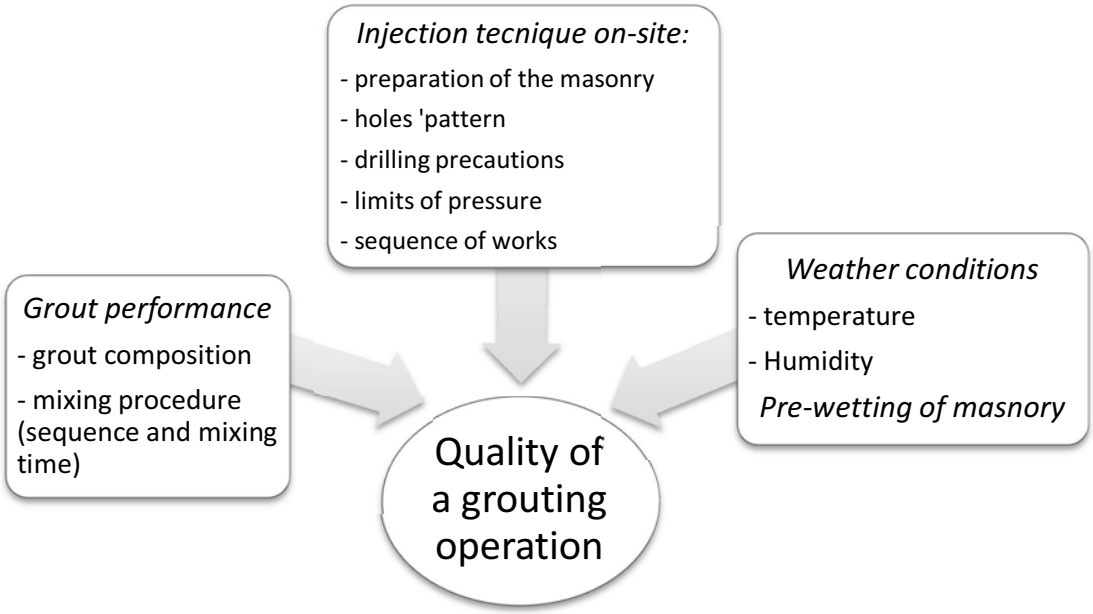

Fig. 3.6 – Factors that affect the quality of a grouting operation.

In order to ensure the quality of a grouting operation, the monitorization of the grout penetration is critical. Indeed, close supervision of the works in an obligatory requirement. It ensures that the designing specifications are followed and it allows accurate records of the whole operation to be made. For this purpose, it is essential to use skilled labour in all the phases in order to ensure the right decisions are made in the event of unforeseen circumstances.

After injection, the work is not yet done. The injected region should be checked after the grout has hardened. One possible and reliable method is to use the same NDT method as was used for the diagnosis of the masonry structure. Thus, it is possible to compare the maps (e.g. by sonic tomography) that are obtained before and after the injection. As shown in Fig. 3.7, if the masonry voids were filled with grout, the sonic velocity will generally increase (which ensure the adequacy of the grout injection). But other NDT can also be used: electrical resistivity, radar technique, etc. They are discussed in Chapter 4.

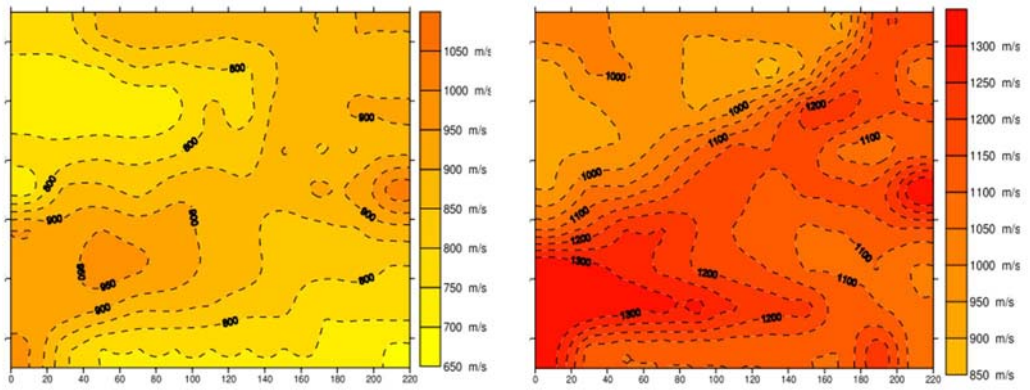

Fig. 3.7 - Results of the sonic tomography: original conditions of the masonry (left); after grout injection (right) (Da Porto et al., 2003)

3.1.2.7 Other injection techniques

Regarding the grout injection, the method studied in this thesis is the mechanical pumped system. In fact, the majority of grouting challenges can be solved using pumped systems (Bras, 2011). However, there are other methods, namely gravity systems and vacuum systems. The best method should be selected based on the nature and condition of the masonry.

Table 3.3 shows a comparison among these different methods of grout injection in terms of application, procedure and constraints.

Table 3.3 – Comparison among different methods of grout injection (Bras, 2011),(Gil, 1994),(Van Rickstal, 2000)

System	When should it be used?	Procedure	Constraints
Gravity grouting	- is advisable to very damaged masonry elements, e.g. to consolidate masonry ruins.	- it consists of letting the grout enter the masonry, with the help of the gravity force.	- it is only effective if the voids inside the masonry are adequately large, once the pressure associated is very low.
Vacuum grouting	- in situations where the use of pressure could be dangerously disruptive and ineffective (e.g. small statues); - in situations where difficulties may occur in confining the grout by pressure, if it spreads beyond the area to consolidate, incurring additional costs.	- a vacuum is first created in part of the structure to be consolidated. To achieve this, all leakage paths away from the pre-defined portion must be sealed. Then the vacuum must be induced, removing all the gases and fluids from within the pores. After, the pressure differential between the atmosphere and the vacuum sucks the grout into the pores.	- resins (higher fluidity) are more suitable than cementitious grouts; - the creation of a complete vacuum system in a masonry element attached to a whole structure is often difficult to carry out on site. Thereby, the method is limited to relatively small elements.
Hand grouting	- it can be an alternative when no other facilities are available. Normally, it is carried out in association with pointing and tamping.	- it consists of forming against the surface of the masonry small clay modelled cups, in which the grout is poured and allowed to flow through the voids of the masonry around the cup. The grout is poured into them until the desired level in the masonry is reached.	- It is a small scale procedure that can only be adapted to local consolidation

3.1.3 Grouting as a strengthening technique

During an earthquake is expected a high degree of damage to the old masonry walls. Since the integrity of the walls is inadequate due to the presence of internal voids, cracks and other discontinuities that seriously affect the seismic resistance. In order to improve the seismic response of

old masonry walls, grout injection (Fig. 3.5) is a widely used consolidation technique since the 80´s (Kalagri et al., 2010; Miltiadou-Fezans, 1990; Vintzileou, 2011). The main goals of this consolidation technique is to increase the homogeneity/compactness, which also increases the adhesion between stones, mortars or other materials inside the masonry and, at the same time creates new bonds (links) between the internal and external leafs of the wall. In this way, the masonry shear and flexural strength are improved, and the monolithic behaviour is re-established without altering the morphology and load-bearing system of the wall (Binda et al., 1997; Miltiadou-Fezans & Tassios, 2013b). Furthermore, the threshold of critical force at which the damage initiates, is increased at the global level leading to overall improvement of the quality of masonry walls. According to Uranjek and Bosiljkov (Uranjek & Bosiljkov, 2012) the behaviour of the wall after grout injection is significantly influenced by the injection grouts performance. For a successful injection, it is necessary to ensure an adequate grout flow within the masonry (porous media) in order to increase the quality of the consolidation (this issue will be studied in Chapter 7 and Chapter 8). This fact is critical, given the heterogeneity of this type of masonry (see 2.2).

Since the old masonries are highly heterogeneous the variance on the strength is also high. Thus, the uncertainty about the strength becomes bigger and hence the probability of failure is elevated. As demonstrated above, grout injection can be a solution to this problem. In fact, as shown in Fig. 3.8, when a good and uniform penetration of the grout inside the masonry is achieved (successful consolidation), there is an increase of the average strength and the reduction of the strength variance. This means that the safety of the masonry is improved and the risk of collapse is lower after a successful grout injection intervention.

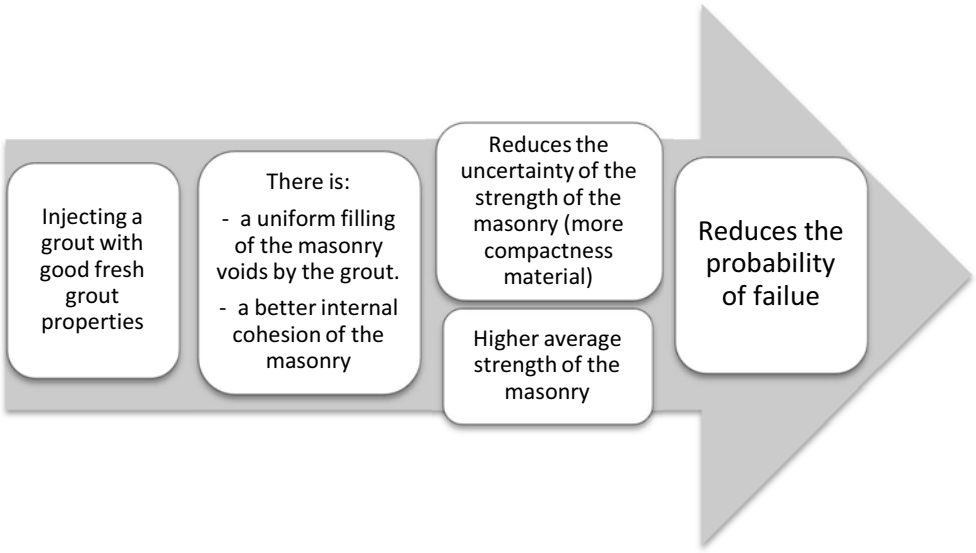

Fig. 3.8 - Relation between the probability of masonry failure and the fresh grout properties

As already demonstrated, the grout injection may be used for strengthening old masonry walls. However, grouting should not be used in masonry walls where the porosity (voids volume) is low (Jorne et al., 2015). In these cases, the application of steel transversal connectors must be performed. The aim of this technique is to improve the connection (mechanical connection) between the two leafs

of the wall avoiding their separation from the inner core, as can be seen in Fig. 3.9. The application of such technique may include, or not, binding material such as grout.

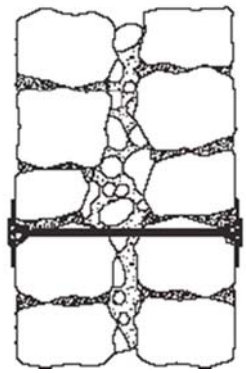

Fig. 3.9 – Face to face connector in wall of two layers (Coias, 2007)

3.2 Grout design for masonry: an overview

Grouts are mixtures of binder with water, with or without special additives. Their design as well as the method of application must fulfil a series of performance requirements, namely injectability, bond strength and compatibility (see 3.3). In what concerns the nature and composition of the masonry materials, the grouts must show compatibility with the original material in terms of chemical, physical and mechanical characteristics in order to fulfil with Charter of Venice (Biçer-Simşir et al., 2009; Kalagri et al., 2010; Vintzileou & Adami, 2009). Thus, it should be underlined the importance of selecting appropriate raw materials for the grout composition, taking into account the properties of the masonry to be injected. The goal is to avoid the negative experiences of the past, and on the contrary ensure the authenticity of historical material and the monumental value of the masonry construction (principles of the Charter of Venice) (Van Gemert et al., 2015a). The fulfilment of these principles is crucial, since the grout injection is an irreversible technique.

3.2.1 Binders

For each application, the grout mix designs may include different types of binders. Regarding hydraulic binders can be subdivided into two main categories, namely cement and lime with hydraulic properties. Cement based grouts were initially pure cement grouts. However, it was proven that their injectability properties were inadequate for filling the small size voids and cracks of historic masonries because of clogging (Axelsson et al., 2009; Eklund & Stille, 2008). Moreover cement grouting leads to higher stiffness values, which may increase structural damage. The reason for this is the significant variation in the deformability and the hygrothermal behaviour of the masonry (usually composed with materials having low strength and high porosity) (Papayianni & Pachta, 2014). Furthermore, it is known (Vintzileou, 2006) that mechanical tests have not confirmed the need for grouts with high cement content. Thus, it can be conclude that the use of grouts with reduced/without cement content is beneficial in prevention of physic-chemical incompatibility with in situ materials (Bras, 2011), meaning an increase in the durability intervention. All this led to the development and investigation of alternative mixes, namely hydraulic lime grouts. Research concerning the use of hydraulic lime based grouts (pure hydraulic lime or in combination with a pozzolanic material) is relatively recent (Baltazar

et al., 2014, 2013; Bras et al., 2010; Kalagri et al., 2010; Vintzileou, 2006). Their similarity with in situ materials may offer a promising solution as long as they also prove to be mechanical efficient.

Concerning lime based grouts, they can also be used in restoration work due to their similarities and therefore compatibility with the original masonry being repaired/conserved (Scannell et al., 2014). In fact, the main advantage of the lime mortar is the compatibility with the materials from old masonries, which is much closer than the cement and even the hydraulic lime. However, as CO_2 has difficulty in reaching the inner of the masonry, the process of carbonation is slow. Thus, the efficiency of these grouts is compromised, since the mechanical resistance of the wall is slightly improved over the long term.

Polymeric grouts offer the highest effectiveness (due to the excellent rheological behaviour) and at the same time they have outstanding mechanical and bonding properties. However, the physical incompatibility with the masonry limits their use in historical buildings.

In Table 3.4 shows the advantages and disadvantages of the binders mentioned above in relation to hydraulic lime. In all of them, the disadvantages have greater weight. For this reason, the hydraulic lime (see 5.2.1.1) was the binder chosen in the injection tests of this work.

Table 3.4 – Advantages and disadvantages of different types of binding agents in relation to hydraulic lime (adopted from (Van Rickstal, 2000), (Toumbakari, 2002) (Van Gemert et al., 2015a)

Types of binding agents	*Advantages*	*Disadvantages*
Polymers (e.g. polyester or epoxy resins)	- Show low viscosity and low critical shear value (good rheological properties). - The absence of the solid particles in suspension (is a pure liquid) that might hinder the flow, make polymers very suitable for injection. - Show a high tensile and adhesion strength. - Low shrinkage and high chemical resistance (in particular to alkalis).	- Poor adhesion to wet surfaces (due to the formation of air bubbles that increases the porosity of the resin and damages the adhesion). - Present different physical properties (moisture transport, thermal expansion) in comparison with masonry materials. - High cost (intervention very expansive). - Mechanical behaviour is not compatible with the materials that are present in historical buildings.
Cements	- Is the most popular binding agent of modern times. - Fast hardening allows to proceed faster in applying new loads to the structure.	- Does not correspond to the binding agent used in most historic masonry buildings (art historians and architects disapprove its use). - Physical properties are different from those present in historical materials (but much closer than in the case of polymers). - After injection, the loss of ductility of the masonry is higher. - High risk (due to C_3A) of the formation of ettringite.

Types of binding agents	*Advantages*	*Disadvantages*
Air limes	- The most compatible with the original materials for the consolidation of ancient masonry. - For centuries has been used for the construction of buildings. - Injectable in fine cracks (due to the fineness of their particles).	- The carbonation of thick layers of lime is a very slow process (due to the slow diffusion of CO_2 through the carbonated layer). - Low mechanical strength.

3.2.2 Admixtures and additions

Grouts, by definition, are mixtures of a binder and water. However, these simple mixes are unable to perform efficient consolidation, therefore requiring the use of additional products. According some authors (Baltazar et al., 2013, 2012a; Binda et al., 2003a; Eriksson et al., 2004; Fernàndez-Altable & Casanova, 2006; Mirza et al., 2002b) the fresh grout properties can be improved with the use of additives in the grout composition, in particular pozzolans that can be added to the grout composition. According to ASTM C618, a pozzolan is defined as a "siliceous or siliceous and aluminous material which, in itself possesses little or no cementitious value but will, in finely divided form and in the presence of moisture, chemically react with calcium hydroxide at ordinary temperature to form compounds possessing cementitious properties". The pozzolans can be either of natural origin or industrial by-products (artificial). The main artificial pozzolans are: silica fume, fly ash and metakaolin. They are widely accepted as providing economic and technical advantages, and moreover, the durability issues are taken into account (Faria et al., 2014).
Another key point in the design of grouts is the use of dispersant admixtures, such as SP, because of its influence on the fresh properties of cementitious mixtures. In fact, the influence of SP on the rheology, stability and water retention is clear, resulting from several phenomena, such as:

(i) the adsorption of SP molecules on binder particles creates a repulsion mechanism between binder particles avoiding their flocculation as well as minimizing the amount of water needed for particle dispersion;

(ii) the dispersing action of SP opposes the sedimentation, so the sedimentation process occurs more slowly and the particles settle more homogeneously (which means lower segregation);

(ii) the SP de-flocculate the grout particles, allowing a higher degree of wettability and consequently reducing the amount of free water (Mikanovic, et al., 2008).

From a global point of view considering rheological, stability and water retention results obtained by some authors (Baltazar et al., 2012a; Petit et al., 2011; Sonebi et al., 2013), it seems that SP is necessary when designing a grout for injection purpose. Its presence seems to be inevitable when the PM injected has very fine voids.

3.2.3 The effect of mixing procedure on penetrability of grouts

The mixing procedure is a critical step in the grout preparation process. Adequate mixing procedure will result in a grout with better injectability properties. High-shear mixing equipment is necessary to

break up agglomerations of finer particles. Usually, the grout is mixed using a high-shear drill mounted mixer (mechanical mixer). The highest speed possible should be used to break the mix components into individual particles.

Toumbakari in (E.-E. Toumbakari et al., 1999) studied the effect of two different mixing procedures. One with a mechanical mixer and another one with an ultrasonic mixer. Ultrasonic mixing improves dispersion, since the action of ultrasonic waves demonstrated that an ultrasonic treatment can easily disperse very fine particles substances. The same work shows that the reduction on the viscosity of the grouts was by approximately 50–60% thanks to the ultrasonic mixing procedure. In addition, the yield stress exhibited by the same grouts was more than four times reduced due to the ultrasonic mixing. This suggests that the mixing procedure has much influence on the rheological properties of the grout. Consequently, ultrasonic mixing procedure can provide better injectability results (especially when the solid phase of the grout has very fine particles) (E.-E. Toumbakari et al., 1999).

3.3 Grout requirements

The working properties are defined as properties of the material in the state in which it is applied, measuring its practical ease of use, while the performance characteristics of the material relate to its long-term behaviour within a masonry structure. The choice of a suitable grout for repairing old structures is not only dependent on the properties of set grout but also on those of fresh grout, which determine how effective it will be in situ.

Regarding the main properties of masonry injection grouts, specific standards are scarce and unclear. Thus, the existing standards related to the cement grout, mortar and concrete are used throughout the work, being adapted in some cases.

3.3.1 Working properties

The injectability capacity of the grout is an essential parameter for a successful intervention. As it is known, the injection in the interior of an old masonry is a challenging issue (Miltiadou-Fezans & Tassios, 2013b). There are several factors (associated with masonry) which may affect the grout injectability, namely: heterogeneity, presence of cracks, voids and discontinuities of different apertures, water absorption of the different masonry materials, etc.

In general the injectability of a grout is dependent on the intrinsic properties listed in Table 3.5.

Table 3.5 – Working properties

Desired working properties	Comments
Low viscosity / good fluidity	- If kept for a proper time, allows the diffusion of the grouts in the fissures and voids.
Good penetrability	- The maximum grain size of the mix, as well as the distribution of various grain sizes (grading curve of the solid phase of the grout) should be compatible with the "minimum width'' of the voids or fissures to be filled. - Fineness combined with the mixing procedure both contributed to the penetrability of grouts.
Good water retention	- It represents the ability of a grout to retain the mixing water during the injection inside dry and high absorptive masonries.
No bleeding / segregation of components (Stability)	- The grout needs to be stable to fill the voids locally and flow to the next void and fill the subsequent one. - Defined by segregation and bleeding and gives an indication of the homogeneity of the PM after injection.
Good workability	- Characterized by rheological parameter plastic viscosity, as well as the procedure of funnel flow time (Marsh cone test).

If these basic characteristics are not satisfied, the grout is not injectable at all, regardless any PM. The properties to measure are depending on a number of parameters and the available procedures refers to different methods, often not correlated one another (Kalagri, et al., 2010). Below the properties that influence the injectability result are detailed, as well as the experimental procedure used.

Fluidity

Vintzileou (Vintzileou, 2006) states that fluidity depends on the grain size, nature and shape of grains and the specific surface of the solid phase. Most studies measure the viscosity of the grout using a flow cone method. Based on the standard ASTM C939-02, the measurement of flow time is connected to the grout fluidity; the longer the flow time, the lower will be the grout fluidity. This test will be further detailed in chapter 5.2.4.1.

Penetrability

As referred by Miltiadou-Fezans (Miltiadou-Fezans & Tassios, 2013a) occasionally literature may not be sufficiently clear about the issue of penetrability; ''penetrability'' does not seem to be always distinguished from ''fluidity'' of the grout - a very important property which, however, may not be manifested at all if larger grains of the grout produce a blockage. Nevertheless, research work has been carried out on penetrability: some authors (Axelsson et al., 2009; Eklund & Stille, 2008; Miltiadou-Fezans & Tassios, 2013a) reiterate the importance of the ratio between the opening of the fissure and the maximum grains in the grout; and this was the approach followed in the present research (see Chapter 5 and Chapter 7).

Water retention

The water retention capability is an important property to be assured, since it represents the ability of a grout to retain the mixing water during the injection inside dry and high absorptive masonries. The ability to preserve water within grout suspension for the longest possible time will allow maintaining good rheological behaviour and grouting stability in order to ensure a successful injection. The measurement of water retention was performed in accordance with the ASTM C941-02 (see 5.2.4.2).

Rheological properties

Vintzileou (Vintzileou, 2006) states that the rheological requirements of the grout enable the grout to diffuse into the masonry. In fact, good rheological properties ensures a homogeneous filling of the cracks and voids in the masonry which provides a monolithic unit after hardening of the grout (Ignoul et al., 2004). The most important rheological parameters are the fluidity, characterized by the Bingham plastic viscosity and the yield stress. Other major issue on rheology of cementitious suspensions is the time dependent behaviour i.e. thixotropic behaviour; this means that in the case of cementitious suspensions the viscosity depends not only on the applied shear stress, but also on the time for which the suspension has been submitted to a shearing stress and on the shear history, which leads to the hysteretic behaviour. Hydraulic lime-based grouts can be seen as thixotropic materials, since they show a shear-thinning and time dependent behaviour as stated in other studies (Baltazar et al., 2013, 2012a; Bras et al., 2013b). During shearing of hydraulic lime grouts, the weak interparticle bonds are broken by the mechanical stress and the network among them breaks down into separate agglomerates (structural breakdown). In the case of a grout intervention if the injection stops, the grout is at rest and the particles will start to flocculate into agglomerates again (structural build-up), leading to a loss of workability (Bras, 2011; Wallevik, 2009); however, a strong shearing may erase the previous effect. These structural changes are dominant and reversible but only on short observation times, which also depend on grout environmental temperature, as will be checked in Chapter 5.

The results obtained by some authors (Baltazar et al., 2014, 2013; Bras et al., 2013b) show that thixotropy constitutes a critical parameter for the grout injection. The results demonstrated that care should be taken during the whole injection process, namely to avoid any stops during injection and to restrict the resting time between the mixing and the injection in order to prevent that flocculation may compromise the application and effectiveness of the grouting intervention. All these issues will be analysed in Chapter 5.

Stability

Grout mixes exhibiting appropriate penetrability and fluidity, should also be checked against their possible instability. Otherwise, blockage may soon appear and the quality of the intervention could be severely affected. In order to achieve a satisfactory injectability, stability of the suspension should be ensured (Miltiadou-Fezans & Tassios, 2013b). Stability is an issue of paramount importance in grout design, because it is a condition to achieve the same properties (porosity, strength, etc.) at every location (homogeneity) within the PM. There are two distinct phenomenona that may occur and disturb the homogeneity: bleeding and segregation.

Bleeding is the outcome of a layer of water at the top of the grout, which was not retained by the suspension. Segregation is the deposit of the heaviest grains from the solid phase at the bottom of the grout (Gil, 1994). These parameters give an indication of the homogeneity of the product. If these basic parameters are not satisfied, the grout is not injectable at all, regardless any masonry support typology (any PM). The chemical and physical properties of the grout solid phase and the presence and amount of any admixtures are important factors on the grout stability, since they influence the equilibrium of the interparticle forces present in the grout suspension after the mixing procedure. In this work, the influence of superplasticizer dosage is studied (see 5.3.1.3). The grout stability can be evaluated through several experimental procedures. They are shown in Chapter 5 and Chapter 7 .

3.3.2 Performance characteristics

The evaluation of the grouts is based on the parameters of the physical-chemical and mechanical compatibility according to the requirements listed in the Table 3.6. This table includes a list of performance properties and suggested criteria. In the literature is rare to find numerical values suggested for performance characteristics. As with working properties, the performance characteristics specified depend on the original materials. The general consensus on injection grouts for old masonries appears to be that the grout should be compatible with the original materials (Biçer-Simşir et al., 2009; Chaudhry, 2007). In fact, the grout needs to be adapted to the original material with regard to three aspects: chemical (including durability), mechanical/structural and physical compatibility (Van Gemert et al., 2015b). This issue is of utmost importance since grout injection is an irreversible technique. For this reason, some authors have studied this issue. For instance: Toumbakari (Toumbakari, 2002) argue that durability of the repair depends on the choice of the grout materials in order to ensure a compatible microstructure with masonry materials. Moreover, other authors (Biçer-Simşir et al., 2009; Miltiadou-Fezans, 1990) concluded that the mechanical strength of the grout should be similar to the original materials.

Regarding mechanical requirements, several authors (Eleni-Eva; Toumbakari et al., 1999; Uranjek & Bosiljkov, 2012) found that the compressive strength of grout injected walls was not directly proportional to the compressive strength of the grouts used for injection. In turn, as previously mentioned, an important parameter for the improvement of the behaviour of old masonry strengthened by grout injection is the bond achieved between grout and the in situ material. Good bonding is vital to the creation of a unified response of the structure to external aggressive agents (Chaudhry, 2007; Eleni-Eva; Toumbakari et al., 1999). Moreover, the bond strength is not necessarily proportional to the compressive or tensile strength of the grout. The bond mechanism between different stones and grouts was also studied by (Uranjek & Bosiljkov, 2012; Vintzileou & Adami, 2009), who performed shear tests, as well as direct tension tests. The results obtained showed the important influence of the substrate characteristics (i.e. the surface roughness, porosity, and initial water content) on the bond properties. All these factors will be studied in Chapter 5 and Chapter 6.

Table 3.6 – Performance characteristics

Desired Performance characteristics		Comments
Physical requirements	Low hydration heat	- High temperatures may adversely affect the bond with the substrate.
	Limited shrinkage	- One of the most important problems in repair is the shrinkage of the repair materials, which result in a poor bond (loss of adhesion) between grout with in situ materials (due to microcracking along the interfaces) (Luso & Lourenço, 2016). Shrinkage is more pronounced in dry environments. - Toumbakari *et al* (Eleni-Eva; Toumbakari et al., 1999) suggest that although autogenous shrinkage is unavoidable, relatively low shrinkage is necessary for a good bond.
	Adequate hardening time	- The setting time must be suited so as not to hinder the injection work in-situ.
	Hygroscopic properties	- Such as limited volume changes due to humidity variations, water insoluble grout, etc. -The expansion of the binder will produce unstable grouts.
	Compatible microstructure	- Compatibility of the grout and the original material.
Chemical requirements	Chemical stability	- Provide stability to chemical reactions between the grout and the in situ materials over time
	Resistance to expansion/ resistance to sulfates	- Resistance to sulphate salts, preventing subflorescence and expansive products, which increase the pressure inside, cracking the grout and eventually damaging the masonry (Binda & Anzani, 1997) - Minimum alkali content
Mechanical requirements	Moderate Compressive strength	Similar to the original materials.
	Young's modulus, modulus of elasticity	Similar to the original materials.
	Flexural strength	- Similar to the original materials. - Reasonable deformability.
	Good adhesion strength/ good shear strength	- Adhesion with the existing masonry components. - The support with high porosity show the highest results (Miltiadou-Fezans, 1990). Thus, the adhesion between grout and brick were much higher than between limestone and grout.

Chapter 4. Diagnosis of the masonry and control of grouting efficiency

4.1 Scope

The control of the effectiveness of a grout requires a previous assessment of the global masonry conditions, which is the basis to justify the grouting procedure. Frequently the design of the masonry is not known and the knowledge of the wall perspective is not enough information to know the inner content (Chaudhry, 2007). Inside the wall there might be cracks, voids and damages, which make it weaker. Two possible ways can be followed to reach this knowledge (Saisi et al., 1999):

(i) SEMI-destructive tests (e.g. Coring, flat-jack test, etc.)
(ii) Non-destructive tests (NDT), as thermography, sonic and radar tests.

Based on the information collected in these tests, it is possible to elaborate a grout repair design. Some elements such as the choice of the most adequate grout, the expected consumption and the operations costs can be evaluated.

After carrying out the grout operation, the global effectiveness must be checked. Destructive and/or non-destructive evaluation techniques should again be performed (Gil, 1994).

4.2 Destructive tests

Among the destructive techniques, coring is one of the most used. The coring enables furthermore to analyse the quality of the inner masonry by visual inspection of the cores (Van Rickstal, 2000). It enables the calculation of the mechanical properties (the measurement of tensile and compressive strength can be obtained respectively by splitting and compressive tests that can be performed on the cores), porosity and composition of the masonry. Eventually the core hole can also be inspected using an endoscope and qualitative information over the existing cracks and internal cavities can be obtained. However, the method has important limitations in practice. It only reveals a local condition. As masonry is a heterogeneous material, many cores must be collected to get representative results. Such procedure can be dangerous, since coring is an intensive job and especially because coring will damage the building. Thus, the numbers of cores must be minimized. A previous study using NDT (e.g. sonic tests) may be an option, since they produce visual charts that enable to identify the relevant areas where the destructive tests should be carried out (Gil, 1994).

The flat-jack test can be an alternative to coring test. As an advantage, it is slightly less destructive test than coring and enables the evaluation of the local in plane compressive state of masonry and its stress-strain relation. Nevertheless, as the coring test, it gives only local information and worse, in this case the information is only about the superficial layer of the wall.

Another destructive technique is offered by the resistographical method. A hole is drilled in the masonry and the force needed to advance is plotted versus the depth. Hard parts of solid and sound masonry need a high force to advance whereas soft and deteriorated parts only need a small force. This method causes less damage to the structure: only some small drilling holes, and provides a transverse scope of the inner masonry (Van Rickstal, 2000).

4.3 Non- destructive tests

A large proportion of existing old masonry buildings throughout the world represents cultural heritage assets. Taking into account that for cultural heritage buildings with artistic value the structural condition should be assessed with the minimal possible intervention, the application of NDT methods for both structural visualization and defect detection play an essential role (Hobbs, 1991). Several NDT methods have been proposed for structural investigation of building elements (Cotič et al., 2013). Contact methods, such as ground penetrating radar (GPR), ultrasonic, sonic and impact echo are especially promising in imaging the inner structure of buildings. On masonry, such methods have been applied for detection of the morphology, localization of voids, determination of the moisture distribution, detection of severe delamination, as well as to control the effectiveness of repair by injection techniques (Anzani et al., 2006; Cotič et al., 2013; Valluzzi et al., 2009). Using the same NDT, before and after grouting, the evaluation of grout effectiveness can be made by comparing the results of NDT.

In Table 4.1 four NDTs are compared, and the differences are described in relation to:

(i) The reliability and limitations of each technique to evaluate in situ the degree of mechanical and physical damage of existing masonries and the efficiency of their strengthening by grouting;

(ii) The different principles that each technique follows (each technique is affected by different parameters);

(iii) The frequency value of the signals (not applied to electrical resistivity). The fundamentals of wave propagation through solid materials allow recognising the limitations and the capabilities to recognise defects. In fact, the capabilities to recognise defects are related to the dominant wavelength of the incident wave and also to the size of the tested element. The wavelength- λ, is a function of velocity- v and frequency – f ($\lambda = v/f$) (Saisi et al., 1999). For a given velocity, as the frequency increases the wavelength decreases, providing the possibility for greater resolution. However, as frequency increases the rate of energy absorption also increases limiting the size of the wall section that can be investigated. The optimal frequency must be chosen considering attenuation and resolution requirements to obtain a reasonable combination of the two limiting parameters.

Table 4.1- Comparison between NDT techniques (Anzani et al., 2006; Chaudhry, 2007; Cotič et al., 2013; Valluzzi et al., 2009; Van Rickstal, 2000)

Test	- From measurements:	- Principle / Test procedure	- Drawbacks / limitations
Sonic test	-is a low cost method enabling a qualitative information about the masonry state (reveal/ locate states of damage in structural elements or portions of walls); -are suitable for detecting voids and cracks in walls of great thickness due to the strength of the signal; -are able to detect the variation of materials in the walls; -are a reliable technique to evaluate the effectiveness of grout injection (allows the control of the distribution of the grout in the masonry).	-origin of the emitted wave: stress waves; -the velocity of the sonic wave depends upon the state of the material (composition, presence of inhomogeneities, voids and deteriorated areas, etc.). The pulse will be transmitted through the material; -cracks and voids imply that the wave has to find another, longer way and this increases the transmission time, or that the wave has to pass the crack through a layer of air, which has a much lower transmission velocity than the surrounding material.	-the input frequency changes with the characteristics of the superficial material, e.g. the high frequency components can be filtered due to the wall structure or to the presence of a thick plaster or a partially detached plaster, etc. -the output signals can have a rather low frequency content. But in this case, sonic tests do not have the resolution requested to detect in detail the wall morphology or small voids. -to visualize the stone-mortar texture behind the plaster, poor localization and resolution is expected due to the near-field effects.
Ultrasonic test	-in comparison with the sonic waves, ultrasonic signals are much more sensible to surface conditions/small samples; the loss of energy (typical of a high frequency wave), leads to a rapid attenuation of the waves.	-the same principle of sonic test, but the frequency of waves is above 20kHz.	-the ultrasonic measurement is only suitable for limited transmission distances.
Electrical resistivity	-the values (electrical resistivity map) are a function of the masonry properties between the electrodes and probes. Thus, the real properties or anomalies of the structure can be estimated.	-it consists in measuring the electrical resistance (R) of the masonry, based on the equation of Ohm-Pouillet: V(volts)= R(ohm) x I (A); -the presence of cracks inside the masonry increases its electrical resistivity. The equipment test needs at least two electrodes and two probes. The electrodes introduce a current in the structure and the probes measure the potential difference between them.	-the humidity influences to a high extend the resistivity values. The more humid the masonry, the lower the resistivity. -the information on the internal state of structure (visualized in the electrical resistivity map) is partly masked due to the influence of the limited dimensions of the masonries (the influence of the boundaries should be eliminated).
Ground Penetrating radar (GPR)	-enables to judge the homogeneity of the structure; -in the case of strong interfaces between the layers can recognise the presence of leaves in a wall; -when sonic tests do not have the resolution requested (due to low frequency) to detect in detail the wall morphology, GPR can be an alternative option.	-origin of the emitted wave: electromagnetic (EM) waves; -GPR is based on the propagation and reflection of high frequency electromagnetic impulses produced by an antenna system, where reflections occur at the interfaces between materials with different dielectric properties (e.g. mortar and stone);	-the technique requires expensive equipment; -the presence of water attenuates the EM waves in order to reduce the maximum thickness of the wall that could be measured. Besides, this attenuation masks the relevant information;

Test (cont.)	- From measurements (cont.):	- Principle / Test procedure (cont.)	- Drawbacks / limitations (cont.)
Ground Penetrating radar (GPR) (Cont)		- use EM signals for the investigation of masonry structures providing 2D and 3D radargrams that show the construction morphology and the type of reinforcement.	-since are negatively influenced by the presence of moisture, Radar tests are not a reliable technique to evaluate the effectiveness of grout injection; -could be disturbed by the diffractions produced by large quantities of small scattering inhomogeneities (as in a rubble masonry); -the reflections may not appear at all the expected positions due to the surface roughness of the materials; -to visualize the stone-mortar texture behind the plaster, poor localization and resolution is expected due to the near-field effects.
IR thermography	-allows the detection of defects within a depth of approximately 10 cm, based on recording IR radiation from the previously heated specimen's surface; -IR thermography is capable of detecting crack patterns in the surface and subsurface of the plaster (through thermal contrasts).	-if masonry materials have different thermal conductivity, thermal contrast is observed in thermal image; -the detection of plaster delamination can be identified because the presence of an air gap slows down the cooling process, due to its lower thermal conductivity than the masonry materials.	-the visualisation of the masonry morphology and the type of connections is hard, due to the limited depth resolution of IR thermography; -the thermal images can be greatly affected on-site, due to non-uniform heating and the variation in plaster thickness. - When conducted outside, the external temperature has an undue influence on the results.

According to the information of other works (Table 4.1), IR thermography has difficulty in detecting cracks/voids within the masonry (in particular very thick walls) due to the limited depth resolution. On the other hand, in sonic, electrical resistivity and GPR tests, a poor localization/resolution of the voids close to the external surface is expected due to the near-field effects. As is well known, in the multi-leaf masonry walls, cracks together with voids may occur anywhere in the masonry structure. Thus, for a correct localization of defects, the fusion of images obtained by sonic tests/electrical resistivity/GPR and IR thermography should be used to increase the reliability of an NDT inspection on-site (Cotič et al., 2013).

As mentioned in Table 4.1, the main concept of ultrasonic and sonic techniques is the same, varying only the frequency which conditions the wave length change (as already explained above). Thus, in laboratory studies – as in the case of this thesis – ultrasonic tests are the most adequate; in real masonries sonic tests should be used. In fact, the choice of technique changes according to the dimensions and compactness of the analysed material. This issue will be detailed in Chapter 8 .

A tomographic image is a computational technique which utilizes an iterative method for processing a large quantity of stress wave transmission data (e.g. ultrasonic pulse velocity taken along many different ray paths). Standard pulse velocity data is used to determine the velocity distribution map within a solid material. Regarding the issue studied, this map represents a "picture" of the masonry

interior. According to several authors (Cotič et al., 2013; Da Porto et al., 2003; Riva et al., 1997; Schuller et al., 1994), the velocity distribution maps obtained by tomography have proven to be quite useful for indicating observable damage and also for indicating the quality (the effectiveness) of repairs in unreinforced masonry. In chapter 8.3.4 it is explained how a tomographic image can be obtained, while in chapter 8.4.5 the obtained tomographs are presented and their usefulness is explained.

Chapter 5. Influence of superplasticizer, temperature, resting time and injection pressure on hydraulic lime grout injectability

5.1 Introduction

The behaviour of a wall after grout injection is significantly influenced by the efficacy of grout injection (Uranjek & Bosiljkov, 2012). For a successful injection it is necessary to ensure an adequate grout flow inside the masonry. This means that it is essential to ensure good fresh properties, such as good rheological behaviour, water retention and stability to allow a good injectability and also to regulate the consolidation quality. Thus, the grout design must take into account all these factors. One of the key points in grout design is the use of dispersant admixtures. The SP is a well-known dispersant admixture whose function is based on repulsive forces (see 3.2.2 and 5.2.1.2). Through SP action, an improvement of fresh grout parameters is expected by increasing the fluidity, water retention and stability (Baltazar et al., 2012a). However, it is well known that fresh grout behaviour of cementitious pastes with SP depends on type and dosage (Baltazar et al., 2013). So this issue will be further detailed, as well as the influence of SP action on hydraulic-lime grout injectability.

According to other studies (Baltazar et al., 2013; Bras et al., 2013b) hydraulic lime-based grouts show a shear-thinning and time dependent behaviour - thixotropic materials. So, the grout viscosity depends not only on the applied shear stress, but also on the time for which the suspension has been submitted to a shearing stress. If the injection is stopped during an intervention, the grout is at rest and the particles will start to flocculate into agglomerates (structural build-up), leading to a loss of workability (Wallevik, 2009). Besides the resting time, the workability loss also depends on grout temperature. Indeed, different environmental conditions lead to different grout microstructure and consequently different injection performances. Thus, it can be stated that temperature and resting time could be crucial parameters in the quality of a grouting intervention. Regarding hydraulic lime grouts limited data are available about the combined effect of temperature, resting time and grout composition on fresh grout performance. For this reason in this chapter is analysed the influence of temperature, resting time and grout composition on the rheological properties, such as yield stress and Bingham plastic viscosity. In addition, the flocculation area that is directly related to the bonds between the binder particles (agglomerates) was also evaluated.

According to some authors (Bras & Henriques, 2012; Miltiadou-Fezans & Tassios, 2013b; Valluzzi, 2005), the grout injectability is a key parameter for a successful intervention, since the injection of the interior of masonry is a challenging matter due to different reasons (see 2.2 and 3.3.1). Thus, in the last stage of this chapter, some injection tests were performed to study the injectability of the studied grouts. The injection setup is similar to that used by other authors in their grout injection tests (Binda et al., 2003a; Bras & Henriques, 2012; Valluzzi, 2005; Van Rickstal et al., 2003). Reduced models were used in order to simulate certain channels/ paths that may exist in the inner core of a multi-leaf stone masonry – porous media (PM). Nevertheless, comparing to literature the outputs achieved are different. In this chapter, the injectability of the grout was analysed based on two equations. One based on the equation of (Bras & Henriques, 2012) that takes into account the time and injection height – injectability rate of the grout. Another created in this work that expresses the percentage of voids that is filled after grout injection. Different grout injectability results were obtained for the various compositions studied and different conditions tested (environmental temperature, resting time and injection pressure). Moreover, these results were compared and correlated with the properties of the

fresh grouts. This goal is particularly relevant due to the absence of information about the real influence of fresh grout properties on the performance of grout injection.

Regarding the grout injectability, the standardized sand column test method (NF P18-891, EN 1771) was applied to evaluate the penetrability, fluidity and stability characteristics of the grout suspensions. Such test was also used in other works (Kalagri et al., 2010; Miltiadou-Fezans & Tassios, 2013a; Oktay et al., 2015). The results from this injection model are compared with the results of the injection model mentioned above. In addition, some considerations about the model that best simulate the injection of a grout in the inner core a multi-leaf masonry are made.

Thus, in summary, this chapter is composed mainly of three phases (graphically demonstrated in Fig. 5.1):

(1) A study of the influence of SP dosage in some fresh grout properties, namely: fluidity, water retention and stability.

(2) Evaluation of the combined effect of temperature and resting time on the grout rheological properties (yield stress and plastic viscosity) and thixotropy (flocculation area), studied through rheometric measurements in order to allow a better understanding of the flow behaviour of HL-based grouts under different environmental temperatures and resting times.

(3) Injection tests performed on reduced models to analyse and correlate the grout injectabilities with the values of fresh grout properties previously studied in the previous phases.

According to Miltiadou and Tassios (Miltiadou-Fezans & Tassios, 2013a, 2013b, 2012) the grout design methodology should be based on the study of grout injectability characteristics: penetrability, fluidity and stability. This research gives continuity to the papers (Baltazar et al., 2014, 2012b) where the influence of mixing procedure and grout composition on the grout injectability were studied. In this chapter the influence of SP dosage, temperature, resting time and injection pressure on the grout injectability was studied through the analysis of the injectability characteristics mentioned above.

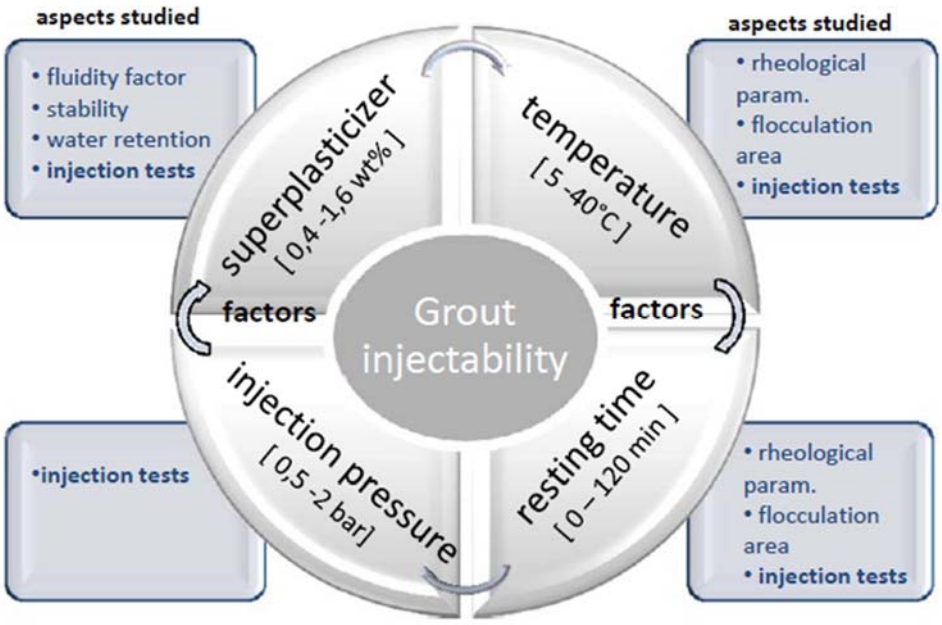

Fig. 5.1 - Factors that influence the grout injectability

5.2 Experimental details

5.2.1 Materials

In this section it will be presented a general description of the materials used for grout composition. As far as the grout performance is concerned there is an important relation between the grouts design variables and its fresh properties. Concerning the grout design, there are two categories of components that must be addressed during grout design, namely basic components (binders and water) and admixtures / additions. The selection of materials depends on a range of factors, including the desired working properties and performance characteristics (see 3.3). Hence, the following topics focus on the materials used in this work and the reasons for their choice.

5.2.1.1 Basic components

- **Hydraulic lime**

As previously mentioned (3.2.1 and 3.3.2), one of the main criteria for the choice of the binder in the assessment and study of the grout composition is the evaluation of potential incompatibility problems with the materials from the original walls, which may jeopardize the performance of whole consolidation process. Thus, the binder chosen was the hydraulic-lime. Comparatively with grouts based on pure cement or organic resins, hydraulic lime provides potentially more compatible grouts with the original materials presented in historic masonries – which was the objective of the study (Valluzzi, 2005; Van Rickstal, 2000).

Regarding the mechanical behaviour, hydraulic lime is an intermediate product between the hydrated lime and cement, since the hardening process involves both the carbonation of the free lime (as pure lime) and the hydration of the calcium silicates and aluminates. In fact, such as cement, hydraulic lime is able to set by chemical reactions (hydration reactions) with water. Thus, hydraulic lime tends to give an acceptable early strength (in contrast with the hydrated lime) and at the same time the wanted ductility is not lost.

The mechanical resistance (and other properties) of hydraulic limes depend on their chemical composition, the manner in which they have been burned, and on the manner they have been slaked or hydrated (Reichel et al., 2005). The composition of hydraulic limestone includes the amount and types of inorganic impurities which give the hydraulic lime its hydraulicity. These impurities include silica, alumina, and ferric oxide (Table 5.2). Depending of the composition, the setting process of the hydraulic lime can be similar to Portland cement. Thus, in order to avoid incompatibility problems, it is essential to know this information when hydraulic lime is being used in injection works where the PM are old masonry walls.

Hence, and based on above, the hydraulic lime was chosen as binder to be used in this research. The hydraulic lime used is a EN459-1:2010 labelled as HL5 and produced in Portugal by Secil-Martingança, which has the characteristics presented in Table 5.1 and Table 5.2, according to the information of the quality control system provided by the manufacturer.

Table 5.1 – Hydraulic lime characteristics [a]

Compression strength at 7 days (MPa)	*>2.0*
Fineness	
	90 µm 15.0%
	200µm 2.0%
Setting Time	
	Start >1h
	End <15h
Expansibility	<2.0mm
Free lime	3.89%
Ignition loss	19.84%
Density	2.85 g/cm^3
Fineness (Blaine)	9400 cm^2/g

[a] As stated in the technical data sheet from the supplier

Table 5.2 - Chemical characterization of HL5 according to XRF results

Compound Name	*Hydraulic lime (%)*
MgO	0,99
Al_2O_3	2,96
SiO_2	10,86
SO_3	1,97
K_2O	0,89
CaO	78,77
TiO_2	0,30
MnO	0,04
Fe_2O_3	2,96
SrO	0,06
Na_2O	0,26
SiC	-

The grain size distribution of HL5 is represented in Fig. 5.2.

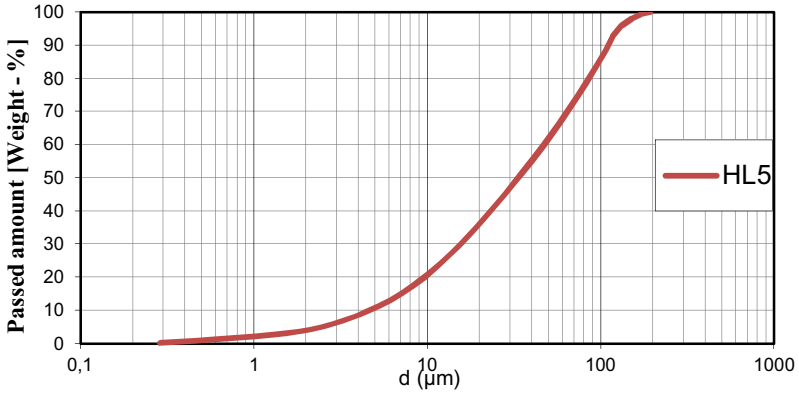

Fig. 5.2 - Grain size distribution of HL5 used in the injection tests

- **Water**

Water is the element which assures fluidity of the grout and enables the hydration of the cementitious components. The determination of the w/b is an important procedure. Water presence improves the rheological behaviour of the mixture, but a too high ratio decreases the mechanical properties and might cause instability of the grout (Baltazar et al., 2012a, 2012b; Mirza et al., 2002b).

There are three types of water in grout. The first is the free water that is responsible for the fluidity and it is the first to migrate by evaporation. The adsorbed water is attached to the surface of the solid phase, reducing its surface energy. The last, the combined water is present on the composition of the hydrated components of the hydraulic binders (Gil, 1994).

5.2.1.2 Admixtures – Superplasticizer

The use of dispersant admixtures is one of the key points in the grout design. The SP is a well-known dispersant admixture whose function is based on repulsive forces. This repulsion action increases the average inter-particle distance and therefore decreases the magnitude of the attractive van der Waal forces, and hence, particle flocculation is reduced or even prevented (Vikan, 2005). Thus, through SP action an improvement of rheological parameters is expected, by reducing both plastic viscosity and yield stress (Baltazar et al., 2012a). However, it is well known that rheological behaviour of grout suspension with SP depends on type and dosage (Baltazar et al., 2013). This issue will be further detailed in this chapter.

The SP chosen was the polycarboxilate (Glenium SKY 617) produced by BASF, which characteristics, according to the information provided by the manufacturer, are listed in Table 5.3.

Table 5.3 - Characteristic of SP

Function	*High range water reducing*
Commercial name	Glenium Sky 617
Structure of the Material	Polycarboxylate
Colour	Brown
Densiity (g/cm^3)	1.05
pH	8
Charge	Anionic
Chloride Content (%)	<0.10
Recommended dosage rate (wt%)	03-0.9

The polycarboxilate belong to the last generation of superplasticizers whose repulsion is a combination of coupled steric and electrostatic effects, known as electrosteric repulsion. Thus, the repulsion action results from two forms: electrostatic repulsion obtained from ionization of the binder particles with identical charges and solid particle repulsion predominantly through steric forces (Artelt & Garcia, 2008; Vikan, 2005). The steric repulsion protects binder particles from flocculation, this repulsion arising from the long side chain polymer which hold the particles far enough so that they cannot join themselves (Fig. 5.3).

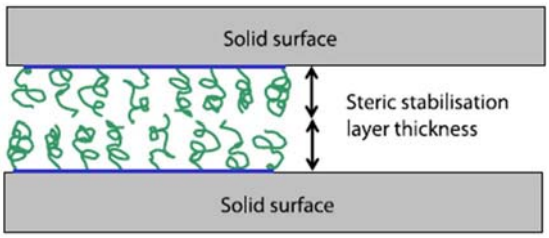

Fig. 5.3 – Repulsion of adsorbed SP disperses the binder particles (Banfill, 2011)

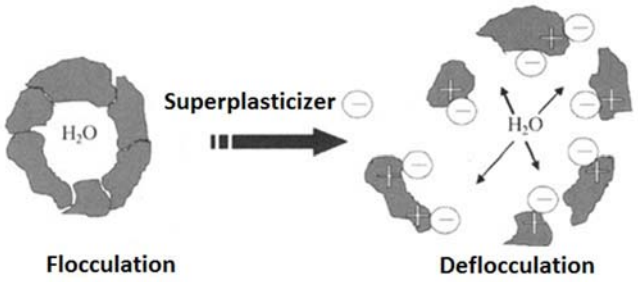

Fig. 5.4 - Superplasticizer effect on flocculation of the binder particles (adapted from (Bjornstrom & Chandra, 2003)

5.2.2 Mixing procedure

The hydraulic lime mixes were prepared at a room temperature of 20 ±2 ºC and a relative humidity of 55 ±5 %. For the preparation of grouts water and hydraulic lime at the temperatures of 5, 20, 30 and 40 ºC were used, and the dry binder was hand-mixed to ensure a homogeneous distribution before the beginning of the mechanic mixing. The mixing procedure adopted was based on the work (Baltazar et al., 2012b). It is divided in three phases. In the first phase, 100% of the binder is added to 70% of total mix water and mixed during 10 min. The remaining water (with diluted SP) is added within 30 s (without stopping the mixer, speed=2400 rpm) - second phase. According to several authors (Aiad, 2003; Bjornstrom & Chandra, 2003; Fernàndez-Altable & Casanova, 2006), the delay of 10 min on the SP addition improves the effectiveness of the dispersing particles. In the last phase, after all materials had been added, the mixing was maintained for 3 min at 2400 rpm. Regarding the mechanical mixing, as concluded by Toumbakari *et al.* (E.-E. Toumbakari et al., 1999), a high turbulence is required in order to obtain an adequate deflocculation of hydraulic lime. In fact, low mixing turbulence leads to a mixture with large flocculates since the low mixing speed is not capable of deflocculating all the formed flocs comparatively with grouts obtained with high (2400rpm) mixing speeds.
The mixer cup had a capacity of 5 litres, with 177 mm diameter and a height of 244 mm. The blade used had a helicoidal shape (as shown in Fig. 5.5) and the gap at the bottom between the blade and the cup was 4 mm ± 1 mm. Each grout sample passed through a 1.18 mm sieve (n. 16 ASTM) before the tests (fresh grout tests and injection tests). As mentioned by certain authors (Eklund & Stille, 2008; Van Rickstal et al., 2003), the granularity of the binder should be fine enough. Thereby, it has to be mentioned that an appropriate mixing procedure should separate flocculated grains since they act as big grains.

Fig. 5.5 - The mixer blade used in experimental work

5.2.3 Fresh grout tests

With the aim to maximize the penetration and diffusion of grout in the PM (i.e., to maximize the injectability of grout), the study of some fresh grout properties is required. According to some authors (Miltiadou-Fezans & Tassios, 2013a; E.-E. Toumbakari et al., 1999; Valluzzi, 2005), the fluidity, water retention and stability have a significant role in the success of the grout injection. If they are not verified, the grout will hardly be injectable regardless of PM (Kalagri et al., 2010; Miltiadou-Fezans &

Tassios, 2012). Based on certain test procedures, it was assessed the fluidity, water retention and stability.

5.2.3.1 Fluidity measurements

This behaviour can be explained as the tests are meant to assess different features of fluidity. Thus, the cone method evaluates the grout viscosity; the spread method reflects the yield strength.

Marsh cone test

Grouts require different flow characteristics depending on the application; therefore it is not surprising that one of the most discussed properties is fluidity or workability. In the literature, it is generally measured by various types of flow cone, of which the Marsh cone (Fig. 5.6) is the most frequently mentioned method (Assaad & Daou, 2014; Baltazar et al., 2014; Biçer-Simşir et al., 2009; Mirza et al., 2002b; Roy & Roussel, 2004; Sonebi et al., 2013). According to ASTM C939-02 the measurement of flow time is linked to the grout fluidity, meaning that the longer the flow time, the lower is the grout fluidity. This test enables a grout design regarding several factors, like SP dosage for instance (Baltazar et al., 2012a). However, some authors, e.g. Bras (Bras, 2011), concluded that the Marsh cone is inadequate for grout design in those cases were fine materials are to be injected (< 4mm), as is the case of the PM studied in this work, since the measurement of flow time with a Marsh cone with Ø=10mm seems insufficiently sensitive. Le Roy and Roussel (Roy & Roussel, 2004) observed that the error obtained with a nozzle diameter of 10 mm is 10 times higher than a nozzle diameter of 6 mm. Other researchers (Roussel et al., 2005) conclude that flow time is not meaningful from the rheological point of view when the flow is not laminar, something that is most likely to occur for higher diameters.

In order to improve the physical significance of Marsh-cone test, Miltiadou-Fezans (Miltiadou-Fezans & Tassios, 2012) creates the fluidity factor test (FFT). This test has some changes relative to standard ASTM C939-02, namely the lower nozzle-diameter of Marsh cone (only 3 mm). Moreover, the flow time is measured for a flow with only Q =100cm^3 instead of conventional 1000/1200 cm^3 used in different works (Assaad & Daou, 2014; Biçer-Simşir et al., 2009; Bras, 2011; Roy & Roussel, 2004; Sonebi et al., 2013). The authors argue that in this way the fluid pressure acting on the nozzle is practically kept constant during the test. In fact, according to the Nehdi results (Nehdi et al., 1997), the pressure gradient on the nozzle (which is the "engine" of the flow in the cylindrical part) decreases as the fluid level in the conical part decreases. The author observed that the pressure gradient variations at the beginning of the test are small (small variations of the fluid height in conical part) and become higher at the end of the test when the phenomenon accelerates. This leads to a constant debit during the first part of the experiment which decreases at the end of the total time needed to empty the cone. Moreover, given the small variation of the fluid height, the influence of the roughness of cone's walls is minimized.

The concept of a fluidity factor F_l is obtained by the equation:

$$F_l = \frac{Q}{A \times t_f} \tag{5.1}$$

where A is the area of the cross section of the nozzle and t_f the flow time. Based on the equation it is possible to state that "more fluid grouts are characterized by higher F_l values, i.e., higher velocities of flow" (Miltiadou-Fezans & Tassios, 2012).

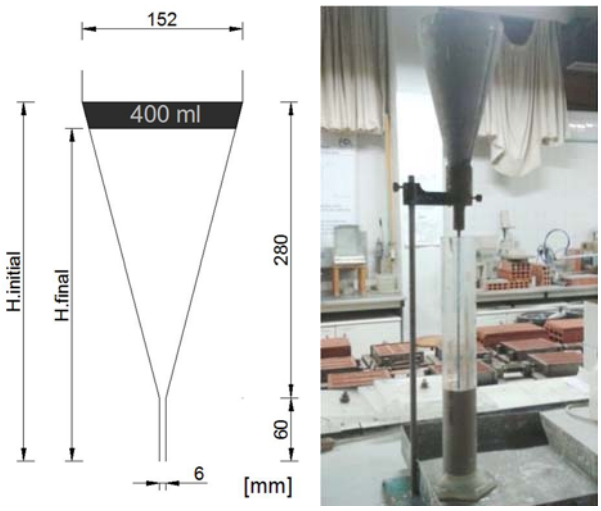

Fig. 5.6 – (a) Marsh cone size; (b) Marsh cone test

In the case of this work, the fluidity was evaluated using a modified Marsh cone having an outlet diameter of 6 mm. And the fluidity factor was measured for a flow with Q =400 cm^3 (100cm^3 revealed to be a low volume to perform this test), which does not induce a high variation of the fluid height inside the cone during the test (Fig. 5.6-a). This volume of grout was placed in the cone through a sieve, which prevented large particles blocking the outlet. It should be referred that before each test, the internal surface of the cone was wetted.

The fluidity factor was measured at three different stages: just after the mixing process (0 min), and after mixing grout for 30 and 60 minutes under the same conditions.

Given the configuration of the Marsh cone used and the volume chosen, the fluidity factor of water is equal to 2744 m/s. The environmental conditions of the laboratory were characterized by 55 ±5% relative humidity and a temperature of 20±2 °C. The Marsh cone test was made for different resting time values: 0, 30 and 60 min after grout preparation.

Mini-slump test

In accordance with the NP EN 445-2008 the mini-slump test is used to determine the fluidity/ workability of fresh grout. This test is based on the measurement of the spread diameter of grout placed into a cylindrical mould. The mini-slump cylinder has a diameter of 39 mm and a height of 60 mm (Fig. 5.7-a). The cylinder is placed in the centre of the horizontal base plate. After pouring the grout into the cylinder without overflow, the upper part of the cylinder was tamped lightly to bleed off any air pockets, and the entire cylinder was gently lifted (Assaad & Daou, 2014; Sonebi et al., 2013). Then, the diameter of the grout after spreading on a horizontal base plate was measured (Fig. 5.7-b). The spread diameter resulted of the average of four diameters, instead of two referred in the standard. Thus, it is achieved a higher accuracy in final result of spread diameter.

According to some authors (Biçer-Simşir et al., 2009; Domone, 1998), the shape and the size of the spread at the stoppage are directly related to the yield stress, since during the test the flow of grout stops when the shear stresses in the sample become smaller than the yield stress. Therefore, the spread diameter can be a relevant parameter for estimating the material yield stress.

Fig. 5.7 - Procedure of mini-slump test. (left) mini-slump cylinder; (right) spreading of the grout after the cylinder to be lifted

5.2.3.2 Water retention test

The water retention is another important property to maximize the injectability of grout, since it represents the ability of a grout to retain the mixing water during the injection inside dry and high absorptive masonries. The ability to preserve water within grout suspensions for the longest possible time will allow the maintenance of good rheological behaviour stability, which are requirements for a successful injection (Assaad & Daou, 2014). The measurement of water retention was performed in accordance with ASTM C941-02. This test determines the time required to remove a certain amount of water from the grout sample. A depression of 5.0 ± 0.2 kPa (controlled by digital manometer) was applied to a Bruckner funnel containing 500 ml of the grout, while a graduated cylinder collected the removed water (Fig. 5.8). The standard recommends that the test ends when 60 ml of water was removed, but only 45 ml were considered since some grouts were unable to lose 60 ml of water. One of the reasons for the difficulty to remove 60 ml of water from the grout it is due to segregation that increases with time because the mixture particles settle to the bottom of funnel preventing the removal of water.

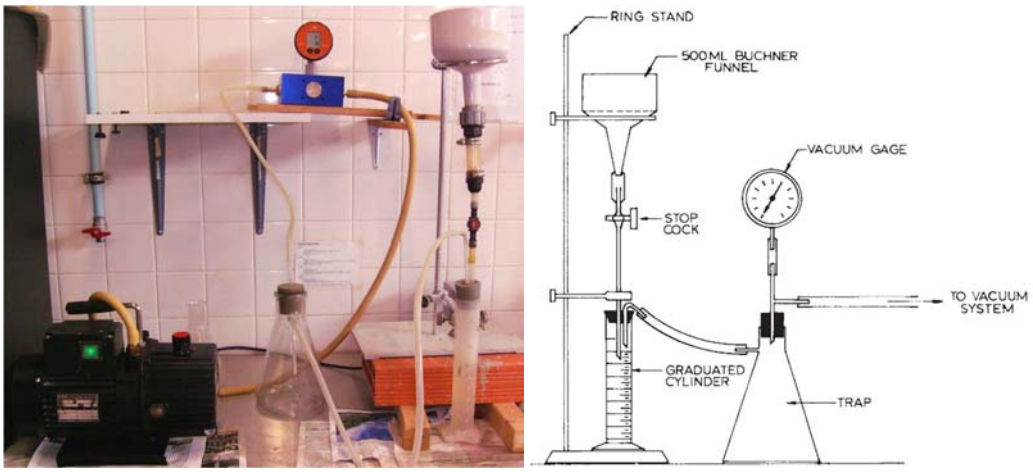

Fig. 5.8 – Device adopted for measurement of the water retention (ASTM C941-02)

5.2.3.3 Stability test

The instability phenomenon like segregation and bleeding causes lower homogeneity in the grout during injection. Thus, an unstable grout the binder particles will sink in injected masonry, the flow slows down causing obstruction of the injection channel and blocks further injection; these effects results in injected zones with a higher binder concentration and others with weaker concentration. In the worse scenario the grout flows away and leaves some empty zones without any binder (Van Rickstal, 2000). Thus, the grout stability is essential to obtain a good injectability (Valluzzi, 2005).
In the present work, grout stability was analysed measuring density variations of the upper zone of a grout volume in rest inside a recipient, a procedure developed by Van Rickstal (Van Rickstal, 2000). The grout samples were placed in a 500 ml cup and a spherical object with a volume of 4.85 cm^3 and a mass of 34.29 g suspended from the balance was immersed into the grout sample (Fig. 5.9). The sphere undergoes buoyancy according to Archimedes' law. This force varies with grout density which changes when instability leads to the deposition of particles at the bottom of cup causing a decrease of density on the top layers. So, during the test the mass variation was recorded with time. The analysis of the results was done in terms of percentages of initial density (for each mass value recorded) throughout the time test. A small variation of mass represents a low variation of grout density, consequently meaning reduced segregation and bleeding. The environmental conditions of the laboratory were characterized by 55±5% relative humidity and a temperature of 20 ± 2 °C.

Fig. 5.9 – Stability test. (a) Equipment used in the experimental work. (b) Sphere hanging over the grout sample

5.2.3.4 Grout rheological test

Test procedure

To study the temperature and resting time effects on grout rheological properties a Bohlin Gemin HR^{nano} rotational rheometer, equipped with a plate–plate geometry (with Ø = 40 mm) and a gap of 2 mm was used. The grout samples were analysed 10 min after the end of the mixing process. In all measurements the rheological protocol adopted was the following: a pre-shearing stage of 60s at a shear rate of $1s^{-1}$ followed by 60s at rest was applied. The pre-shearing was applied in order to homogenize the sample and therefore ensure a similar initial state for all samples. Then, the shear rate was increased from 0 to 300 s^{-1} and an analogous decreasing from 300 s^{-1} to rest was applied. This range of shear rate was chosen based on the range which is of interest to injection grouts. Each shear rate was applied long enough (i.e. 6 s for shear rates up to 4 s^{-1} and 2 s for shear rates over than 4 s^{-1})

in order to ensure the attendance of the steady state, before measurements took place. A solvent trap was used to prevent drying of the grout samples during testing. The effect of temperature on rheological properties was studied over a range of 5 to 40ºC. Thus, a fridge and a climatic chamber were used to maintain the temperature of the materials, as well as the mixing equipment at the desired levels. However, the mixing was made at room temperature for practical reasons. All rheological measurements were performed at the desired temperature which was maintained by means of the rheometer temperature unit control. The procedure enabled the determination of the yield stress, plastic viscosity and flocculation area. They will be addressed below.

Grout rheological parameters

The rheological behaviour of fresh hydraulic lime grouts is similar to other cementitious materials with a shear-thinning behaviour (Bras et al., 2010); this behaviour can be explained by the increasing of shear rate that causes a dispersion of the particles flocs leading to viscosity decrease (Phan et al., 2006). Moreover, Roussel (Roussel et al., 2010) stated that the flow behaviour also depends on solid volume fraction, hydration process and chemical factors as action of admixtures.

Hydraulic lime grouts can be seen as a viscoplastic fluid, showing a plastic response until the yield stress is reached and viscous behaviour for higher stress levels. Depending on their mix-proportioning and the considered range of shear rates, the grout may display Newtonian (i.e. constant apparent viscosity) or shear-thinning (i.e. decreasing apparent viscosity with shear rate). For low shear rates, the grout behaves linearly and may be described by Bingham equation. In this way, the Bingham model (Eq. 5.2) can be used to fit the experimental data in order to estimate the Bingham plastic viscosity and yield stress (Baltazar et al., 2013; E.-E. Toumbakari et al., 1999):

$$\tau = \tau_0 + \eta_p \times \dot{\gamma} \tag{5.2}$$

where τ is the shear stress (Pa), τ_0 is the yield stress (Pa), η_p is the plastic viscosity (Pa.s) and $\dot{\gamma}$ is the shear rate.

Since a smaller yield stress and plastic viscosity means an easier injection process, they can be used as control factors to know if a grout is suitable to be injected. In relation to yield stress, in terms of injection process, it is associated to the minimum stress that is necessary to apply for the suspension to start flowing. In other words, as concluded by Roussel (Roussel et al., 2010), yield stress corresponds to the energy that has to be applied to the system in order to break a network of interaction between particles. It originates from colloidal and contact interactions between particles and depends on the volume fraction and nature of the solid (binder) particles. It is also affected by the presence of SP. On the other hand, Bingham plastic viscosity represents the flow resistance once flow is initiated. Taking into account the grout injectability performance, the level of colloidal interactions between suspension particles should be low in order to obtain a low flow resistance and hence the grout flows easily.

To give response to the aforementioned issues the influence of different temperatures and resting times on the rheological behaviour of grouts was studied.

Thixotropic behaviour

Wallevik concluded that the thixotropic behaviour of cement paste is related to microstructure changes (i.e. flocculation, dispersion and re-flocculation of the binder particles) and the time needed for such changes to take place (Wallevik, 2009). The flocculation depends on the various interactions that arise between the particles of grout suspension. According to Roussel (Roussel et al., 2010), for a cementitious paste, surface forces (or colloidal interactions), Brownian forces, hydrodynamic forces or various contact forces between particles interplay. In function of the size of the particles in the suspension, one or several of these interactions can dominate. Wallevik in (Wallevik, 2005) proposed that there are basically two kinds of flocculation (phenomenon also known as coagulation). The first type is the reversible flocculation, where two flocculated binder particles can be separated (i.e. dispersed) again, i.e., some external forces bring the suspension back to a previous structural state. These reversible changes often dominant in short observation times, correspond to thixotropy (Roussel et al., 2010). Other changes, in particular consequences of the hydration phenomenon, are irreversible. From that arises the second type of flocculation (called permanent flocculation) where two binder particles can no longer be separated. This leads to what is often described as "workability loss".

In this work, the coupled effect of temperature and resting time on the thixotropic behaviour of the grout is studied. Based on the experimental procedure developed by Bras *et al.* (Bras et al., 2013a) (already described above) it was possible to calculate the flocculation area (which is related to the grout workability loss during its hydration) for the grouts tested at different temperatures (from 5 to 40 ºC) and different resting times (from 0 to 120min). The flocculation and deflocculation areas have the dimension of energy related to the volume of the sample sheared (Eq. 5.3).

$$A = \mathrm{P}a.s^{-1} = \frac{N.m}{s}.\frac{1}{m^3} = \frac{energy}{volume} \tag{5.3}$$

For flocculation phenomena the area A of the flow curve in the range 300 s^{-1} – 0 s^{-1} (step down test) indicates the energy that is required to build-up the grout microstructure. On the other hand, de-flocculation values are related to the energy that is required to break down the microstructure (Bras et al., 2013a). The value of flocculation area is the area below the flow curve. This area is calculated by integration of the polynomial expression of the flow curve in a graph shear stress vs. shear rate.
The flocculation tendency is mainly important when the flow tends to stop which enables an increase of the particle flocculation phenomenon. Thus, a lower flocculation area is always desirable.

5.2.4 Injection tests

To analyse the influence of temperature, resting time and injection pressure on grout injection some injectability tests were conducted. Since it is hard to reproduce a real masonry and it is difficult to visualize what is happening inside the PM being injected, simplified models were created to improve the knowledge about the physical mechanisms that take place during injection and that determine the penetration of the grout in the masonry. Similar models were used in previous publications (Bras & Henriques, 2012; Kalagri et al., 2010), which try to simulate the inner core of a multi-leaf stone masonry. The reduced models allowed quantifying the grout injectability at two different resting times

(0 and 60 min) and four different temperatures (5, 20, 30 and 40 ºC). The models (Fig. 5.10) were prepared using transparent Plexiglas cylinders – diameter 144 mm and height 300 mm – as in ASTM C943.

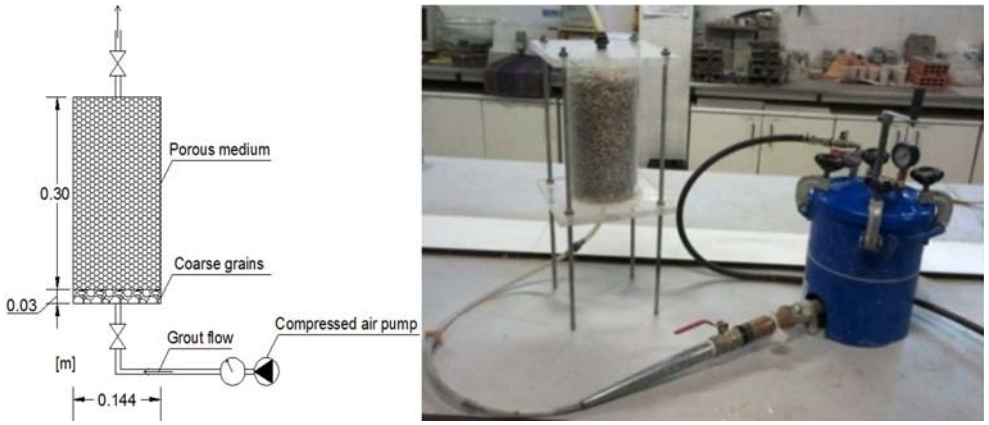

Fig. 5.10 - Setup for injection tests used in lab

Theses cylinders were filled with a PM consisting of a mix of fine and coarser siliceous sand, trying to reproduce as much as possible the voids size distribution and permeability of the inner core of a masonry wall. Following the assumptions of Van Rickstal (Van Rickstal, 2000), the cylinders were filled in three layers (10 cm per layer). At each fraction, they were densified by vibrating the cylinder. At the bottom of the cylinder, a distributing layer of coarse grains ensures a good distribution of the grout. For injection purposes a device based on previous works (Binda et al., 2003a; Bras & Henriques, 2012; Valluzzi, 2005) was used (Fig. 5.10).

In this chapter, the gradation of PM was chosen based on the research conducted in Chapter 7. Thus, the PM results from the combination of four different sizes of sands (40% course, 40% medium, 15% fine and 5% very fine) (Fig. 5.11 and Fig. 5.12). Table 5.4 shows some parameters to characterise the PM that are described in detail in 7.3.2. All parameters (except PM porosity) are obtained from grain size distribution curves shown in Fig. 5.12.

Table 5.4 - Porous medium characteristics

	Porous medium chosen
d(90) [mm]	8.27
d(15) [mm]	1.30
W_{nom} [mm]	0.195
P.M. porosity [%]	42.7
Specific Surface (mm^2/mm^3)	2.14

* the diameter through which 90% of the total mass passes
** the diameter through which 15% of the total mass passes
*** $W_{nom} \sim 0.15 \times D_{15}$ (see 5.2.7)

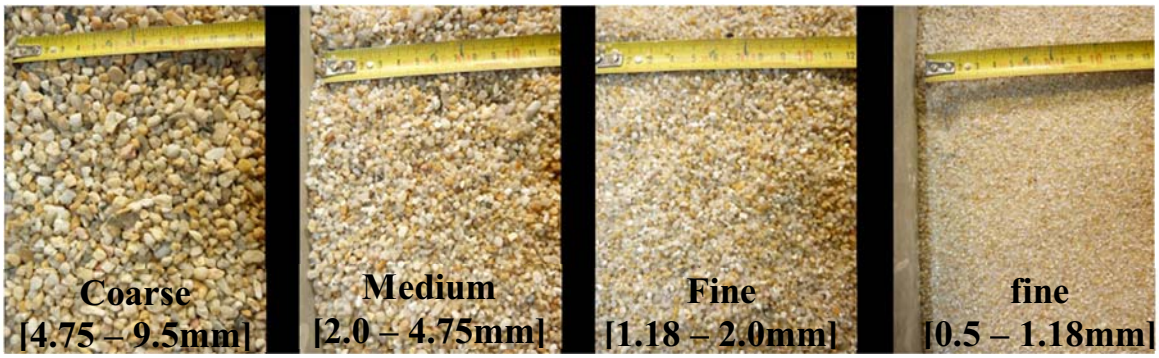

Fig. 5.11 - Four different grain size ranges (coarse, medium, Fine, fine)

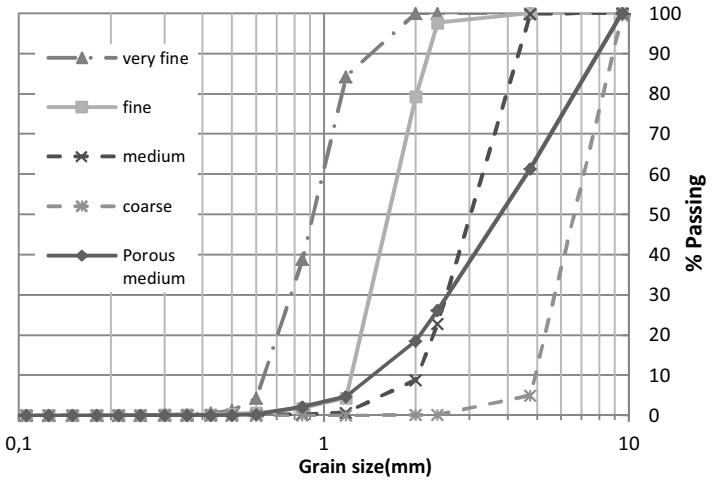

Fig. 5.12 – Grading curve of the PM and of each different sand

The reduced models (Fig. 5.10) were injected at constant pressure of 0.5, 1 and 2 bar, with the grout being injected from bottom to top based on the procedure developed in (Bras & Henriques, 2012; Valluzzi, 2005). The PM and all raw materials were pre-stored at the targeted test temperature before injection. Thus, during the injection, the targeted temperature is reached by the fresh grouts as well as the PM.

The penetration of the grout into the PM is directly dependent on the injection pressure, which influences the pressure at the inlet of the injection holes. For higher injection pressures, the grout can penetrate in finer voids. In addition, the grout will pass easier and faster into the PM. Thus, the amount of water (of the grout suspension) absorbed by the particles of PM is lower and therefore the particles remain better in suspension. However, as already addressed in 3.1.2.4, the pressure is restricted to a few bars in order to avoid any structural damage caused by the internal pressure within the masonry. The injection pressure values for masonry found in literature range between 0.2 – 2 bar (Binda et al., 1997; Bras & Henriques, 2012; Valluzzi, 2005; Van Rickstal, 2000). Thus, in this work the injection pressures used were: 0.5, 1 and 2 bar.

5.2.5 Injection capacity of the grout

According to Kalagri (Kalagri et al., 2010), the injectability capacity of the grout constitutes a key parameter for a successful intervention. Thus, in present work the goal was to get the injection capacity of the grout as a function of the PM. Each PM can be characterized by porosity, grain size

distribution and voids size average (Table 5.4). In the absence of a formal quantitative definition for injectability, Bras and Henriques (Bras & Henriques, 2012)created an equation – Eq.5.4 to quantify the injectability of the grout, taking into account the height of injection - h_{inj} and the time of injection - injectability rate of the grout. In the present work, this equation was slight altered in order to achieve more accurate injectability results, since the accuracy of measurement of h_{inj} within a cylinder is always low. Thus, the volume of grout injected (m/ρ), the volume available to grout injection inside the PM (*Vv*) and the time of injection are considered. In addition, it was created other equation (Eq.5.5) to express the concept of the injectability as the ratio between the volume of grout injected (m/ρ) and the volume available to grout injection inside the PM (*Vv*). Defined in this way, injectability can be expressed in l/m^3 (litres of injected grout per cubic metre of voids to be injected), dimensionless (if the volume of the grout is expressed in m^3) or in percentage of the total volume to be injected. Thus, the equations 5.4 and 5.5 for grout injectability (at a given injection pressure) are proposed:

$$I_{rate}(Bras) = \frac{1}{t} \times \frac{h_{inj}}{h_{total}} \Rightarrow I_{rate} = \frac{1}{t} \times \frac{\frac{m}{\rho}}{V_V} \tag{5.4}$$

$$I = \frac{\frac{m}{\rho}}{V_V} \tag{5.5}$$

where I is the grout injectability (-), I_{rate} is the injectability rate of the grout (s^{-1}), m the injected mass during the injection process (kg), ρ the density of the grout (kg/m^3), V_v the voids volume of PM (m^3), t is the time of injection and h_{total} is the height of the cylinder. By measuring the weight of the cylinders before and after injection it was possible to determine (by knowing the density of the grout) the quantity (volume) of injected product. Additionally, knowing the volume of voids (measured by the saturation of water before injection), it was possible to calculate the effective performance of injection in each PM.

In section 5.3.3 and Chapter 7 (7.5.1.1 and 7.5.1.2) the aforementioned equations are used and the results obtained are analysed.

5.2.6 Injection tests using NF P 18-891

In the field of hydraulic grouts for injecting historic masonry structures, systematic research has been undertaken, using the standardized sand column test (described in the French standard NF P 18-891, as well as in the European standard EN1771), that was conceived by Paillère and Rizoulières in the Laboratoire Central des Ponts et Chaussés (LCPC, France). The test was developed initially for the control of injectability of polymers for the repair of concrete structures (Paillère & Rizoulières, 1978). Recently, in works of several authors (Nuno G Almeida et al., 2012; Biçer-Simşir et al., 2009; Kalagri et al., 2010; Miltiadou-Fezans & Tassios, 2013a; Oktay et al., 2015; Papayianni & Pachta, 2014), the grout injectability was also evaluated using the standard sand column-test. This test is particularly interesting since it enables simultaneously to control the fluidity, penetrability and stability. The

column used in the injectability tests (Fig. 5.13) is a transparent plexiglass cylinder with a height of 36 cm and an inner diameter of 22.6 mm. It was kept in a vertical position and gradually filled with a PM consisting of a mix of fine and coarser siliceous sand (Fig. 5.11). This mix of different granular sands does not simulate masonry itself (which is hardly reproducible in laboratory), but tries to reproduce as much as possible real situations of the inner core of a masonry wall. The use of different gradings of sand enables to simulate voids of different aperture, which can be characterized by a nominal value of voids aperture – W_{nom} - nominal lower value of the aperture of fissures ($W_{nom} \sim 0.15 \times D_{15}$, where D_{15} is diameter of the PM grain, corresponding to 15% passing). Furthermore, these gradings of sand are reproducible.

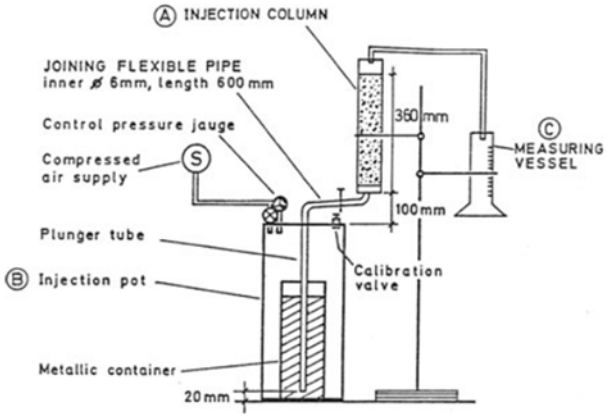

Fig. 5.13 - Setup of the sand column injectability test (Miltiadou-Fezans & Tassios, 2013a)

The column is injected from bottom to top under constant pressure (0.75 bar). The time the grout takes to reach the top of the column (T_{36}) and the time measured to collect 100ml in the vessel C (Fig. 6) are recorded. According to EN 1771, NF P 18-891 and The Getty institute (Biçer-Simşir et al., 2009), the grout injectability is evaluated based on these two parameters. In order to be considered injectable in the sand column, the grout must reach the top of the column (T_{36} value should be less than 50 sec), as well as to flow in the vessel C (Kalagri et al., 2010; Miltiadou-Fezans & Tassios, 2013a). Following this approach, the grout injectability was assessed at three different temperatures (5, 20 and 40 ºC), two different resting times (0 and 60 min) and different SP dosage (0.4 -1.6wt.%).

5.3 Results and Discussion

5.3.1 Effect of superplasticizer on fresh grout behaviour

Regarding to the grout composition, certain parameters play an important role on the fresh grout behaviour, such as binder type, water/binder ratio (w/b) and SP dosage (Baltazar et al., 2014, 2013; Bras & Henriques, 2009). For that reason, it is extremely important to study the different parameters that are involved in grout composition and their influence on fresh state behaviour. In the present work, a w/b content (0.5) was chosen (and maintained in all grout compositions) in view of the results reported in the literature where the materials studied were the same (Baltazar et al., 2013; Bras & Henriques, 2012; Miltiadou-Fezans & Tassios, 2012; Valluzzi, 2005). On the other hand, the dosage of SP was changed. Given the knowledge of the literature on this issue (Baltazar & Henriques, 2014; Baltazar et al., 2013), the range of 0.4 -1.6wt.% was chosen.

5.3.1.1 Fluidity measurements

Fluidity (Marsh cone test)

The Marsh cone test was used to study the loss of fluidity of different grouts with time as recommended by Aitcin (Aïtcin, 1998). The influence of SP on hydraulic lime grouts fluidity was studied for the resting times 0, 30 and 60 min. The results are presented in Fig. 5.14. SP dosages of 0.4, 0.8, 1.2 and 1.6 wt% were tested. For a grout with 0.4 wt% the fluidity factor at 60 min is too low when compared to other compositions (Fig. 5.14). As expected (Mirza et al., 2002b; Yamada et al., 2000), regardless the resting time, the fluidity factor increase with an increase in the SP dosage until the saturation point (SP = 1,2%) remaining afterwards practically unchanged. The saturation point appears to correspond to the maximum degree of dispersion of the grout particles, above which there will be no improvement in fluidity. According to some authors (Banfill, 2011; Miltiadou-Fezans & Tassios, 2012) a higher SP concentration will lead to reverse effect. This phenomenon is called depletion attraction, which is caused by an excessive concentration of SP in the liquid phase that will be the source of an osmotic pressure over the binder particles forcing the particles to flocculate and causing negative effects, such as stability problems (segregation and bleeding). Another aspect illustrated in Fig. 5.14 is that the higher the resting time, the bigger is the variation of the fluidity factor between the highest and lowest SP dosage. This behaviour can be attributed to a higher amount of SP available to disperse the particles, resulting in a larger dispersion of the grout particles during the test, since the SP imposes repulsive forces that prevent the particle flocculation (Banfill, 2011). For that reason, this characteristic of SP is more critical for the longer times tested (as illustrated in Fig. 5.14).

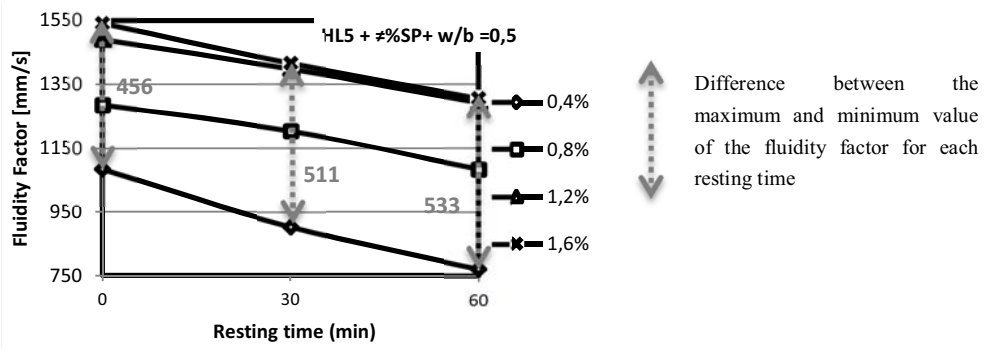

Fig. 5.14 - Influence of SP dosage on fluidity factor for 0, 30 and 60 min of resting time after grout preparation

Spread diameter (Mini-slump test)

As already mentioned to the Marsh cone test, the influence of SP on hydraulic lime grouts fluidity was studied for the resting times 0, 30 and 60 min. From Fig. 5.15, in accordance with Marsh cone results, the grout workability is higher for a higher SP dosage. In fact, regardless of the resting time, a significant difference in the spread diameter can be detected between 0.4-1.6 wt% SP (Fig. 5.16). Some authors (Sonebi et al., 2013; Svermova et al., 2003; Yamada et al., 2000) also noted that due to the better deflocculation of the particles in the suspension, the SP dosage has great effect on the mini-slump results. Besides, as it can be seen in Fig. 5.16, for higher resting times the spread diameter decreases which is related to workability loss of the grout.

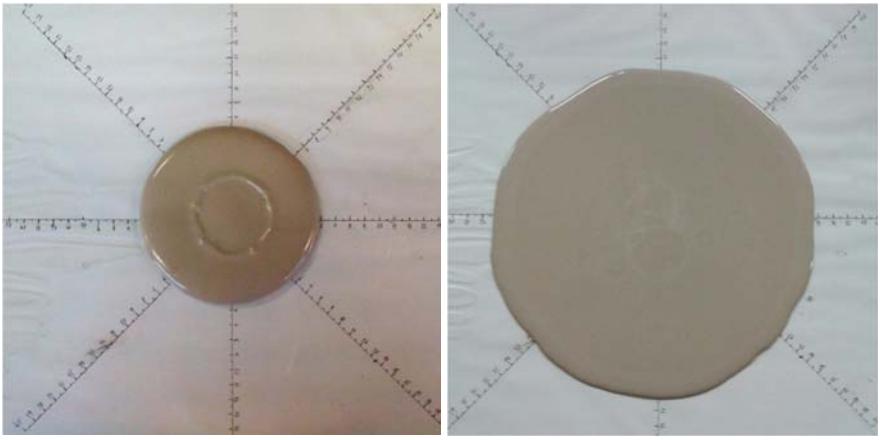

Fig. 5.15 – Spread diameter of grout with 0.4 wt% SP (left), and 1.2 wt% SP (right)

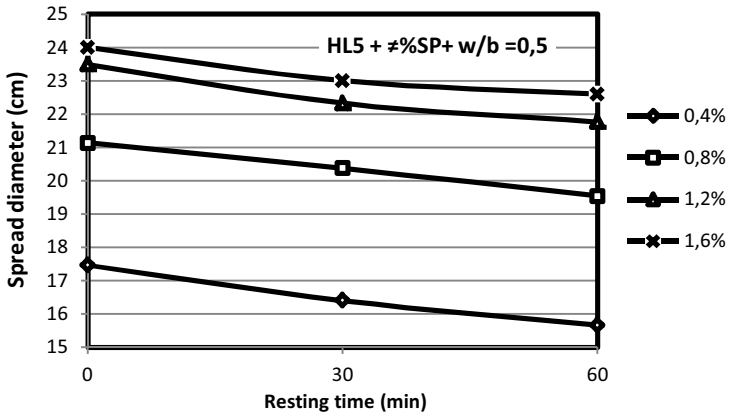

Fig. 5.16 - Influence of SP dosage on spread diameter for 0, 30 and 60 min of resting time after grout preparation

5.3.1.2 Water retention

Grouts should have the capacity of retaining water to ensure the preservation of their rheological proprieties and consequently a good flow during injection into PM. The loss of water inside the masonry can work as a blocking mechanism for injection process (Bras & Henriques, 2012; Van Rickstal, 2000) due to the increase of the internal friction and collision among solid particles (which means more energy required to breakdown the structure), leading to a decrease of dispersion degree and hence a reduction of injection capacity (Assaad & Daou, 2014). So, it is essential to inject a grout with high water retention time which means a grout with good capability to retain the mixing water (Uranjek & Bosiljkov, 2012).

In the case of change of SP dosage, the degree of dispersion (it is dependent of SP dosage) determines the water retention capacity since it allows more particles to be wetted and therefore more water is absorbed on the particles surface and less water is free to bleed (Biçer-Simşir et al., 2009). As observed in Fig. 5.17.a this phenomenon has more impact up to 1.2wt% SP. Based on the work of Bombled (Bombled, 1974), an increase of water retention can also mean an increase of grout stability. This issue will be addressed in the next section.

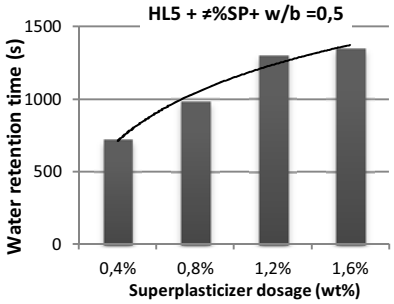

Fig. 5.17 - Influence of SP dosage on water retention time

5.3.1.3 Stability

The percentages of initial grout density up to 70 min after the mixing process for different SP dosages are presented in Fig. 5.18. It is observed that the grout stability is significantly improved until a SP dosage of 1.2 wt%. In fact, the dispersive action of SP opposes sedimentation, since the sedimentation process occurs more slowly and thus the particles settle more homogeneously (Assaad & Daou, 2014). If the SP dosage is too low (for a certain w/b chosen), the distance between the binder particles becomes much small. As a result, the internal friction between closely-packed particles increases and consequently the aggregated particles tend to sink by gravity (sedimentation process) resulting in a reduction of the grout stability (Assaad & Daou, 2014) . In these conditions, the equilibrium of the interparticle forces is not reached and hence the grout cannot be used. For that reason, a SP dosage of 0.4 wt% and 0.8 wt% should not be used.

On the other hand, as mentioned by Miltiadou and Tassios (Miltiadou-Fezans & Tassios, 2012), for higher percentages of SP, possible instability side effects (bleeding and segregation) should be checked. The same authors created an equation (Eq.5.6) which enables to calculate the values (w/b) for which the grout starts to exhibit segregation.

$$(\frac{w}{b})_{segr} \cong 0.8 + (\frac{S_A}{6000}) - 1.7 \times (SP) \tag{5.6}$$

where S_A is the surface specific (cm^2/g). According to this Eq. 5.6, for a 1.6 wt% of SP the w/b is too high and for this reason the grout exhibits segregation, which means that is not stable along the time (Fig. 5.18).

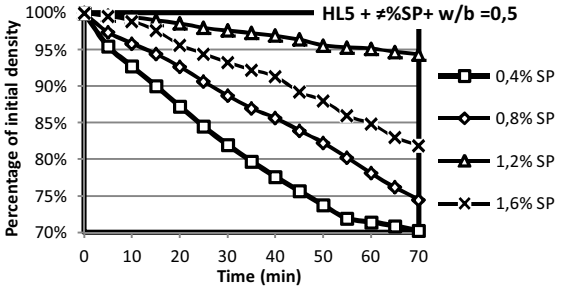

Fig. 5.18 - Percentage of initial density versus time for different SP dosages, according to the proposed stability test

In order to control the grout stability, Van Rickstal proposed to accept a fluctuation of ±5 % for the density measure as a stability criterion (Van Rickstal, 2000). According to Fig. 5.18, for a resting time of 60 min, the composition of 1.2 wt% SP is the unique that satisfies the stability criterion.

Furthermore, as demonstrated in other tests (Fig. 5.14, Fig. 5.17 and Fig. 5.18), this grout composition always shows a good performance. So, it is chosen to be tested in the sections where is evaluated the influence of resting time and temperature on grout rheology (section 5.3.2).

5.3.2 Evaluation of the combined effect of temperature and resting time on grout rheology

As previously mentioned, the temperature affects the kinetics of hydration which determines the variation in grout rheological behaviour over time. Then, the coupled effects of various resting times (from 0 to 120min) and environmental temperatures (from 5 to 40 °C) on the yield stress, plastic viscosity and flocculation area were analysed. Based on the conclusions obtained in section 5.3.1, the grout composition tested at this stage was 1.2 wt% of SP.

5.3.2.1 Yield stress and plastic viscosity

From the results illustrated in Fig. 5.19 and Fig. 5.20, it is clear that the rheology of a grout suspension strongly depends on temperature and resting times. As observed by Petit (Petit et al., 2010) there are changes in rheological properties for different temperatures and resting times, which are related to the evolution of the restructuring of the microstructure, binder hydration, interaction between binder and SP and variation of free water content.

For a grout temperature higher than 20ºC a workability loss can be detected (i.e. an increase of yield stress and plastic viscosity). However, it is worth noting that the workability loss is more significant for temperatures above 30 °C. According to Bras *et al.* (Bras et al., 2010) for high temperatures it is expected an increases of the microstructure density of the grout which can increase the yield stress. Nevertheless, in this work only for resting times higher than 30min it is possible to observe a significant increase of the yield stress with the increase of the temperature.

Regarding the range of 5 to 20ºC for both rheological parameters, it is observed a slight evolution as was also obtained by Mirza *et al.* (Mirza et al., 2013). There is a decrease of plastic viscosity with the increase of temperature from 5ºC to 20ºC which can be attributed to an increase in the Brownian motion of the particles. On the other hand, the increase of yield stress is due to the fact that the thermal agitation (related to the Brownian motion phenomenon) is counteracted by faster reaction kinetics of the lime hydration and by the increase in electrostatic forces of lime particles caused by the temperature increase. According to the PFI (Particle flow interaction)-theory (Wallevik, 2009) with the evolution of hydration reactions most of the binder particles start to be permanently connected between each other (irreversible physical bonds) causing a significant increase of the yield stress which leads to a penetrability loss since the yield stress influences the grout filling ability. Thus, as concluded by Roussel (Roussel et al., 2010), Brownian motion only plays a minor role on rheological behaviour of cementitious suspensions. Indeed, it is dominated by the effect of attracting interparticle forces. Therefore, the yield stress is thus dictated by the structure of the interaction network and can be seen as a sensitive measure of the forces acting between particles, namely electrostatic forces and van der Waals forces.

Based on the achieved results it cannot be stated that the environmental temperature of 20ºC leads to the best grout rheological behaviour, as reported by Bras *et al.* (Bras et al., 2010). In general, the

results show that for grout temperatures ranging between 5 ºC and 20 ºC that the minimum stress that is necessary to apply for a grout to start flowing, as well as the velocity at which a given grout will flow, is practically independent of temperature. Nevertheless, it should be noted that these experimental results are not directly comparable since the experimental work carried out by Bras *et al.* is not consider the use of SP.

In respect to the resting time, the fresh grout showed a time-increasing yield stress and a time-increasing plastic viscosity regardless of the temperature, similar to the results obtained by some authors (Mirza et al., 2013; E.-E. Toumbakari et al., 1999; Yamada et al., 2000). However, the evolution is not constant. For the reasons already mentioned, there is a larger increase for higher temperatures.

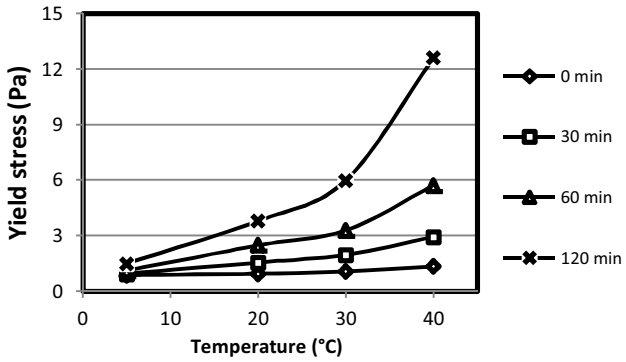

Fig. 5.19 - Influence of temperature and resting time on yield stress for grouts with 1.2%wt of SP

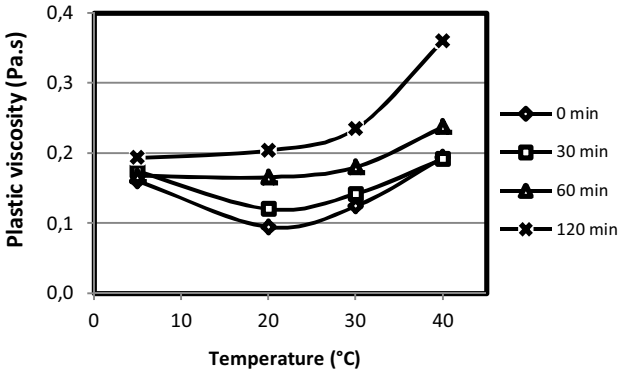

Fig. 5.20 - Influence of temperature and resting time on plastic viscosity for grouts with 1.2%wt of SP

5.3.2.2 Flocculation area

The flocculation area is plotted in Fig. 5.21 as a function of resting time and temperature. Based on the achieved results it is clear that the flocculation area increases with resting time for all the temperatures studied, what reflects the thixotropic behaviour of the grouts studied (at rest there is structural build-up of the grout) (Assaad & Daou, 2014). Nonetheless, two trends are observed depending of the resting times. For higher resting times (60 and 120min), the flocculation area increases with temperature, especially for temperatures above 30 ºC. Regarding the lower resting times (0 and 30 min), there is a slight decrease of flocculation area with an increase in temperature up to 20ºC; nevertheless, the flocculation area starts to increase in temperatures higher than 20ºC (with the largest increase above 30ºC). Thereby, it can be stated that for the lower resting time 20ºC is the optimum temperature. This

behaviour can be attributed to temperature increase and hydration growth. The temperature increase leads to faster hydration reactions and therefore a quicker flocculation (rapid change in the grout microstructure). Furthermore, the growth of hydration products on the surface of the binder particles will cover the adsorbed layers of SP which results in a progressive loss of SP dispersion action. However, for lower temperatures (such as 5ºC) the grout approaches the water freezing point, which leads to the formation of strong hydrogen bonds. Furthermore, according to Brownian motion, random motion of the particles is temperature-dependent. This means that for lower temperatures, the molecular agitation decreases (grout particles are closer to each other), thus the lower freedom state causes a higher flocculation area (quicker microstructure build up). However, as illustrated in Fig. 5.21, for higher resting times (60 and 120 min) this phenomenon (thermal agitation) is counteracted by faster reaction kinetics of the lime hydration caused by the increase of the temperature. Thus, it is possible to conclude that for higher resting times, thixotropic behaviour is dominated by the hydration effects.

Based on the results obtained, it can be stated that thixotropy constitutes a critical parameter for the grout injection. To prevent that the flocculation compromises the application and effectiveness of the grouting intervention, the resting time (between the mixing and the injection process) should be restricted, especially for high temperatures.

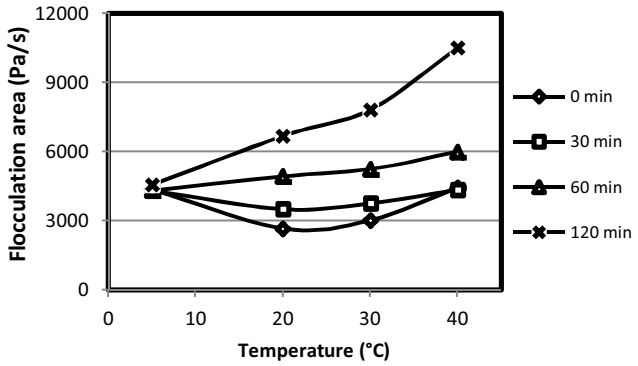

Fig. 5.21 - Influence of temperature and resting time on Flocculation area for grouts with 1.2%wt% of SP

5.3.3 Grout injectability as function of environmental temperature, resting times, SP dosage

In this chapter, the purpose of the injection tests was to check the influence of fresh grout parameters on grout injectability. More specifically, it was checked if the conclusion drawn from the data obtained in the fresh grout tests at different temperatures (5, 20, 30 and 40ºC) and different resting times (0 and 60 min) are in agreement with the injectability values. Regarding the grout composition, all compositions (0.4 -1.6 wt% SP) were tested in order to evaluate the effect of the considerations indicated in sections 5.3.1 and 5.3.2 on the results of injection tests. As mentioned in section 5.2.5, two different equations were used to study the injectability of the grouts. The difference between both equations is the existence of a parameter (injection time) in the injectability rate equation (Bras & Henriques, 2012).

5.3.3.1 Influence of temperature and resting time

The grout injectability as function of temperature and resting time is shown in Fig. 5.22. As it can be seen, the high injection capacity is achieved for the temperature of 20°C. In contrast, for the temperature of 40°C it is observed the lower injectability. As shown in the rheological tests (Fig. 5.19 and Fig. 5.20), the worst grout rheological behaviour (higher viscosity and yield stress) is obtained for the temperature 40°C. In fact, for higher temperatures (above all for higher than 30ºC), higher amount of water is evaporated from the grout suspension during the injection. As result, the internal friction and collision among solid particles increase, leading to higher yield stress (Assaad & Daou, 2014) and hence a lower penetration in the PM is achieved. Besides the rheological parameters mentioned above, the flocculation phenomenon analysed as a function of the resting time and temperature is particularly important during a grout injection (Van Rickstal, 2000). The results of injectability test show that the grouts with higher flocculation area (Fig. 5.21) present lower injectability. In fact, higher flocculation means stronger attraction forces among binder particles and hence the dispersion is not so easily achieved.

The resting time is another variable that influences the performance of grout injection. In fact, in most cases there is a reduction of grout injectability between the resting time 0 and 60 min (Fig. 5.22). The results of resting time of the 120 min are not shown due to the difficulty to inject the grout. These results are associated to the increase of flocculation of the binder particles (structural build-up) along time, which means a lower number of free binder particles (loss of workability) (Assaad & Daou, 2014). According the PFI - theory (Wallevik, 2009), as already referred, there are two kinds of flocculation: reversible and permanent. With longer resting times, more and more binder particles become permanently connected (permanent flocculation) what contributes to the workability and penetrability loss and hence the grout cannot flow.

Table 5.5 – Voids volume, grout volume and injection time for grouts with different temperatures and resting times (grouts with 1.2 wt% of SP); injection pressure = 1 bar

Temperature (°C)	Resting time (min)	Voids volume (cm^3)	Grout volume (cm^3)	Injection time (s)
5	0	2140	2012	25
	60	2168	1973	35
20	0	2182	2160	26
	60	2172	1933	34
30	0	2179	2157	26
	60	2143	1886	37
40	0	2161	1988	26
	60	2153	1701	40

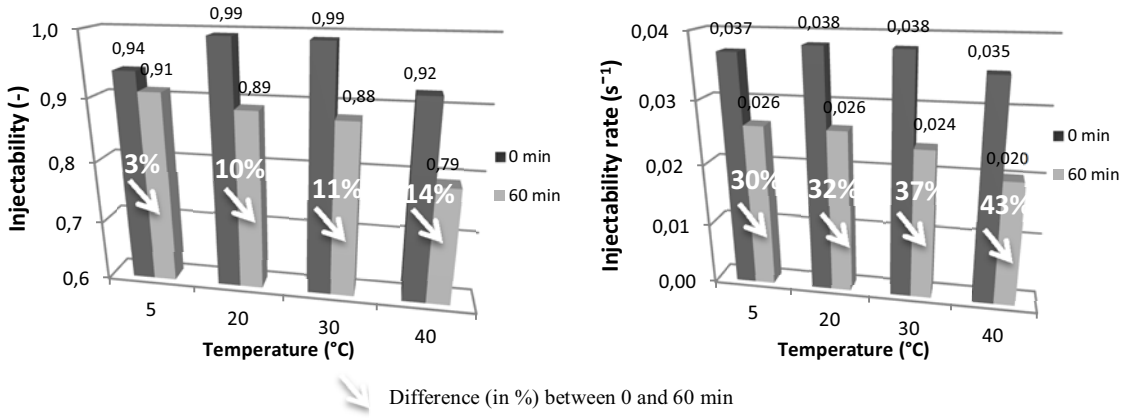

Fig. 5.22 –Influence of temperature and resting time on grout injectability (left) and injectability rate (right) for grouts with 1.2 wt% of SP; injection pressure = 1 bar

5.3.3.2 Influence of superplasticizer dosage

According to Van Rickstal (Van Rickstal, 2000), there are three blocking mechanisms. The first mechanism depends on the granularity of the binder. Since the flocculated binder grains act as big binder grains (which contribute to prevent the grout injection), it seems to be impossible to produce an injectable grout without SP. They have a deflocculating action which causes a drastic reduction in the magnitude of attraction forces (i.e. the total potential energy interaction between particles is reduced (Wallevik, 2009), and therefore particle flocculation is reduced or even prevented (Roy & Asaga, 1979; Vikan, 2005). Thus, the reduction of the tendency to flocculate during hydration phase leads to a lower injectability loss along the time. As can be seen in Fig. 5.23-a, the grout with 1.2 wt% of SP shows the lowest difference between the resting times 0 and 60 min (10% on injectability and 24% on injectability rate). Regarding the fluidity measurements (see Fig. 5.14) the increasing of SP concentration causes a decrease in the grout viscosity. Such results are in agreement with the injectability results presented in Fig. 5.23. This agreement was proved experimentally by Miltiadou and Tassios (Miltiadou-Fezans & Tassios, 2012). The authors concluded that a grout is able to penetrate certain PM if its fluidity is higher than a specific threshold F_l (fluidity factor) value. From different PM and different grouts (with fineness ranging from 4000 to 10000 cm^2/g; the binder used in this work has 9400 cm^2/g - Table 5.1), Miltiadou and Tassios proposed an empirical formula (Eq.5.7) which gives a minimum required F_l for each W_{nom} – see 5.2.7). Basically, this expression estimates the necessary fluidity in order to ensure penetration into a given PM.

$$\min F_l \approx [1.2 - 45 \cdot (W_{nom} - 0.1^2) \cdot 10^3, (mm/s) \tag{5.7}$$

According to Eq.5.7 for a W_{nom} = 0.196mm (0.15 x 1.30mm) (D_{15}= 1.30mm, see Fig. 5.12), the min F_l is 785mm/s. As the composition with 0.4 wt% of SP at 60min of resting time has a lower F_l (F_l = 761mm/s - Fig. 5.14), the injectability value (0.42) is low (Fig. 5.23). Regarding the composition with 1.6 wt% of SP at 60min of resting time has a high F_l (F_l = 1305mm/s - Fig. 5.14), though the injectability value is not high. In this case, there is another phenomenon related to the instability (already mentioned in 9.2.2), which has a higher influence. In fact, as emphasized by the Miltiadou and Tassios (Miltiadou-Fezans & Tassios, 2013b), an appropriate penetrability and fluidity is not

enough to achieve a satisfactory injectability. Indeed, the stability (that is the second mechanism (Van Rickstal, 2000) of a suspension against segregation or excessive bleeding should be ensured, since when flow slows down the binder particles in an unstable grout sink to the bottom of the flow channel (Miltiadou-Fezans & Tassios, 2013b). This narrows the channel and thereafter can result in the blockage of the injection. As shown in stability results (Fig. 5.18), the grout with 1.2 wt% of SP shows the best results. The addition of SP (until the optimal dosage) significantly improves the stability and consequently the injectability of the grout for both resting times tested.

The third possible blocking mechanism is the result of water absorption by the masonry (causing negative consequences on the rheological properties) (Assaad & Daou, 2014; Van Rickstal, 2000). When meeting a dry and absorptive masonry it is important to use a grout with excellent water retaining properties. Thus, to prevent this problem, the water retention capacity of grout should be controlled. The study of the effect of addition of certain admixtures, as conducted in this work, may be a possible way (see section 9.2.2). From Fig. 5.17, it can be seen that the grout with 1.2 wt% has a high water absorption capacity and consequently the volume of grout injected into the PM is also high (Table 5.6) which means a high injectability (Fig. 5.23).

Therefore, taking into account the results obtained, it can be argued that the three blocking mechanisms must be checked in order to achieve an adequate injectability.

Table 5.6 - Voids volume, Grout volume and Injection time for grouts with different SP dosages and different resting times (injection temperature at 20°C); injection pressure = 1 bar

SP dosage (%)	Resting time (min)	Voids volume (cm^3)	Grout volume (cm^3)	Injection time (s)
0.4	0	2159	2008	85
	60	2137	898	60
0.8	0	2189	2145	34
	60	2165	1689	65
1.2	0	2182	2160	26
	60	2172	1933	34
1.6	0	2186	2164	24
	60	2136	1388	22

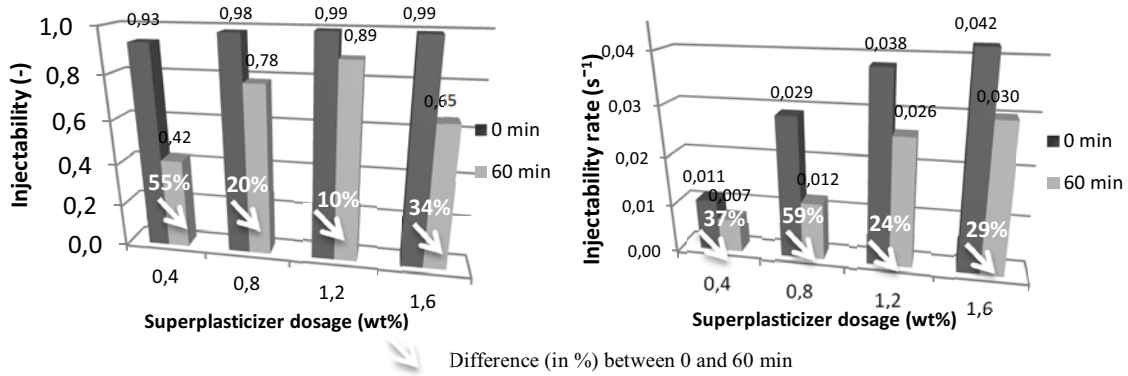

Fig. 5.23 - Influence of the SP dosage on grout injectability (left) and injectability rate (right) for different resting times and a temperature of 20 ºC; injection pressure = 1 bar

According to (Eklund & Stille, 2008), besides rheology the filtration tendency is another factor that limits the injection capacity. The filtration tendency is a characteristic whereby a plug of particles can be formed at a void opening or in a constriction within the void/channel preventing further penetration

(see 7.2). Commonly the maximum grain-size of the binder is the conditioning effect present on the "groutability ratio" criterion in order to evaluate the grout injectability (grout penetrability), which in reality may not be correct. As observed in this work and the literature (Miltiadou-Fezans & Tassios, 2013a), the small-sized particles have higher tendency to flocculate into larger agglomerates, when compared to larger grain-sizes. Thus, it can be pointed out that a suitable dosage of SP is essential to prevent the flocculation of small grains of the binder, since the flocculation phenomenon has a significant effect on the level of filtration tendency of the grout, and thereby in the grout injectability.

5.3.3.3 - Correlation between grout injectability and fresh grout parameters

A general correlation between the values of each fresh grout parameter (Fig. 5.14 and Fig. 5.18; Fig. 5.19-Fig. 5.21) and the corresponding values of injectability (Fig. 5.22 -Fig. 5.23) is presented in Fig. 5.24. This figure summarizes some observations already mentioned, namely that injectability (dimensionless) depends mainly on yield stress and water retention, while the injectability rate (s^{-1}) is more influenced by the plastic viscosity and the fluidity factor (F_l). Flocculation area shows low correlation level for both injectability equations.

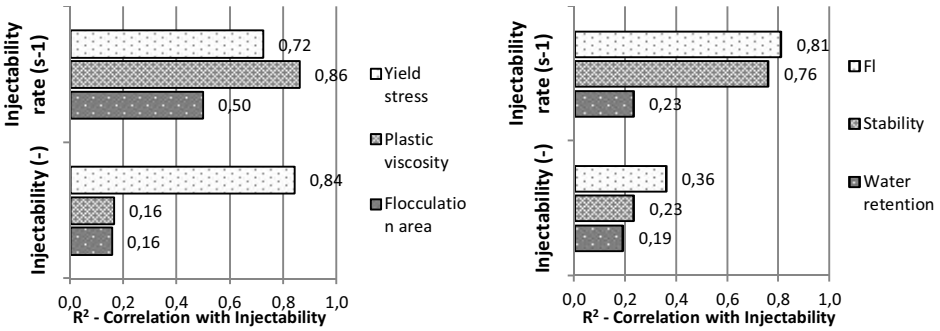

Fig. 5.24 – Correlation between grout injectability and fresh grout parameters

5.3.4 Injection tests using NF P 18-891

Table 5.7 shows that for lower dosages of SP the grout is considered not injectable, since the grout flow is interrupted and do not reach the top of the column (36 cm). Nonetheless, when the SP dosage is close to optimal dosage (1.2wt %), the grout is considered injectable (even not respecting the penetrability criteria mentioned above). In fact, as observed in Table 5.7 the grout flow reaches the top of the column and has a high flow in the vessel. Such results confirm that the presence of SP in grout composition minimizes the particle flocculation phenomena, since the electrostatic connections between particles and the agglomeration (due to immediate hydration of the fines) are reduced.

Based on the work of several authors (Kalagri et al., 2010; Miltiadou-Fezans & Tassios, 2013a), for a grout suspension to achieve a satisfactory injectability, it is required a suitable penetrability and fluidity, as well as an appropriate stability. Indeed, if any instability (excessive bleeding or segregation of solid grains) appears during injection, the grout flow may be blocked which can affect the quality of the intervention. For that reason, when the resting time is equal to 60 min, the composition of 1.2 wt% SP (that respect the stability criterion - Fig. 5.18) is the unique that is considered injectable (Table 5.7).

Furthermore, the grout flow increases significantly with the increase of SP content (until optimal dosage) due to the increase of fluidity. As the presence of SP retards the hydration of the grout suspension (the dormant stage of the hydration process is prolonged), the rheological behaviour (more precisely the yield stress and plastic viscosity) is maintained in adequate conditions for a longer period of time (Heikal et al., 2005). Nevertheless, it should be noted that when SP dosage is too high (above of optimal dosage - 1.2 wt%), the stability criterion is not ensured Fig. 5.18 and thereby a satisfactory injectability is not achieved. So, it is crucial to choose a suitable SP dosage, especially in the case of a high value of resting time.

Given the results obtained in this chapter, it can be conclude that the selection of an appropriate SP dosage can be done based on the fresh grout tests (see 5.3.1) and the sand column test. Moreover, particularly the latter test, it can be checked if the grain size distribution of solid materials of the grout is appropriate taking into account the gradings sand of the PM, i.e., the lower apertures of the voids. This issue will be address in Chapter 7.

Table 5.7 - Sand-column test results for grouts with different SP dosages and injected at different resting times (injection temperature at 20ºC)

		Flow in the column (36 cm)		**Flow in the vessel (100 ml)**		
% SP	*time (min)*	height of injection (cm)	injection time (T_{36}) (s)	Volume reached (ml)	injection time (s)	grout flow (ml/s)
0,4	*0*	13,5	11,3	-	-	-
	60	5,5	20,8	-	-	-
0,8	*0*	33,8	12,5	-	-	-
	60	14,4	15,8	-	-	-
1,2	*0*	36,0	7,5	100**	27,1	3,7
	60	36,0	10,4	30	25,2	1,2
1,6	*0*	36,0	5,6	100**	11,6	8,6
	60	32,5	9,7	-	-	-

* All values are the average of three results with similar performance

** Maximum volume collected

As already concluded in 5.3.2, the temperature affects the rheology of hydraulic lime grouts and consequently the grout injectability is also affected. According to Table 5.8, the flow of grouts at 40ºC and 0 min showed a good result. In fact, there is an improvement in fluidity since the increase of temperature changes the adsorption capacity of the superplasticizer (Heikal et al., 2005). However, when the resting time is equal to 60min, the worse rheological behaviour is detected when the temperature rises to 40 ºC. Thus, it can be concluded that the resting time should be taken into account during grout injection. As seen in Table 5.7 and Table 5.8, for higher resting time, the grout injection performance decreases. But the influence of the resting time is dependent on injection temperature and grout composition (in particular the SP dosage). For higher temperatures and lower dosage of SP, the influence of resting time in the grout injectability increases. In both cases the rheological behaviour is severely affected along the resting time. More specifically, there is a significant increase of the particle flocculation phenomenon (Fig. 5.21). Thus, an increase of temperature results in a shorter time where an appropriate grout injectability is achieved (especially if a low dosage of SP is used), as observed for temperature 40ºC (Table 5.8). In contrast, for lower temperatures (5ºC) the fresh grout properties do

not change much along 60 min (Fig. 5.21) and therefore the grout injectability is not affected significantly (Table 5.8).

Table 5.8 – Sand-column test results for grouts injected at different temperatures and resting times (SP = 1.2wt %)

		Flow in the column (36 cm)		**Flow in the vessel (100 ml)**		
Temperature (°C)	*time (min)*	height of injection (cm)	injection time (T_{36}) (s)	Volume reached (ml)	time (s)	grout flow (ml/s)
5	0	36,0	8,5	100**	50,5	2,0
	60	36,0	9,5	33	17,3	1,9
20	0	36,0	7,5	100**	27,1	3,7
	60	36,0	10,4	30	25,2	1,2
40	0	36,0	7,3	100**	35,7	2,8
	60	0,0	-	-	-	-

* All values are the average of three results with similar performance

** Maximum volume collected

Comparing the results of the two models of injection tests mentioned above, the injection results show the same trends. Actually, as noted in 5.3.3 and 5.3.4 the same conclusions are reached. Nevertheless, in the following chapters, the model of injection tests shown in 5.2.5 was chosen. Indeed, the injection test using the French standard NF P 18-891 was not used due to two reasons: a) the diameter of the column (22.2mm) is too small for aggregate sizes studied in this work (especially the coarser PM with size between 4.75-9.5mm); b) due to geometric configuration of the column, the path of the grout during the injection is only one-dimensional, rather than three-dimensional, as in the case of adopted model (see 5.2.5) and reality.

5.3.5 Grout injectability as function of injection pressure

On the one hand, as stated in section 5.2.5, the penetration of the grout into the PM is directly dependent on the injection pressure. On the other hand, taking into account the findings achieved by Baltazar *et al.* (Baltazar et al., 2014) related to the pressure and grout rheological properties, an injection pressure of 0.5 bar achieves the best grout rheological performance. So, it was compared the injection capacity of the grout for 0.5 and 1 bar in order to evaluate the influence of injection pressure on injection tests. The grouts with resting time equal to 0 min and 1.2 wt% of SP was chosen, that showed a high performance for an injection pressure equal to 1 bar (Fig. 5.22). From Fig. 5.26-a, comparing the two injection pressures, there was not noticed a significant difference in grout injectability. However, it was noticed a great difference in injectability velocity which is confirmed by the injectability rate values (a reduction of about 35% - Fig. 5.26-b).

As can be seen in Fig. 5.22, the grout injectability is low for grouts with resting time equal to 60min and 1.2 wt% of SP. Thus, the injection pressure was increased to 2 bar in order to increase grout injectability. However, as observed in Fig. 5.27-a, the injectability value remains low. In certain cases, due to high turbulence created by the high injection pressure, the percentage of voids filled - Injectability (-) decreases (Fig. 5.27). Moreover, according to Petit *et al.* (Petit et al., 2011), an increase in plastic viscosity and yield stress are obtained when the pressure increases, since the friction between the solid particles is augmented.

From the injections tests, it was observed that injection pressure just has some influence on rate of grout injection. Indeed, the higher is the injection pressure, higher is the velocity of injection - Inj (s^{-1}). Nonetheless, regarding the percentage of voids filled there is no significant improvements on the effectiveness of grout injection. Indeed, the yield stress has more influence on the grout filling ability, a smaller yield stress, meaning an easier injection process, with lower pressures, as occurred on the grout with resting time equal to 0 min (Fig. 5.26).

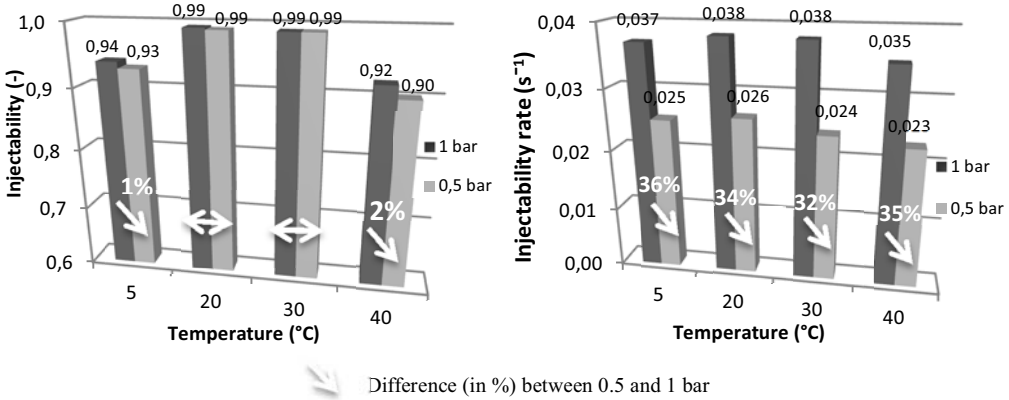

Fig. 5.26 – Influence of the injection pressure on grout injectability (left) and Injectability rate (right); with SP= 1.2wt% at 0min for different temperatures

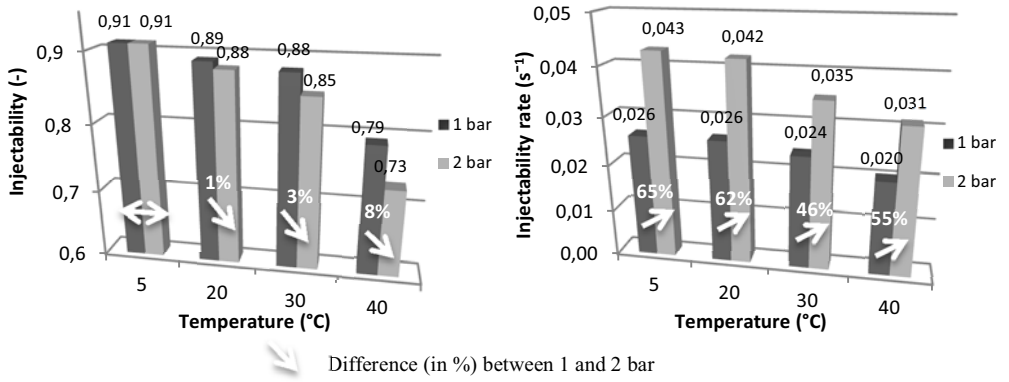

Fig. 5.27 - Influence of the injection pressure on grout injectability (left) and Injectability rate (right); with SP= 1.2wt% at 60min for different temperatures

5.4 Conclusion

The main achievements obtained with the present work are summarized in Table 5.9.

Table 5.9 – Influence of SP dosage, resting time and temperature on fresh grout parameters and injectability values

		Fluidity factor	Water retention	Stability	Injectability (-)	Injectability rate (s^{-1})
Addition of SP [0.4-1.6wt%]		⇧	⇧	⇗ 1.2% ⇘ (0.4% – 1.6%)	⇧	⇧
		Plastic viscosity	Yield stress	Flocculation area	Injectability (-)	Injectability rate (s^{-1})
Increase of resting time [0-120min]		⇧	⇧	⇧	⇩	⇩
Increase of the temperature [5 – 40ºC]	0 min	5ºC ⇘ 20ºC ⇗ 40ºC	5ºC ⇨ 40ºC	5ºC ⇘ 20ºC ⇗ 40ºC	20ºC ⇘ 5ºC ⇗ 40ºC	20ºC ⇘ 5ºC ⇗ 40ºC
	30 min	5ºC ⇘ 20ºC ⇗ 40ºC	40ºC ⇘ 20ºC ⇨ 5ºC	5ºC ⇘ 20ºC ⇗ 40ºC	-	-
	60/120 min	40ºC ⇗ 20ºC ⇨ 5ºC	40ºC ⇗ 5ºC	40ºC ⇗ 5ºC	5ºC ⇘ 40ºC	5ºC ⇘ 40ºC
Increase of the injection pressure [0.5-2bar]		-	-	-	0.5 ⇨ 2	0.5 ⇗ 2

- The use of SP confirmed a worthy contribution on the fresh parameters (working properties) of hydraulic lime grouts. An adequate presence of SP leads to an increase of fluidity, water retention and stability. In fact, for the PM used (with presence of fine particles (0.15 - 2 mm), the injection tests clearly confirmed the positive influence of SP dosage on the injectability rate and the grout injection capacity. Nonetheless, SP replacement above 1.2wt% may be considered excessive, since some instability phenomena can occur.

- Concerning the fresh state behaviour, the experimental tests showed that rheology of hydraulic lime grouts strongly depends on temperature. The worse rheological behaviour was detected when the temperature increases from 20 to 40 ºC, especially in 30-40ºC range. Therefore, if the consolidation is performed in warm climates (above 30ºC) starting early in the morning and ending at higher temperatures, special attention should be paid to the variation of the grout injection performance during those periods. In contrast, for lower temperatures (below 20ºC) the fresh grout properties do not change much. Nevertheless, for temperatures lower than 5 ºC there is a danger of frost and this can be detrimental to the solidified state of the grout.

- The injection tests (both models used) also revealed that the resting time should be taken into account during grout intervention, especially when the flow tends to stop enabling an increase of the particle flocculation phenomena, which causes a considerable reduction on grout injectability. So, a low resting time is desired, in particular in the cases of grouts with low wt% of SP or when the injection temperature is high. Concerning the temperature, the planning of a consolidation work with grouts should take into account that the influence of resting time varies over the day and mainly over the climatic seasons.

- It should be pointed out the correlation between the results of fresh grout parameters and those injection tests. The injectability (dimensionless) depends mainly on yield stress and water retention, while for the injectability rate (s^{-1}) the plastic viscosity and fluidity factor are the most influential parameters.

- The two models of injection tests show similar results. Nonetheless, in the French standard NF P 18-891 the successful of injection results is lower due to geometric configuration of the column. The path of the grout during the injection is only one-dimensional, rather than three-dimensional, as in the case of other model and reality. Furthermore, the diameter of the column (22.2mm) is too small for aggregate sizes studied in this work. For that reason, the French standard NF P 18-891 will not be adopted in the next chapters.

- Regarding the injection pressure, it was observed that only has some influence on the rate of grout injectability. Actually, the higher is the injection pressure, higher is the velocity of injection - Inj (s^{-1}). Nonetheless, regarding the percentage of voids filled there is not significant improvements on the effectiveness of grout injection when injection pressure is increased.

Through the present research, it was shown the influence of SP dosages as well as the importance of a suitable temperature, resting times and injection pressure on the improvement of injectability of hydraulic lime-based grouts. In the next chapter, the effectiveness of grout consolidation will be checked through ultrasonic tests and mechanical tests on PM injected with these grouts.

Chapter 6. Combined effect of superplasticizer, temperature and resting time on hydraulic lime grout consolidation

6.1 Introduction

In general, the main goals of grout consolidation are to increase the compacity (especially in the inner core), which also increases the cohesion and adhesion between stones, mortars or other materials inside the damaged masonry. Furthermore, some new bonds between the internal and external leafs of the wall are created, which enables to reinstate the collaboration between external and internal leaves. This increases structural integrity and overall stability, which improves the monolithic behaviour and therefore the resistance to seismic forces (Binda et al., 1997; Miltiadou-Fezans & Tassios, 2013b)(Van Gemert et al., 2015a). According to Uranjek and Bosiljkov (Uranjek & Bosiljkov, 2012) the behaviour of the wall after grout injection is significantly influenced by the efficacy of grout injection. For a successful intervention, it is consensual that grouts should have high injectability, low or no shrinkage and good bond to masonry materials (represented by a PM, such PM is used to simulate the infill material of the inner core of three-leaf masonry). Regarding the injectability, its importance was studied in the previous chapter. The shrinkage is a property with high influence on interfacial bond strength between grout and PM. Since additional stress on the interface is created, some cracks appear and hence loss of adhesion between grout and PM is observed (Mirza et al., 2002a; Toumbakari, 2002). Concerning the mechanical strength of the PM after injection, the results confirmed that the mechanical properties of the grout (compressive and flexural strength) are not the main factors. Actually, the interfacial bond strength between grout and PM particles, which is evaluated by splitting and direct-shear test, has more importance.

The shear capacity resistance of inner core of masonry (in particular the shear bond strength of the grout-PM interface) was evaluated from direct-shear tests in several PM. To reduce the horizontal deformability of the different leaves of the masonry (out-of-plane deformations), the shear bond strength must be high. In fact, the shear failure planes generated in the inner core (e.g. in seismic actions) may cause high horizontal pressure on the external leaves and thus increase the risk of collapse of the masonry (Mazzotti et al., 2014; Silva et al., 2014a).

The effectiveness of grout consolidation in small models (cylinders) was also evaluated through tomography. As demonstrated in other articles (Da Porto et al., 2003; Mojmir et al., 2012), ultrasonic tomography may be used to detect voids/flaws (evaluating the homogeneity) and to evaluate the efficiency of grout injection. Ultrasonic test is a NDT technique and thus it does not present any risk of damage for the cylinder (PM after injection). The test consists in the measure of the transit time of ultrasonic pulses (stress waves) in cylinder. This transit time and the calculated ultrasonic pulse velocity result in basic information about the compacity of the cylinder under investigation. The presence of inhomogeneities, voids and damaged areas in the cylinder is detected by low ultrasonic velocities in the tomographs.

This chapter is part of a larger study which analyses the performance of the grout injection, taking into account fresh and mechanical properties of the grout, grout injectability and the mechanical strength of the PM after injection. The grout fresh properties were analysed in a previous chapter and several considerations of that chapter are taken into account in the discussion of the results of this chapter. In this chapter, the main objective was to study the influence of superplasticizer (SP) dosage, temperature (for injection and cure) and resting time on grout consolidation, as graphically demonstrated in Fig. 6.1.

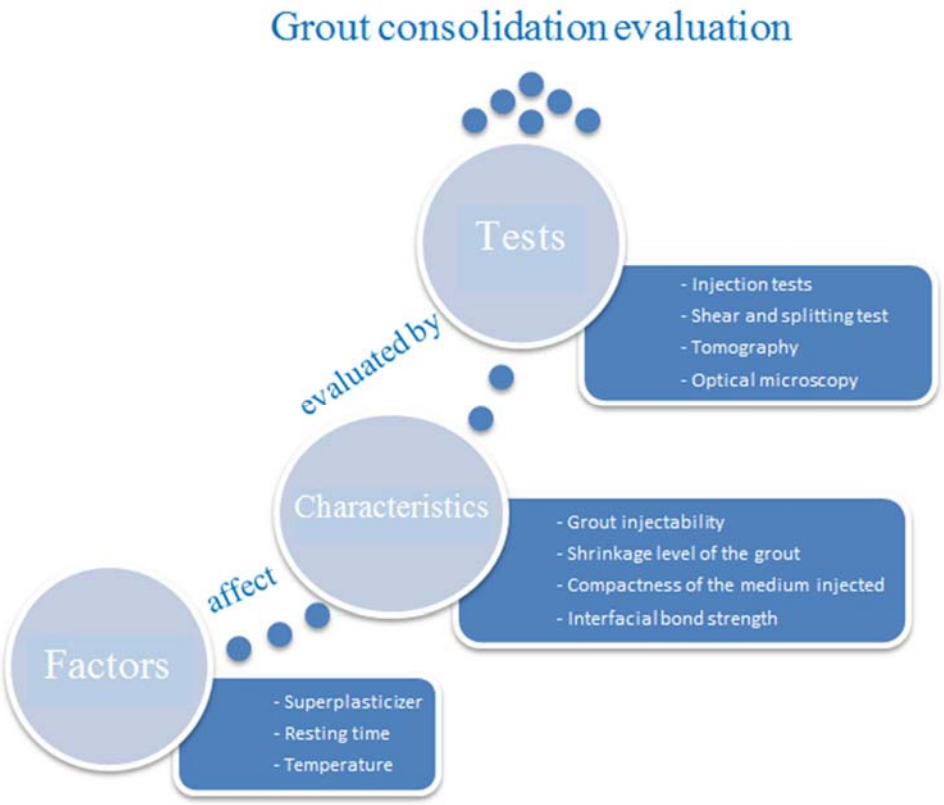

Fig. 6.1 – Grout consolidation evaluation

6.2 Grout design

The choice of a suitable grout to increase the consolidation within the old masonries is dependent on the properties of hardened grout, as well as of fresh grout. The fresh grout properties were reported in chapter 5.3. Regarding the hardened state, in order to improve the mechanical behaviour of the old masonry injected, a suitable mechanical resistance and good bonding properties of the grout should be chosen. These characteristics may be affected by many parameters, namely the type of binder, the water/binder ratio, the type and percentage of superplasticizer and the curing temperature. Taking account the findings reported in the literature where the materials studied were the same (Baltazar et al., 2014, 2013; Bras & Henriques, 2012; Miltiadou-Fezans & Tassios, 2012; Valluzzi, 2005), the HL5 hydraulic lime - EN459-1 (binder), the Glenium Sky 617 (SP) and a water/binder content (0.5) were chosen. According to Baltazar et al (Baltazar et al., 2014), for a water/binder ratio lower than 0.5, the water available may not be enough to ensure a plenty lime hydration. On the other hand, a water/binder ratio higher than 0.5 can result in a weak porous structure, and hence in a lower mechanical strength. The dosage of SP was investigated and varied in the range 0.4 -1.6 wt%. Furthermore, three different curing temperatures (5, 20 and 40ºC) were evaluated.

6.3 Grout mechanical properties

In order to check the influence of the grout mechanical strength on the grout consolidation of old masonry wall, a testing campaign was undertaken. All samples were submitted to compressive and flexural strength tests following standard (EN 1015-11, 1999). The flexural strength of the grouts was

measured on 40x40x160 mm prismatic specimens, whereas the two broken halves were used for the determination of compressive strength. The test machine was a Z50 Zwick with 50 kN loadcell. For flexural strength determination, a pre-load of 10N was first applied and then a loading rate of 0.2 mm/min until the failure. With respect to compressive strength, the pre-load was equal to 50N and the loading rate was 0.7 mm/min. The variations on compressive and flexural strength of grouts at the maturity age of 28 days with different SP dosages and different curing temperatures are given in Table 6.1 and Table 6.2, respectively. Each test was repeated on six specimens and arithmetic average of the test results is presented.

As stated by Demir and Baspinar (Demir & Serhat Baspinar, 2008), SP does not react by a chemical action on hydrated products, even so it affects the grout microstructure and changes the morphology and size of lime hydration products (changing the porosity - Table 6.3). From Table 6.1, the increase of SP is advantageous for the grout mechanical strength. Such result can be explained through the higher dispersion of the mixture resulting in a higher hydration rate (there is a better wettability of the binder particles). The optimum SP dosage is equal to 1.2wt%. The 1.6 wt% dosage exhibited the lowest results due to instability phenomena that were observed in chapter 5.3.1.3. For this reason, grouts with this SP dosage were not used in the injection tests.

Table 6.1 - Influence of SP dosage on grout compressive strength and flexural strength results at 28 days and 20ºC of curing temperature

	SP dosage (wt%) %			
	0.4	**0.8**	**1.2**	**1.6**
Compressive strength [MPa]	4.11 (5,8)	4.92 (8,1)	5.32 (4,7)	3.25 (8,9)
Flexural strength [MPa]	1.12 (8,7)	1.64 (7,7)	2.36 (8,2)	1.01 (9,3)

* Coefficient of variation is indicated in brackets (%)

The curing temperature can influence the hydration rate (Arrhenius law) and, thus the stability and the transformation of the hydrates (Rojas & Cabrera, 2002). In the case of high temperature (40ºC), the initial fast hydration causes more rapid precipitation of the hydration products. This fast hydration in the initial stage leads to a more heterogeneous distribution of the hydration products, which results in a coarser porosity (Table 6.3) and a weaker interlocking between hydrates (Lothenbach et al., 2007). So, a lower value of mechanical strength (compressive and flexural strength) is obtained to high temperatures (Table 6.2). On the other hand, when the curing temperature is low, the start of hydration is slower, allowing more time for diffusion of the dissolved ions before the hydrates precipitate. Thus, the hydrates are more homogeneously distributed resulting in a lower porosity (Table 6.3) and stronger interlocking between hydrates (Lothenbach et al., 2007) and therefore in a higher mechanical strength (Table 6.2). However, the maximum values of mechanical strength are not attained at 5ºC (lower temperature studied), but at 20ºC. As also observed by Mirza et al (Mirza et al., 2013), there is an optimum curing temperature.

Table 6.2 - Influence of temperature on grout compressive strength and flexural strength results at 28 days for grouts with 1.2 wt% of SP

	Temperature (ºC)		
	5	**20**	**40**
Compressive strength [MPa]	3,90 (5,5)	5.32 (11)	2.87 (7,6)
Flexural strength [MPa]	1.71 (5,8)	2.36 (5.3)	0.91 (11.6)

* Coefficient of variation is indicated in brackets (%)

Regarding the physical characterization, the mass loss, shrinkage and porosity of each grout were taken into account (Fig. 6.2, Fig. 6.3 and Table 6.3, respectively).

Fig. 6.2 shows that the mass values decreased between 20-30%. The influence of SP dosage is low. All grouts show the same trend and similar mass loss. In contrast, there are significant differences when the curing temperature changes. When the curing temperature is equal to 40ºC, a high water quantity is released by evaporation and thus the mass loss is higher (Fig. 6.2 –right). The evaporation rate depends on several factors. The temperature is definitely a major factor.

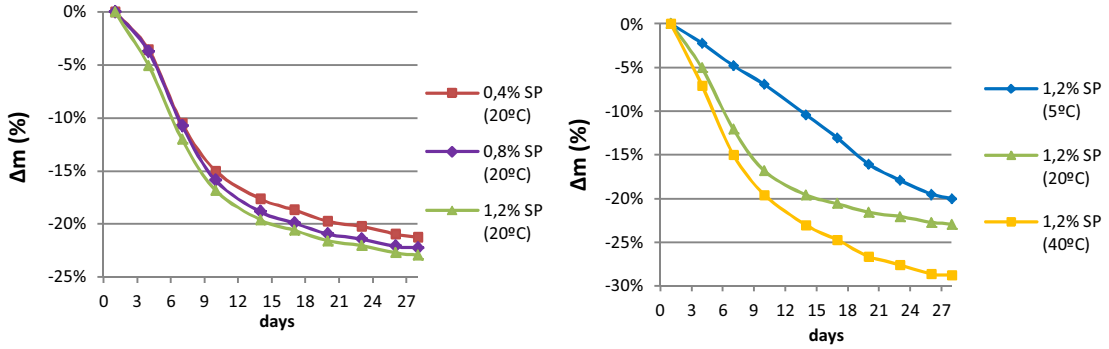

Fig. 6.2 – Mass loss during the curing time; for different % of SP (left) and different temperatures (right)

According to (Brás, 2011), the evaluation of grout shrinkage is important since the formation of shrinkage cracks induces additional stress that can affect the interface mechanical bond (i.e. the adhesion) between grout and PM particles. In order to reduce the micro-cracking along the interfaces, Mirza et al (Mirza et al., 2013) stated that the reduction of grout shrinkage is required.

Grout cumulative shrinkage measurements (autogenous and drying shrinkage) were performed using prismatic specimens (4x4x16 cm3). These specimens were removed from the moulds 24h after being mixed and stored at temperature of 5, 20 and 40ºC. Length changes of the prisms were measured along the curing time using a length comparator.

The drying shrinkage is the shrinkage occurred during the drying phase of the specimens (more significant during the first 3 days - see Fig. 6.3). It can arise through the evaporation of the water molecules held by capillary tension in small capillaries (5–50 nm), as well as from the water removed in surface area of C-S-H (Wongkeo et al., 2012). For this reason, the shrinkage phenomenon was more pronounced at 40ºC (Fig. 6.3-right). For this temperature, the loss of capillary water (due to the evaporation) is high, which contribute to the volume change of the material (and therefore the tensile stress is developed) and thus increasing the degree of drying shrinkage (Mirza et al., 2013). In general, the shrinkage tends to stabilize after the tenth day.

The influence of SP is less significant than the temperature. According to Fig. 6.3-left, a higher dosage of SP causes lower cumulative shrinkage. The higher resistance obtained at higher dosages of SP (SP increases the hydration rate - Table 6.1) enables to counter the drying shrinkage (Alsayed, 1998).

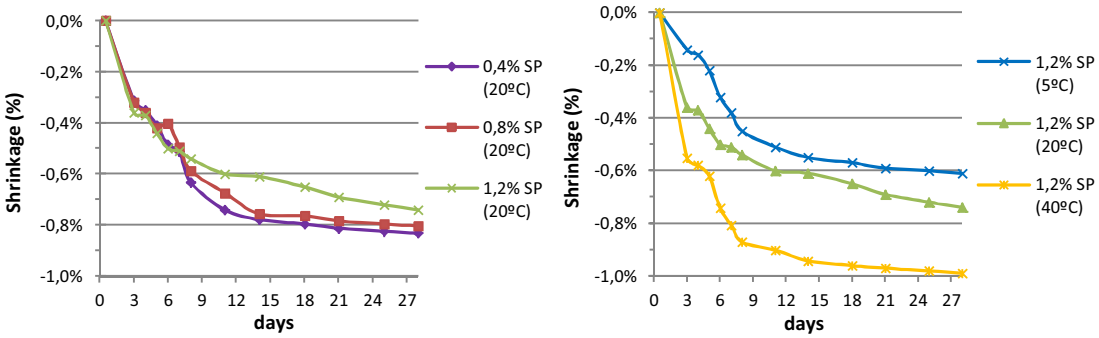

Fig. 6.3 – Cumulative shrinkage (%), for different % of SP (left) and different temperatures (right)

As already mentioned, the grout microstructure is influenced by SP dosage. Table 6.3 shows that the dosage 1.2wt% leads to a more robust grout microstructure (lower porosity), which is consistent with the compressive strength results (Table 6.1). The same correlation was observed for the temperature.

Table 6.3 – Porosity of the grouts

	SP dosage (wt%); T=20ºC				Temperature (ºC); %SP=1.2		
	0.4	**0.8**	**1.2**	**1.6**	**5**	**20**	**40**
Porosity (%)	48.8 (4.3)	48.4 (5.6)	40.6 (3.6)	49.3 (7.3)	48.8 (3.2)	47.6 (3.9)	50.7 (5.3)

* Coefficient of variation is indicated in brackets (%)

6.4 Physical and mechanical properties of the PM injected

6.4.1 Experimental details

Since the main purpose of grout injection is the structural consolidation of old masonry, the approach chosen was to evaluate the mechanical properties of the injected structure. Using the injected cylinders that were analysed in 5.3.3, the mechanical properties are evaluated at 45 days after mixing. The injected cylinders were placed and cured in the chamber at temperatures of 5, 20 and 40ºC. Subsequently, a physical and mechanical evaluation was performed.

The Plexiglas cylinders were removed from the hardened samples and the ultrasound pulse velocity was measured in order to obtain the tomographs (Fig. 6.4-1). After that the cylinders were cut in 3 slices (Fig. 6.4-2) and each of these slices was measured (Fig. 6.4-3). Thereafter, the shear strength and tensile splitting were determined (Fig. 6.4-4 and Fig. 6.4-5).

Fig. 6.4 - Ultrasound pulse velocity test (for a cylinder); 2) slice of the cylinder; 3) measure of the cylinder; 4) and 5) shear and splitting test, respectively (for a slice of cylinder)

6.4.2 The mechanism bond – interfacial bond strength

Interfacial strength is related to the interfacial bonding between grout and PM particles. The thinner the interfacial bonding, the higher the interfacial bond strength (Caliskan, 2003), regardless of types of the PM particles. In general, this interfacial bonding between grout and PM particles is a weak interfacial zone where cracks propagate preferentially. The formation of this weak interface is due to the water filled spaces around the PM particles (microbleeding water) and the wall effect of packing of hydraulic binder grains against the relatively flat PM particle surface (Rao & Prasad, 2002; Xuan et al., 2009). The result is that a zone closest to the PM particle contains predominately small grains and has a significant higher porosity, while larger grains are found further out. This phenomenon is a random process resulting in a heterogeneous interface bonding (Scrivener et al., 2004).

The nature of the interfacial zone depends on the microstructure characteristics of the PM particles. Three types of mechanisms are possible at the interface: physical interaction, physical – chemical interaction and mechanical interlock (Rao & Prasad, 2002). Regarding this work, as the particles of PM show smooth surface, if only physical interaction takes place, the interfacial bond strength should not be high. Other mechanisms must be relevant, namely the chemical interactions where the surface can interact with the hydration products of the grout matrix resulting in a very strong bond. Moreover, the grout matrix should penetrate in the pores resulting in a significant mechanical interlock (Rao & Prasad, 2002). In order to analyse this phenomenon, the importance of the SP (which provides the deflocculation of the hydraulic lime particles), as well as the curing temperature (associated with different resting times) are studied subsequently.

6.4.3 Splitting Test

The indirect tensile strength test was carried out according with ASTM C 496 test procedure. This test consists on applying a compressive force along the length of a cylindrical specimen at a prescribed rate until failure occurs (Fig. 6.4 - Fig. 6.6). To apply the load along two opposite longitudinal lines and prevent possible irregularities on specimen lateral surface from causing stress accumulation, two wood stripes (5 mm thick, 15 mm width) were inserted between the loading platens and the specimen (Fig. 6.6-b). The load applied induces tensile stresses on the plane perpendicular to the load. The test is considered valid only if the failure occurs along the load direction in the middle of the specimen (as shown in Fig. 6.6-b).

The tensile strength is calculated at the theoretical failure section where the tensile stress is maximum:

$$T = \frac{2F}{\pi \times l \times \emptyset} \qquad (6.1)$$

where T is the splitting tensile strength (MPa), F the maximum applied load indicated by the testing machine (N), l the length (mm), and $\emptyset$ is the diameter (mm).

The diameter of the samples is 144 mm and the height 80 mm, a value that is lower than the prescription of the standard. This reduced height was required to allow the evaluation of the effectiveness of the injection at three different levels.

Making a parallelism with the old masonries, the results of tensile splitting tests of cylinders (which represent the inner core of the strengthened masonry wall) can be used to estimate the ability of grout to improve the tensile strength of ancient masonry walls with this type of pore size distribution (Uranjek & Bosiljkov, 2012).

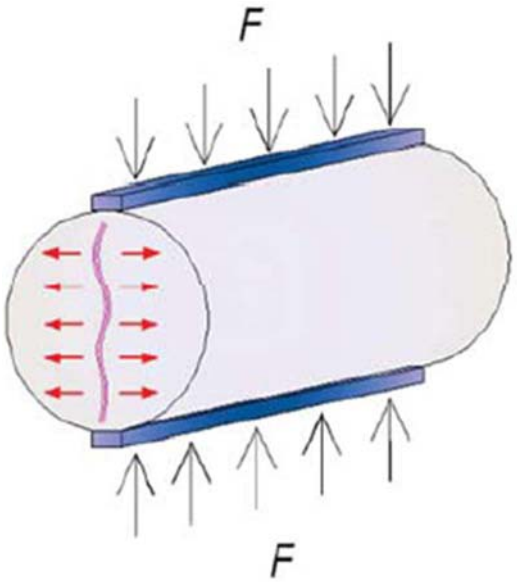

Fig. 6.5 – Compressive force and failure mode in splitting test (Luso, 2012)

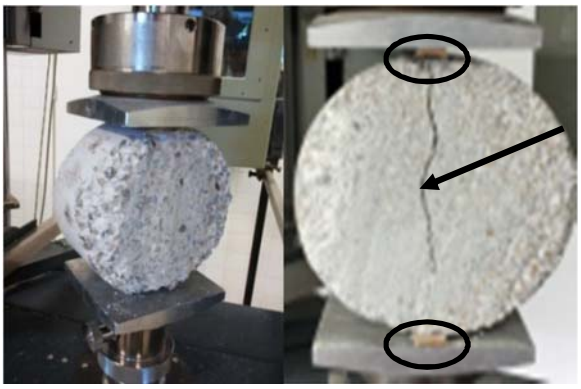

Fig. 6.6 - Device adopted for the splitting test. a) the specimen prior to the test -and b) after the test with the crack on the plane containing the applied load

6.4.4 Direct-shear test

As regards the resistance to seismic action, masonry shear strength is the most important parameter to be evaluated. A number of tests have been proposed so far to define the characteristic shear strength - τ (Mazzotti et al., 2014). The test adopted is based on the triplet test (defined by EN 1052-3) which allows quantifying the shear bond strength of the sample through sliding shear failure (Caliskan, 2003; Milosevic et al., 2013). This test enables to evaluate the interfacial bond between grout and PM particles, as well as the interlocking effect of the PM particles along the failure surface. Together with splitting tensile strength, the shear bond strength evaluates the interfacial bond strength between the materials of PM injected.

The test apparatus is schematized in Fig. 6.7. A metallic plate with 20 mm thick was positioned under a half part of the specimen. The load was applied on the top of other metallic plate that was positioned on the other half part of the specimen. Through metallic plates, a good stress distribution and a good contact between the specimen and the plates of the loading machine used for applying compression load was ensured.

Fig. 6.7 - The apparatus of the shear test (based on triplet test) and the crack pattern of specimen after the shear test

This test allows the evaluation of the adhesion/cohesion between grout and PM particles and the measuring of the maximum shear bond strength – τ_{DS} (MPa) by applying only one equation (Eq.6.2):

$$\tau_{DS} = \frac{F_V}{A} \tag{6.2}$$

Where F_V [N] is the ultimate shear load and A [mm^2] is the area of sliding shear failure (Fig. 6.7) which is given by the product of the height and the diameter of the cylinder);

6.4.5 Tomographic calculations

Given the objective of the work, it was decided to use tomography to evaluate the effectiveness of grout injection. As in other works of literature (Da Porto et al., 2003; Valluzzi et al., 2009), it was evaluated the penetration and diffusion of the grout into the PM by evaluating its compactness after injection (Bosiljkov et al., 2010; Da Porto et al., 2003)(Cantini et al., 2012). As explained below, the zones where the grout cannot penetrate are detected by tomography.

Considering the small size of the models used in the laboratory, the use of ultrasonic tomography (the tomographs are generated from the ultrasonic results at a frequency equal to 54 kHz) is more suitable. The ultrasonic test was done according to ASTM C597-09, and it is explained in detail in 8.3.3. The ultrasonic tomography enables the creation of a tomographic image that is a map of the velocity distribution on a plane section of the structure under investigation (Concu et al., 2009). As the ultrasound velocity depends on the compactness of the PM injected (i.e., depends on the presence of voids), the performance of grout injection in such PM can be analysed through the tomographs (Concu et al., 2010; Ferraro et al., 2013; Schullerl et al., 1997). To obtain the ultrasonic tomographs along the height of the cylinder, a system of measuring points, i.e., a mesh grid was established (see 8.3.4). The data collected in this mesh grid are processed in GEOTOM CG software through an iterative method (SIRT algorithm) and the outputs are tomographs (2D and 3D) of the cylinder analysed (see 8.3.4).

6.4.6 Optical microscopy

The interfacial zone between grout and PM particles plays a major role in controlling the bond properties and consequently may strengthen or weaken the PM injected. For this reason, it was studied using optical microscopy. The porosity and the bond between materials at the interface were the main focus of the investigation.

Following the mechanical testing, samples (inside the PM injected) were selected and cut to gain samples of approximately 30mm x 30mm x 15mm. An appropriate surface preparation was carried out including grinding, polishing and protecting the surface with an epoxy resin with fluorescence dye to prevent damage of the air void edges (Alterman et al., 2014). The resin used was the EpoFix that is a cold-setting resin based on two fluid epoxy components (resin and hardener) (Table 6.4). Epofix is specially developed for impregnation of porous specimens. Due to its low viscosity, EpoFix can penetrate into the majority of pores and cracks of the specimens. In addition, it shows a low shrinkage and good mechanical properties in the cured state.

Table 6.4 - Technical data of EpoFix Resin provided by the manufacturer

Components	Resin/Hardener
Mixing ratio vol/vol	15/2
Mixing ratio weight/weight	25/3
Pot life	30 min *
Curing time	8 hours *
Max. temp. while curing	75°C
Linear shrinkage	insignificant
Viscosity	550cP (20°C)/150cP (50°C)
Moulds	silicone, phenolic, polyethylene

*for 30g and temperature equal to 20°C

To prepare the samples, the procedure followed was:

1. Degrease the specimen before it is placed in the mould
2. Mix 15 parts by volume of resin with 2 parts by volume of hardener in a paper cup and stir carefully for at least 2 minutes.
3. Heat the Epofix mixture at 50°C in order to obtain a mixture with a lower viscosity, thereby ensuring a greater penetration into the pores of the specimens.
4. For porosity measurements, or to obtain a contrast, Epofix can be colored by adding Epoxy - Dye to the resin before mixing (Fig. 6.8-a).
5. Pour the mixture carefully over the specimen in the mould, so that no air bubbles are caught, and let the mixture harden. The air within the sample is removed using a desiccator (Fig. 6.8-b and c).
6. After curing, Epofix can be cut, ground, polished, grilled, etc. (Fig. 6.8-d and e).

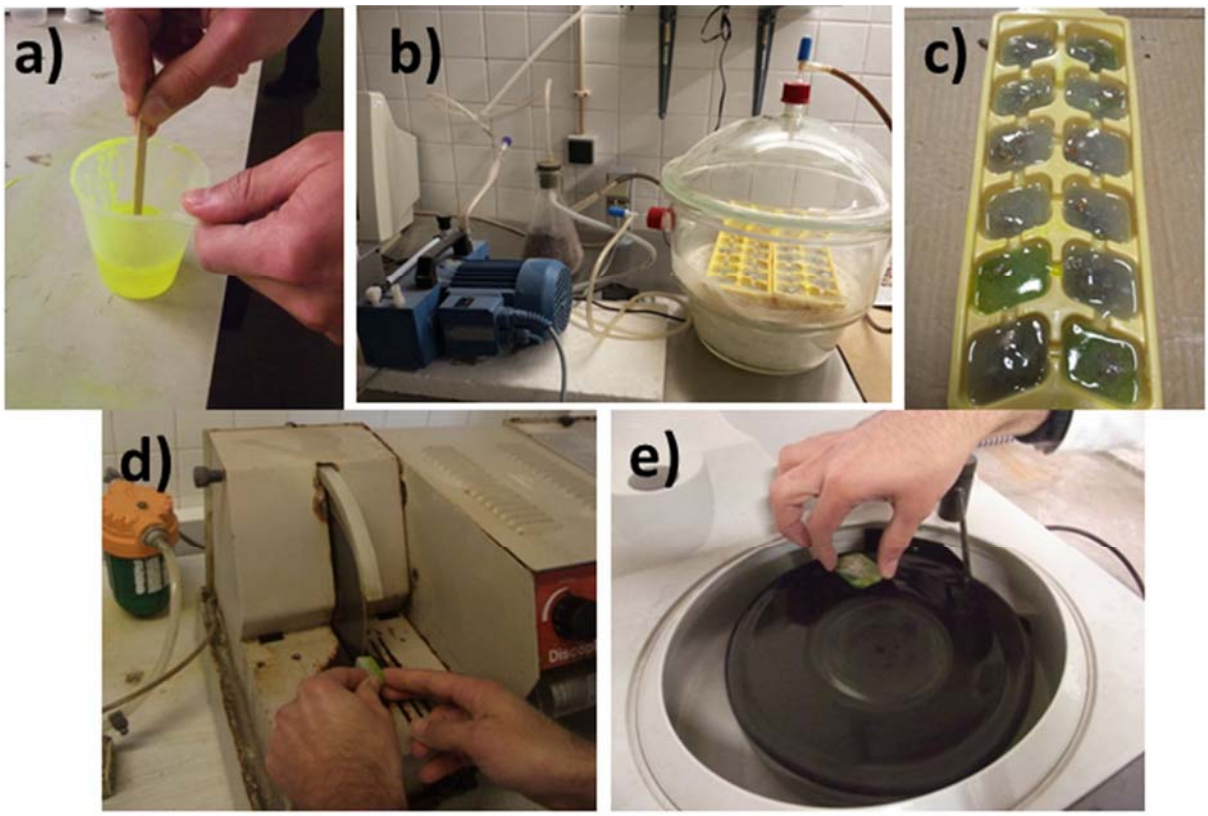

Fig. 6.8 - Preparation of the samples that are observed in Olympus microscope

An image of the interface zone, using an Olympus microscope (Fig. 6.9) capable of 70x magnification was carried out. The aim was to evaluate the compactness/density of the interfacial zone. It was found that the magnification equal to 7x and 20x produced the most useful images for the image analysis.

Fig. 6.9 –Optical microscopy using an Olympus microscope

6.5 Results and Discussion

6.5.1 Splitting Test, Direct-shear test and Optical microscopy

The results of mechanical tests of injected cylinders showed, that the behaviour of the PM after grout injection is significantly influenced by the injection's grout ability to fill the voids among PM particles and to establish a good interfacial bond with PM particles (Mojmir et al., 2012). Regarding this issue, Uranjek and Bosiljkov (Uranjek & Bosiljkov, 2012; Uranjek et al., 2014) inspected the split surfaces of the cylinders (PM injected) after mechanical tests. They observed that the prevailing mode of failure in tensile splitting test was through the bond between the PM particles and the grout – adhesive failure, regardless of injected grout. This kind of failure means that the interfacial bond strength value is lower than the tensile strength value of the grout and PM particles itself (cohesive failures).

As observed in Table 5.6, the SP dosage and resting time have much influence on grout injection capacity. Such fact was confirmed through visual observations on the cylinders (Fig. 6.10) and cross-section of the cylinders (Fig. 6.11) and optical microscope image (Fig. 6.12). For this reason, the results obtained in both mechanical tests (Table 6.5) have a high variation depending on the SP dosage (together with resting time) used in grout injection. The SP enables the deflocculation of the hydraulic lime particles, increasing the grout injectability (more voids filled - Table 5.7) and therefore a stronger mechanical interlock with the PM particles along the failure surface is established (Rossignolo, 2009). Furthermore, a denser bond between grout and PM particles is achieved, since the spaces between PM particles (i.e. porosity) are significantly reduced (Fig. 6.12). Thus, the grout with the best injectability capacity (1.2 wt% of SP - Table 5.6) shows the best interfacial bond strength (Table 6.5), which confirms that a good adhesion (bond) along the interfaces grout-PM particles is dependent on the grout injectability. Regarding the splitting tensile strength, the increase was in the range of 0.52-1.13 MPa for resting time equal to 0min, and 0.43-0.95 MPa for resting time equal to 60min. Similar trends were observed for the shear bond strength (Table 6.5). In fact, the maximum shear bond strength was

reached for grout with the best injectability (1.2wt% SP at 0 min) and the minimum was reached for grout with the lowest injectability (0.4wt% SP at 60 min). As observed the shear bond strength can be significantly different (depending on the grout injectability), nevertheless, the same sliding shear failure mode was observed in all the shear tests (Fig. 6.13).

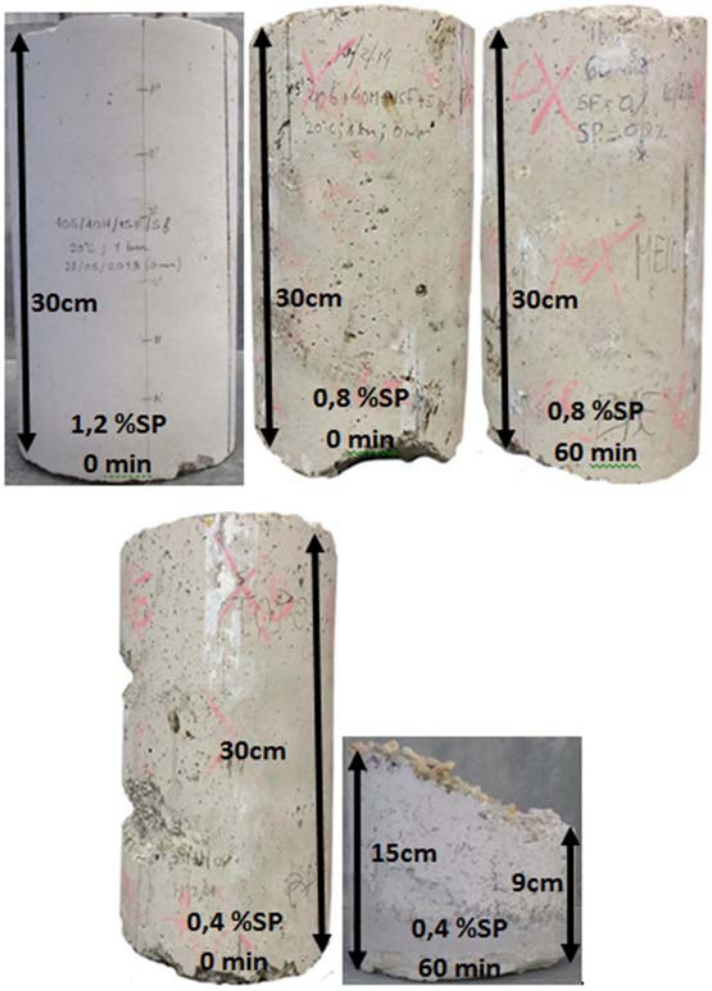

Fig. 6.10 – Inspection of the cylinders after curing time

Fig. 6.11 - Top view of slices at bottom level

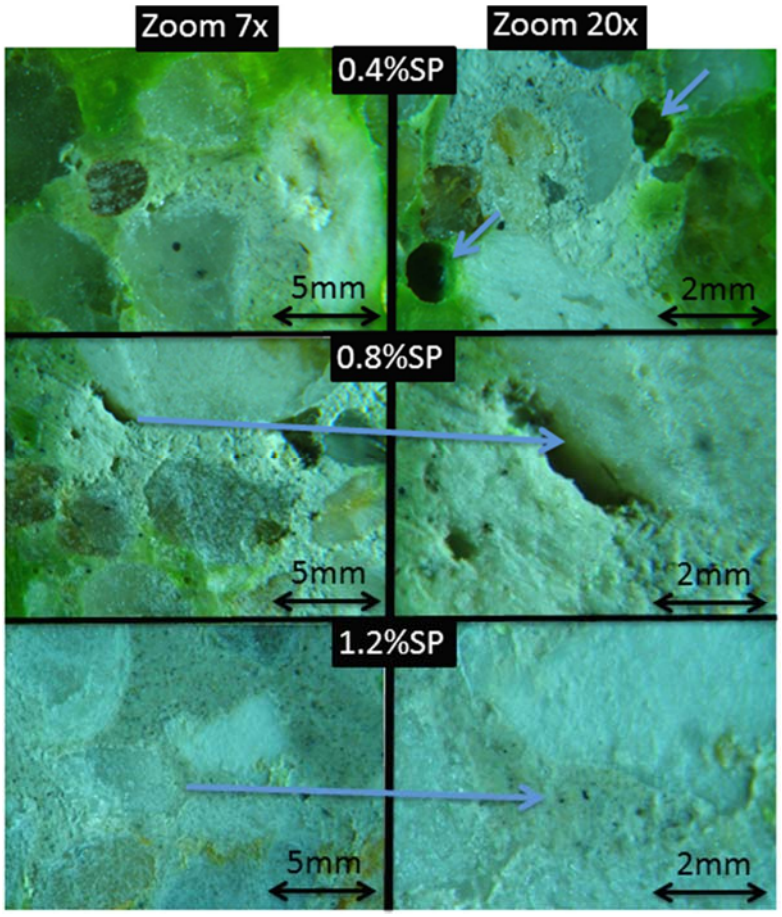

Fig. 6.12 – Different grout injectabilities for different SP dosages in grout composition (optical microscope image); the green colour (impregnation of the resin) represents the voids of the samples analysed

Fig. 6.13 - Sliding shear failure mode

The importance of the adequate SP dosage (which enables the deflocculation of the hydraulic lime particles) is more evident when the resting time increases. As already observed in injection tests (Table 5.7), in mechanical tests when the resting time is equal to 60 min, the results are very poor for lower SP dosages (Table 6.5). Under these conditions, the grout rheological behaviour is no longer suitable for obtaining a satisfactory injectability.

Table 6.5 – Splitting tensile strength and shear bond strength for grouts with different wt% of SP injected at 20ºC

Porous medium		Splitting tensile strength [MPa]					Shear bond strength [MPa]				
		Bottom	Middle	Top	Average	Gradient [MPa/m]	Bottom	Middle	Top	Average	Gradient [MPa/m]
0 min	0,4%SP	0,50	0,65	0,41	0,52	-0,56	0,98	1,05	0,73	0,92	-1,56
	0,8%SP	0,70	0,70	0,62	0,67	-0,50	1,12	1,05	0,90	1,02	-1,38
	1,2%SP	1,10	1,20	1,10	1,13	0,00	1,87	1,93	1,66	1,82	-1,31
60 min	0,4%SP	0,43	X	X	0,43	X	0,78	X	X	0,78	X
	0,8%SP	0,64	0,66	0,51	0,60	-0,81	1,15	1,10	0,98	1,04	-1,75
	1,2%SP	1,01	0,95	0,89	0,95	-0,75	1,61	1,71	1,34	1,55	-1,69

According to injection results, when the injection temperature is equal to 40ºC and the resting time is null, the grout is considerable injectable (Table 5.5). The performance is even better than 5ºC. Nevertheless, the curing temperature of 40ºC shows the worse mechanical results. As observed in 6.2 and by other authors (Mirza et al., 2013), the curing temperature is also a factor with influence on the physical and mechanical behaviour of the hydraulic lime grouts (Fig. 6.3 and Table 6.2). As already referred, the curing temperature can influence the hydration rate (Arrhenius law) and, thus, the stability and the transformation of the hydrates (Rojas & Cabrera, 2002). Thus, the high temperatures prejudice the densification of the interface zone (which should be as dense as possible). Since the filling of this region due to the deposition of hydration products (especially calcium hydroxide) is reduced (Scrivener et al., 2004). Indeed, the fast hydration leads to a rapid and heterogeneous deposition of hydration products, which leads to a coarser porosity in interfacial zone.

The shrinkage level is another property that depends on the curing temperature (see 6.2). As seen in Fig. 6.3-right, for higher temperatures the shrinkage level is higher. Given that cracks associated to shrinkage usually appear on the interface grout - PM particles (subtract), the grout adhesion to the surface of PM particles is also dependent on shrinkage level. A low shrinkage is required to achieve a good interfacial bond strength (Silva et al., 2014a) .

Based on the deposition of hydration products and shrinkage phenomenon (Fig. 6.3), it can be stated that the interfacial bond strength is lower (Table 6.6) for higher curing temperatures (40ºC).

Regarding the resting time, the PM with a resting time equal to 0 min have interfacial bond strength on average 1.2 times higher (for splitting tensile strength and shear bond strength) than the PM injected with a resting time equal to 60min. The different injectability performance (studied in 5.3.3.1) is the reason for such result.

Table 6.6 - Splitting tensile strength and shear bond strength for grouts with 1.2wt% of SP exposed to different curing temperatures

Porous medium		Splitting Tensile Strength [MPa]					Shear bond strength [MPa]				
		Bottom	Middle	Top	Average	Gradient [MPa/m]	Bottom	Middle	Top	Average	Gradient [MPa/m]
0 min	5ºC	1,03	1,09	1,03	1,05	0,00	1,79	1,82	1,53	1,71	-1,63
	20ºC	1,10	1,20	1,10	1,14	0,00	1,87	1,93	1,66	1,82	-1,31
	40ºC	0,97	1,06	0,72	0,92	-1,56	1,74	1,69	1,30	1,58	-2,75
60 min	5ºC	1,02	1,00	0,96	0,99	-0,38	1,72	1,73	1,42	1,62	-1,88
	20ºC	1,01	0,95	0,89	0,95	-0,75	1,61	1,71	1,34	1,55	-1,69
	40ºC	0,63	0,87	0,44	0,64	-1,19	1,12	1,05	0,77	0,98	-2,19

The influence of the grout properties on the improvement of mechanical properties of the PM injected were reported by several authors (Kalagri et al., 2010; Uranjek et al., 2014). Regarding the influence of mechanical strength of the grout on the mechanical strength of PM injected, the authors concluded that is reduced. Kalagri *et al* (Kalagri et al., 2010) stated in particular that the compressive strength of the grout is not the decisive property in order to increase the strengthening of the PM. For these authors, the fresh grout properties that influence the injectability capacity have higher preponderance. Based on the results obtained, it is confirmed a good correlation between grout injectability and the mechanical strength of the PM injected.

6.5.2 Tomography

Regarding the SP dosage, the velocities presented in Fig. 6.14 show a remarkable scatter, varying between 510 and 2880 m/s. Concerning the resting time equal to 0 min, the average velocity value for grouts with 0.4 %SP corresponded to 1350 m/s and 2450 m/s for grouts with 1.2 %SP. These results seem to indicate that the injection of the grout 1.2 %SP was successful in filling the significant voids of the PM (Fig. 6.15), which is in accordance with mechanical results (Table 6.5) and injection tests (Table 5.6). In contrast, low velocity values are encountered in some zones of the PM with 0.4 %SP (Fig. 6.15) which means a lower injectability of the grout in these zones. The tomographs suggest that this grout is severely affected by the plug formation and consequent obstruction of the voids (see 5.3.3.2). This is confirmed by visual observation where some voids were detected (Fig. 6.16). Furthermore, a remarkable difference was noticed between the bottom slice and the top slice (Fig. 6.14). Actually, a negative gradient velocity is observed due to decrease of the ultrasonic velocity along of the PM. These results confirm the mechanical results shown in Table 6.5.

When the resting time is equal to 60 min, the ultrasonic values shown in tomographs are quite lower in comparison with grouts injection with resting time equal to 0 min. Moreover, the ultrasonic velocities showed a significant scatter, especially the PM injected with grout 0.4 %SP (with minimum and maximum values of 500 and 2750 m/s, respectively).

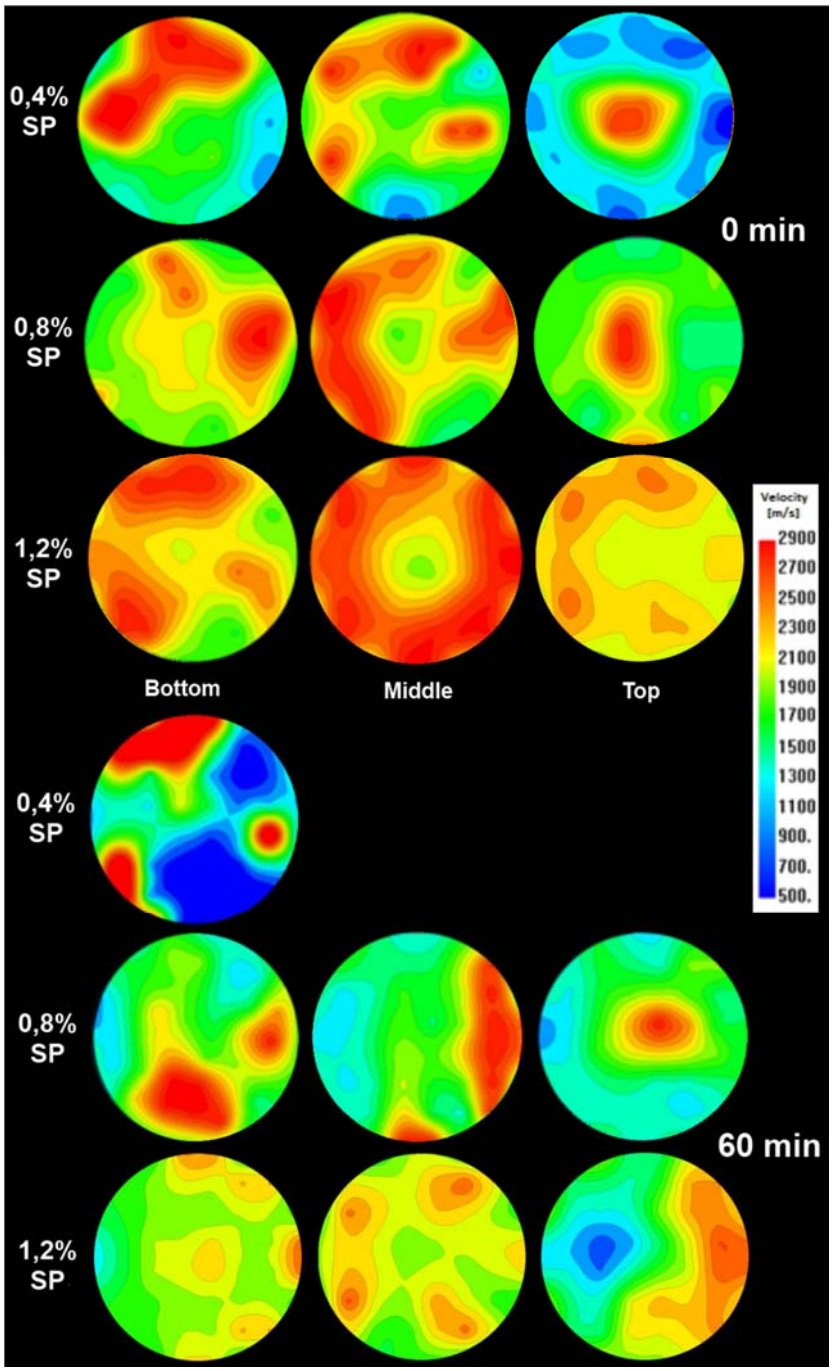

Fig. 6.14- Ultrasonic horizontal tomography for cylinders injected with grout with different wt% SP at the temperature 20°C and the resting time: 0 and 60 min

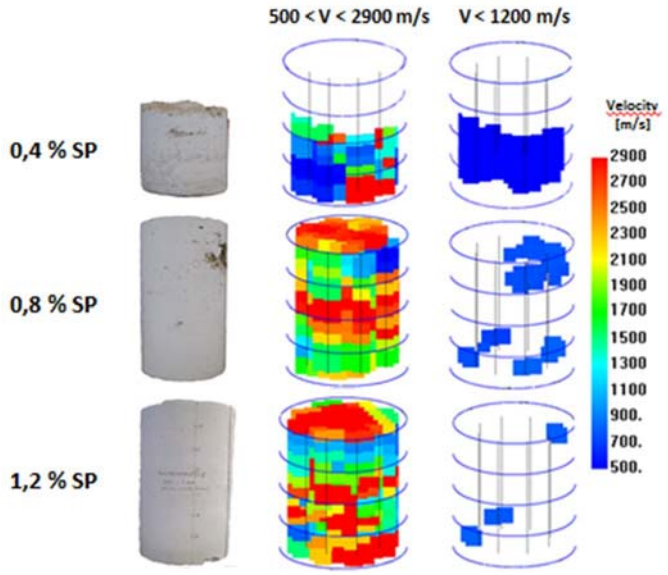

Fig. 6.15 – 3D ultrasonic horizontal tomography for cylinders injected with grout with different wt% SP at the temperature 20°C and the resting time: 60 min, V< 1200m/s represents the voids

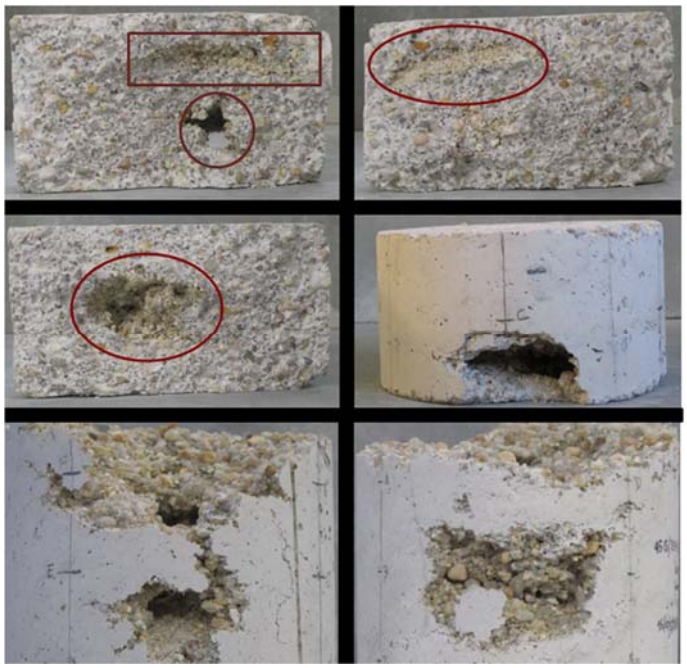

Fig. 6.16 - Slices of cylinders 0.4 wt% SP with voids due to the plug formation and consequent obstruction of the void

Fig. 6.17 shows that the ultrasonic pulse velocity decreased at higher temperatures (for any resting time), indicating that the PM injected was less dense and more porous. In fact, the lower ultrasonic velocities were measured for temperature equal to 40 °C. The mean value of ultrasonic velocity for resting time = 0 min was equal to 1950 m/s, and decreased to 1400 m/s when the resting time = 60min. Indeed, in the latter case there are significant voids that were not successfully filled (Table 5.5). As observed in the tomographs (Fig. 6.17) there is a considerable area with ultrasonic velocity lower than 1200 m/s. On the other hand, the higher ultrasonic velocities were generally obtained when the specimens were injected and cured at 20 ºC, showing the importance of curing temperature (besides

the injection temperature) in attaining a good compactness of the PM. In fact, when the curing temperature is not high, the hydrates are more homogeneously distributed (the dissolved ions have more time for diffusion before the hydrates start to precipitate) resulting in smaller pores (Lothenbach et al., 2007). In the case of resting time = 60 min, the tomographs of the temperature equal to 5 ºC have the highest ultrasonic velocities. As concluded in 5.3.2 and as shown in Table 5.5, for lower temperatures the fresh grout properties are properly maintained during the resting time due to the delay of the hydration reactions.

As observed in all tomographs, the increasing of velocity (related to the reduction of attenuation) in the medium slices suggests an increase in density and homogeneity. This improvement was confirmed by the mechanical tests (see Table 6.6), which show an increase in resistance capacity for the medium slices. This trend was verified for both resting times (0 and 60min). In top slice the tomographs seem to suggest a decrease of the compactness and homogeneity (Fig. 6.17). The existence of ultrasonic velocities lower than 1200 m/s indicates the presence of significant voids in the top slice (especially for cylinders with higher temperature and resting time), which means a bad level of consolidation – confirmed by mechanical results (Table 6.6).

As concluded in other works of the authors (Da Porto et al., 2003; Mojmir et al., 2012), the ultrasonic test has sensitivity to evaluate the effectiveness of the grout injection. Thus, the huge variability of the ultrasonic velocities (shown in the tomographs - Fig. 6.14, Fig. 6.15 and Fig. 6.17) is related to the different amounts of grout injected (i.e. different injectabilities of grout), which is consistent with the results of injection tests (5.3.3).

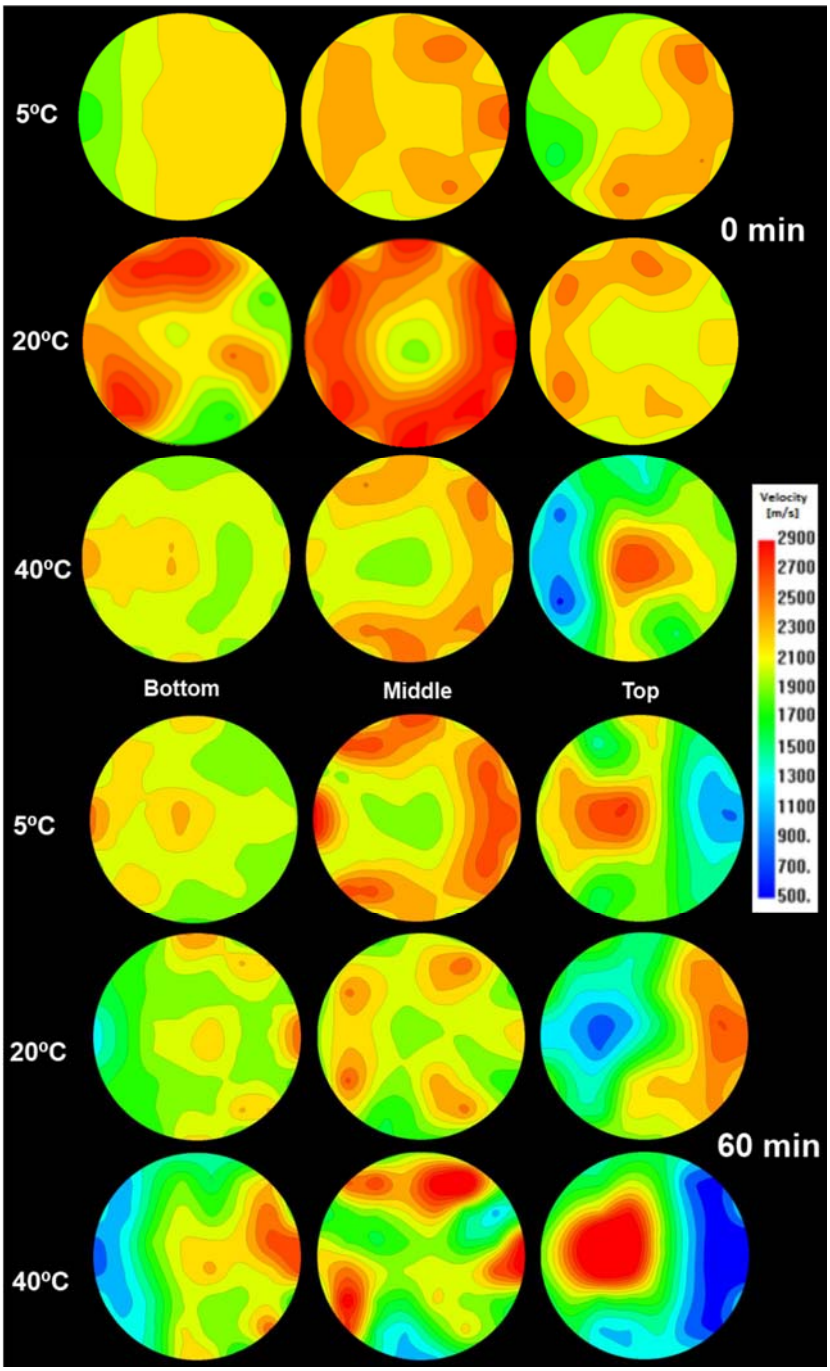

Fig. 6.17 - Ultrasonic horizontal tomography for cylinders injected with grout with 1,2wt% SP at the temperatures: 5, 20 and 40°C and the resting time: 0 and 60 min

6.6 Conclusion

The following remarks can be drawn from the evaluation of the results of the experimental research carried on:

- The results confirmed that the mechanical properties of the grout (compressive and flexural strength) are not the main factors that control the mechanical strength of the PM injected. The grout injectability (with influence on the compactness / cohesion of the PM after injection), as well as the interfacial bond strength (evaluated by splitting tensile strength and shear bond strength) between grout and PM

particles have more importance. The grout shrinkage level (which is related to the cracks that appear on the interface grout - PM particles) is one of the main factors that can affect the interfacial bond strength (the ability of the grout to achieve a solid bond with PM particles). The SP dosage and especially the curing temperature showed a significant influence on the grout shrinkage level.

- The injection and curing temperature have influence on the compactness of the PM after injection. The best results are dependent on the resting time value. 20ºC of temperature is the best for 0 min and 5ºC is the best for 60min. The temperature 40ºC exhibits the worst results, especially for resting time = 60min when the grout injectability is low (fresh grout properties are severely affected). Moreover, in the case of high curing temperature, the fast hydration in the initial stage leads to a more heterogeneous distribution of the hydration products which results in bigger pores (coarser porosity) and, consequently, lower interfacial bond strength (lower interlocking and adhesion between grout and PM). In addition, for this temperature, the level of grout shrinkage is high which also contributes to affect the interfacial bond strength.

- SP enables the deflocculation of the hydraulic lime particles, increasing the grout injectability and therefore a stronger mechanical interlock with the PM particles along the failure surface (adhesive failure) is established. The 1.2wt% dosage has the best results (especially for resting time = 60min).

- Regarding direct-shear test, the same failure mode (sliding shear failure) was observed in all PM. Nevertheless, the shear bond strength is significantly different, depending on the injectability of the grout and the adhesion at the PM-grout interface (interfacial bond strength).

- Tomographs and mechanical tests showed a decrease in compactness and homogeneity at the top slice of the cylinders (especially for cylinders with higher temperature and resting time) – the farthest area from the initial injection point.

Chapter 7. Injection capacity of hydraulic lime grouts in different porous media

7.1 Introduction

Grouts for injection should be adequately designed to achieve the best performance from the injectability point of view. This means that fresh grout properties, such as rheological properties are of prime importance, since adequate rheological properties are an essential criterion to allow the correct flow of the grout inside the masonry to ensure the filling of the voids (Kalagri et al., 2010; Valluzzi, 2005). The most important rheological parameters are the plastic viscosity and the yield stress (that were analysed in Chapter 5). Other important properties are the granularity of the binder before mixing (Ignoul et al., 2004), since both rheology and penetrability depend on the particle size of the grout. According to Eriksson (Eriksson, 2002) the most important PM features affecting penetrability are aperture size, variability in aperture and magnitude of contact areas, sometimes referred to as tortuosity. In relation to this issue, the aim of this work is to investigate how the penetration of hydraulic lime grouts stops or gets blocked, and to increase the understanding for the different mechanisms affecting this effect. The stop mechanisms are important to consider during grouting as well as in grouting design in order to understand the processes and to optimise the grouting performance. Research work from different domains of the literature (masonry grouting and soil/rock grouting) has been carried out on penetrability, with some authors defending the importance of the ratio between available opening of the void/channel of the PM to be injected and the maximum particles sizes of the solid phase of the grout (Eklund & Stille, 2008; Miltiadou-Fezans & Tassios, 2013a) and (Axelsson et al., 2009). In the present work, several criteria already established by different authors were evaluated and related with the grout injection capacity of the present study. Thus, it was possible to identify the appropriate criteria to express the penetrability of the grout used in different PM.

The effectiveness of a grout injection depends not only on the characteristic of the mix, but also on the knowledge of wall type (Valluzzi, 2005). Therefore, it is of utmost importance to know precisely the morphology of the wall section, the composition of the materials constituting the wall, distribution and size of cracks and percentage and distribution of voids (Binda et al., 2003a, 1997). It is noted that the permeability and moisture content are also important properties in the assessment of injectability (Van Rickstal, 2000). The relation between the parameters mentioned above (calculated by standard tests) and grout injectability tests is evaluated in the present research.

Injectability tests were used to study the penetrability of grouts. Two materials with different water absorption coefficients were used in order to study the influence of grout water loss to PM in grout injectability. Taking into account the conclusions of the chapter 5.4, the injection setup explained in chapter 5.2.5 was chosen. Different grout injectability results are obtained for the various PM studied. Furthermore, these results are compared with the results obtained by other authors (Bras & Henriques, 2012; Valluzzi, 2005; Van Rickstal et al., 2003), that used similar injection setup and similar PM.

7.2 Literature survey - Penetrability of grout

7.2.1 Penetration capability

The penetrability is related to the filling of the existing voids and fissures, directly contributing to the strength, tightness and durability of the masonry. To do so, the grout should be able to pass through the "narrowest" possible width of such discontinuities and overcome flow-resistances, in order to reach the maximum possible internal volume of masonry voids. The limiting factors appear to be the rheology (flow properties) and filtration tendency (plug formation) of the grout (Eklund & Stille, 2008). Both must be optimised to attain adequate penetration of the grout. According to several researchers (Axelsson et al., 2009; Eriksson, 2002), yield stress is one of the important rheological parameters in predicting penetration capability of fresh grout given that no plug formation has occurred. The filtration tendency is a characteristic (Fig. 7.1) whereby a plug of particles can be formed at a void opening or in a constriction within the void/channel preventing further penetration (Eklund & Stille, 2008).

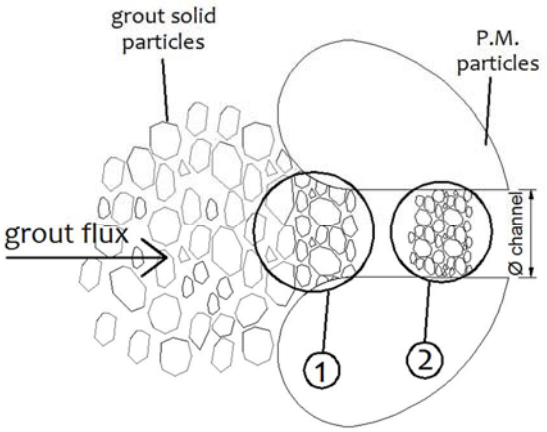

Fig. 7.1 - Plug formation at the entry to a void (1) and obstruction of the void (2). Adapted from (Eklund & Stille, 2008)

The filtration tendency is related to the grain-sizes of the grout. There are various ways of describing directly or indirectly the grain-size distribution. One common method refers to the use of the d_{95} value, which corresponds to the mesh size of a sieve through which 95% of the binder material passes. This value is also used for describing the maximum grain-size, which in reality may not be correct. Therefore, it should be taking into account the increased tendency for small particles to flocculate into larger agglomerates (Eklund & Stille, 2008), when compared to larger grain-sizes. In fact, small grain-sizes are also important in what refers the analysis of filtration tendency of the grout.

7.2.2 Apertures calculated by different methods

The flow path through the PM can be described by means of porosity, pore size distribution, hydraulic conductivity or theoretical aperture. The advantage of using the latter is that it can be easily compared to the particle size of the grout, thus making it easy to describe the injectability.

Two different methods have been used in order to determine the theoretical aperture with sands *b*. One method is to use the Kozeny–Carman equation (Carman, 1956), see Eq (7.1).

$$b_{K-C} = \frac{n}{(1-n) \times S} \times \sqrt{12 \times C_3} \quad (7.1)$$

The shape factor constant (to take into account the shape and tortuosity of channels) C_3 was set at 0.2. This value included simultaneously the notions of equivalent capillary channel cross-section and tortuosity. The porosity n is determined for each PM, as is mentioned in the section 7.3.2, the specific surface S (mm^2/mm^3) is determined from the grain distribution curves, following Eq. (7.2) (Axelsson & Gustafson, 2007) (Table 7.6).

$$S_{S,i-(i+1)} = \frac{\alpha_{i-(i+1)}(p_{(i+1)} - p_i)}{\ln\left(\frac{d_{(i+1)}}{d_i}\right)}\left(\frac{1}{d_i} - \frac{1}{d_{(i+1)}}\right) \quad (7.2)$$

In this equation α (-) is the shape factor (to take into account the shape of the grains, the factor is 6.1 for rounded grains and 7.7 for angular grains), p (%) is the passed amount in a certain sieve and d (mm) is the size of the sieve mesh.

The Eq (7.1) was developed considering the total available volume between the particles of PM. Thereby, it can be considered as a model for determining the available aperture for a Newtonian fluid. The Kozeny–Carman equation was developed for hydraulic characterisation of the sand (in the present chapter the PM studied were considered as sand) and implies that a Newtonian fluid (water) is used. However, since grouting is generally performed with a Bingham fluid, there is a rheological difference. According to Axelsson (Axelsson et al., 2009), b_{eqv} for a Bingham fluid can be expressed using the porosity (n) and specific surface (S):

$$\boldsymbol{b_{eqv} = \frac{8}{\pi \times S \times (1-n)}} \quad (7.3)$$

This expression was developed for a Bingham fluid and, therefore, it is not describing the same available aperture as the previous equation, as illustrated in Fig. 7.2. The shaded area in the right of the figure represents the area available for a suspension (Bingham fluid) whereas closer to the contact point between the PM particles, only water (Newtonian fluid) will be able to penetrate. Thus, the penetrability of a Newtonian fluid is in the range of 3-5 times bigger than for a Bingham fluid, such as suspensions (Axelsson et al., 2009). This means that b_{eqv} should be in the range of 3-5 times larger than the apertures developed for Newtonian fluids (b_{K-C}). Table 7.1 summarizes the different parameters used to evaluate the penetrability of the grout inside the PM.

Table 7.1 - Summary of the different parameters for determining the penetrability from available space considering grouting with a suspension (Bingham fluid) and hydraulic measurement with water (Newtonian fluid)

Parameter	Rheological model
$\boldsymbol{b_{K-C}}$	Newtonian
$\boldsymbol{b_{eqv}}$	Bingham
$\boldsymbol{\frac{D_{15}^{soil}}{d_{85}^{grout}} > 25}$	Bingham
$\boldsymbol{b_{K-C} > 3\text{-}5 \times d_{95}}$	Newtonian

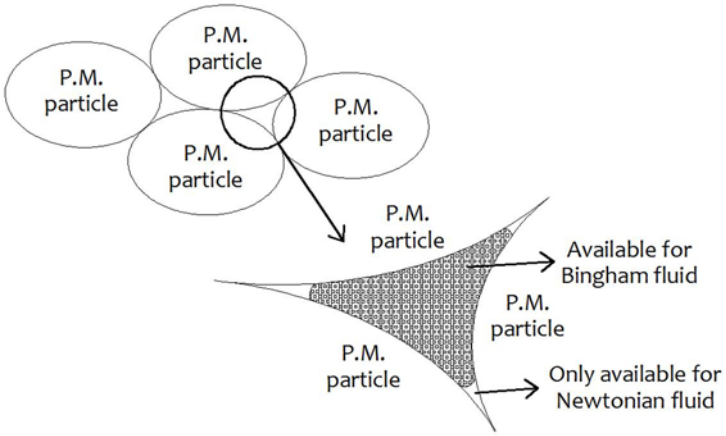

Fig. 7.2 - The available area between PM particles for a Newtonian fluid (e.g. water) and a Bingham fluid (suspension). Adapted from (Axelsson et al., 2009)

In the field of soil grouting, the penetrability of hydraulic grouts has been studied by a number of authors, e.g. Mitchell (Mitchell, 1982) who established in 1982 several rules of thumb for the injectability of PM. More recently, the same rules were used by Axelsson (Axelsson et al., 2009). The use of these rules for the present PM leads to the results presented in Table 7.2.

Table 7.2 - Rules of thumb of Mitchell (Mitchell, 1982) for injectability as a function of the grain distribution for PM

Criteria	Grouting consistently possible	Grouting not possible
$\frac{D_{15}^{soil}}{d_{85}^{grout}}$	> 25	< 11
$\frac{b_{K-C}}{d_{95}^{grout}}$	> 5	< 3

Notation: D_{15}^{soil} = diameter of the soil grain, corresponding to 15% passing
d_{85}^{grout} = diameter of the grout grain, corresponding to 85% passing
d_{95}^{grout} = diameter of the grout grain, corresponding to 95% passing

7.2.3 Different criteria to evaluate the penetrability of the grout

As already stated in different literature (Axelsson et al., 2009; Eklund, 2005; Miltiadou-Fezans & Tassios, 2013a; Paillère & Guinez, 1984), for a granular suspension (such as hydraulic lime grout) to be able to penetrate in a certain PM, the grain size distribution of its solid phase should be compatible with the characteristic dimensions of the PM (apertures, voids, interfaces, etc.) to be injected. Thereby, penetrability conditions are frequently expressed in terms of the ratio (n) between the size of the larger solid particles of the grout (d) and a ‘‘representative’’ diameter of channels or a width of channels to be injected (W_{nom}). This ratio expresses the practical need of the grout solid particles to be significantly smaller than the characteristic aperture to be penetrated. Several phenomena are behind this ratio, namely the friction that exists due to the irregular form of the solid particles, the electrostatic connections between particles and the agglomeration due to immediate hydration of the fines (Miltiadou-Fezans & Tassios, 2013a). In last decades different authors have established different relationships (criteria) in order to assess the penetrability of hydraulic grouts. More recently, Miltiadou-Fezans and Tassios created one table (Table 7.3) which gives the different criteria the same

format: $d < W_{nom}/n$. According to the same author, when W_{nom} is not known, as in the case of granular media, it is possible to assume the approximation: $W_{nom} \sim 0.15$ x D_{15}. In accordance with Dantu (Dantu, 1961) this value corresponds to the diameter of the smallest path passing through grains of the same size D_{15}.

Table 7.3 - Grain penetrability conditions, according to literature. Table adapted from Miltiadou-Fezans and Tassios (Miltiadou-Fezans & Tassios, 2013a)

Author	Criterion: $d<W_{nom}/n$	Grouted medium
Johnson (Johnson, 1958)	$d_{85}<W_{nom}$ / 3,75	Fine granular soil
Mitchell (Mitchell, 1970)	$d_{100}<W_{nom}$ / 3	Fissured medium
Littlejohn (Littlejohn, 1983)	$d_{85}<W_{nom}$ / 3,75	Fine granular soil
Littlejohn (Littlejohn, 1983)	$d_{100}<W_{nom}$ / 5	Fissured medium
Hutchinso (Hutchinson, 1981)	$d_{max}<W_{nom}$ / 3	Fine granular soil
Cambefort (Cambefort, 1977)	$d_{100}<W_{nom}$ / 1,5 to 2	Fissured medium
Léonard (Léonard, 1961)	$d_{85}<W_{nom}$ / 0,75 to 3	Fine granular soil
Papadakis(Papadakis, 1959)	$d_{100}<W_{nom}$ / 1,5 to 3	Fine granular soil
Paillère & Guinez (Paillère & Guinez, 1984)	$d_{100}<W_{nom}$ / 1,5 to 2,3	Tests in "sand column"
Miltiadou-Fezans(Miltiadou-Fezans & Tassios, 2013a)	$d_{85}<W_{nom}$ / 5±1	Tests in "sand column"
Miltiadou-Fezans(Miltiadou-Fezans & Tassios, 2013a)	$d_{99}<W_{nom}$ / 2	Tests in "sand column"

Notation: d_{85} = diameter of the grout grain, corresponding to 85% passing
$d_{100} = d_{max}$= "maximum" diameter of the grout grains

From Table 7.3, it should be emphasized that the criteria from Paillère and Guinez (Paillère & Guinez, 1984) and Miltiadou-Fezans and Tassios (Miltiadou-Fezans & Tassios, 2013a) are resulted of the evaluation of the grout penetrability using sand column tests (used in the standard NF P18-891). These authors studied in a more precise way the relationship that exists between the grading of the solid phase of the grout and the penetrability of hydraulic grouts. In this way, in the experimental results of Miltiadou and Tassios (Miltiadou-Fezans & Tassios, 2013a), a great variety of solid phases (of materials commonly used in the composition of hydraulic grout) was taken into account for the formulation of penetrability grading criteria. The criteria are: $d_{85}<W_{nom}/5±1$ that relates d_{85} and W_{nom} and studies the phenomenon "wall flocculation blocking effects". The other criterion $d_{99}<W_{nom}/2$ aims to ensure that the few grains with a size of "d_{99}" do not produce any "friction blocking" (see Fig. 7.3).

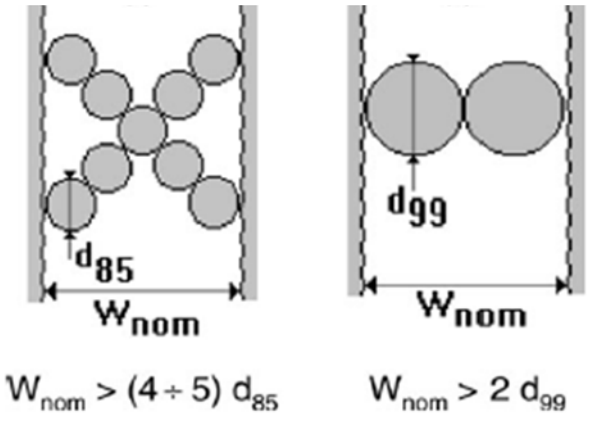

Fig. 7.3 – Schematic derivation of the maximum grains able to flow through a void (Miltiadou-Fezans & Tassios, 2013a)

7.2.4 Relation between penetrability and yield stress

According to the conclusions of some authors (Baltazar et al., 2013; Bras, 2011; Eriksson, 2002), yield stress can be associated to the ability of the grout to fill the voids and its ability to flow when a given shear stress is applied. The knowledge of the yield stress τ_0 enables to understand if a fluid will flow or not, since it represents that ability to flow.
According to Buckingham Reiner equation (Bras & Henriques, 2012), the shear stress (τ) at the wall of the cylindrical channel will be:

$$\tau = \frac{\Delta P}{L} \times \frac{D}{4} \quad (7.4)$$

Where D is the diameter of the void, ΔP is the difference of injection pressure in the channel and L the length of the channel. Since the injection pressure is constant, the shear stress at the wall will decrease when the grout penetrates the channel because L, the length filled by grout, is increasing. When shear stress at the wall is lower than the yield stress of grout the flow will stop. This is expressed by the following Eq. (7.5):

$$\frac{\Delta P}{L} \times \frac{D}{4} \leq \tau o \quad (7.5)$$

Knowing the maximum L of the injection tests, the pressure adopted in the injection tests (see 7.4.3) and the yield stress (see 7.3.1), according to Eq 7.5 it is possible to obtain the minimum void diameter (D_{min}) of the PM to be injected. It is important to emphasize that two of various assumptions followed by Buckingham equation are: the grout flow does not change in time and occurs inside a void with the shape of a cylindrical tube. Given the heterogeneity (variability in size of the apertures) of PM studied in this work, these assumptions are hardly respected.

7.3 Materials studied

7.3.1 Grout design

Grout design involves the study of its behaviour in the fresh state, requiring some performance characteristics such as high fluidity, good water retention, stability and limited or no bleeding (Miltiadou-Fezans & Tassios, 2013b; E.-E. Toumbakari et al., 1999; Valluzzi, 2005) in order to maximize the injectability of grout in the PM, thus maximizing the penetration and diffusion of grout (Valluzzi, 2005). All these characteristics have their particular role in the success of the grout injection. If they are not satisfied, the grout will hardly be injectable regardless of PM (Kalagri et al., 2010; Miltiadou-Fezans & Tassios, 2013a). In order to analyse these characteristics several tests based on the following experimental procedures were performed.
Grout fluidity can be evaluated by its rheological behaviour at fresh state, which could be characterised by several rheological parameters including yield stress and plastic viscosity. The yield stress represents a threshold value, since it enables the understanding if a grout will flow or not. When the applied stress is below of the yield stress the grout does not flow – Eq. 7.5. Regarding the plastic viscosity, it represents the flow resistance once flow is initiated. The lower the grout viscosity the easier and faster the grout will flow and therefore the grout will lose less mixing water by absorption

(Van Rickstal, 2000). The rheological measurements were performed using the procedure shown in chapter 5.2.4.4.

Another parameter to characterize the fluidity of grouts is the flow time, which was measured through the procedure of funnel flow time (Marsh cone test), according to standard ASTM C939-02 and already explained in 5.2.4.1.

Concerning stability, the segregation of solid particles or excessive bleeding should be avoided since otherwise blockage may soon appear and the quality of the grouting intervention could be severely affected (Valluzzi, 2005). In this chapter the stability of the grouts was analysed by the bleeding test, based on standard ASTM C 940. According to this standard 800 ml of freshly mixed grout was poured into a 1000 ml graduated glass cylinder and covered. The height of bleed water was noted after complete sedimentation (three hours after the grout mixture). The final bleeding was calculated according to the expression:

$$Final\ \ Bleeding(\%) = \frac{V_W}{V_l} \times 100 \tag{7.6}$$

where, V_W = volume of decanted bleed water, ml; V_l = volume of sample at beginning of test, ml.

An excess of bleeding in a grout means that there is a substantial amount of free water on the surface of the unset grout. According to Toumbakari (Toumbakari, 2002) a grout has a good behaviour if the bleeding is less than 5%. Thus, in accordance with Table 7.5, it is possible to conclude that in terms of stability, the grout chosen presents a good behaviour. However, it should be noted that this test only gives discrete results that do not allow checking the evolution of density gradient of the grouts. Thus, a new test procedure is also used (already explained in 5.2.4.3) aimed at checking the density variation along the test time of a grout in resting conditions. In this chapter, the analysis of the results was done with the coefficient of variation of density throughout the test in relation to the initial density. So, a small coefficient of variation represents a low variation of grout density, consequently meaning reduced segregation and bleeding. Comparing the coefficient of variation of density obtained (CV=0.07) to the grout chosen with the grouts tested by other authors (CV between 0.12 and 0.31) (Baltazar et al., 2012b; Van Rickstal, 2000), it was concluded that this grout in terms of stability has a high performance.

The water retention capability is another important property to be assured in order to maximize the injectability of grout, since it represents the ability of a grout to retain the mixing water during the injection inside dry and high absorptive masonries. The measurement of water retention was performed in accordance with ASTM C941-02 and already explained in 5.2.4.2.

The grout composition used in the injection tests of this chapter (shown in Table 7.4) takes into account the findings reported in the literature (Miltiadou-Fezans & Tassios, 2012; Valluzzi, 2005) and previous conclusions obtained in 5.4. The main goal was to assess the fluidity, stability and penetrability characteristics in function of the water to solids ratio and/or the percentage of SP.

Table 7.4 - Grout composition tested

Binder	**W/b**	**SP**	**% SP**
HL5	0,5	Glenium Sky 617 (BASF)	1.2

The binder used was the same as previous HL5 hydraulic lime (EN459-1) produced in Portugal by Secil-Martingança, which has the characteristics presented in Table 5.1 according to the information of the quality control system provided by the manufacturer. The grain size distribution is represented in Fig. 5.2. From this curve, it is possible to obtain d_{85}(98μm), d_{95}(129μm) and d_{99} (206 μm) values.
The water/binder ratio (w/b) tested was 50% in weight (Table 7.4). According to the literature and particularly following the recommendations proposed by Valluzzi (Valluzzi, 2005), a minimum value of water/binder of 55% (in weight) should be used, although in this case only 50% was used due to the presence of the SP.
Concerning the use of the SP it became evident throughout the test campaign (performed in Chapter 5) that it was virtually impossible to formulate a grout with adequate injectability without using either a SP or an excessive amount of water that would lead to a grout with stability problems of bleeding or segregation. Analogous results were obtained by Valluzzi (Valluzzi, 2005). After various preliminary attempts with different dosages of SP (see 5.3.1), the same as previous polycarboxilate-based superplasticizer (BASF Glenium Sky 617) was chosen with a dosage of 1.2% in weight.
Comparing the injectability characteristics of the grout chosen with hydraulic lime grouts tested by other authors (Table 7.5), it can be concluded that this grout has a high performance in terms of fluidity, stability and water retention. It should be stressed that the materials and tests used in this research are the same as in other works mentioned in Table 7.5.

Table 7.5 Injectability characteristics of the grout selected in comparison with literature

	Parameters / Tests	Grout selected	Literature
Injectability characteristics	Yield stress [Pa], resting time = 0 min	0.95	1.04 (Bras & Henriques, 2012); 12.74; 0.47(Baltazar et al., 2012a)
	Plastic Viscosity [Pa.s], resting time = 0 min	0.10	0.15 (Bras & Henriques, 2012); 0.057(Baltazar et al., 2012a)
	Flow time (s) (Marsh cone test Diam.=10 mm), resting time = 0 s	9.3	9.1 (Baltazar et al., 2014) ; 22 (Bras, 2011)
	FFT (mm/s x 10^3) (Marsh cone test Diam.=6 mm), resting time = 0 s	1.5	0.1-2.2* (Miltiadou-Fezans & Tassios, 2012)
	Final Bleeding (Stability Test) [%]	2.1	0.33 - 4.8 (Bras & Henriques, 2012)
	Coefficient of variation of density (Stability Test) [-]	0.07	0.12 - 0.31 (Baltazar et al., 2012b) **(Van Rickstal, 2000)
	Water retention capability (time needed to remove 30 ml of water) (sec)	1554	1626 (Baltazar et al., 2012a)

* Marsh cone diameter = 3mm
** The binder used was cement, in all the other cases, the binder was the hydraulic lime

7.3.2 Porous media for injection tests

In order to study the grout injection capacity some injectability tests were made. Given the difficulties to reproduce a historical masonry due to their high heterogeneity (Valluzzi, 2005) and to the difficulty of reproducing the characteristics of ancient mortars (C. Almeida et al., 2012; Binda & Anzani, 1997), the inner core of old masonries were simulated by combining three different crushed limestone sands (hereafter mentioned as stone) and three different crushed bricks (hereafter mentioned as brick) (Fig. 7.4). The same method but with different materials was used in works of other authors (Bras & Henriques, 2012; Valluzzi, 2005; Van Rickstal, 2000). The materials were washed, dried and sieved to

obtain diverse grain size distributions to enable the simulation of different permeability of masonries. Five different grain size media types (of different proportion of limestone and crushed brick, i.e., 10 PM in total) were adopted to simulate different masonries (Fig. 7.5 and Fig. 7.6).

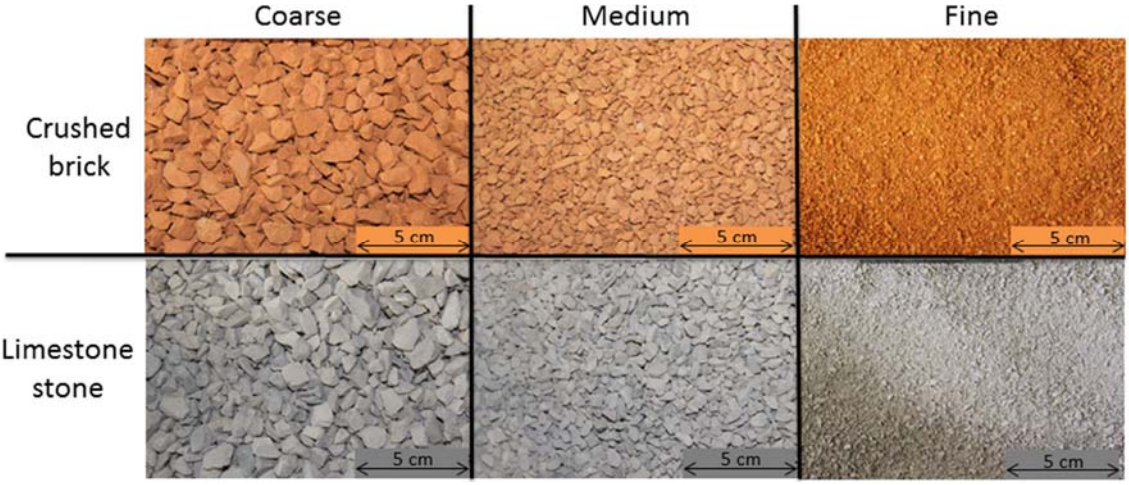

Fig. 7.4 - Three different grain size ranges (fine, medium, coarse). Crushed brick (up picture) and Limestone sand (down picture)

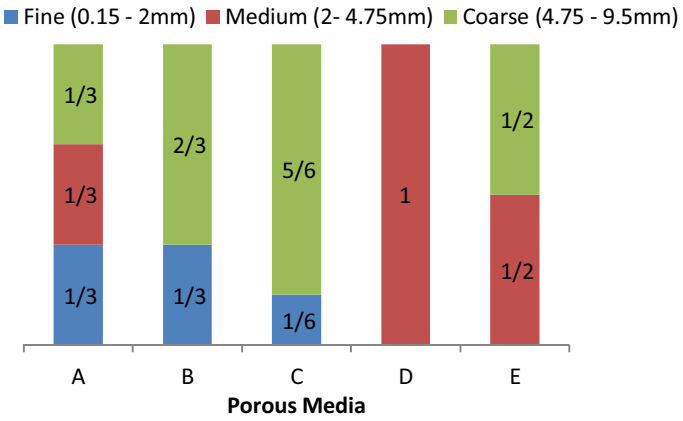

Fig. 7.5 - Different grain size ranges of the PM studied

Fig. 7.6 - PM A_{stone} (left picture) and E_{stone} (right picture)

In accordance with the survey of the sections of multi-leaf masonry done by certain authors (Binda & Anzani, 1997; Bras, 2011) some important parameters were adopted (Table 7.6) to characterize the dimension and distribution of voids of the different PM. These parameters are: the voids size average (which correspond to d_{50} - the diameter through which 50% of the total mass passes) (Bras & Henriques, 2012), as well as the parameter d(90), d(15) and d(10) (respectively the diameter through which 90%, 15% and 10% of the total mass passes) and the % of the total mass that passes through ASTM nº20 sieve (0.85mm). The parameters above mentioned are obtained from grain size

distribution curves shown in Fig. 7.7. The impact of these parameters on injectability value will be analysed in the section 7.5.1.1. Furthermore, the grain size distribution of each PM (Fig. 7.7) allows the determination of nominal lower value of the aperture of voids or interfaces to be injected. Since the calculation of the aperture depends of the specific surface value (shown in Table 7.6) and the latter is calculated from the grain size distribution of each PM.

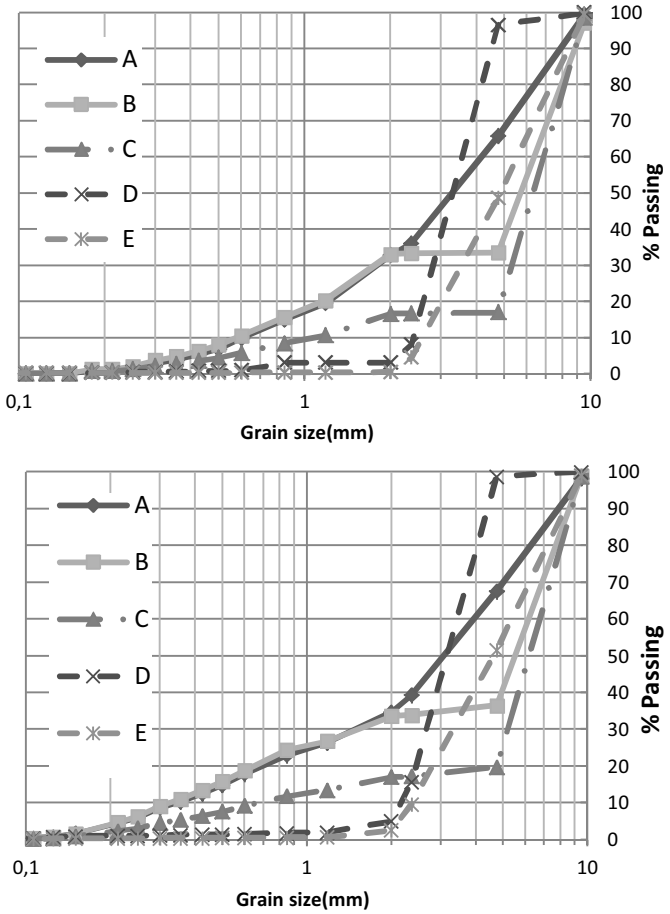

Fig. 7.7 - Grain size distribution for media types A, B, C, D, E used for cylinders grout injection. Limestone PM (above picture) and crushed brick PM (below picture)

According to other authors (Bras & Henriques, 2012; Valluzzi, 2005), the total porosity of each PM type was evaluated by measuring the volume of water that could be injected inside each cylinder (Table 7.6). It is worth to note that this parameter does not give the value of porosity that the grout can penetrate inside the PM, which in fact is much smaller, since the volume accessible depends on the fluid behaviour (Fig. 7.8). In fact, the solid particles of the grout suspension (Bingham fluid) cannot enter all of the voids as can a Newtonian fluid (see section 7.5.1.5). As shown in Table 7.6 the percentage of total porosity measured was approximately between 40-55%, which is a typical range of percentages in research of masonry walls, if only the dimension of the inner core are computed (Valluzzi, 2005). The voids size average (2.5-6mm) was another characteristic with values similar to the old masonry characterization studies carried out by other authors (C. Almeida et al., 2012; Binda et al., 2000, 1997; Valluzzi, 2005), meaning that the methodology proposed in this work for testing grout injectability in a different PM follow a good strategy.

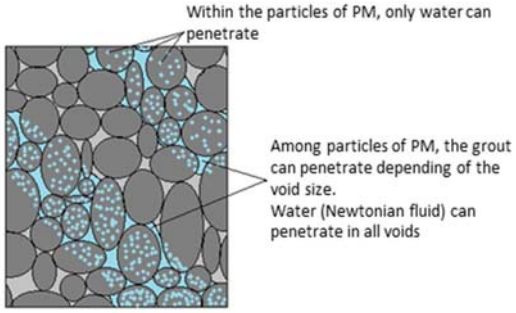

Fig. 7.8 – Depending on the fluid, the accessible volume varies

Table 7.6 - PM characteristics

	Porous media type									
	A		B		C		D		E	
	stone	*Brick*	*stone*	*Brick*	*stone*	*Brick*	*stone*	*Brick*	*stone*	*Brick*
Voids size average [mm]	2.67	2.42	5.23	5.02	6.09	5.97	3.22	3.06	4.28	4.09
d(90) [mm]	8.17	8.22	8.97	8.82	9.00	8.97	4.58	4.50	8.62	8.59
d(15) [mm]	0,85	0,50	0,81	0,47	1,78	1,52	2,55	2,34	2,93	2,66
d(10)[mm]	0.60	0.34	0.58	0.32	1.08	0.67	2.41	2.17	2.66	2.38
% of the total mass that passes through n^0 20 sieve	15.0	23.0	15.7	24.4	8.4	11.8	3.1	1.8	0.3	0.7
PM porosity [%]	41.2	48.1	39.3	48.7	44.6	51.5	50.4	56.6	48.4	55.4
WA_{0h} (%)	4.2	18.0	3.8	16.8	1.6	12.9	1.8	14.2	1.5	12.0
WA_{24h} (%)	5.6	19.4	3.9	19.1	2.2	16.2	2.2	14.3	1.5	12.5
Specific Surface (mm^2/mm^3)	5,03	6,06	4,90	5,84	3,17	3,38	2,86	2,63	2,02	1,72

To study the water absorption (WA) capacity of each PM the European standard EN 1097-6 was used. From Table 7.6 is possible to observe the high water absorption capacity of brick PM when compared to the limestone PM, which is in accordance to the literature (Cachim, 2009). The knowledge of water absorption capacity of the particles of PM is of utmost importance during the injection of grouts. Then, in addition to the total water absorption capacity (WA_{24h}), the water absorption for initial time (WA_{oh}) was also determined for these PM (see Table 7.6). This allows a perception of the amount of water absorbed by the particles of PM (Cachim, 2009) during the injection process, which influences the grout fluidity and consequently the grout injection capacity. The results show that brick PM create more resistance to the flow of grout. On the other hand, since the water absorption of the brick particles is very high, it is expected a high bonding strength between the grout injected and the PM particles (see 8.4.2).

7.4 Procedure

7.4.1 Mixing procedures

The hydraulic lime mixes were prepared at room temperature 22±1.5˚C and 53% of relative humidity. For the preparation of grouts ordinary tap water was used and dry hydraulic lime was hand mixed to ensure a homogeneous distribution before the beginning of the mechanical mixing. The mixing procedure was already detailed in chapter 5.2.3.

7.4.2 Permeability tests

When designing a model to describe the injection process, the permeability will be one of the main parameters of the masonry that influence the penetration, evolution and distribution of the grout inside the masonry. The test setup to measure the permeability of the reproducible masonry samples is shown in Fig. 7.9- a). The time required for a certain volume of water to fill the PM was measured (PM particles were saturated before the test). Thus different water flows (q) in function of different applied pressure (ΔP) were obtained. The Eq.7.7 (Van Rickstal, 2000) based upon Darcy's law conditions (that is, laminar flow and a low pore water velocity, such that the inertia term in the Bernoulli energy equation can be ignored (David Carrier, 2003)), provides the permeability of the PM:

$$q = \frac{k \times A}{\mu \times L} \times \Delta P \tag{7.7}$$

Where: q = water flow (m^3/s);
K = permeability (m^2);
A = area of the tube (m^2);
μ = dynamic viscosity of water (Pa.s);
L = length of the tube (m);
ΔP = applied pressure difference (Pa).

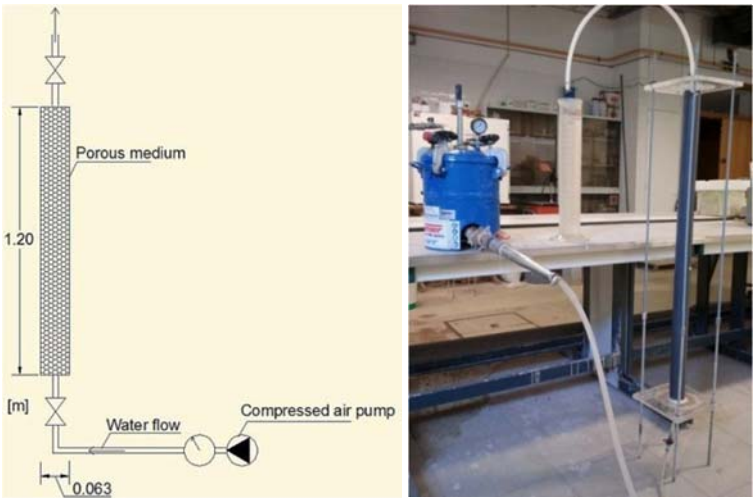

Fig. 7.9 - Setup for permeability measurements using Darcy's law

This test provided the permeability of the different PM (Table 7.7) that were used to determine the influence of the permeability on the injection process and on the diffusion of the grout inside the masonry. According to Table 7.7 the permeability of crushed brick PM is lower than limestone PM for any PM type. One of the reasons, as shown in Table 7.6, is the lower size of finer particles – d(10) of brick PM. Thus, due to the higher resistance to the passage of the water (since the voids available between particles are smaller), the flow rate will be lower and hence lower permeability values are achieved (Eq.7.7). Comparing the values of permeability with PM characteristics shown in Table 7.6, it can be concluded that the permeability depends not only on the porosity of PM, but also of the

specific surface and d(10). Indeed, the best relation is between the permeability and d(10). There is a range values of d(10) and permeability to finer PM (A and B) and another range values to coarser PM, while the PM C has a value between these two ranges. Therefore, it can be assumed that the permeability of a PM depends mainly of the quantity of fine particles. The parameters average voids size and maximum dimension seem to have lower relevance.

Table 7.7 - Permeability for different media porous studied

	Porous media type									
	A		**B**		**C**		**D**		**E**	
	stone	*brick*	*stone*	*brick*	*stone*	*brick*	*stone*	*brick*	*stone*	*brick*
Permeability - K [10^-11 m²]	1,13E-10	0,99E-10	1,64E-10	1,60E-10	5,76E-10	3,88E-10	8,47E-10	7,98E-10	8,46E-10	8,08E-10
Permeability - K [Darcy]	113	99	164	160	576	388	847	798	846	808

The relation between pressure (Pa) and water flow (m^3/s) that crosses the PM for two different types of grain size distributions can be observed in Fig. 7.10. In what concerns the fine PM B the relation is almost linear, whilst the coarse PM C has a significant increase to low pressures, followed by slight increase of water flow to higher pressures. The reason for these different evolutions is related to the Young-Laplace equation (León, 1998) which relates the capillary pressure with the voids diameter, having a proportional inverse growth. On the fine PM low pressures the water cannot penetrate inside the finer pores, resulting a lower water flow. Thus, it is necessary to increase the pressure for the water to penetrate into the finer pores (Fig. 7.10.a). Concerning coarse PM, as they have pores of larger diameter, low pressure of water can penetrate in almost all pores, resulting a quick increase water flow to low pressures (Fig. 7.10.b-c). Regarding the coarse PM C and E, it can be seen that water flow of PM E is almost 5 times higher. The reason is the higher value of d(10) (Table 7.6). Thus, it was confirmed again that the finer particles size has a great influence on the permeability value. These results fit well with Hazen equation ($k = C_H.d(10)^2$, where C_H is the Hazen empirical coefficient) (David Carrier, 2003), where the permeability value is directly dependent of the parameter d(10). Besides that, in the Kozeny-Carman equation the smaller particles of PM also have the most influence on the value of K (David Carrier, 2003).

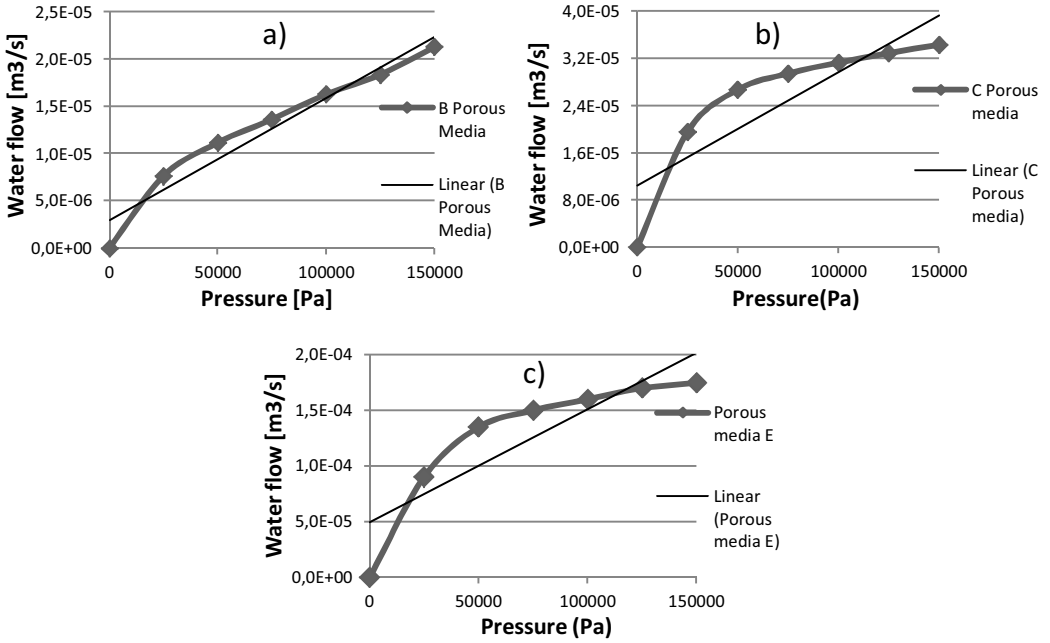

Fig. 7.10 - Different evolutions of discharge as a function of pressure, for fine PM B - a) and coarse PM C - b) and E - c)

7.4.3 Injection Tests

Following the procedure explained in 5.2.5, injectability tests were performed to study the injectability of the grout in different PM. The cylinders (reduced models shown in 5.2.5) were filled with one of the media types trying to reproduce as much as possible real situations, such as the inner core of a multi-leaf masonry. For each PM three samples were used, i.e., three cylinders were filled, for a total of 60 elements. The filled cylinders were injected from bottom to top with fresh hydraulic lime grouts immediately after grout preparation (Bras & Henriques, 2012; Valluzzi, 2005). Given the results reached in 5.3.5, in this chapter the injections tests were performed at constant pressure of 1 bar.

It is worth noting that these injection tests do not simulate the injection within the masonry, but offer the possibility of experimentally:
- evaluate the minimum fineness of the PM that allows the chosen grout to be injected;
- understand the grout flow inside PM for the different grain size distributions used;
- observe the relationships between injection capacity of grout and media grain size distributions.

7.4.3.1 Porous media with different moisture content

As it is not expected that masonries are always dry, the media of some cylinders were pre-wetted by simple injection of water (in accordance with experiments of Valluzzi (Valluzzi, 2005), Van Rickstal (Van Rickstal, 2000) and Anzani (Anzani et al., 2006), as shown in Fig. 7.11. After the injection of water the valve at the bottom of the cylinder was opened to allow the water to flow out of the sample. Half an hour later the same sample was injected with the hydraulic lime grout. It was noticed that water injection washed out the finer particles, creating major flow channels. Injection tests for the five media types were done with and without pre-wetting of the PM. Through the comparison of the values of injectability for these two categories it is possible to evaluate the effect of the water content of PM on the injectability of the grout. Some authors, like Bras (Bras et al., 2013b) and Van Rickstal (Van

Rickstal, 2000), noted the influence of water content of PM to be injected as a factor able to influence grout injection capacity.

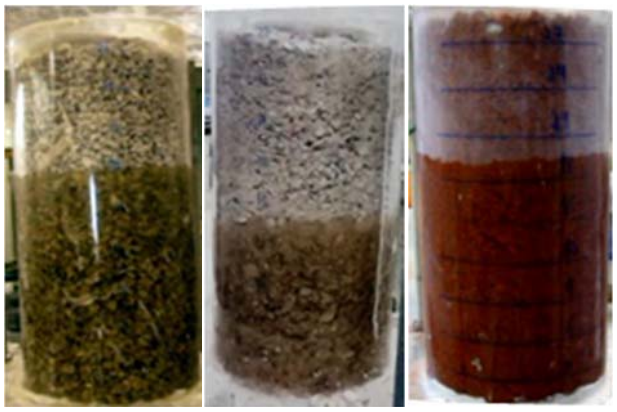

Fig. 7.11- Cylinders filled with media type E_{stone} (left), A_{stone} (central) and A_{brick} (right) being injected by water. The flow was uniform but with different velocities of injection

7.5 Results and discussion

7.5.1 Injection tests

7.5.1.1 Injection capacity of grout for the different porous media

The main objective of this research was the comparison of the performance of the selected grout in terms of its capacity of penetration and injection in different PM. Injectability (calculated by Eq4)) was analysed for two different situations: (i) grout in dry PM and (ii) grout in pre-wetted PM. From Table 7.8 it is possible to observe that coarser PM (C, D and E) with higher porosity and higher size of finer particles - d(10) (Table 7.6) - have injectability values roughly 1,5 times higher than those of the finer PM (A and B). This is observed especially in limestone PM. In what concerns brick PM, this difference is slighter and PM C shows an intermediate behaviour between fine and coarse PM. Comparing the injectability of PM between these two materials, in general terms it is observed that there is no great difference. The total mean-square-deviation (MSD) for each material confirms this fact (Table 7.8). On the one hand, the crushed brick PM have higher porosity (Table 7.6) which leads to higher mass/volumes of grout to be injected (Table 7.8); furthermore, the particle surfaces have lower roughness, which cause a decrease of the resistance to the injection flow (this phenomenon is more pronounced in a fluid more viscous like grout than in the water). But has significantly higher water absorption (Table 7.6) provoking an increase of the overall resistance to the grout flow. This is due to the increase in viscosity and a decrease of the aperture (Van Rickstal, 2000) resulting from the absorption of water by the PM that renders a good penetration more difficult to achieve. In what refers to finer PM (A and B), for both materials, PM B (with only fine and coarse size particles) present lower injectabilities than PM A (with the three different range particles size) (Fig. 7.5). The reason is related with the fact that during injection, when a grout reaches a large void, no pressure can be built up in the neighbourhood of that void. Due to this low pressure, the grout will enter the fine channels only over a short distance, with thixotropy, water absorption and instability of the grout causing the blocking for further injection in these finer channels. When the large void is finally filled, the pressure can increase again, but too much water of the grout is absorbed in the fine channels to restart flowing.

In terms of the injectability of dry or pre-wetted PM, the former present higher values for both of the materials studied. The bigger differences are present in crushed brick PM (see MSD in Table 7.8), especially for finer media. In this case, the parameter with the highest impact is the water absorption due to the higher specific surface that results from the finer media (Table 7.6). As water absorption is higher in the case of crushed brick PM (Table 7.6), these PM absorb more water in the pre-wetting phase, leaving a lower free volume for the grout to be injected. Thus, their injectability values will decrease.

Table 7.8 - Injectability and Volume injection for different PM

	Injectability (-)					volume injection (l)			
P.M.	*Lime stone*		*Crushed Brick*		P.M	*Lime stone*		*Crushed Brick*	
	Dry	wetted	Dry	wetted		Dry	wetted	Dry	wetted
A	0,57	0,58	0,75	0,61	**A**	1,27	1,17	1,66	1,27
B	0,54	0,48	0,71	0,46	**B**	0,85	0,80	1,39	1,00
C	0,96	0,88	0,80	0,74	**C**	2,32	1,95	2,14	1,92
D	0,96	0,91	0,97	0,82	**D**	2,67	2,34	2,82	2,25
E	0,97	0,92	0,89	0,84	**E**	2,61	2,36	2,56	2,30
MSD*	0,08	0,10	0,04	0,11	Average	1,94	1,72	2,11	1,75
MSD*	0,09		0,08		Average	1,83		1,93	

$$* MSD = \frac{(y_1-y_0)^2+(y_2-y_0)^2+\ldots+(y_n-y_0)^2}{n};\ y_0 = target\ value = 1$$

From the analysis Table 7.8 it is possible to observe a close relation with some of the PM characteristics presented in Table 7.6, namely with parameter d(10), % of the total mass that passes through nº20 sieve, and voids volume. According to Fig. 7.12 these parameters are the most important for masonry characterization regarding injectability, independently whether PM is dry or wet at the time of injection. In fact three ranges of values for these parameters can be identified: one for the finer PM A and B, a second for the coarse PM D and E and a third to PM C that lies between the other two ranges (Fig. 7.13). The same happens with the values of injectability. Thus, the above parameters revealed in general to be adequate for the establishment of an injectability characteristic. The other parameters - voids size average and d(90) - did not seem appropriate since the correlation with injectability is very low (Fig. 7.12).

As shown in 7.4.2, the permeability is related to the parameter d(10) – according to Hazen equation (David Carrier, 2003). As injectability is related to the permeability of the PM (Fig. 7.15), so the influence of the parameter d(10) on the grout injectability is understandable. Moreover, as mentioned in 7.2.1, during the injection process the finer particles tend to agglomerate (Eklund & Stille, 2008) which causes the decrease of the voids diameter. Thus, the phenomenon of clogging up the finer channels is more visible, i.e., there is an increase of constrictions and resistance to the grout flow.

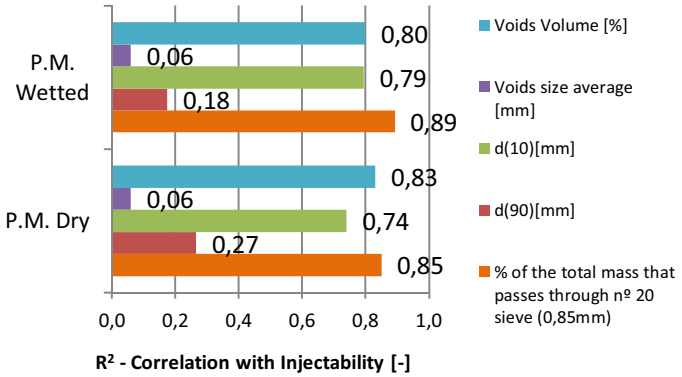

Fig. 7.12- Correlation between Injectability and PM characteristics (taking into account the injection results of limestone and crushed brick PM)

The analysis of the relations between injectability and certain PM parameters is presented in Fig. 7.13, from which it can be seen that higher voids volume are associated with higher injectabilities. This association, however, can only be established for the same material. When the analysis is between different materials, there are other parameters, as the water absorption capacity, which may have a relevant preponderance. Thus, in Fig. 7.13 and Table 7.6 it is possible to observe that brick PM have a higher porosity. In what concerns the grout volume injected (Table 7.8) they are similar in both PM, confirming what was previously written about the Newtonian fluids (water, the fluid that was used to determine the voids volume) able to penetrate into more voids than Bingham fluids (grout suspension). The higher the water absorption of a PM, the higher is the difference between grout injected and the voids volume.

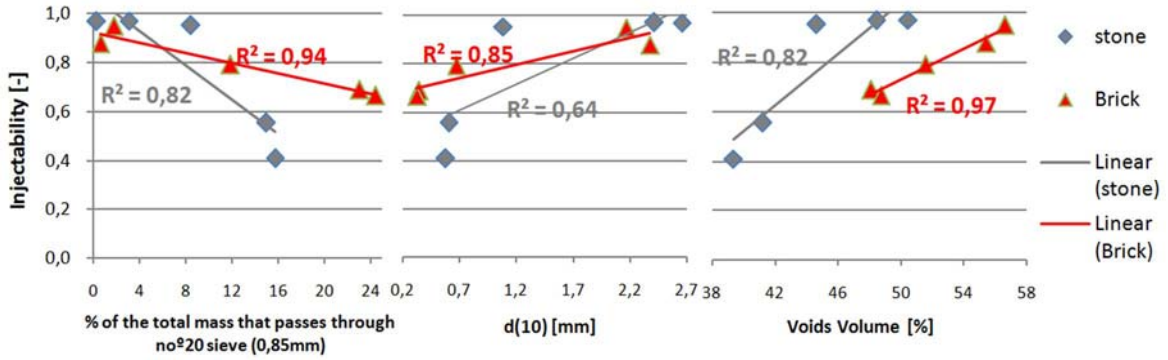

Fig. 7.13 - Relation between Injectability values and certain parameters of the PM

7.5.1.2 Injection capacity of grout taking account the injection time

As mentioned in section 5.2.6, Bras and Henriques (Bras & Henriques, 2012) followed a different approach to study the injectability of the grout. Comparing with the equation proposed in this article, the main difference is the introduction of another parameter: the time of injection. Thus, following the approach of Bras, the rate of grout injectability is analysed. Fig. 7.14 is an outcome of using this approach.

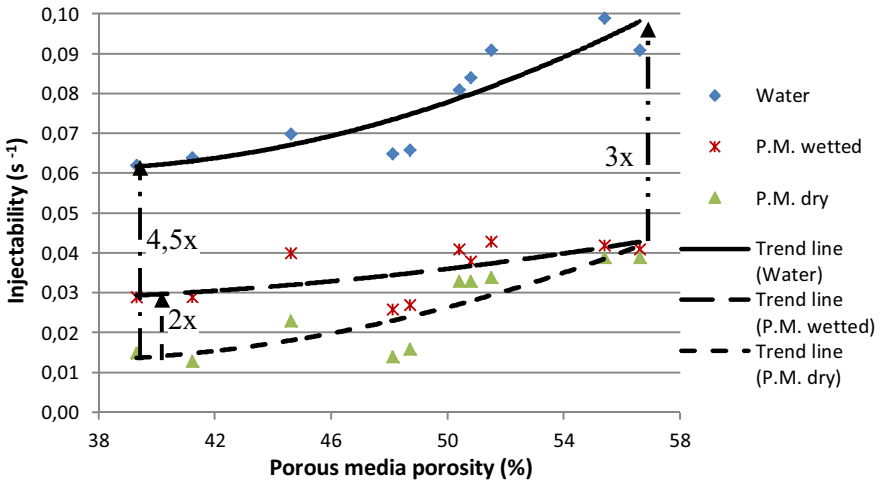

Fig. 7.14 - Injectability (calculated by the equation of Bras) curves for water, PM wetted, PM dry for the different PM tested, taking account the PM porosity injected [%]

The injectability of grouts when compared with the results obtained with water presents significantly lower values (Fig. 7.14), in particular for the PM A and B with low porosity (Table 7.6), where the ratio between injection capacities reached 4,5 times. However, for higher porosity the ratio decreases to 3 times. These results fit with the conclusions obtained by Bras and Henriques (Bras & Henriques, 2012). In fact, it seems that the yield stress value has more relevance in injectability of a fluid for finer PM, whereas for coarser PM, viscosity forces and inertia effects become more expressive.

From Fig. 7.14 it is possible to observe that coarser PM with higher porosity (Table 7.6) and permeability (Table 7.7) have values of grout injectability approximately 2-3 times higher than those of the finer PM. The amount of grout injected, as well as the rate of grout injectability are greater for the coarse PM because the resistance to the grout flow is lower once the pore system has voids/channels with higher aperture (Table 7.9).

The grout injectability is higher when PM is wetted at the time of injection (Fig. 7.14). This difference (in average about 37%) can be explained by considering that the resistance to flow has been reduced by the water injection, leading to the PM with a higher conductivity (Van Rickstal, 2000), consequently higher velocity injection (i.e. rate of grout injectability). The higher differences are present in finer PM due to higher water absorption capacity of finer particles (Table 7.6). Thus, in what concerns the rate of grout injectability, it is more beneficial to use pre-wetting in finer PM than in coarse PM. In fact, in these cases the grout will only flow through the larger voids, since at the time of grout injection the finer voids are already filled with water (during the pre-wetting these capillaries absorb water due to the high capillary pressure - Young-Laplace equation), hence hindering the penetration of the grout.

In general the values of injectability (s^{-1}) obtained are higher than the values obtained by Bras and Henriques (Bras & Henriques, 2012). One reason can be the higher PM porosity and voids size average of the PM studied in this work (Table 7.6), compared to the PM used by Bras. Thus, the aperture of the voids in the pore system is higher which results in higher injectability of the grout. Other reason can be the better rheological behaviour of the grout used in injection tests compared to the grouts used by Bras (Table 7.5). Indeed, the lower viscosity and yield stress contribute to obtain a grout with higher fluidity and penetrability, respectively (Miltiadou-Fezans & Tassios, 2013a, 2012).

From Fig. 7.15, as expected, the increase of permeability of PM leads higher values of injectability - I(s^{-1}). However, for high permeability values (higher than 750 Darcy) this trend is non-existent. As already mentioned, for coarser PM (C, D and E) the viscosity forces and inertia effects have more relevance than the aperture of the voids. In fact, if the PM has not small voids, an increase of the voids aperture does not necessarily mean an increase of the injectability (despite the increase in permeability). So, it was confirmed again that the finer voids of a PM has the main role in the injectability values.

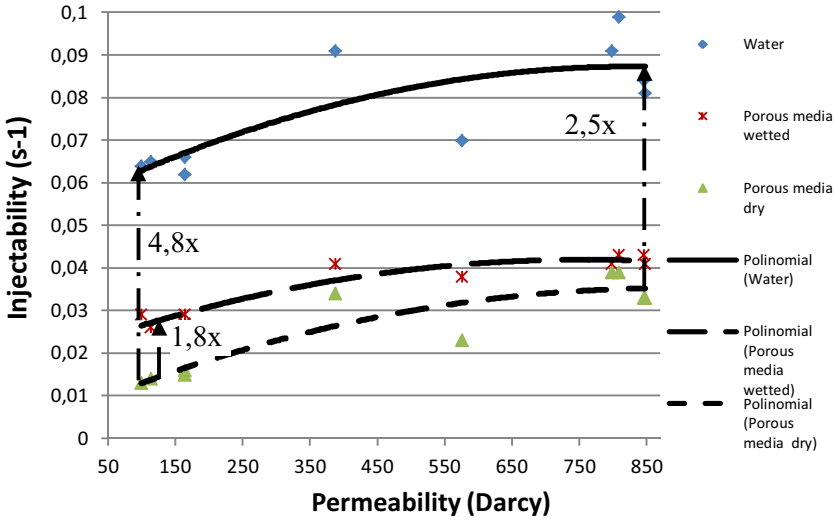

Fig. 7.15 - Injectability (calculated by the equation of Bras) curves for water, PM wetted, PM dry for the different PM tested, taking account the permeability (Darcy) of each PM

7.5.1.3 Visual inspections during the injection of the cylindrical models

During the injection test a movie was made to allow the visual analysis of grout penetration inside the cylinders. The following remarks can be made: (a) while injecting the dry material a segregation took place between the water (absorbed by the finer material) and the remaining part of the grout (Fig. 7.16); (b) when the finer material formed a complete layer through the section of the cylinder, the flow was interrupted (Fig. 7.17.a-f); (c) when an injection blocks, it is not possible to restart the flow by increasing the pressure; d) when the finer material does not exist or is just present in a small quantity the injection was successful (Fig. 7.18). These results are in accordance with the literature (Bras & Henriques, 2012; Kalagri et al., 2010; Valluzzi, 2005).

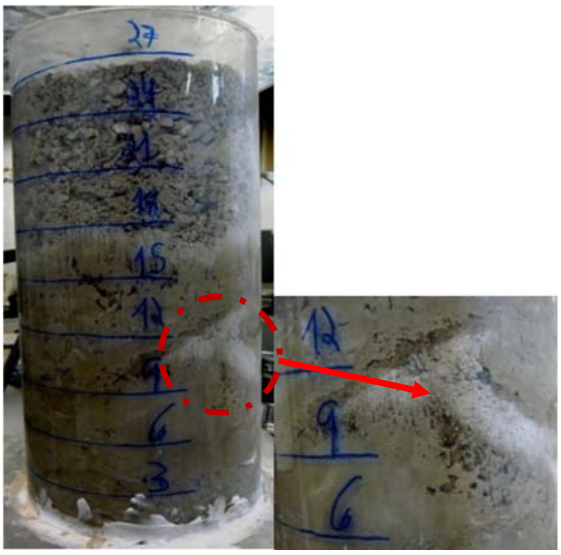

Fig. 7.16 - Cylinders filled with media type $B_{,stone\ dry}$ after injection (segregation took place between the water and the remaining part of the grout)

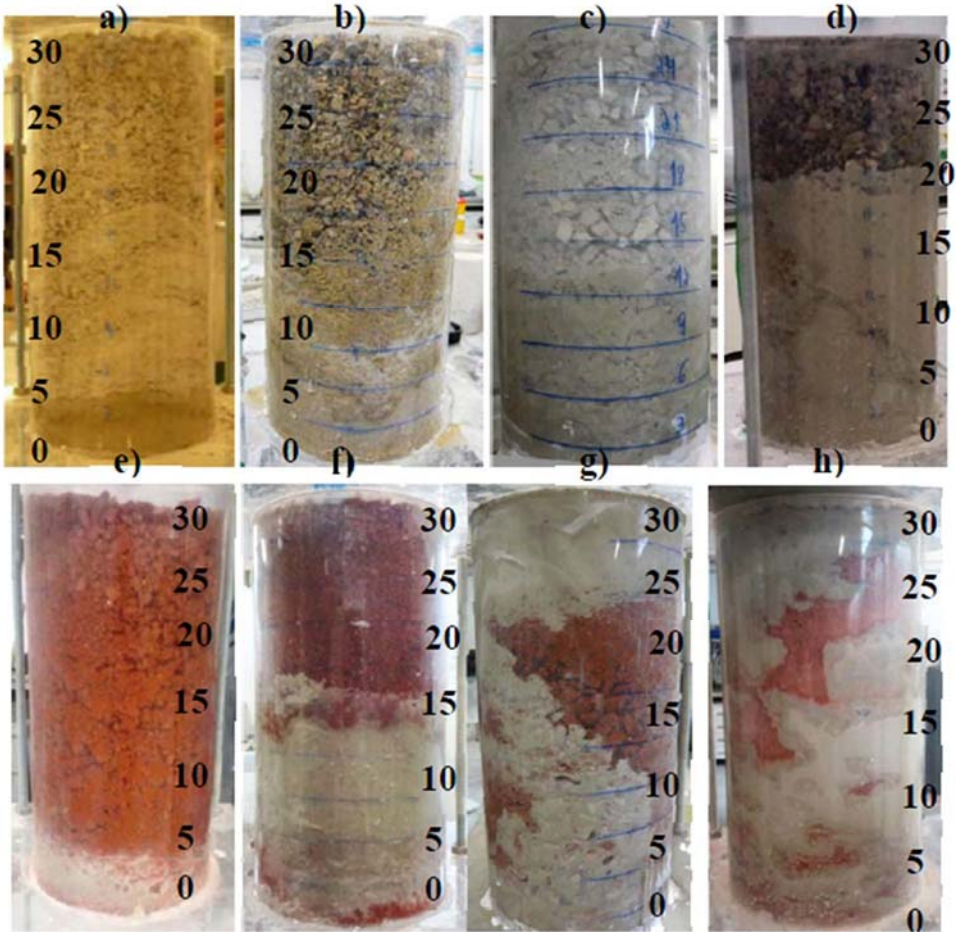

Fig. 7.17 - PM a) $A_{,stone\ dry}$, b) $A_{,stone\ wetted}$, c) $B_{,stone\ dry}$, d) $B_{,stone\ wetted}$, e) $A_{,brick\ dry}$ f) $A_{,brick\ wetted}$, g) $B_{,brick\ dry}$ and h) $B_{,brick\ wetted}$ being injected

For the same PM, the height of injection is higher when the PM is wetted previously to the injection of the grout (Fig. 7.17.a-b, Fig. 7.17.c-d and Fig. 7.17.e-f). One of the reasons is the reduction of flow resistance due to the water injection, leading to a PM with a higher conductivity. Van Rickstal (Van

Rickstal, 2000) noted that the conductivity to water of a dry PM is smaller than the one of a wet sample, concluding that the conductivity of a PM is related to water content. Considering the results obtained the same phenomenon happens with the grout. Regarding the crushed brick B PM, the grout was able to advance until reaching the top but leaving part of the voids empty because the resistance to fill these voids is high (Fig. 7.17.g-h). Moreover, as explained above, in the crushed brick PM the water absorption is significantly higher, what hinders the grout injection process.

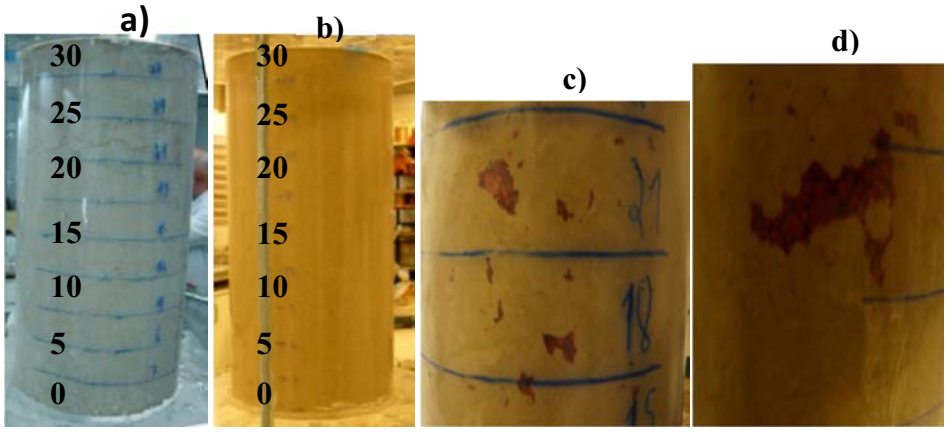

Fig. 7.18 - Cylinders filled with media type a) $D_{stone,dry}$ b), $E_{stone,dry}$ c) and d) $C_{brick,dry}$ being injected

The injection of PM A and B (PM composition with higher amount of fines) was not successful in laboratory, even when PM were wetted. Taking into account that the situation in the cylindrical containers is better than in reality from the point of view of injectability, given the fact that they have a larger number of connected voids when compared with real masonry (Binda et al., 2003a), it can be concluded that this grout will not be injectable inside a masonry with similar characteristics. However, these types of PM (A and B) only represent the cases where the voids cannot be directly reached (when the grout is not allowed to flow through paths with discontinuities or small openings) and/or when the width of the voids is not large enough when compared with the dimension of the grout's grains (Miltiadou-Fezans & Tassios, 2013a; Valluzzi et al., 2004). In contrast, the grout injection inside PM D and E has good penetration and diffusion of the grout (Fig. 7.19.a-b). Regarding PM C, it was observed that the injection inside the cylinders of this PM were not complete, as shown in Fig. 7.18.c-d and Fig. 7.20. The reason for this fact is the presence of dry fine particles (with small size and high water absorption) which prevents the penetration of the grout flux. In section 7.5.1.5 this issue will be addressed in detail.

From these tests (see Fig. 7.17) it becomes clear that pre-wetting cannot solve the penetrability issues which is in accordance with the injectability tests performed by Valluzzi (Valluzzi, 2005), where no differences were found in cylinders preliminarily wetted, in comparison with the anhydrous ones. Moreover, according to some authors (Valluzzi, 2005; Van Rickstal, 2000) pre-wetting causes a lower mechanical strength of the samples (as it will be seen in chapter 8.4.2). Therefore, pre-wetting has to be used with much precaution.

7.5.1.4 Visual inspections after injection of the cylindrical models

The cylinders of Fig. 7.19 were cut into three slices (bottom, medium and top levels) 45 days after being injected and an inspection of each slice was made (Fig. 7.20) to assess the degree of success of

the injection in terms of penetration and diffusion of the grout A remark can be made regarding the presence of high quantity of zones not injected during the injection of PM with finer material (PM A and B), leaving large voids as shown in Fig. 7.19 and Fig. 7.20.

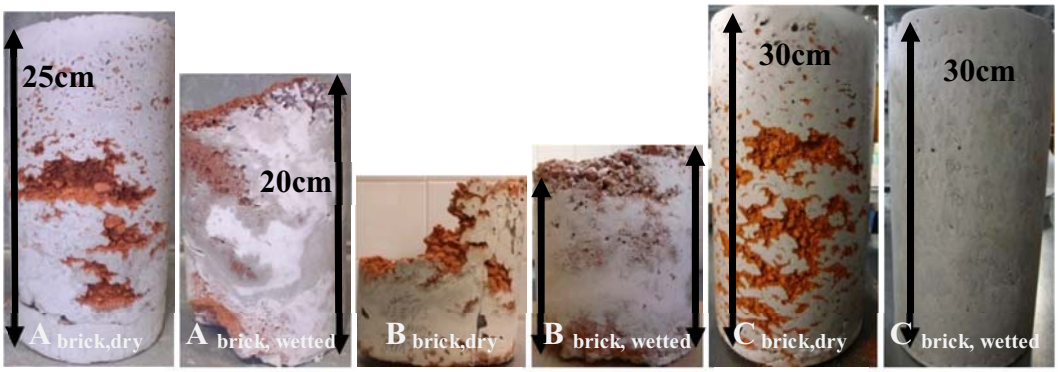

Fig. 7.19 - Cylinders 45 days after being injected

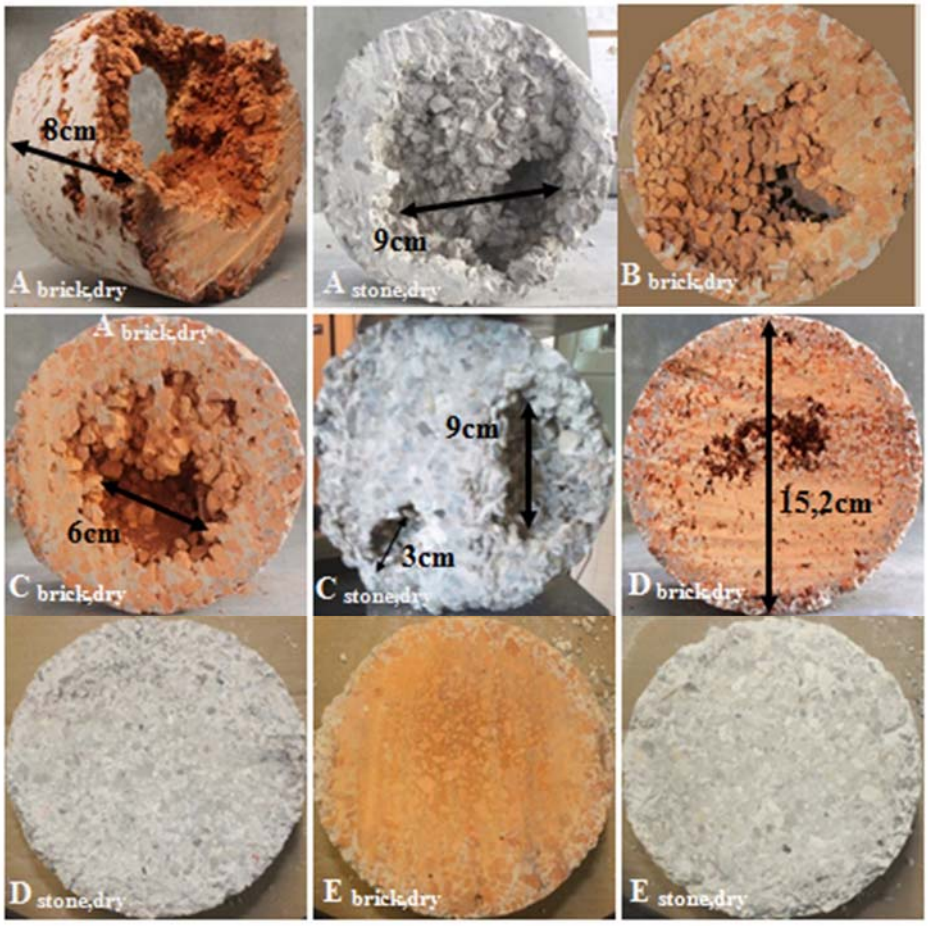

Fig. 7.20 - Slices of cylinders at different levels

7.5.1.5 Penetrability results

Evaluation of different apertures in grout penetrability

Using the porosity and the specific surface determined from the grain size distribution curves (Fig. 7.7) of each PM presented in Table 7.6, an evaluation of the aperture (b_{K-C}) in the PM was performed (Table 7.9). The results obtained imply that the PM A and B are hardly injectable, if the rules aforementioned (see 7.2.2) are considered, which may explain the failure of the injection. In relation to the PM D and E the rules are verified (exception D_{brick}), thus not causing any fail during the injection process. In particular the PM C are close to what is considered to be injectable (the rules are not totally verified). This may explain why the injection was not totally successful in some parts of the cylinder. These observations are in strict accordance with visual inspections (Fig. 7.19 and Fig. 7.20).

Table 7.9 Determined apertures for the different PM used in the experiments and the ratios between the PM and the grout

Porous Media		b_{K-C} (mm)	b_{K-C}/d_{95}^{Grout}	$D_{15}^{soil}/d_{85}^{Grout}$
A	stone	0,22	1,7*	8,5*
	Brick	0,24	1,8*	5,0*
B	stone	0,20	1,6*	8,1*
	Brick	0,25	2,0*	4,7*
C	stone	0,39	3,1**	17,8**
	Brick	0,49	3,8**	15,2**
D	stone	0,55	5,0	25,5
	Brick	0,77	6,0	23,4**
E	stone	0,72	5,6	29,3
	Brick	1,12	8,7	26,6

* PM not injectable; ** PM starts to create plug formation (filtration tendency)

According to Eriksson (Eriksson, 2002) and Eklund (Eklund, 2005) the most important PM features affecting penetrability are aperture size, variability in apertures and magnitude of contact areas. As the finer PM present lower aperture sizes and higher variability in apertures and magnitude of contact areas (i.e., higher specific surface), grout penetrability problems may arise.

Newtonian fluid vs. Bingham fluid

The aperture determined for the Bingham fluid (called equivalent aperture - b_{eqv}) is typically 3–5 times larger than the Newtonian fluid (water), as shown in Table 7.10. Thus, as stated earlier, the penetrability of a Newtonian fluid (water) or a Bingham fluid (grout suspension) differs. In fact, the solid particles of the grout suspension cannot enter all of the voids a Newtonian fluid can. It also means that the available space in each PM that can be filled with water is not the same as the space that may be filled with the grout. In fact, the results show that for each PM the volume of injected grout is lower than the volume of injected water. For this reason injectability values are lower than 1 (Table 7.8). Considering the aforementioned, it is possible to state that the measured porosity, which is done with water, is not a representative measurement for the available volume for a grout suspension.

Table 7.10 The equivalent aperture for a Bingham fluid and the ratio compared to the aperture determinant for Newtonian fluids

Porous Media		b_{eqv} (mm)	b_{eqv} / b_{K-C}
A	stone	0,86	4,0
	brick	0,81	3,4
B	stone	0,86	4,2
	brick	0,85	3,4
C	stone	1,45	3,7
	brick	1,56	3,2
D	stone	1,80	3,3
	brick	2,23	2,9
E	stone	2,44	3,4
	brick	3,32	3,0

Analysis of the influence of filtration rate on grout penetration blockage

The curves that represent the mass of injected grout over time for each PM were plotted in Fig. 7.21. During the first part of injection process the injection curves have a linear increase, while for the last part of the injection the curves show a different behaviour. The coarse PM present a constant flow of the same magnitude in all the tests. In relation to finer PM, from Fig. 7.21 it can be seen that a limited penetration occurred. After an initial penetration, the inclination of injection curves become null, what means that the penetration in the PM was not total (the top of the cylinder was not reached). The evolution of injection curves are in full agreement with the injectability values (Table 7.8) and the visual inspections performed the cylinders after 45 days of injection tests (Fig. 7.19 and Fig. 7.20).
By analysing the grout injection curves in Fig. 7.21 and the grout injectability values present in Table 7.8, certain conclusions regarding the penetrability and stop mechanisms can be made:
1. For PM A and B, the results presented in Table 7.9 indicate that limited penetration occurs due to the narrow voids between the particles of PM. In the lower part of the cylinder the presence of grout was obvious, but along the height the flow paths were successively blocked, the grout solid particles being unable to enter the available aperture – a stop mechanism called clogging (Axelsson et al., 2009), leading to an absence of grout at the top as shown in Fig. 7.16.a. As referred by Eklund and Stille (Eklund & Stille, 2008), the plug formation (Fig. 7.1) is probably influenced by a stochastic phenomenon. From the experiments it was possible to observe that both the time for the plug to occur and the position where it occurred vary in the different tests.
2. According to Table 7.9, PM C is close to the threshold for which penetration is possible. The hypothesis is made that in critical parts of PM only single grout particles, but not the entire grout suspension, are able to penetrate the PM, therefore starting the filtration of grout solid particles as shown in Fig. 7.18.d, Fig. 7.19 and Fig. 7.20.
3. The grout will be able to penetrate PM D and E, as confirmed by visual inspection which showed homogenous grout penetration along the cylinder height (Fig. 7.19 and Fig. 7.20).

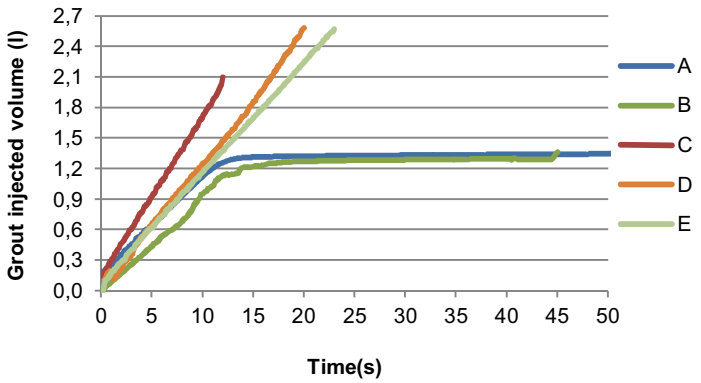

Fig. 7.21 - Grout volume injection vs. time to brick PM wetted

Concerning whether pre-wetting of PM before the grout injection may have any benefit concerning the penetration, it was observed that in finer PM the magnitude of filtration process is lower. In fact, as shown in Fig. 7.16.a and Fig. 7.16.c a higher height of injection is reached when the PM is pre-wetted. However, the grout volume injected is lower (Table 7.8), because as already stated during the pre-wetting the capillaries can absorb water due to capillary pressure what subsequently hinders the grout injection process.

In summary, three main conclusions can be drawn regarding the penetrability of hydraulic grouts:

– The penetrability depends on the ratio between the aperture size and the maximum grains in the grout.
– Close to the limit of what is considered penetrable there is filtration of grout grains.
– The water content of PM before the injection affects the filtration rate; more water means higher height (length) of grout penetrability; however the grout volume injected is lower.

Analysis of the grout penetrability using different criteria

According to the values of Table 7.11, some criteria created from different fields of the present work showed a slight agreement with the injectability results, namely the criteria proposed by Johnson, Littlejohn, Cambefort, Papadakis and Paillère & Guinez. The criteria created by Miltiadou-Fezans and Tassios are to be the most suitable. As highlight, for the cylinder D the criterion $d_{85}<W_{nom}/5\pm1$ is verified to limestone PM and not for the brick PM (although the criterion has been almost fulfilled). In fact, as can be seen in Fig. 7.19 the injection was not entirely perfect for $D_{,brick}$. The reason can be lower size of particles to brick PM (Table 7.6), resulting in lower W_{nom} value; consequently the magnitude of filtration process is higher. As regards the criterion $d_{99}<W_{nom}/2$, for both PM is found to be verified which in the reality it is not correct, as mentioned above. Therefore, the use of a single groutability ratio criterion is not sufficient to ensure penetrability into very fine voids of PM. Indeed, as concluded by Miltiadou-Fezans and Tassios (Miltiadou-Fezans & Tassios, 2013a) the upper part of the entire grading curve of the binder must be taken into account. Thus, specific grading criteria should be verified in order to evaluate if the grout can be injected in a certain PM.

Table 7.11 - Verification of the condition $d<W_{nom}/n$ based on different authors

		P.M.									
		A		**B**		**C**		**D**		**E**	
Author	**n value**	stone	Brick	stone	Brick	stone	Brick	stone	Brick	stone	Brick
Johnson	W_{nom}/d_{85} (n > 3,75)	1,31	0,77	1,25	0,73	2,73	2,34	**4,02**	**3,88**	**4,49**	**4,08**
Mitchell	W_{nom}/d_{100} (n > 3)	0,66	0,39	0,63	0,36	1,37	1,17	2,08	2,01	2,32	2,11
Littlejohn	W_{nom}/d_{85} (n > 3,75)	1,31	0,77	1,25	0,73	2,73	2,34	**4,02**	**3,88**	**4,49**	**4,08**
Littlejohn	W_{nom}/d_{100} (n > 5)	0,66	0,39	0,63	0,36	1,37	1,17	2,08	2,01	2,32	2,11
Hutchinso	W_{nom}/d_{max} (n > 3)	0,66	0,39	0,63	0,36	1,37	1,17	2,08	2,01	2,32	2,11
Cambefort	W_{nom}/d_{100} (n > 1.5 to 2)	0,66	0,39	0,63	0,36	1,37	1,17	**2,08**	**2,01**	**2,32**	**2,11**
Léonard	W_{nom}/d_{85} (n > 0,75 to 3)	**1,31**	**0,77**	**1,25**	0,73	**2,73**	**2,34**	**4,02**	**3,88**	**4,49**	**4,08**
Papadakis	W_{nom}/d_{100} (n > 1,5 to 3)	0,66	0,39	0,63	0,36	1,37	1,17	**2,08**	**2,01**	**2,32**	**2,11**
Paillère & Guinez	W_{nom}/d_{100} (n > 1,5 to 2,3)	0,66	0,39	0,63	0,36	1,37	1,17	**2,08**	**2,01**	**2,32**	**2,11**
Miltiadou-Fezans	W_{nom}/d_{85} (n > 5 ±1)	1,31	0,77	1,25	0,73	2,73	2,34	**4,02**	3,88	**4,49**	**4,08**
Miltiadou-Fezans	W_{nom}/d_{99} (n > 2,0)	0,66	0,39	0,63	0,36	1,37	1,17	**2,08**	**2,01**	**2,32**	**2,11**

Bolded values indicate that the condition $d<W_{nom}/n$ is partially satisfied.
Bolded and underlined values indicate that the condition $d<W_{nom}/n$ is satisfied.

Buckingham Reiner model (yield stress vs. penetrability)

Given the maximum L of the injection tests (0.3m), the pressure adopted in the injection tests (ΔP = 1 bar) and the yield stress (τ_0=0,63 Pa), the minimum void diameter (D_{min}) of the PM to be injected is equal to 0,0075 mm (according to Eq.7.5). As can be seen in Table 7.9 and Table 7.10, the apertures calculated for all PM are much bigger than D_{min}. Therefore, according to Buckingham Reiner model an homogeneous filling in all PM should have been achieved. Nevertheless, as can be seen in 7.5.1.3 and 7.5.1.4, in PM A and B it is not observed. As aforementioned the variability of shape of channels inside PM (not only cylindrical channel such as it is considered in the model of Buckingham Reiner) could also be a possible explanation for the difficulty that occurs when the grout is injected in these PM. Another possible explanation for the non-homogeneous filling observed in these PM can be the higher water absorption of these PM (Table 7.6). The loss of water that occurs in grout leads to an increase of yield stress which means that Eq. 7.5 may be satisfied - flow will stop in some channels - meaning that grout will try to flow through other available channels, leading to the non-homogeneous filling.

7.6 Conclusions

The present study allows the following conclusions:

(a) Given the large variety of masonry types and materials and in order to better take into account the mentioned difficulties of hydraulic-lime grout to penetrate in extremely fine voids, the importance of

evaluating the injectability of a grout for each specific case before intervention (by injecting plexiglass cylinders containing samples of the real materials of the masonry to be repaired) was highlighted in this work. Similar conclusions were also obtained by other authors, such as Bras (Bras & Henriques, 2012), Kalagri (Kalagri et al., 2010), Valluzzi (Valluzzi, 2005) and Van Rickstal (Van Rickstal, 2000).

(b) The results of injectability show that the percentage of filling varied between 46% and 97% for the different PM. The reason for the upper value to be lower than 100% is due to the fact that the voids volume was determined with water (Newtonian fluid), which is able to penetrate into more voids than the grout (Bingham fluid). This phenomenon may also explain the similarity of grout volume injected in both PM, in spite of the brick PM having a higher porosity.

The value of injectability of a grout in a given media is mainly affected by the permeability, voids volume, size of the finer particles - d(10), rough surface and the water absorption capacity of the media particles. Depending on the grain size distribution and the type of material of PM, the parameters referred have different influence on injectability. Thus, it is necessary to characterize all parameters of the PM so that the injection capacity of the grout can be estimated.

Comparing the differences of injectability values between coarse and fine PM, it is observed that these values are higher when using the equation proposed by Bras *et al* (Bras & Henriques, 2012). In addition to the amount of grout injected, the equation by Bras also takes into account the rate of grout injectability, which has a great influence on the results. Furthermore, from these injectability results it seems that the yield stress value has more relevance for finer PM, whereas for coarse PM, viscosity forces and inertia effects become more significant.

(c) The increase of permeability of PM leads higher values of injectability - $I(s^{-1})$. However, for high permeability values (higher than 750 Darcy) this trend is non-existent. In fact, the parameter d(10) that is associated with the aperture of smaller voids/channels has the main role. When a PM has not small voids, an increase of the voids aperture does not necessarily mean an increase of the injectability (despite the increase in permeability).

(d) According to the visual inspections during the injection of the cylinders, it was concluded that for high amounts (over 33 wt%) of the finer material (0.15-2 mm) the reliability of the injection technique is jeopardized (Kalagri et al., 2010). In these cases the grout flow tends to stop during the injection process, enabling an increase of the particle flocculation phenomena, as observed with PM A and B. Thus, it can be concluded that this grout will not be injectable inside a masonry with similar internal characteristics. The visual inspections also showed that pre-wetting of the PM cannot solve the grout penetrability, since at the time of grout injection the finer capillaries are already filled with water (due to its high capillary pressure - Young-Laplace equation), hence hindering the penetration of the grout. The only advantage of pre-wetting is to increase the grout injection velocity, since the flow resistance is reduced by the water injection, therefore increasing the rate of injectability. However, pre-wetting should be used with much precaution, as also stated by some authors (Valluzzi, 2005; Van Rickstal, 2000).

(e) In the light of the achieved results, some conclusions can be drawn regarding the penetrability of hydraulic lime grout:

1- The penetrability depends on the ratio between the aperture size and the maximum particle size in the grout. When the grout solid particles are not able to enter the available aperture pathways clogging occurs. This happens in PM A and B, for which the rules established by Axelsson and colleagues are not observed. Close to the limit of what is considered penetrable according these rules filtration occurs, i.e. the grout enters the available aperture but some solid particles of the grout stop in constrictions and gradually block the pathways. This stop mechanism happens in some critical zones of PM C. When the rules are respected (cases of PM D and E), homogeneous penetration of grout suspension is achieved.

2- The penetrability of a fluid is dependent on the aperture of the area between the particles of PM and a function of the fluid type. Moreover, the variability in apertures and the magnitude of contact areas are also important PM features that affect the fluid penetrability.

3- The water content of PM before the injection affects the filtration rate; more water means lower filtration tendency. However, as already mentioned, in general this fact does not improve grout penetration.

4 - From the study of hydraulic lime grout penetrability following different approaches, it was possible to conclude: a) the grain size distribution of the grout solid phase should be compatible with the characteristic dimensions of the discontinuities to be injected (voids, fissures, interfaces, etc.); b) one "groutability ratio" criterion is not sufficient to ensure penetrability into very fine discontinuities of masonry. In reality, as already established by Miltiadou-Fezans and Tassios (Miltiadou-Fezans & Tassios, 2013a) the upper part of the grading curve of the grout solid phase has to comply with specific grading criteria, depending on the granularity of the PM to be injectable; c) knowing grading curve of the binder can predict if a given PM can be injectable.

5- According to the grout penetrability results obtained, the Buckingham Reiner equation is not the best way to check whether a grout is able to penetrate in a specific PM. The high variability of shape of the channels inside these types of PM contradicts the assumptions of the equation, which should not be used. However, as already concluded by other authors (Axelsson et al., 2009; Bras & Henriques, 2012; Eriksson, 2002), the injection tests revealed that yield stress may be used as a control index for the application of injection grouts.

Chapter 8. Evaluation of consolidation of grout injection in different porous media

8.1 Introduction

As mentioned in Chapter 6 and Chapter 8, an important parameter for the improvement of the behaviour of old masonry strengthened by grout injection is the bond between grout and the in situ material, which is not necessarily proportional to the compressive or tensile strength of the grout. The bond mechanism between different PM and grouts was also studied by Adami and Vintzileou (Adami & Vintzileou, 2008), who performed shear tests, as well as direct tension tests. The results obtained showed the important influence of the substrate characteristics (i.e. the surface roughness, porosity, and initial water content) on the bond properties. In order to study the above parameters, in the hardened state the cylinders that resulted from injection tests (see 7.5.1) were evaluated through non-destructive techniques (NDTs) and mechanical tests.

In what concerns the mechanical tests, splitting tests were performed to different injected PM. This study aims to contribute to a better understanding of the prevailing mode of failure and the influence of the type of material, distribution of voids size and water content of the particles (at the time of injection) in the mechanical bonds at the interfaces (grout - PM). Furthermore, it is also analysed the strength gradient along the height of the cylinder, as well as the relation with the effectiveness of grout injection for each PM.

Among the various NDTs, acoustic techniques, based on measurements of the characteristics of acoustic waves propagating through the material, appear to be of great usefulness since they are non-invasive, easy to use and provide relevant information about internal morphology of the injected material (see 4.3). Thus, they are often used in laboratory for materials characterisation and structural diagnosis (Riggio et al., 2012). Acoustic analysis is based on a simple principle of physics: the propagation of any wave will be affected by the medium through which it travels. Thereby, changes in measurable parameters associated with the passage of a wave through a material can be correlated with changes in the physical properties of the material (Anzani et al., 2007; Cantini et al., 2012; Uranjek & Bosiljkov, 2012). Thus, in the present work, ultrasonic tomography was used to evaluate the effectiveness of grout injection for the strengthening of multi-leaf stone masonry walls, since it is possible to obtain a qualitative information about the compactness of the PM from the outputs of ultrasonic tomography (Da Porto & Modena, 2003). In this way, the locations in which injection is more difficult to penetrate (areas of masonry consisting of solid stones or a mixture of different particles which prevent the injection of grout) can be detected (Uranjek & Bosiljkov, 2012; Zanzi et al., 2001) (Fig. 8.1). To this end, a comparative tomography of PM after injection was carried out. The tomographs were obtained with specific software, in the present case GeoTom CG. The software take as input a data set of travel-time measurements and compute a three-dimensional model of velocity in the material containing the ray paths (Cantini et al., 2012; Jackson & Tweeton, 1996). The SIRT (Simultaneous Iteration Reconstruction Technique) iterative method was implemented to solve the system in both programs in order to easily obtain a map of the wave velocity distribution in the tomographic section (Fig. 8.1).

The tomographic analysis also allowed establishing a relation with mechanical results. From the tomographs it was also possible to identify different density gradients along the height of the cylinder, since there is a relation between the velocity of the ultrasound and the compactness of the media (Epperson & Abrams, 1989; Miranda et al., 2010). Being so, this research has special relevance due to

lack of information about the study of grout injection capacity in physical models filled with different PM (simulating old masonries), through tomography and mechanical tests, when compared to the amount of information that already exists for injectability tests (Bras & Henriques, 2012; Miltiadou-Fezans & Tassios, 2013a; Valluzzi, 2005; Van Rickstal, 2000).

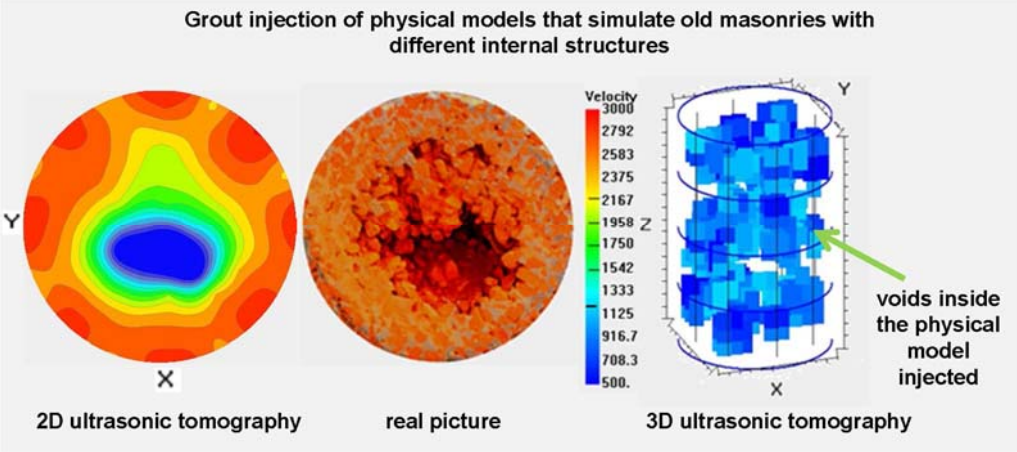

Fig. 8.1 - Evaluation of the grout injectability through ultrasonic tomography

8.2 Material studied

8.2.1 The mechanism bond

Research conducted by several authors (Vintzileou & Adami, 2009) indicated that the bond between grout and PM is of both chemical (because of the reactions between the materials in contact along the interfaces) and (mainly) mechanical. Mechanical bond depends on characteristics of the substratum, such as density, surface porosity and pore size, roughness, water content and water absorption capacity. Thus, it is extremely important to know the values of these properties for the different PM studied. In addition, it also depends on the properties of the binding material, in particular its chemical composition, fineness, setting time and expansibility phenomena.

8.2.2 Porous media properties

8.2.2.1 Porous structure

To study the water absorption capacity and porous structure of the particles of each PM, the cumulative pore size distribution was evaluated using the mercury intrusion porosimetry (MIP) with an AutoPore IV 9500 mercury porosimeter (Fig. 8.2). The brick and limestone samples with a dimension about 3,5 cm (Fig. 8.3) were dried in an oven at 105^0C before testing. In the MIP test, the samples were evacuated to 50 μmHg (6.7x10-6 MPa) and subsequently, was started the intrusion process of low-pressure which was generated between 0.0138-0.2068 MPa to gradually force the mercury into the pores on the surface of the sample. After the low-pressure stage, the penetrometer was then installed in the high pressure port to perform the analysis of high pressure. The pressure was then increased from 0.2758 MPa up to a maximum pressure of 206.8 MPa (30 kpsi), being able to penetrate into pores as small as 7 nm in diameter. By tracking pressures and intrusion volume during the experiment, it is possible to get a measure of the pore structure. The in-pore invasion process is

governed by the Washburn-Laplace equation (Eq 8.1) in which the size of intruded pore accesses, assimilated to cylindrical capillaries, are inversely proportional to the applied pressure:

$$p = \frac{2\Upsilon \times \cos(\theta)}{r} \qquad (8.1)$$

Where p is the mercury injection pressure (Pa), Υ is the surface tension of mercury (N/m), θ is the contact angle between the solid and mercury, and r is the pore radius (micron). In this study, as in other previous studies with similar materials studied (Barbhuiya et al., 2009; León, 1998; Yajun & Cahyadi, 2003), a constant contact angle θ of 140° and a constant surface tension of mercury Υ of 0.485 N/m were assumed in the computations of pore volumes.

Fig. 8.2 - mercury porosimeter used in tests

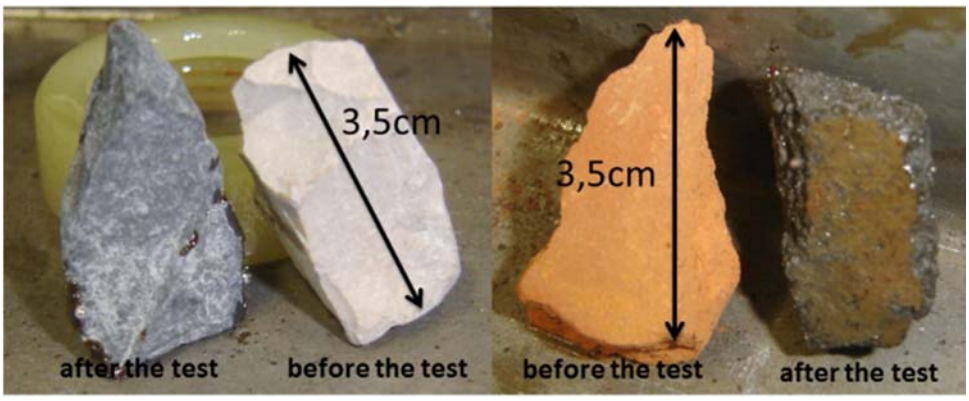

Fig. 8.3 – Limestone and brick samples before and after the MIP test

From the graphic presented in Fig. 8.4 (each curve is the average of three tests) it can be observed in both samples the inexistence of a pore diameter to which the highest slope of mercury injection (threshold diameter (Diamond, 2000) corresponds. However, the curvature of cumulative pore size distribution of limestone is more pronounced, which indicates a narrow distribution of the pores. Indeed, the main pore diameter is significantly larger in brick (0.015 - 4.5 μm) than for the limestone samples (0.025 - 0.045 μm). Moreover, the area below the cumulative intrusion curve is much higher in brick samples. Thereby, it is possible to state that brick samples, with higher porosity and pores size, have higher water absorption capacity when water or grout is being injected. These results fit well

with the water absorption (WA) capacity of each PM (Table 7.6) calculated by the European standard EN 1097-6. The knowledge of water absorption capacity of the particles of PM is of utmost importance during the injection of grouts (Bras & Henriques, 2012; Van Rickstal, 2000). This allows a perception of the amount of water absorbed by the particles of PM during the injection process, which influences the grout fluidity (consequently the grout injection capacity) and the mechanical bond between the grout - PM particles, since the water that is absorbed by the surface particles of PM forces the binder grains to stick to its walls creating an interfacial layer (grout - PM particle) with high binder content which provides a better bond between both. Thus, on one hand, brick PM create more resistance to the grout flow and, on the other hand, establishes a greater bond with the grout.

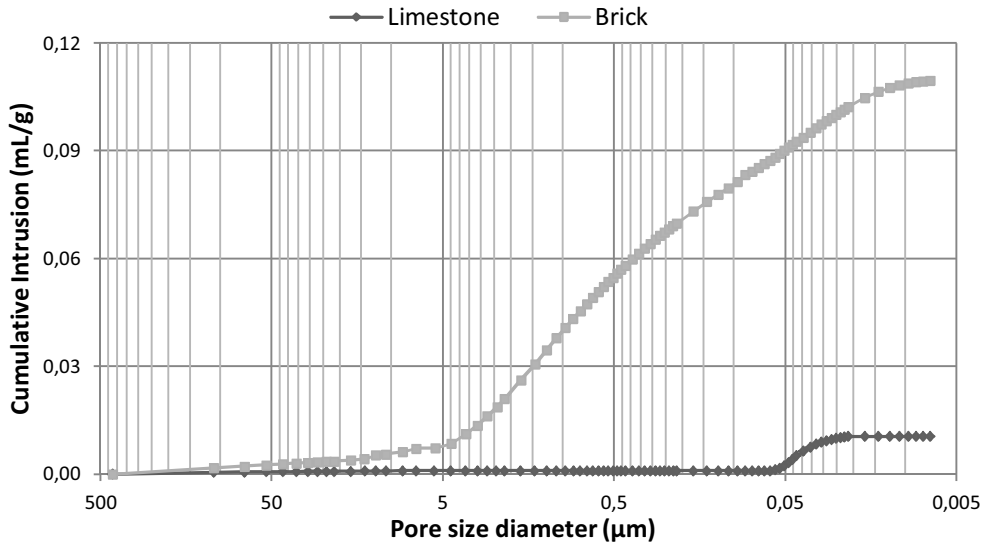

Fig. 8.4 - Cumulative pore size distribution to brick and limestone samples

Another output from MIP is the bulk density, porosity and median pore diameter (Webb, 2001). The bulk density is equal to the mass of the bulk quantity divided by the bulk volume (this volume includes all pores, open and closed). The porosity is calculated based on the mercury intrusion volume at the maximum pressure. The median pore diameter - D_{avg} (µm) is calculated from the equation:

$$D_{avg} = \frac{4 \times I_{tot}}{A_{tot}} \qquad (8.2)$$

where I_{tot} is the total specific intrusion (mL/g) and A_{tot} (m^2/g) is the total specific pore area. The results of porosity and median pore diameter are in consonance with the graph of cumulative pore size distribution (Fig. 8.4). As shown in the curves of cumulative intrusion, the area below of the curve is much higher in brick samples. Furthermore, the pores distribution focuses more on the area of the bigger pores, and thereby the D_{avg} is higher.

The results of density and ultrasound velocity are in accordance with the porosity, because the first two increase while the latter decreases, as expected. In fact, stone particles with lower porosity have higher bulk density (3,60 g/cm^3) than brick particles (2,00 g/cm^3).

Table 8.1 - Hardened properties of the limestone and crushed bricks

	Limestone	Crushed brick
Median Pore Diameter - D_{avg} [μm]	0,038	0,520
Bulk density[g/cm^3]	3,60	2,00
Porosity[%]	2,70	21,89
Ultrasound Velocity[m/s]	5044	2253

8.2.2.2 Wettability

The grout wettability quantifies the wettability of a solid surface by a grout. For the same grout, wettability depends on the type of surface in terms of water absorption capacity and roughness (Klein et al., 2012). Therefore it is possible to conclude that the grout wettability is directly related to the bond between grout and PM particle, meaning that when a grout has high wettability the bond with PM is generally also high. In this work, the grout wettability was characterised by contact angle measurements. The contact angle (Fig. 8.6) is a quantitative measure of the solid angle (θ) of a fluid on a given surface (Pichot et al., 2012), determined in this work with a sessile drop apparatus (Goniometer KSV instruments - Fig. 8.5) using PM particles (which are polar as most construction materials). Firstly, the PM particle was placed in a horizontal position in the sessile drop apparatus. Afterwards, a droplet of grout was carefully dispensed onto the PM particle and an image of the droplet making contact with the glass surface was captured by a video camera (Fig. 8.7). The image was subsequently processed with software (by KSV instruments) to determine the contact angle.

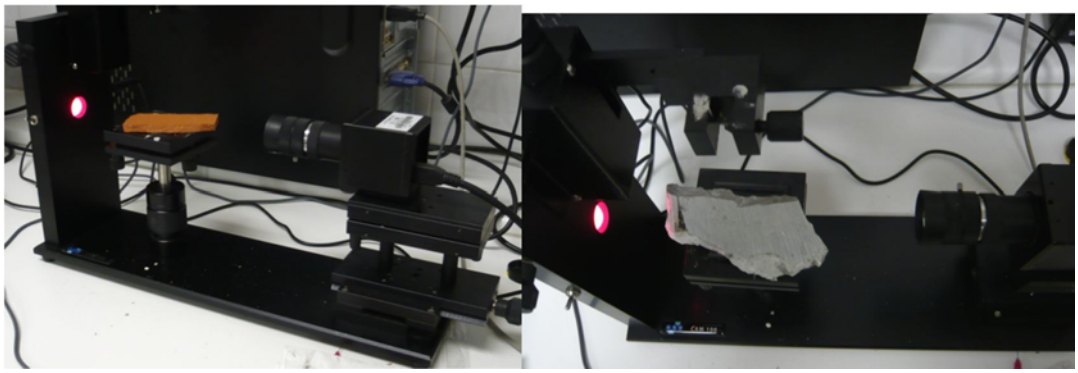

Fig. 8.5 - Goniometer KSV instruments

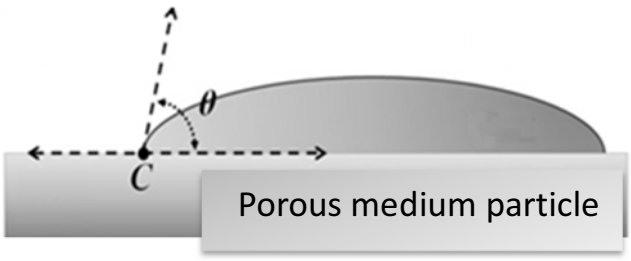

Fig. 8.6 - Contact angle (θ) measurement of a liquid drop on a PM substrate (adapted from) (Pichot et al., 2012)

A high contact angle - Fig. 8.7.b indicates a grout with low affinity for the polar surface (poor wetting). This means that a lower contact angle - Fig. 8.7.a is desirable to get a grout with higher wettability and, as a result, with greater bond. But, on the other hand, the grout wettability is directly related with the

grout retention capability and it can also be seen as an indicator of its fluidity, because high water loss (high wettability) is a drawback in grout flow capacity (Baltazar et al., 2014). Thus, in what concerns the evaluation of the effectiveness of grout injection it should be taken into account that the contact angle has an opposite trend for the grout fluidity and the bond strength between grout and the PM particles. Table 8.2 shows the contact angles of grouts with different PM. As seen, the contact angle is higher in stone particle surface and when PM particle is wetted. The results show a considerable variation which means a significant alteration on grout wettability.

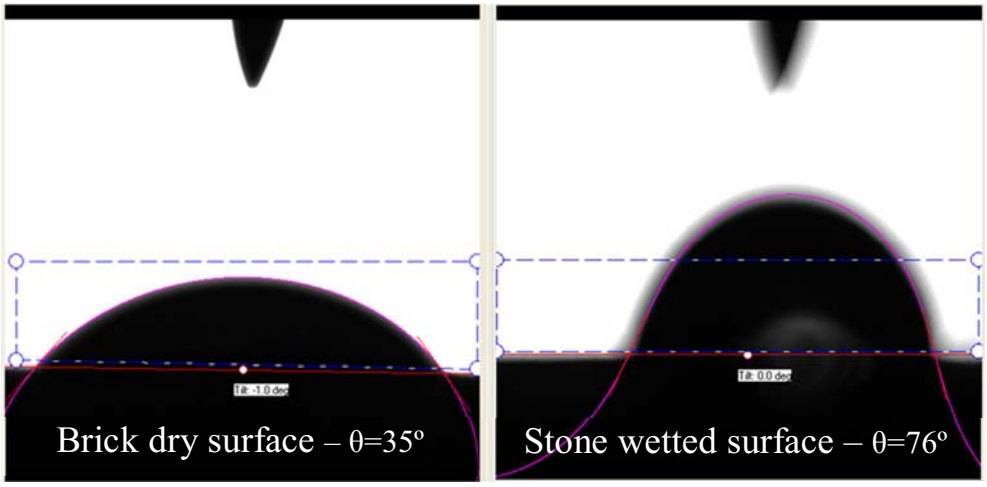

Fig. 8.7 - Contact angle (θ) measurement of a grout drop onto the PM particle captured by a video camera

Table 8.2 - Contact angle (θ) between grout and particle surface of PM

PM		Contact angle - Θ (º)
Stone	Dry	48
	Wetted	76
brick	Dry	35
	Wetted	54

8.2.3 Grout design, samples and general characterization

As already mentioned in Chapter 5, Chapter 6 and Chapter 7, grout design involves the study of the behaviour of a suspension in fresh and hardened state. Together with the previous tests, grout strength determination was made to the grout used in injection tests of the Chapter 7 (see Table 7.4). In order to determine mechanical characteristics of the formulated grouts a testing campaign was undertaken and the samples were submitted to flexural and compressive strength tests following standard (EN 1015-11, 1999). Prismatic grout samples (160x40x40 mm) - Fig. 8.8.a were cured in a controlled atmosphere at 20±2ºC and 60±5% relative humidity until the age of the test. Testing was performed at the ages of 28 and 90 days. For flexural strength determination (Fig. 8.8.a), a pre-load of 10N was first applied and then a uniform rate of 0.2 mm/min until the failure. With respect to compressive strength (Fig. 8.8.b), the pre-load was equal to 50N and the uniform rate was 0.7 mm/min (both tests are explained in detail in chapter 6.3). For both situations, the failure occurred within a period of 30s to 90s, using a Z50 Zwick mechanical test machine with 50 kN capacity. Following the same settings (in the Z50 Zwick machine) of compressive test, the splitting (Fig. 8.8.c) and shear test (Fig. 8.8.d) were performed.

Fig. 8.8 –a) Flexural test, b) Compressive test, c) Splitting test, d) shear test

The mechanical properties of the grout studied are present in Table 8.3. Regarding flexural and compressive strength, the grout shows good mechanical performance in comparison to the results found in the literature. On the other hand, the shear strength and splitting tensile strength show lower values compared to other mechanical tests.

Research conducted by several authors (Kalagri et al., 2010; Toumbakari, 2002) indicated that the intrinsic mechanical properties of the grout have not extreme relevance. Ignoul in (Ignoul et al., 2004) also indicated that intrinsic mechanical properties of grout hardly influence the final strength of a deteriorated masonry wall. Ignoul suggested that the adhesion strength to the cracks and void surfaces in the masonry are more important. Thus, based on the standard ASTM C 496, the grout adhesion strength to the PM particles was studied (see 8.3.2).

Table 8.3 - Mechanical properties of the grout selected

	Parameters / Tests	Grout selected	Literature
Mechanical Properties	Flexural strength [MPa] - 28d	2,36	2.11-2.47 (Bras, 2011); 0.6-1.7(N.G. Almeida et al., 2012); 1.02-1.9 (Kalagri et al., 2010)
	Flexural strength [MPa] - 90d	2,85	2.29-2.52 (Bras, 2011); 0.88-2.52(Kalagri et al., 2010)
	Compressive strength [MPa] - 28d	5,32	2.82-4.08 (Bras, 2011); 3.23 (Jorne et al., 2012); 6.1(L. G. Baltazar et al., 2013); 1.7-3.4 (C. Almeida et al., 2012); 1.53-3.1(Kalagri et al., 2010)
	Compressive strength [MPa] - 90d	7,45	4.5-8.16 (Bras, 2011); 2.56-4.88 (Kalagri et al., 2010)
	Splitting tensile strength [MPa] - 28d	0.25	-
	Shear strength [MPa] -28d	0.34	-

As conducted for the porous structure of the particles of each PM, there was obtained the median pore diameter, bulk density and porosity from MIP tests (Table 8.4). In comparison to the hardened properties of PM particles (Table 8.1), the grout shows a microstructure with lower density and more porous. Nevertheless as checked in studies by Binda and Toumbakari (Binda et al., 2003a; Eleni-Eva; Toumbakari et al., 1999), low density grouts will perform better in a wall as compared with high density grouts. Regarding the median pore diameter is important to know the value, because the bond strength between grout and the PM particles depends on the properties of the binding material, in particular the porous structure. This issue will be detailed in 8.4.2.

Table 8.4 - Hardened properties of the grout selected

	Grout
Median Pore Diameter - D_{avg} [μm]	0,108
Bulk density[g/cm^3]	1,44
Porosity[%]	46,1

8.3 Procedure

8.3.1 Mechanical properties

In the first part of this chapter it was mentioned that the mechanical properties of the grout are not much relevant since pure grout will not be present in the injected masonry. Instead it is more useful to test the mechanical strength of the injected cylinder samples. For this purpose cylinders were kept in normal laboratory conditions for 45 days (T=20ºC and R.H.=65%) after the injection. The characterization of the mechanical properties was carried out only for the samples in which the grout reached the top of the cylinder (PM types C, D and E) – see 7.5.1.4.

The Plexiglas cylinders were removed from the hardened samples and the ultrasound pulse velocity was measured in order to obtain the tomographs (Fig. 8.9-1). After that the cylinders were cut in 3 slices (Fig. 8.9-2) and each of these slices was also analysed for ultrasound pulse velocity (Fig. 8.9-3) and the tensile splitting strength (Fig. 8.9-4) was determined.

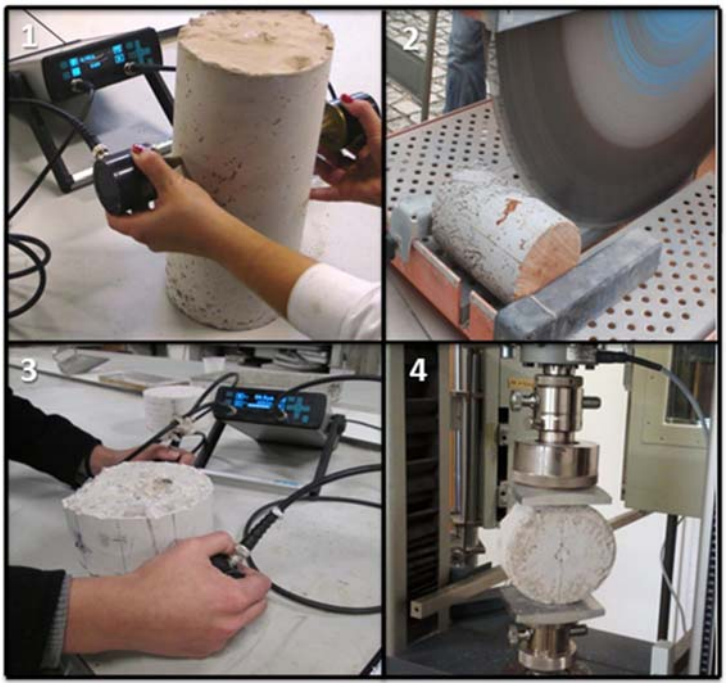

Fig. 8.9 - 1) Ultrasound pulse velocity test (for a cylinder); 2) slice of the cylinder; 3) and 4) ultrasound pulse velocity and splitting test, respectively (for a slice of cylinder)

8.3.2 Splitting tests

Splitting test was performed in accordance with the procedure described in chapter 6.4.3.

8.3.3 Ultrasonic pulse velocity tests

The ultrasonic technique is based on the generation of ultrasonic impulses at a selected point of the sample. Based on the time (measured by a pundit equipment) that the impulse takes to cover the distance between the transmitter and the receiver, the overall quality and homogeneity of the tested cylinder can be assessed (Moropoulou et al., 2013; Panzera et al., 2011; Uranjek & Bosiljkov, 2012). In general terms, more compacted materials with higher density will have high wave propagation velocities. Instead, air interfaces (or voids) within a cylinder will cause variations in the pulse velocity, since the wave pulse is forced to circumvent the internal air void, the time of propagation for the assumed path through the void centre is increased, causing in this way, the decrease of the apparent velocity. Thus, air interfaces are registered as places with very low wave propagation velocity (Naik et al., 2004).

It is worth noting that the wave propagation is not only affected by intrinsic characteristics of the materials mentioned above. Actually, there are external factors (namely humidity and temperature) that can modify the wave propagation (ASTM C957-02, 2002; Leucci et al., 2014). Thus, it is important to control these variables in order to correctly estimate the wave velocity in the investigated material (cylinder). For this reason, the cylinders were tested at room temperature 20 ˚C and dried prior to be tested.

The choice of appropriate frequency depends on the type of the evaluated material, since the attenuation magnitude of the ultrasonic waves (that varies according to the heterogeneity degree of the material) is dependent on the value of selected frequency (Anzani et al., 2007). For a higher frequency, higher is the attenuation of the wave energy which affects the quality of the signal detected by the receiver transducer (Concu et al., 2009). In this work, considering the scale of the samples used in the laboratory (see 7.4.3) the use of ultrasonic tomography was chosen. It was used ultrasonic transducers with 54 kHz which are able to locate small anomalies, such as minor flaws/voids (Schullerl et al., 1997). In these conditions sonic tests (low frequencies, lower than 20 kHz) were not appropriate to study the injectability of the grout. Indeed, low frequency pulse tests limit the identification of smaller flaws and voids due to the higher energy and resistance to attenuation in the presence of multiple cracks and flaws, what may not be critical when testing in situ real masonries (as is often used). However, it is important to note that the main concept of both techniques is the same, varying only the frequency which conditions the wave length change.

In what concerns the format of the transducers, there are several types (Whittingham, 2007). The linear transducers are the most common. They have the advantage of a good resolution in the near field (Fig. 8.10), which is beneficial for small models typically used in the laboratory. However, they are not indicated for materials with curve surface (as the cylinders used in this work) because they cannot wrap conformably the material surface causing the creation of air gaps. So, transducers with reduced surface (sector transducer) were used, as can be seen in Fig. 8.11. Actually, the difficulty of the coupling of the transducers with the surface is underlined by standard ASTM C597-09 and some authors (Kashif et al., 2016). Thus, to obtain an adequate coupling, an ultrasound gel (viscous material) was used.

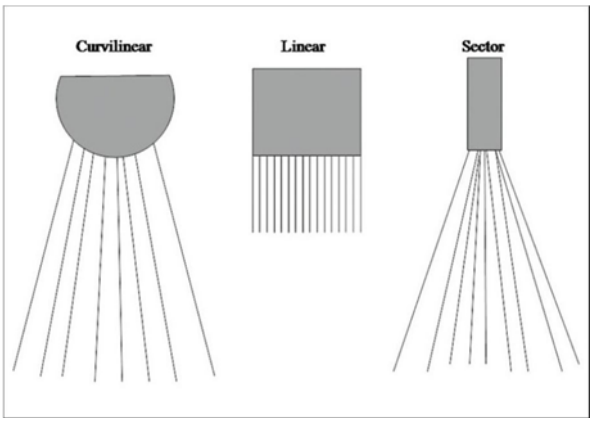

Fig. 8.10 – Different types of ultrasonic transducers

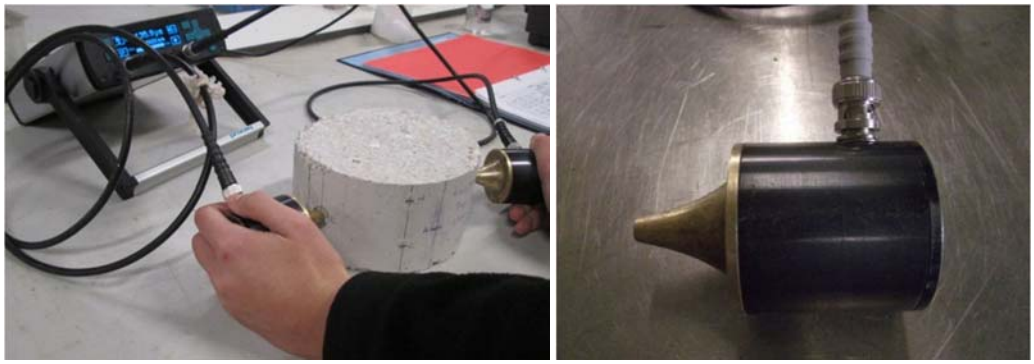

Fig. 8.11 – Ultrasonic test with sector transducers

The ultrasonic tests were aimed at controlling the effectiveness of the injection by evaluating the compactness at different heights (Cantini et al., 2012; Zanzi et al., 2001). Thus, the measurements were performed in the middle of each slice corresponding to the three levels (bottom, middle and top) of each cylinder (Fig. 8.9). To obtain the average ultrasonic velocity of each slice to detect the penetration and diffusion of the grout, a system of measuring points, i.e., a grid pattern, was established (Fig. 8.12). The grid refinement is dependent on the: sample size, variability expected and the accuracy required (Cantini, 2012).

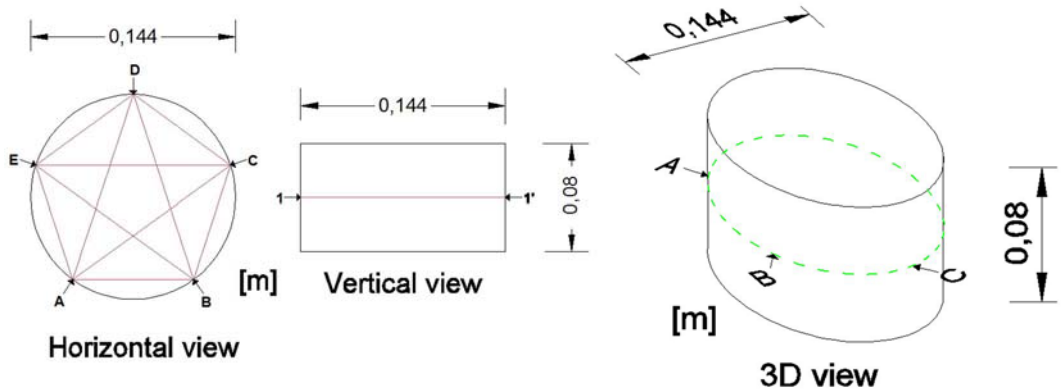

Fig. 8.12 - Scheme of the mesh grid used to measure the average ultrasonic velocity for each slice of the cylinders

8.3.4 Ultrasonic tomography

The direction in which the maximum energy is propagated is at right angles to the face of the transmitting transducer; however, it is possible to detect pulses travelling through material in some other direction (Panzera et al., 2011). In other words it is possible, to make measurements of pulse velocity (BS EN 12504-4, 2004) by placing the two transducers on either:

(i) opposite faces - direct transmission (Fig. 8.13.a), the ultrasonic wave is transmitted by a transducer (emitter) through the tested object and received by a second transducer (receiver) on the opposite side;

(ii) the same face - indirect or surface transmission (Fig. 8.13.b), the propagation of ultrasonic waves occurs between points that are located on the same surface of the material;

(iii) adjacent faces - semi-direct transmission (Fig. 8.13.c).

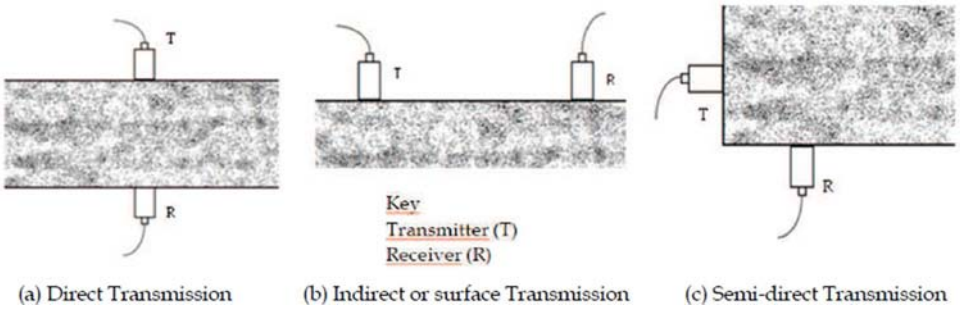

Fig. 8.13 – Methods of propagation and receiving ultrasonic pulses (Panzera et al., 2011)

Direct transmission is the most sensitive, and indirect transmission the least sensitive testing arrangement (Panzera et al., 2011). Direct Transmission is very effective, since the broad direction of wave propagation is perpendicular to the source surface and the signal (stress wave) travels through the entire thickness of the item (Concu, et al., 2009). In contrast, in the indirect transmission the wave propagation travels only in the surface of the material. Indirect measurements are not recommended in ASTM C 597 and it is often stated that indirect measurements are not reliable. Thus, indirect transmission is used when only one face of the sample/material is accessible (Yaman et al., 2002). In the laboratory, access is generally available to opposite surfaces of a test specimen and ultrasonic tests are commonly conducted using direct transmission. However, the direct transmission has some limits. The major limit consists in describing the wave's characteristics of the sample using for each path only one value of that characteristic, i.e., hypothesising that the mean value is homogeneous along each wave path. This assumption prevents the identification of the position of the detected anomaly inside the sample/cylinder. An effective way to overcome this limit is to use tomography which allows the reconstruction of an image of the inside of the cylinder (Concu et al., 2009). The tomographic imaging is a computational technique (GEOTOM CG is the software used) that utilises an iterative method (SIRT algorithm) for processing a large quantity of data (ultrasonic pulse velocities) collected on the external surface to reproduce the morphological internal structure of a sample (Bliylikzt, 1998; Cantini, 2012; Zanzi et al., 2001). The final output is a map of the velocity distribution on a plane section of the structure under investigation (ultrasonic horizontal tomography) and in all structure - cylinder (3D tomography), which allows the evaluation of the effectiveness of repair technique (Concu et al., 2010; Ferraro et al., 2013; Schullerl et al., 1997).

The section of the cylinder investigated was marked by a mesh grid (Fig. 8.14) whose dimension was related to the distance between two subsequent transmission or receiving points and a certain resolution in order to detect the areas where grout cannot penetrate (Cantini, 2012).

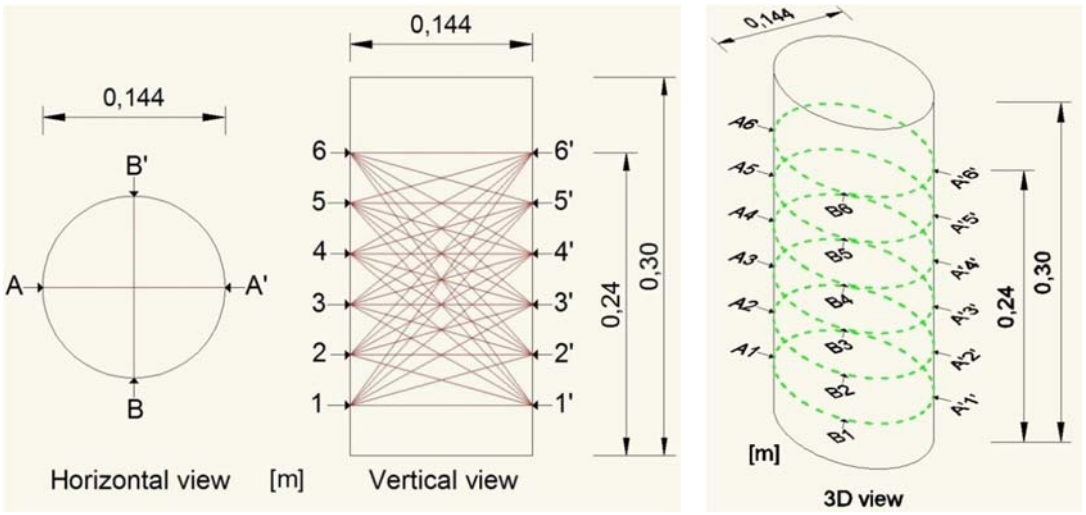

Fig. 8.14 - Scheme of the mesh grid to obtain ultrasonic tomographs along the height of the cylinder

8.4 Results and discussion

The characterisation of the mechanical properties of the samples (in which the grout injection reaches the top of the injection) was done with direct ultrasonic measurements, splitting tests and ultrasonic tomography.

8.4.1 Visual inspections after injection of the cylindrical models

After 45 days the cylinders were cut and an inspection of the degree of success of the injection in terms of penetration and diffusion of the grout was possible. A remark can be made regarding the presence of large amount of not injected zones for PM with finer material, as shown in Fig. 8.15 - a). In contrast, when PM do not have any presence of finer particles, a high effectiveness of grout injection is achieved (Fig. 8.15 - b-c)).

Fig. 8.15 - PM C (left), D (middle) and E (right picture). The core in the left picture displays a big void

8.4.2 Splitting test

Splitting tests enable the determination of grout bond to the PM injected. Only a grout with good behaviour will improve the load bearing capacity of masonry (Bras, 2011). The splitting tensile

strength values are reported in Table 8.6. It can be remarked that the strength values are ranging from 0.18 to 0.40 MPa for limestone PM and from 0.24 to 0.62 MPa for crushed brick PM depending on the effectiveness of injection. These results fit well with similar results reported in the literature (Binda et al., 2001). Samples C showed a lower strength (both for crushed brick and limestone), probably because of the lower porosity and the lower aperture of the voids of PM (Table 7.6) before injection (causing phenomena of filtration and blockages to the grout flow) induces lower amounts of injected material (Table 8.5 and Fig. 8.16) (C. Almeida et al., 2012; Axelsson et al., 2009; Binda & Anzani, 1997), i.e., lower effectiveness of grout injection capacity (Fig. 8.15 and Fig. 8.25). Another reason is related to the fact that PM C has more quantities of fine particles (causing higher specific surface). Thus, there exists more suction of water by the aggregate (for both materials), resulting in diminution of water in the area surrounding the porous surface of the aggregate. This reduction is maximum at the interface aggregate-grout, causing a delay of the hydration process and decreasing the mechanical characteristics.

Table 8.5 – PM porosity [%] and grout mass injected [kg] for the different PM used

Porous Media		Porous media porosity [%]		Grout mass injected [kg]	
		stone	***Brick***	***stone***	***Brick***
A	*Dry*	41,2	48,1	2,15	2,81
	Wetted			1,97	2,15
B	*Dry*	39,3	48,7	1,43	2,35
	Wetted			1,36	1,69
C	*Dry*	44,6	51,5	3,92	3,62
	Wetted			3,30	3,24
D	*Dry*	50,4	56,6	4,51	4,76
	Wetted			3,95	3,80
E	*Dry*	50,8	55,4	4,41	4,33
	Wetted			3,98	3,89
Average		**45,3**	**52,1**	**3,1**	**3,3**

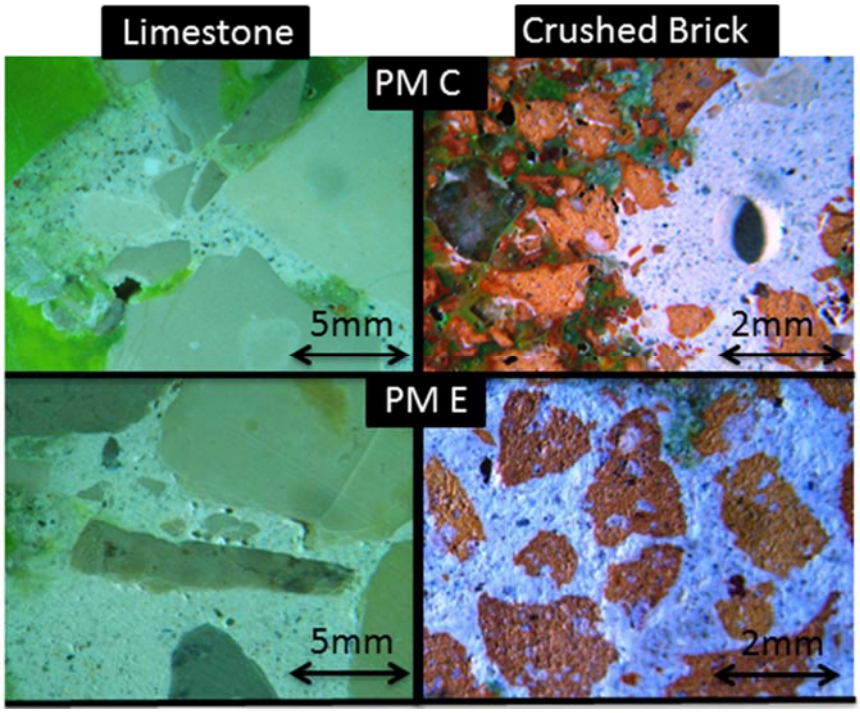

Fig. 8.16 - Different grout injectabilities for different PM (optical microscope image); the green colour (impregnation of the resin) represents the voids of the samples analysed

From Table 8.6, it is obvious that the mechanical results highly depend on the position of the specimen in the original sample. For some samples (cylinders) the relation between mechanical strength show a positive gradient (i.e. increase of the strength values along the height of the cylinder) whereas for other there is a negative gradient. Two phenomena can cause a density gradient. While the grout is going up through the cylinder filled with PM particles, its W/C ratio decreases because the particles absorb some of the water. This water absorption leads to an increase of the density of the grout also contributing to an increase of its cohesion resulting in a positive gradient strength (Table 8.6). But it happens only if the PM is dry at the time of injection. On the contrary, when PM is pre-wetted before the injection the w/b ratio is higher (because the grout does not lose so much water to the PM) which causes an increase of free water amount that contributes to increase shrinkage and instability phenomena - segregation and bleeding (L. G. Baltazar et al., 2013; Luso, 2012). Shrinkage is one of the most important problems in what concerns injections; as mentioned in Chapter 6 a relatively low shrinkage is required for a good bond. In relation to the instability phenomena, the separation of liquid phase of grout (water) and solid phase (binder) will increase, yielding a difference in binder concentration that can occur vertically (especially for higher heights) due to gravitational settling of the binder grains, as shown in Fig. 8.17. These phenomena are more significant if the grout is not very stable and if the water retaining properties of the grout are poor. This observation has important consequences for practical works. The upper zone of an injected masonry may loose too much binder and therefore become weaker than the bottom zone, the stiffness being negatively affected. In this work, a negative strength gradient is also clearly noticeable when analysing the strength results (Table 8.6). Therefore, besides the hydrostatic pressure also the strength gradient can limit the maximum injection height (Van Rickstal, 2000).

Fig. 8.17 - Cylinder $C_{stone,,wetted}$ (left picture) and $C_{brick,wetted}$ (right picture) 45 days after of the injection time

In the case of PM C the density gradient is negative in both situations. The resistance of the fine voids to the flow increases at greater distance from the injection hole. Due to this increasing resistance finally the yield stress will not be reached at the front of the injection (Van Rickstal, 2000). This blocking mechanism produces a slow obstruction of the injection. When the grout loses too much water the viscosity and the yield stress become too high to make any further penetration possible. This phenomenon is more visible when PM have fine particles, which is the case of PM C (Fig. 7.20 and Fig. 8.25).

Table 8.6 - Splitting tensile strength [MPa] for different cylinder parts (bottom, middle and top) of PM C, D and E

Splitting Tensile Strength [MPa]		***Limestone***					***Crushed Brick***				
Porous Medium		bottom	middle	top	**Average**	Gradient [MPa/m]	bottom	middle	top	**Average**	Gradient [MPa/m]
C	*dry*	0,28	0,24	0,22	**0,24**	-0,38	0.41	0.21	0.11	**0.24**	-1,88
	wetted	0,25	0,20	0,10	**0,18**	-0,94	0.38	0.21	0.13	**0.24**	-1,56
D	*dry*	0,25	0,28	0,30	**0,28**	0,31	0.47	0.56	0.58	**0.54**	0,69
	wetted	0,25	0,22	0,15	**0,21**	-0,63	0.54	0.52	0.54	**0.54**	0,00
E	*dry*	0,33	0,40	0,47	**0,40**	0,88	0.54	0.62	0.72	**0.62**	1,13
	wetted	0,33	0,31	0,18	**0,27**	-0,94	0.62	0.62	0.56	**0.60**	-0,38

According to the results of Vintzileou and Adami (Vintzileou & Adami, 2009) the prevailing mode of failure in the tensile splitting test was the bond between the PM particles and the grout (adhesive failure – see 6.5.1), regardless of the type of material analysed. In all PM, higher values (by 75% approximately) of the splitting tensile strength were obtained for brick PM when compared with the limestone PM (Table 8.6). This is attributed to the better mechanical adhesion achieved of the interface grout-brick particles consequence of its higher grout wettability (higher grout affinity with the particle polar surface as shown in contact angle results - Table 8.2) (Eleni-Eva; Toumbakari et al., 1999; Vintzileou & Adami, 2009), which promotes the emergence of important chemical reactions in the contact area between particles surface and the grout paste during the hydration process. On the other hand, in case of non-porous aggregates (limestone aggregates have average size pores much smaller than the brick aggregates, as shown in Fig. 8.4), there is no release of ions from the surface of the aggregate susceptible of combining with ions derived from the hydrated grout. Therefore, a simple deposition of constituents of grout hydrated, i.e., a physical connection is established on the aggregate surface.

Comparing the splitting tensile results of various cylinders (Table 8.6), it is possible to observe that for both materials PM E has the highest results. As the prevailing mode of failure in splitting test is through the bond between grout and PM particles, for PM without relevant voids such as PM D and E the one with lower number of interfaces (Fig. 8.15) will have the higher mechanical results, which in this case is PM E.

The water content of the interfacial zone is another parameter with extreme relevance on the bond between the grout and the PM particles. As PM particles are completely embedded in the grout, they absorb the water of the grout which provides a better adhesion between both. By injecting water the masonry will be saturated and, although the grout will pass easier (since it is more fluid), the contact angle between grout and particles surface will be higher (poor wetting, meaning poor bond). Furthermore, the W/C ratio of the grout after injection will remain very high, producing a weaker binding material in the hardened state. The little absorption needed for a good adhesion between grout and masonry does not occur and the mechanical improvements will be poor (Luso, 2012; Valluzzi, 2005; Van Rickstal, 2000). Moreover, after the injection process the water content is higher in case of pre-wetted PM. Thus, in these cylinders the difficulty in the penetration of CO_2 inside the cylinder is increased, which causes a delay in increasing the resistance of the hardened samples since the hardening process of hydraulic lime, in addition to the hydration of the calcium silicates and aluminates also involves the carbonation of the free lime (Park, 2008).Thus, it is possible to state that although pre-wetting can improve the penetration of the grout inside the masonry, it has deleterious effects on mechanical strength, strength gradient and stability of the injected grout. The only exception is $C_{brick,dry}$ (see Table 8.6) due to poor effectiveness of the injection in this PM, especially in the upper zones (Fig. 8.25).

When comparing the values obtained with those reported in literature (Bras & Henriques, 2012) and (Van Rickstal, 2000), it can be noticed that they are lower. The reason is the smaller height of the samples (about 80mm) when compared with the height of the cylinders tested by other authors (about 300mm). Thereby, in this case the Poisson effect along the axis of applied load is much higher.

8.4.3 Ultrasonic velocity test

The measurement of pulse ultrasonic velocity by transmission in a material is a relatively simple and fast test, as explained previously. From Table 8.7 it is possible to observe a velocity variation in function of the height above the injection point, i.e., there is a velocity gradient depending on the height of injection. Since there is a relation between the velocity of the ultrasound and compactness and density of the media (Epperson & Abrams, 1989; Miranda et al., 2010), the presence of density gradients can be inferred. The gradient is negative in the case of injections of wet PM and positive when the PM is dry at the time of injection. In the case of dry PM one phenomenon can explain the positive density gradient. While the grout is going up through the cylinder its w/b ratio decreases because the PM absorb some of the water, which lead to an increase of the density of the grout. This phenomenon was also reported by Van Rickstal *et al*.(Van Rickstal et al., 2003). The only exception is $C_{,brick,dry}$ (Table 8.7) due to the obstruction created by dry finer particles to the grout flux along the height of injection, as shown in Fig. 8.25.

Table 8.7 - Vertical distribution of the Ultrasonic velocity (m/s) measured in different cylinder parts (bottom, middle and top)

Ultrasonic velocity (m/s)		**Limestone**					**Crushed Brick**				
Porous Medium		bottom	middle	top	**Average**	**Gradient**	bottom	middle	top	**Average**	**Gradient**
C	*dry*	1839	1994	2066	**1966**	+	1924	1890	1581	**1799**	-
	wetted	1896	1655	1644	**1732**	-	1663	1508	1474	**1548**	-
D	*dry*	1920	2021	2079	**2040**	+	1849	1853	1929	**1877**	+
	wetted	2124	2087	1874	**2028**	-	2027	1978	1987	**1997**	-
E	*dry*	2352	2409	2472	**2444**	+	1825	1841	1878	**1881**	+
	wetted	2337	2335	2108	**2260**	-	2123	2098	2036	**2086**	-

From Table 8.7 it can be seen that for each limestone PM the velocity values of pre-wetted samples were lower, due to the higher amount of free water after the grout injection. As a result, after hardening it is observed a larger number of voids in the cylinder which attenuates the ultrasonic waves. Indeed, the voids in the interior of cylinders act to scatter some of the initial energy of the compressional wave pulse away from the original wave path. Such results fit well with similar results obtained by Anzani *et al*. (Anzani et al., 2006), Panzera *et al*. (Panzera et al., 2011) and Naik *et al*.(Naik et al., 2004). In fact, after pre-wetting of PM not all the injected water flow away, so for the same PM the grout mass injected in wetted PM is smaller than in dry PM, as shown in Table 8.5. After the injection process the dry PM does not have any presence of free water. In contrast, in pre-wetted PM free water is present which means that during the curing process when the water evaporates, some voids within the PM are left.

According to Panzera *et al*. (Panzera et al., 2011) and Anzani *et al*. (Anzani et al., 2007), for heterogeneous materials such as the PM studied in this work, ultrasonic velocity value depends not only on porosity but also on attenuation due to dispersion at the internal interfaces PM particles–grout. Since when a propagating wave pulse impinges on an interface, a portion of the wave energy is scattered away from the original wave path (i.e., dissipation of energy occurs). Thus, as shown in Table 8.7, for coarser PM (D and E) without relevant voids after injection, the PM D with more interfaces present lower values of ultrasonic velocity.

Regarding the brick PM, from Table 8.7 it is clear that pre-wetting can solve penetrability problems (the obstruction to grout injection is reduced), since the average ultrasonic velocities are higher for PM wetted. On the other hand, since there is no water absorption out of the grout, the mechanical strength of these particular samples is very poor, as shown in splitting test results (Table 8.6). Therefore, as already stated by Van Rickstal, pre-wetting has to be used with caution (Van Rickstal, 2000).

Comparing the presence of grout after the injections for different PM with the ultrasonic velocity values (Table 8.7), it can be observed one reasonable relation, as shown in Fig. 8.18. Indeed, it is clear that the higher the presence of grout in a PM (i.e., a better quality of injection), the greater is the ultrasonic velocity measured since the presence of voids is lower.

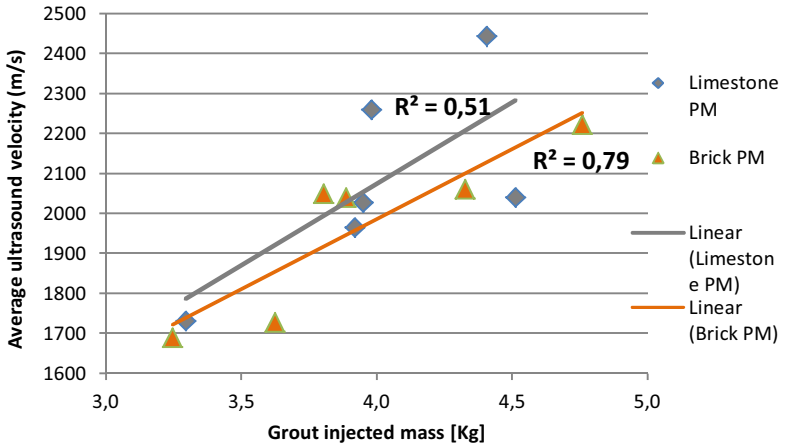

Fig. 8.18 - Relation between Grout injected mass [kg] with ultrasonic velocity [m/s]

Given the results obtained, it is possible to infer that the direct ultrasonic tests can be used to improve the injection technique and to control the penetration and diffusion of the grout during the injection tests on laboratory. Thus, these results can be used in the construction of the tomographs in order to accurately detect the areas where the grout cannot penetrate. It is worth noting that in old real masonries, the construction of the tomographs should be done based on sonic tests rather than ultrasonic results. The presence of large voids and discontinuities do not allow recording the signal of ultrasonic waves due to the high attenuation of waveform energy. This conclusion is in accordance with the results of some authors as Anzani *et al.* (Anzani et al., 2006) and Da Porto *et al.* (Da Porto & Modena, 2003).

8.4.4 Relation among experimental tests results that characterise the grout injection

Some of the results shown previously were combined and analysed together with the radar graph of Fig. 8.19, in which the average of the results for different PM are represented in percentage (100% being the highest value for each test result). From this graph some general relations already reported can be observed, namely the relation between the amount of injected grout (in mass) with the ultrasonic velocities (US) and between the results of splitting tensile strength (ST) and the inverse of contact angle (1/θ). Concerning the first relation, it is clear that the higher the presence of grout in a PM (i.e., a better quality of injection), the greater is the measured ultrasonic velocity since there are less voids. Regarding the second relation, it is observed that higher 1/θ values correspond to higher splitting tensile strengths due to the stronger bonds between grout and the particle surface of PM. Taking into account the splitting test results displayed in Fig. 8.19, the bond strength between grout and PM particles has greater importance than the percentage of voids filled with the grout, i.e., the mass of injected grout for each PM (Table 8.5). Actually, limestone PM exhibited lower splitting tensile strength values than brick PM, in spite of the similar injectabilities of grout in either PM (Table 7.8).

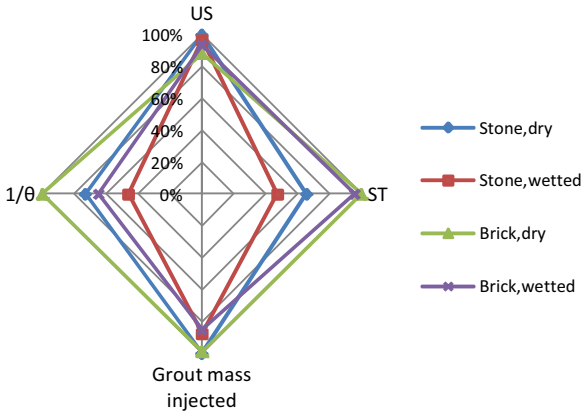

Fig. 8.19 - Relation among experimental tests (ultrasonic, splitting, contact angle and injection test) results that characterise the grout injection

For each PM material, the relation between splitting tensile strength and ultrasonic velocities is presented in Fig. 8.20. It is possible to observe that there exists a great coherence. Thus, when ultrasonic tests show an increase of the ultrasonic velocity, it is possible to conclude that the mechanical characteristics follow the same trend. Similar results were also obtained by Miranda (Miranda et al., 2010). It is worth noting that this relation could not be verified if in the same graph different materials of PM are present. In this case, there are several factors (already mentioned in 8.4.2) that influence the splitting test results and not only the number of voids and interfaces (related to the ultrasonic velocity) that each PM has.

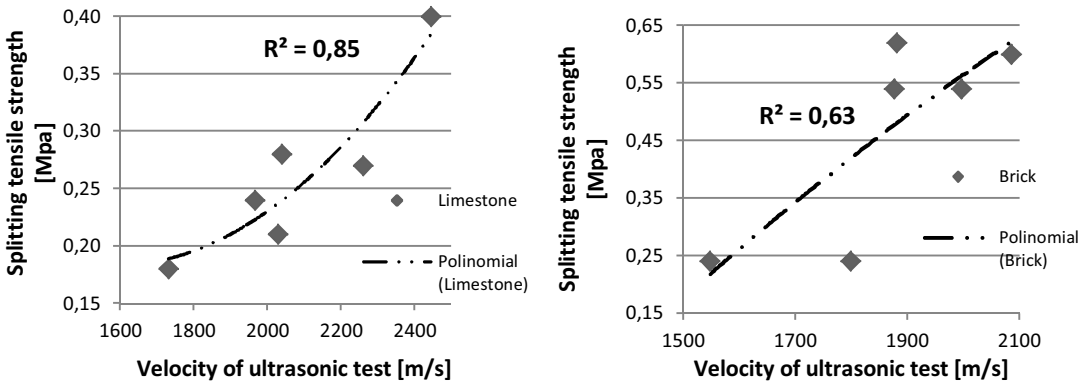

Fig. 8.20 - Relation between splitting tensile strength and ultrasonic velocities. Limestone PM (left picture), Crushed brick PM (right picture)

8.4.5 Tomography

8.4.5.1 Methods and algorithms

The tomographic imaging is a computational technique that utilizes an iterative method for processing a large quantity of data (ultrasonic velocities) collected on the external surface to reproduce the morphological internal structure of the cylinder injected (Cantini, 2012; Zanzi et al., 2001). The software used in order to obtain the tomographic image is the GeoTomCG. The tomographic calculations of GeoTomCG are based on iterative procedure to determine the velocity pattern, which provides the best fit to measured first-arrival traveltimes between sources and receivers transducers.

An initial velocity pattern is assumed. This initial pattern is often an uniform velocity. The first-arrival traveltimes for the initial velocity pattern are calculated, and then the differences between those calculated traveltimes and the measured traveltimes are used to adjust the velocity pattern to reduce the root-mean-square of those differences. The adjusted velocity pattern is used in the next iteration. That sequence is performed iteratively until additional iterations do not improve the fit (Lehmann, 2007). During the tomographic calculations of GeoTomCG two algorithms are used: Forward modelling and Inversion.

Forward modelling in GeoTomCG calculates the first-arrival traveltimes between sources and receivers for a pattern of velocity. This algorithm is performed by ray tracing and travel-time computation with either straight or curved raypaths. The straight-ray approximation allows very rapid calculation of model travel times, but its validity diminishes with large velocity contrasts. So, given the heterogeneity of the samples studied, it is possible to conclude that is not suitable. Curved-ray calculations involve a great deal more of computation, but are more accurate for strong contrasts (Jackson & Tweeton, 1996). There are three methods: "ray-bending", "network theory" and a hybrid approach that uses both the network and ray-bending methods which causes longer execution times, but is the most accurate of the approaches available (Jackson & Tweeton, 1996), since it can solve the main problems associated with other methods. For this reason, this was the chosen method. As regards ray-bending, the problem is that the calculations may converge to a local minimum rather than a global minimum time path. However, this problem is solved through the use of network method where all paths correspond to global minimum travel time (which means first-arrival paths). The problem of network method is that the paths are rather angular and appear "unphysical", but they can be iteratively improved by the bending algorithm (Jackson & Tweeton, 1996).

In relation to Inversion algorithm calculates the adjustments to the velocity pattern to improve the fit to the first-arrival traveltimes. GeoTomCG performs inversions with the simultaneous iterative reconstruction technique (SIRT) (Lehmann, 2007). Another technique established to perform ultrasonic tomography of a sample is the RAYPT (Ray-projection technique), a constrained optimisation technique designed for imaging discrete anomalies in a uniform background material, which it is not the case of cylinders studied and for this reason was not used.

The calculations with SIRT are based on a three-dimensional rectilinear grid of node points, with intervening volume elements or voxels. Values of velocity are specified at the nodes, and calculated within voxels by multiple linear interpolation. SIRT calculations modify an initial velocity model by repeated cycles of three steps: forward computation of model travel times, calculation of residuals, and application of velocity corrections. The cycle repeats through a specified number of iterations. In GeoTomCG, the weighting of velocity correction factors for grid-points is proportional to the sum of the fractions of raypaths in voxels that share that point. The alternative of weighting proportional to the length of raypaths in surrounding voxels (used in ancient software like 3DTOM) gives too much influence to long slanted raypaths (Jackson & Tweeton, 1996).

The output of this technique is a map of the velocity distribution on a plane section, as well as a 3D, of the structure under investigation, which allows the evaluation of the effectiveness of repair technique (Schullerl et al., 1997). In an imperfectly elastic material (as the cylinders studied in this work), intrinsic attenuation causes an exponential decay of wave amplitude with distance from the point

source, since the waves lose some energy due to internal friction (depending on the magnitude of the loss of the physical properties of the medium) (Bliylikzt, 1998; Jackson & Tweeton, 1996). Thus, it is worthwhile to note that the tight grid of measurements used (Fig. 8.14) allowed defining more precisely the shape of the voids, thus achieving a sharper resolution, with the drawback of implying longer measuring and computational times. This observation fits well with the results obtained by Concu *et al*. (Concu et al., 2010, 2009) and Cantini *et al*. (Cantini, 2012). This last author noticed the influence of the density of the ray path map (that depends directly on the mesh grid chosen), highlighting the benefit of some redundancy for a better resolution of the tomographs; this allows a noise reduction in the velocity map and a better detection of the local inhomogeneities.

8.4.5.2 Ultrasonic Tomographs

In this section the ultrasonic tomographs will be compared with the photos that were taken during the inspection tests of the cylinders and with the mechanical results presented in 8.4.2. Ultrasonic tomographs of horizontal sections for each level (bottom, middle and top) of the ultrasonic grid (Fig. 8.12) were obtained. These ultrasonic velocities are influenced by local voids along their paths, thus the results reported for each level can indicate significant differences depending on the area and location of voids present.

Some results from cylinders characterised by the presence of fine material are worthy of attention. It is the case of PM C_{dry} it shows low velocities in zones that before the injection presented finer PM material. This trend is systematically observed on the cylinders filled with this specific PM (for both materials: brick and limestone), resulting in a non-homogeneous state after injection. Regarding the tomographs, in case of the medium slice of $C_{stone,dry}$ (Fig. 8.21-left), more voids are concentrated in the core (characterised by the lowest values of ultrasonic velocity ranging between 1100-1300 m/s). Related to the borders, the reasonable velocities (from 1700 to 2200 m/s) indicate that there were not too many voids present. These results are consistent with the inspections conducted on cylinders after being cut in slices, as shown in Fig. 8.21-left below. The top slice of cylinder $C_{stone,dry}$ is shown in Fig. 8.21-right, showing a two layer pattern with a higher velocity at the compact region of the cylinder and lower velocity in two zones where there are two voids: a large on the right side and a small one in bottom left side of the sample, as shown in Fig. 8.21-right below. In this way, some of the ray-paths of the horizontal tomographies crossed these voids, which attenuate the ultrasonic waves in these areas.

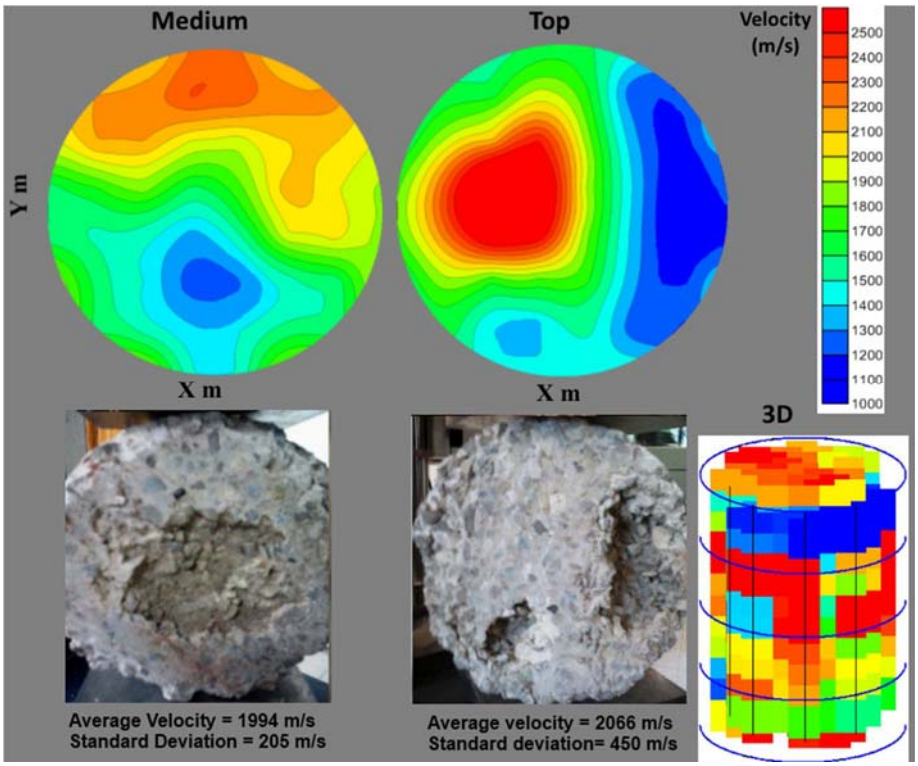

Fig. 8.21 - Ultrasonic horizontal tomography for cylinder $C_{stone,dry}$: medium level (left above) and top level (right above); Inspection after cutting of the cylinder $C_{stone,dry}$: medium level (left below) and top level (middle below), and 3D ultrasonic tomography (right below)

In case of the medium slice of the $C_{brick,dry}$ (Fig. 8.22- left), more voids are concentrated in the core (characterized by the lowest values of ultrasonic velocity ranging between 1000-1300 m/s). Related to the edges/borders, the high velocities (from 2300 to 2500 m/s) indicate a good compactness. The results are consistent with the inspections conducted on cylinders after being cut in three slices, as shown in Fig. 8.22-left below. The Fig. 8.22-right represents the slice of the top of cylinder $C_{brick,dry}$. This tends to show a two layer pattern with a higher velocity region at the upper side of the cylinder and lower velocity on the bottom side. Actually it presents a large void (as shown in Fig. 8.22-right below), where some of the ray-paths of the horizontal tomographies crossed the large void, which attenuate the ultrasonic waves.

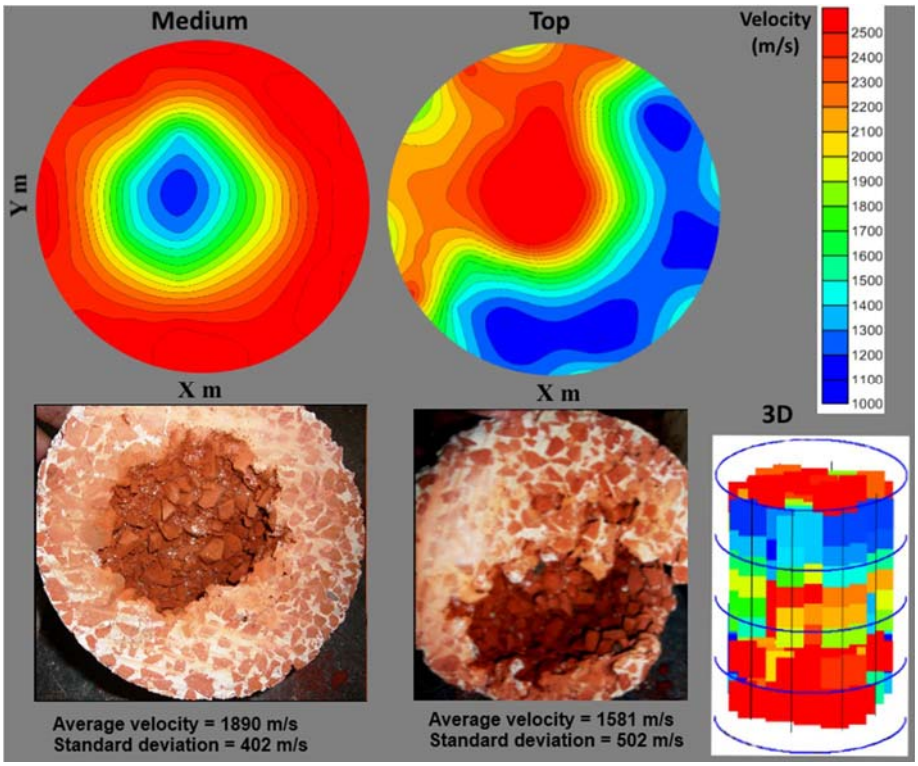

Fig. 8.22 - Ultrasonic horizontal tomography for cylinder $C_{brick,dry}$: medium level (left above) and top level (right above); Inspection after cutting of the cylinder $C_{nrick,dry}$: medium level (left below) and top level (middle below), and 3D ultrasonic tomography (right below)

The highest ultrasonic velocities were generally localised in PM with higher porosity and without fine particles, as is the case of $E_{brick,dry}$ (Fig. 8.24), thus revealing an effect of homogenisation of the cylinder created by the grout injection. The results show a homogeneous distribution of velocities (Fig. 8.23 - below) which seems to indicate that the grout injection was effective. Compared to cylinder $C_{brick,dry}$ (Fig. 8.22 and Fig. 8.24) the contrast velocities are smoother and the velocity range is restricted to about 2320-2380 m/s (Fig. 8.23 -below). Therefore, contrary to the cylinder $C_{brick,dry}$, the cylinder $E_{brick,dry}$ presents a compact section characterised by the absence of large voids, i.e., the voids between particles of PM (before injection test) was successfully filled (Fig. 8.24). The results obtained by tomography were confirmed after cutting the cylinders, where it was possible to observe the absence of large voids and the aggregates connected perfectly with the grout (Fig. 8.23 - above), which is of the utmost importance in relation to the injection of a masonry. Indeed, as mentioned in 3.1.3 the reduction of the risk of failure depends highly on the degree of homogeneity of the masonry after injection. With a uniform filling the variance on the strength decreases and this way the reliability is improved.

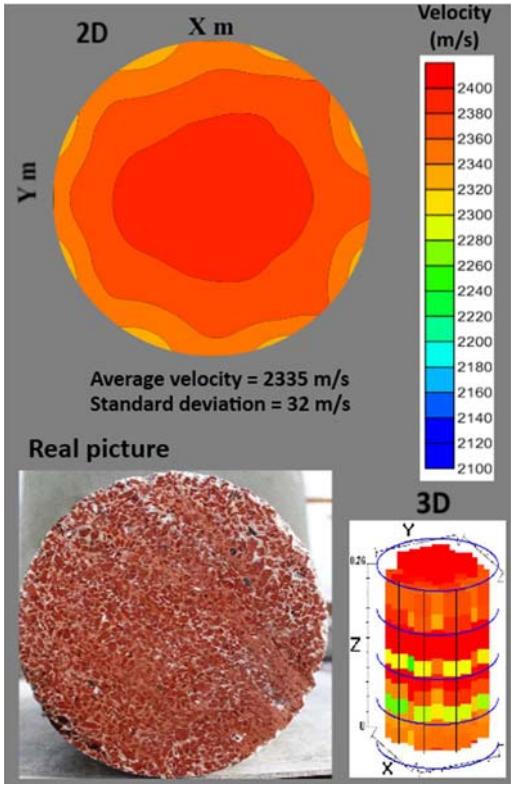

Fig. 8.23 - Cylinder $E_{brick,dry}$: Inspection after cutting of the cylinder (left below), 2D ultrasonic horizontal tomography (left above) and 3D ultrasonic tomography (right below)

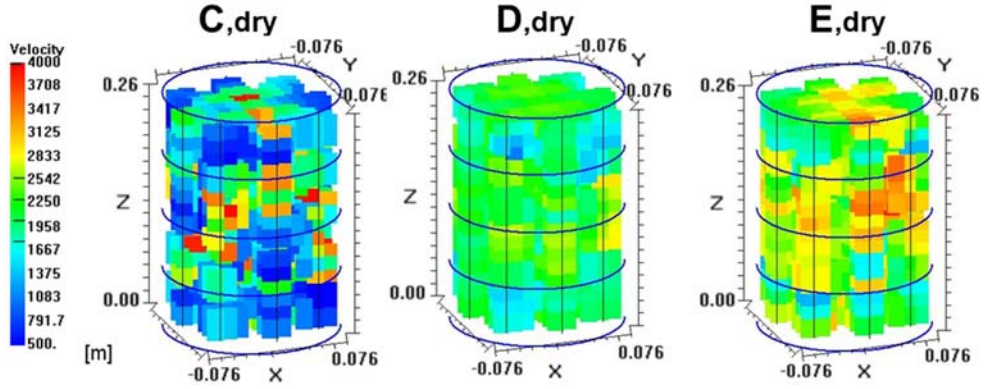

Fig. 8.24 - Results of the ultrasonic tomography (by GeoTom CG) - 3D tomographies for cylinders of dry brick PM

Ultrasonic tomographies in three different levels were carried out on cylinder $C_{,brick,wetted}$, as shown in Fig. 8.25. The tomographs show coherence with the results of Table 8.7 in terms of vertical distribution of the ultrasonic velocity and confirmed preliminary outcomes from visual inspection to cylinder complete (Fig. 8.25- lower right hand corner), which clearly indicated bad grout injection. The test with cylinder $C_{,brick,wetted}$ showed that velocity decreases from bottom to top, indicating that the voids volume is significantly higher near the top level (Fig. 8.25). In fact, the upper horizontal tomography was characterised by smaller values of ultrasonic velocity than the lower horizontal tomography (ultrasonic velocity on the sections ranged between 1000-1700 m/s and 1000-2500 m/s, respectively). The difference in cylinder consistency that was noted during cutting may also be detected from the comparison of the horizontal tomographs and the mechanical results along the

height of the cylinder (Table 8.6). The tomographs displayed in Fig. 8.25 show, in general, that the low values of ultrasonic velocity (around 1000-1200 m/s) allow the identification of areas in bad conditions, whereas areas with high velocities (higher than 1700m/s) indicate that this is a solid area of the cylinder, without voids, which shows that the voids had been successfully filled.

According to Concu (Concu et al., 2009) the attenuation has a very high sensitiveness to all kind of material discontinuity which causes energy loss, since in a medium with discontinuities wave energy is partitioned at each interface encountered by a wave, into reflected and transmitted fractions. Thereby, it is clear that a similar case to $C_{,brick,wetted}$ an excessive attenuation can be occurred, which can cause a significant decrease of ultrasonic velocity in the tomographs (Buyukozturk, 1998; Ferraro et al., 2013). In case of this type of samples with low compactness, lower frequencies ultrasonic waves (the transducers used in this work have ultrasonic frequency of 54 KHz) would be more appropriate because of its higher energy content and resistance to attenuation in the presence of multiple voids (Buyukozturk, 1998).

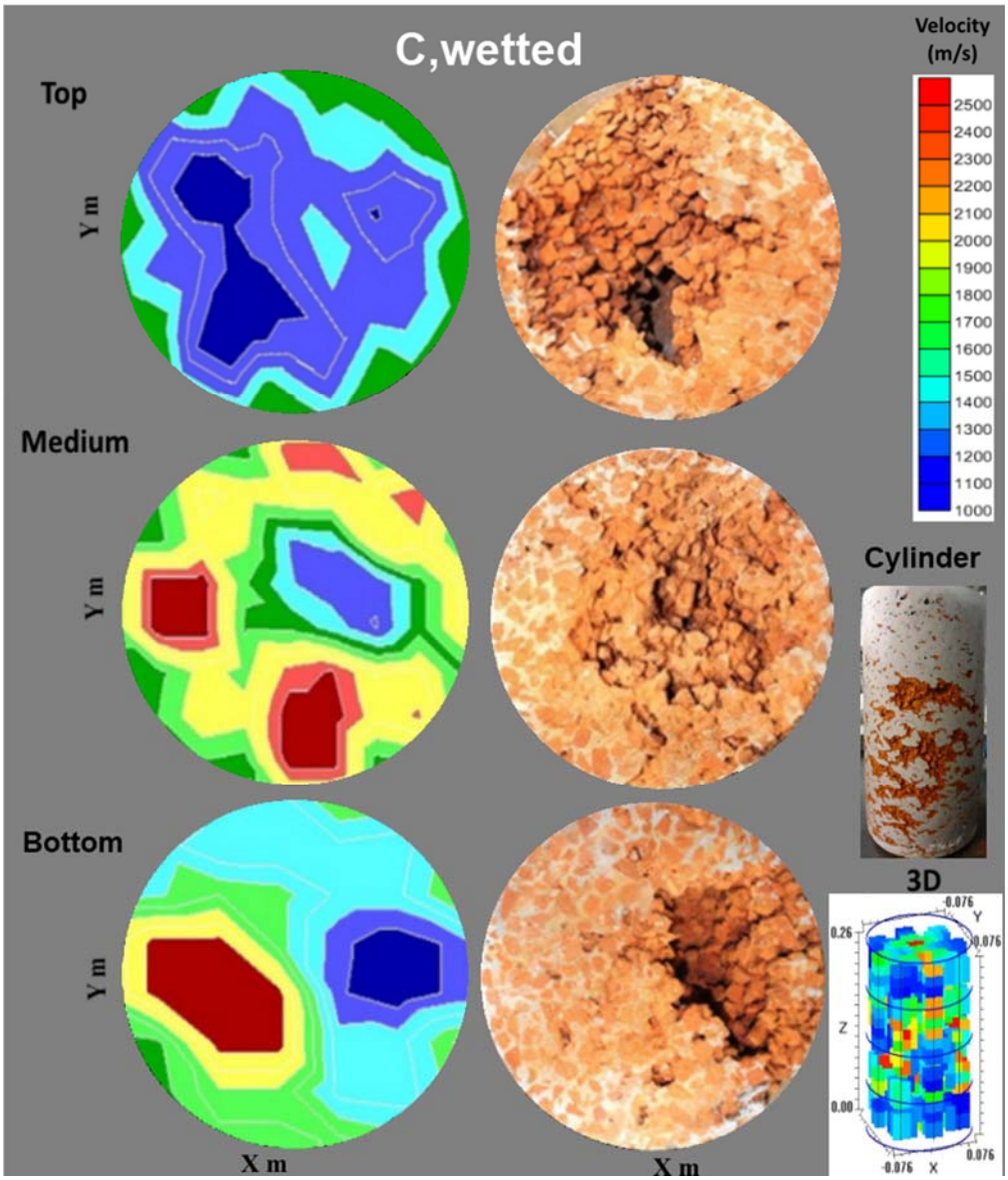

Fig. 8.25 - Results of the ultrasonic tomography for cylinder $C_{brick,wetted}$; horizontal tomographies, in levels: bottom, medium and top of the cylinder. 3D ultrasonic tomography (right picture)

The comparison between the 3 levels of the tests, for cylinder D_{stone} is reported in tomographs of Fig. 8.26. These also show consistency with the results of Table 8.7: vertical distribution of the ultrasonic velocity. When PM is dry at the time of injection, the velocities show an increase towards the upper part of the cylinder (Fig. 8.26-left). In fact, the lower horizontal tomography was characterized by smaller values of ultrasonic velocity than the upper horizontal tomography (average values of velocity on the sections were about 1920 and 2079 m/s, respectively). In the case of pre-wetted PM the inverse happened. The difference in cylinder consistency that was noted during cutting may also be detected from the comparison of the horizontal tomographs. While the mean value of velocity is about 2124 m/s for the tomography at bottom, the mean value on the top section decreases to about 1874 m/s (Fig. 8.26-right).

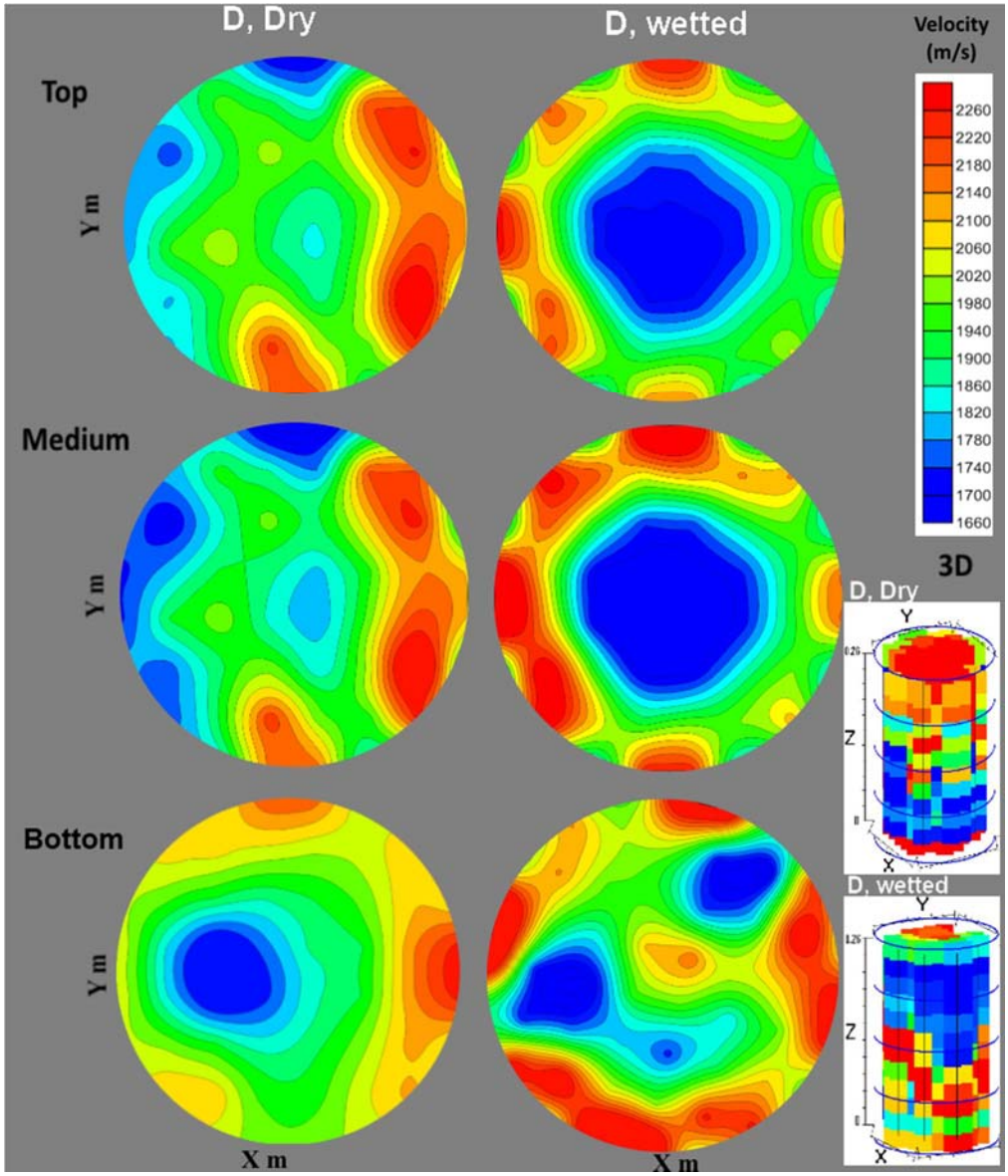

Fig. 8.26- Ultrasonic horizontal tomography: $D_{stone,dry}$ (left pictures) and $D_{stone,wetted}$ (medium pictures) in levels: bottom, medium and top of the cylinder. 3D ultrasonic tomography (right pictures)

As already mentioned, for the tomographs of Fig. 8.25, ultra sonic velocities around 900-1200 m/s correspond to areas that were not injected. The 3D tomographs from Fig. 8.27 confirmed the results

showed previously. In fact, PM C has a considerable area along the cylinder with an ultrasonic velocity lower than 1200m/s (see Fig. 8.21, Fig. 8.22 and Fig. 8.25). In contrast, in PM D and E the area is reduced (see Fig. 8.23 and Fig. 8.26). In the case of PM wetted the area is even non-existent (Fig. 8.27), which proves that the voids present prior to injection were successfully filled by grout.

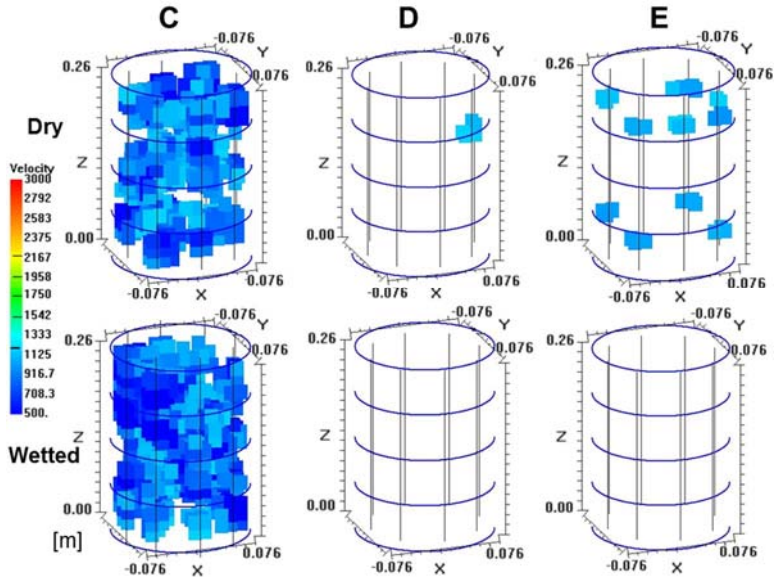

Fig. 8.27 - Results of the ultrasonic tomography (by GeoTom CG) - 3D tomographies (vel. < 1200 m/s) for cylinders of brick PM

Most of the applications found in the bibliography, use these results as qualitative information to assess the compactness and detect damage patterns of the masonry (Da Porto & Modena, 2003; Miranda et al., 2010; Valluzzi et al., 2009). In this work the tomographs were generated using ultrasounds, allowing the evaluation of the extent of grout penetration inside the PM with different materials, particle size and water content at the time of grout injection.

8.4.5.3 Seismic resistance after grout injection

The seismic resistance of the old masonry multiple leaf walls is seriously affected due to the presence of internal voids, cracks and discontinuities between the two external leaves in a multiple leaf wall. Some of the problems/ drawbacks of these masonry walls are poor flexibility, differential stiffness and absence of monolithic behaviour in the lateral direction which originates weak resistance to earthquake (Chaudhry, 2007). In order to attain the desired level of seismic resistance, compactness of the masonry is an essential principle towards strength gain. Based on the results obtained from the physical models (simulating old masonries), it can be stated that the compactness can be reached by injecting the grout and its effectiveness can be controlled through the ultrasonic tomography. This confirms the use of sonic tomography for in situ applications to compare the initial masonry state with the injected one and, therefore, to evaluate the improvements achieved from the seismic resistance point of view.

8.5 Conclusions

The main achievements attained at the present work were:

- Ultrasonic and mechanical tests showed density and strength gradients that are originated from different penetration and diffusion capacity of the grout along the injected PM.

- Pre-wetting process can improve the penetration of the grout inside the PM. However, it has deleterious effects on the mechanical strength and strength gradients of the injected PM. In fact, the mechanical strength of the pre-wetted samples is very poor in comparison with those that were not pre-wetted, especially the upper zones. Indeed, the bond strength of the interfaces is affected in the pre-wetting process, since there is no absorption of grout within the capilars (especially the finer capilars - Young-Laplace equation) because the capilars are saturated and therefore the little absorption needed for a good adhesion between grout and PM particles does not occur.

- Splitting tests confirmed that the prevailing mode of failure occurs at the interface PM particles - grout. The obtained strength values were in the range of 0.1 to 0.63 MPa depending on the effectiveness of injection and the bond properties of the interfaces. The bond properties of the interfaces are affected by the characteristics of the particle surface and can be evaluated by the measurement of contact angle. Crushed brick PM show higher grout wettability (higher grout affinity measured in contact angle test) which means a better mechanical adhesion is established at the interface resulting in higher values in the splitting test.

For both materials PM C with lower porosity and lower aperture of the voids of PM (due to the presence of fine particles) lead to the lowest strength. From the results of splitting tests it became obvious that the mechanical characteristics are highly dependent on the position of the specimen in the cylinder. The results obtained show that the bottom specimens have the highest values causing a negative tensile strength gradient.

- According to the experimental work, ultrasonic velocities can be successfully used to evaluate the quality of an injection. For this purpose, it is essential to choose a suitable frequency, as well as the format of the transducer in order to wrap conformably the material surface. From the results it was possible to find a reasonable agreement between the increase in ultrasonic velocity and the quantity of injected grout. Furthermore, the results were in accordance with visual inspections and can detect non injected areas inside the cylinders. This evaluation also shows a good agreement with the mechanical results.

- The ultrasonic results also show that for heterogeneous materials, the ultrasonic velocity depends not only on compactness but also on attenuation due to dispersion at the internal interfaces PM particles–grout, since when a propagating wave pulse impinges on an interface, a portion of the wave energy is dissipated.

- The inspection of the slices of each of the cylinders confirmed the correspondence between the ultrasonic tomographs and the reality. Thus, it was confirmed that tomography is a useful tool to control the effectiveness of grout injection (Miranda et al., 2010), evaluating the extent of grout penetration inside the PM. It should be noted that while tomography is a useful tool for this purpose, the technique used to supply the required data may vary as a function of the dimensions of the

analysed object. While in laboratory studies – as in the case of this work – ultrasonic tests are the most adequate, in real masonries sonic tests should be used. In fact, the large voids and discontinuities present within the structure of the old masonries do not allow recording the signal of ultrasonic wave due to the high attenuation of waveform energy. Thus, in the case of highly non-homogeneous material with large volume, the choice of sonic tests is more convenient, since the frequency is lower and hence the waveform attenuation is also lower.

- Given the heterogeneity of the samples (PM with different grout injections capacities) studied, the SIRT iterative method instead of RAYPT is more appropriate to perform the data inversion in the ultrasonic tomography technique. In what refers the ray tracing calculation, the curved-ray calculations are more accurate (especially for strong contrasts) to define more precisely the shape and size of the voids.

Chapter 9. Evaluation of the grout injectability and types of resistance to grout flow

9.1 Introduction

As regards injectability (related to the penetration and diffusion capacity of the grout), permeability, voids size distribution and water absorption of the media particles are the most important properties of the PM (see Chapter 7). Depending on the grain size distribution of PM particles, the parameters referred have different influence on injectability. Thus, it is necessary to characterize all parameters of the PM so that the injection capacity of the grout can be estimated (see 7.3.2 and 7.5.1). In this chapter to evaluate the injection performance of the grouts in function of the PM, small scale models (cylinders created in laboratory) already shown in previous chapters have been used. Nevertheless, the dimensions of the cylinders are different. Moreover, in this chapter the granulometry of each PM is not constant along the height of injection. The aim was to evaluate the grout injectability in PM filled with different layers (with different grain size distributions) and different permeabilities and voids distribution along the PM. It was also analysed the reliability of various rules of thumb (already shown in 7.2.3) to check the injectability of a grout in a given PM. Furthermore, it was possible to detect the resistances created by the PM to the grout during the flow. The knowledge of these resistances is crucial to estimate the grout penetration in the internal voids of a PM, allowing to detect when a grout is not injectable in a particular PM.

According to (Gil, 1994; Van Rickstal, 2000), Darcy's law clearly shows a partial inadequacy to model the injection tests. Indeed, the use of Darcy's law led to faster injections through the PM than the experimental results. This suggested that the overall media resistance was underestimated when using this theory. In fact, there is an additional resistance to the grout flow that is ignored by Darcy's law, which is due to the granular nature and the ability to establish bonds of the cementitious grouts. The referred authors implemented in their works the theory of a physical resistance at the fluid (grout) front, called front resistance. This resistance emphasizes the importance of the permeability and granulometry of the front layer. The authors concluded that when this kind of resistance is overcome, it is easier for the rest of the grout to flow through the same front layer. Nonetheless, the injection tests carried out in this work showed that this front resistance is not adequate to model the grout injection. So, an additional resistance was introduced (resistance of suspension- R_s). This resistance depends on the size of the grout solid particles, the size of the voids of the front layer and the void size distribution of the layers already injected.

Following the same procedure of the chapter 7.4.3.1, pre-wetting of the PM was done before grout injection. Some authors (Bras & Henriques, 2012; Eriksson et al., 2004; Gil, 1994) argued that this procedure is able to improve the penetration of the grout inside the PM. Since water content of the PM is a parameter that has influence on the grout injectability, its influence was taken into account for the determination of R_s.

In addition to the fresh state, the grout injection performance was also analysed in the hardened condition. Through tomography, it was also assessed the grout injection capacity in different PM. As concluded in 8.4.5, ultrasonic tomography may be used to detect voids (evaluating the homogeneity) and to evaluate the efficiency of grout injection.

This research gives continuity to the previous chapters where the performance of the grout injection was analysed (in fresh and hardened state). In this chapter, the main aims are: the study of grout

injection in PM with different grain size distributions along the injection, the evaluation of Darcy's law and front resistance in grout injection tests and the creation of an additional resistance to the grout flow (R_s), allowing a more accurate evaluation of the injection.

9.2 Materials studied

9.2.1 Porous media for injection tests

In contrast with other chapters (see 5.2.5 and 7.3.2), the granulometry of each PM is not constant along the height of injection. Six granulometry fractions (coarse – C, medium –M, fine – F, very fine – f, M+F and M+f) were adopted in order to simulate different permeabilities and void size distributions (Fig. 5.11 and Fig. 9.1).

Table 9.1 lists some characterization parameters of each fraction. They have already been adopted in Chapter 5 and Chapter 7, and also in literature (Bras, 2011). As explained in 5.2.5 and 7.3.2, the parameters voids size average, d(90), d(15) and specific surface are obtained from grain size distribution curves (Fig. 9.1). For each granulometry fraction, the nominal lower value of the aperture of voids is represented by W_{nom} ($W_{nom} \sim 0.15 \times d_{15}$) (Miltiadou-Fezans & Tassios, 2013a). The impact of this parameter on penetrability of the grout will be evaluated in 9.4.1. Porosity was estimated by measuring the volume of water that can be filled into each particle size fraction (Bras & Henriques, 2012; Valluzzi, 2005). In these previous studies, the range for the total porosity was between 40% and 55%. In this study, the total porosity of each cylinder is in the range 43-46%. In section 9.4.1 some parameters will be evaluated based on the values presented in Table 9.1.

Table 9.1 – Granulometry fractions characteristics

	C (coarse)	*M (medium)*	*F (fine)*	*f (very fine)*	*50%M + 50% F*	*50%M + 50% f*
Voids size average* [mm]	7.01	3.20	1.68	0.93	2.13	1.70
d(90) [mm]**	9.02	4.44	2.21	1.48	4.15	4.13
d(15)* [mm]**	5.25	2.63	1.30	0.68	1.43	0.78
Wnom [mm]	0.79	0.39	0.19	0.10	0.21	0.12
P.M. porosity – n (%)	45,5	45.6	46.2	46.3	43.9	43.0
Specific Surface (mm^2/mm^3)	0.98	2.21	3.93	6.92	3.07	4.56
Permeability (m^2) x 10^{-10}	8.64	6.55	4.90	2.65	5.51	2.88

*** correspond to d50—the diameter through which 50 % of the total mass passes**

**** the diameter through which 90% of the total mass passes**

***** the diameter through which 15 % of the total mass passes**

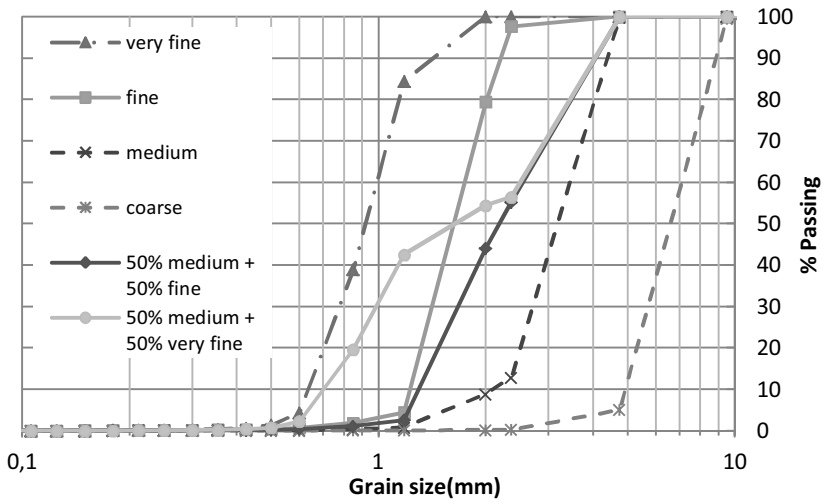

Fig. 9.1 - Grain size distribution of the different ranges sizes particles and the PM used for cylinders grout injection

In order to analyse the physical phenomena that occur during the penetration of the grout when the PM is not constant along the height, three types of PM (easily reproducible) were created (Fig. 9.2). Then, plexiglass cylinders with 100 mm in diameter and 450mm in height were used to perform injection tests in such PM. The cylinders were split into three layers of 13.5 cm each, which were filled with the fractions referred above (Fig. 9.1). The first type (type 1) of PM is completely homogeneous, i.e., each layer was filled with the same granulometry fraction. In the second type (type 2), the granulometry of the middle layer was different from the other two layers, typically finer with the exception of PM F,C,F. The aim of this layout is to evaluate what happens when a grout meets a layer with lower permeability. The third type of PM had the middle layer vertically split in two distinct granulometries (type 3). In the other layers, as in type 2, the coarse particle size was used (C). The objective of the PM type 3 is to assess the progress of grout injection, when a high permeable granulometry fraction is in parallel with a low permeable fraction.

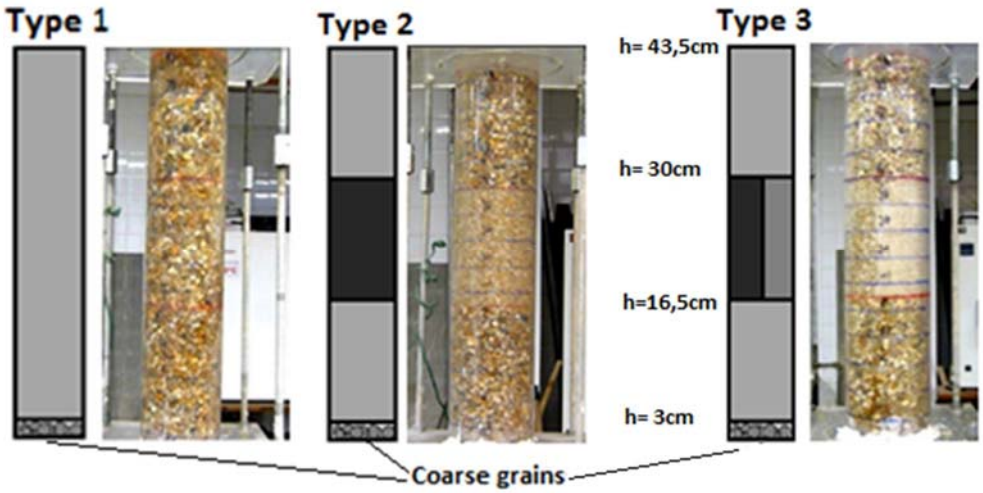

Fig. 9.2 - Layout of uniform sample (type 1), horizontally split sample (type 2) and vertically split sample (type 3)

Fig. 9.3 shows the layout of the different fractions to the eleven PM. These PM will be analysed below. All PM may be reproducible.

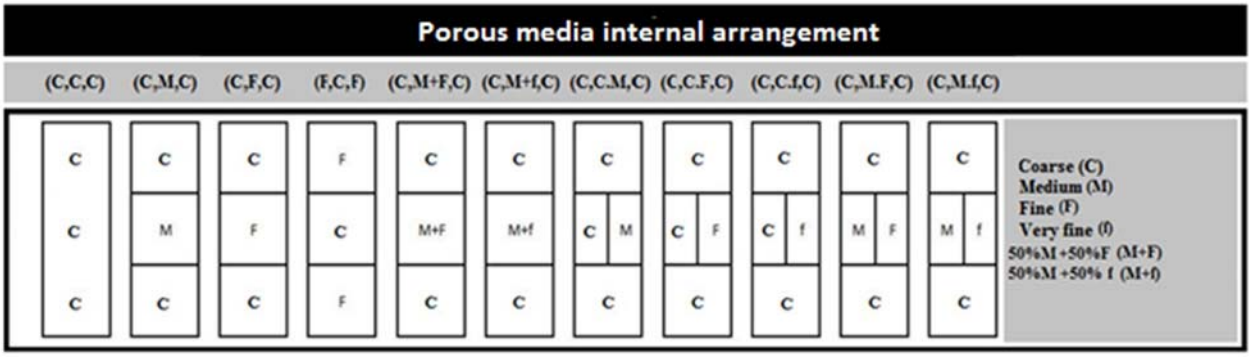

Fig. 9.3 – Layout of PM internal arrangement

Permeability is one of the main PM parameters that influence the evolution and diffusion of the grout. The test setup to measure the permeability of different size fractions was accurately described in 7.4.2. Table 9.1 shows the permeability of the different granulometry fractions that were used to create different PM; the permeability of finer fractions is lower than the coarse fractions. In fact, the resistance to the passage of water is higher for finer fractions. One reason is the smaller particle size, resulting in a smaller aperture of the voids - W_{nom} (Table 9.1). Furthermore, the higher specific surface (Table 9.1) of the finer fractions leads to higher water absorptions – a phenomenon that is explained by the Young-Laplace equation, which also contributes to increase the water flow resistance, thus causing a lower flow rate resulting in lower permeability values (see 7.4.2).

9.2.2 Grout design

9.2.2.1 Grout composition

The formulation of the grout was chosen based on the conclusions of the Chapter 5 and some guidelines and recommendations of several authors (Baltazar et al., 2013; Valluzzi, 2005) and used a HL5 hydraulic lime (EN459-1) produced in Portugal by Secil-Martingança. The water/binder ratio (w/b) was 50% in weight with 1.2wt% of superplasticizer (polycarboxilate Glenium SKY 617 produced by BASF).

9.2.2.2 Mixing procedures

The hydraulic lime mixes were prepared at room temperature of 21 ±2 ºC and a relative humidity of 57 ±5 %. For the preparation of grouts water at the temperatures of 18±1 ºC was used and the dry hydraulic lime was hand-mixed to ensure a homogeneous distribution before the beginning of the mechanic mixing. The mixing procedure was already detailed in chapter 5.2.3.

9.3 Procedure

9.3.1 Injection tests

The injections tests were made using similar procedure to (Kalagri et al., 2010; Valluzzi, 2005; Van Rickstal, 2000). The injections were conducted on cylindrical specimens that were prepared to simulate the infill material (the inner core) of three-leaf stone masonries. The progress of the grout flow inside the plexiglass cylinder was recorded on video, as well as the injected grout mass, measured

by the balance. The video recordings provide the progress of the grout, whereas the weights enable to quantify the amount of injected grout in function of time and to estimate the amount of unfilled voids. Both recordings enable the analysis of the injectability of the grout.
The injection pressure for all these experiments was 0.7 bar (0.07 MPa). The cylinders filled with PM with different fractions were injected from bottom to top using the grout mixes described in 9.2.2.1.
Each PM was dry prior to injection; in addition each PM was also tested after being pre-wetted. In this latter case the particles of the PM were wetted through simple water injection (p=0.7 bar), and then water is let out of the sample. However, at the time of grout injection, the surface of PM particles is still wet. The consequences of pre-wetting for grout injectability were studied in chapter 7.5.1. In this chapter, the goal is to verify if the ineffectiveness shown in PM (A-E) is confirmed in PM with another layout. It should be noted that due to the pre-wetting operation, the particles are saturated which means that the grout contact angle is higher. For this reason, it is expected an improvement in grout flow.

9.3.2 Different criteria to evaluate the penetrability of the grout

As concluded in 7.6, the grain size distribution of the grout solid phase must be compatible with the aperture of the voids of the PM in order to improve the injectability of a hydraulic lime grout. Miltiadou-Fezans and Tassios (Miltiadou-Fezans & Tassios, 2013a) studied this issue and as mentioned in 7.2.3, these authors proposed two specific grading rules: $d_{85} < W_{nom}/5 \pm 1$ and $d_{99} < W_{nom}/2$ in order to achieve grouts with high penetrability.
In the field of soil grouting, Mitchell (Mitchell, 1982) established several rules of thumb for the injectability of PM. One of these rules is presented in Table 7.2. This rule is expressed as the ratio between the aperture of the small voids (represented by D_{15}^{soil}) of the PM to be injected and the size of the larger solid grains of the grout (represented by d_{85}^{grout}). When this rule is not verified (ratio <11), the clogging effect occurs since the grout solid particles are not able to enter the available aperture pathways. When the rule is respected (ratio >25), homogeneous penetration of grout suspension is achieved. In the range between what is considered not penetrable and penetrable (between 11 and 25), the filtration phenomenon occurs, i.e. the grout enters the available apertures but some solid particles of the grout stop in constrictions and gradually block the pathways. According to (Bras & Henriques, 2012), the filtration tendency of the mixture may be affected by hydration of binder grains. Furthermore, the small amount of binder fines must be controlled because the fine materials in suspension coagulate very easily due to interparticle interactions. To counter this, the use of superplasticizers enables the development of repulsive forces due to the adsorption of the polymers on the surface of the grains (E.-E. Toumbakari et al., 1999).

9.3.3 Different types of resistance in a grout injection

9.3.3.1 Use of Darcy's law to model the injection tests

From injection tests observations, Van Rickstal (Van Rickstal, 2000) and Gil (Gil, 1994) built a mathematical model to describe the grout injection. The model takes into account the physical mechanisms that occur during the penetration of the grout through the PM. At first they tried to model

the injections using Darcy's law, governing the laminar flow of fluids through porous materials. The flow is considered to be laminar since the Reynolds number, which characterize the nature of flow for used fractions (Table 9.2) are below the range that indicates turbulent flow. The unique exception is the coarse fraction (Re >10).

Table 9.2 – Reynolds number for the fractions used in PM type 1, 2 and 3

Fraction (mm)	Reynolds number (Re)
(C) (4,75 - 9,5)	13,5
(M) (2,0 - 4,75)	7,1
(F) (1,18 - 2,36)	2,1
(f) (0,5 - 1,18)	*
(M+F) (1,18 - 4,75)	3,7
(M+f) (0,5 - 4,75)	2,2

*Grout is not able to penetrate this fraction

The analytical results (reached with Darcy's law) and the experimental results (from injection tests) were compared in (Gil, 1994; Van Rickstal, 2000). They noted a partial inadequacy of Darcy's law to model the injection times of grout through a PM (Fig. 9.4). In fact, the analytical model simulates a faster injection than the one experimentally observed, indicating that the resistance offered to the grout flow has been underestimated. This work evaluates the additional resistance to the grout flow (which is not considered by Darcy's law) based on the experimental results.

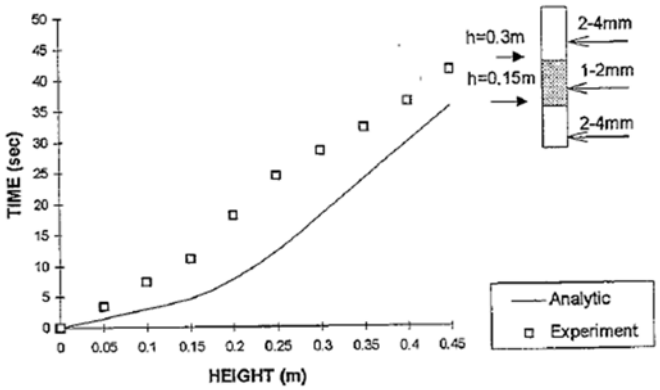

Fig. 9.4 – Darcy's law applied to injection tests (horizontally splitted cylinder) (Gil, 1994)

9.3.3.2 Front resistance theory

The observations mentioned above enabled to develop the front resistance theory. The front resistance theory is based on the hypothesis that beyond the overall media resistance (given by Darcy resistance), there is an additional resistance to the flow at the grout front. At the front, the fluid has to break through the media voids in order that its solid particles can penetrate.

The front resistance (R_{front}) physically indicates the importance of this front resistance in relation to the overall injected media resistance. It is function of the size of the solid particles of the grout and the size of the media voids (Gil, 1994). Making an analogy with electrical resistance arrangement in series,

the total resistance $\boldsymbol{R_{total}}$ can be expressed through the two resistances, the Darcy resistance ($\boldsymbol{R_{Darcy}}$) and the $\boldsymbol{R_{front}}$:

$$\boldsymbol{R_{total}} = \boldsymbol{\Sigma R_i} = \boldsymbol{R_{Darcy}} + \boldsymbol{R_{front}} = \frac{\int \mu(\boldsymbol{z}).\boldsymbol{dz}}{\boldsymbol{k_{media}}.\mathrm{A}} + \boldsymbol{R_{front}} \quad (9.1)$$

Where, μ is the dynamic viscosity of the *grout* (Pa.s), $\boldsymbol{K_{media}}$ is the intrinsic media permeability of the media fraction (m^2) and $\boldsymbol{A}$ is the total cross section area of the cylinder (m^2).
To obtain $\boldsymbol{R_{front}}$ (Pa.s/m^3), in addition to $\boldsymbol{R_{Darcy}}$ (Pa.s/m^3) it is also required $\boldsymbol{R_{total}}$ (Pa.s/m^3), which is calculated from:

$$\boldsymbol{q_{grout}} = \boldsymbol{\rho_{grout}} \times \frac{(\Delta \boldsymbol{P})}{\boldsymbol{R_{total}}} \quad (9.2)$$

Where, $\boldsymbol{q_{grout}}$ is the grout flux (Kg/s), $\boldsymbol{\rho}$ the density of the grout (Kg/m^3) and $\Delta \boldsymbol{P}$ is the applied pressure to the grout (which is considered constant for these injection tests).

9.3.4 Hardened state

In order to study the bond between injection grout and PM particles, it is useful to test the mechanical strength of the injected cylinder samples. For this purpose the cylinders (with the same geometric configuration of other cylinders used in other chapters 6.4 and 8.4) were kept for 45 days after the injection in laboratory conditions (T = 20ºC and R.H. = 60%). After the end of the curing time, the Plexiglass cylinders were removed from the hardened samples and the ultrasound pulse velocity was measured in order to obtain the tomographs (9.3.4.1). After that the cylinders were cut in 3 slices, and for each of these slices the splitting tensile strength was determined.

9.3.4.1 Tomographic calculations

To obtain the tomographs (2D and 3D), the data collected in the ultrasonic tests are processed in GEOTOM CG software through an iterative method (SIRT algorithm). The ultrasonic tests and the creation of the tomographs are described in 8.3.3 and 8.3.4, respectively.

9.3.4.2 Mechanical characterization through splitting tests

Splitting test was performed in accordance with the procedure described in chapter 6.4.3.

9.4 Results and discussion

9.4.1 Injection tests

9.4.1.1 Water and grout injectability in different fractions

Three types of injections were performed: plain water; grout in dry PM and grout in pre-wetted PM. The injection capacity was assessed for the three types of PM referred in 9.2.1.

According to the visual inspections (Fig. 9.5-b) during the injection of the cylinders, the grout was not injectable through the layer filled with very fine fraction (particles smaller than 1.18mm), their presence led to a very small voids size and therefore the grout flow is interrupted. Only water (Newtonian fluid) can be injected through this media. When the finer material does not exist the injection was successful (Table 9.5). These results are in accordance with the rules mentioned in 9.3.2 (and Chapter 7) that express the practical need of the grain size distribution of the grout solid particles should be compatible with the aperture of the voids to be injected. The binder used for the present work has a $d_{85}^{grout} = 0.098\ mm$ and $d_{99}^{grout} = 0.189\ mm$. Thus, it is possible to observe (Table 9.3) that for fractions f and M+f the previous rules are not respected, which may explain the failure of the injection. In relation to the fraction C and M, the rule is checked, thus not causing any fail during the injection process. Regarding the fractions F and M+F, the first rule of Table 9.3 ($D_{15}^{soil} / d_{85}^{grout}$) is only partially verified. This may explain why in some parts of the PM the grout injection was not totally successful. Actually, this rule fits well with the injection results. Other rules lead to results that were not in accordance with the injection tests shown in Table 9.5.

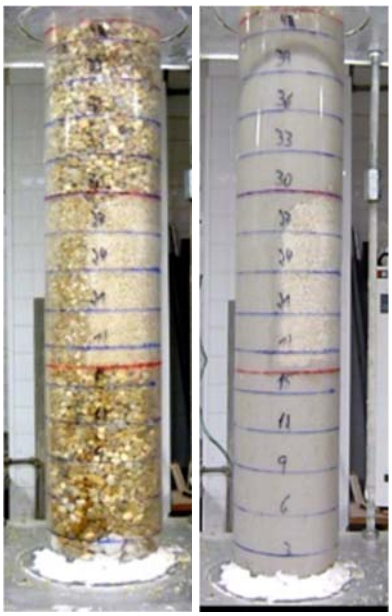

Fig. 9.5 - PM (C,M.f,C) before (left picture) and after (right picture) grout injection

From these injection tests and as already observed in 7.5.1, the aperture of the voids and the fluid type (if Bingham, Newtonian, etc.) are the main factors that affect the penetrability of a fluid. In the case of a granular suspension (e.g. hydraulic lime grout), the grain size of the solid phase must be taken into account. According to the rules shown in Table 9.3, a binder with high grain size is not beneficial to grout penetration, since it will tend to obstruct the flow, preventing grout penetration. Furthermore, the variability in apertures is also an important PM feature (Fig. 9.1) that affects fluid penetration. For this reason, the grout injectability is very low in the fraction M+f.

Table 9.3 - Verification of several criteria in order to assess the grout injectability

Criteria	C	M	F	f	M+F	M+f
$\frac{D_{15}^{soil}}{d_{85}^{grout}}$	53,7	26,9	13,3	6,9	14,6	8,0
W_{nom}/d_{85} (n> 5±1)	8,06	4,04	1,99	1,04	2,19	1,20
W_{nom}/ d_{99} (n> 2,0)	4,17	2,09	1,03	0,54	1,13	0,62

- Green = PM injectable
- Yellow = PM starts to create plug formation (filtration tendency)
- Red = PM not injectable

9.4.1.2 Grout and water flow in the injections of PM types 1, 2 and 3

The volume of grout injected when compared with the results obtained with water showed significantly lower values (Table 9.4), in particular for PM with low permeabilities (PM with finer fractions). From Table 9.4 it is possible to observe that coarser PM (with C and M fractions) with higher W_{nom} and permeability (Table 9.1) have values of grout flow approximately 2–3 times higher than those of the finer PM. As regards the porosity (voids volume), the value is similar for all fractions (Table 9.1). Nevertheless, the grout volume injected is very different, which confirms that the penetrability of the water – a Newtonian fluid (used to determine the voids volume) is significantly higher than a Bingham fluid (grout suspension) (see 7.5.1).

The higher presence of fine particles causes an increase of specific surface of PM (Table 9.1), therefore higher water absorptions are observed. This effect is especially problematic in the case of grout injectability in dry PM. Thus, the grout flow is higher when PM is wetted at the time of injection (Table 9.4). This difference (in average about 13%) can be explained by the reduction of the resistance to flow by water injection. This reduction is explained by the decrease of the grout wettability and the grout filtration rate (see 9.4.1.4). The grout filtration rate is also minimized through the use of SP, which enables the development of repulsive forces on the surface of the suspension grains, resulting in a lower flocculation/coagulation rate (Baltazar et al., 2014) (E.-E. Toumbakari et al., 1999).

The grout mass injected is lower for wetted PM (Table 9.4). Indeed, the finer channels are already filled with water due to its high capillary pressure (Young-Laplace equation) at the time of grout injection, preventing the grout injection in these voids (Fig. 9.7). So, the unique benefit of pre-wetting is to increase the grout flow (cm^3/s) which is directly dependent on the volume injected and on the injection time. As the flow resistance (see 9.4.1.4) is reduced by water injection, the injection time is reduced and therefore there is an increase of grout flow.

Table 9.4 – Mass injected, volume injected, grout and water flow in all PM

		Porous media internal arrangement											
		(C,C,C)	(C,M,C)	(C,F,C)	(F,C,F)	(C,M+F, C)	(C,M+f, C)	(C,C|M, C)	(C,C|F, C)	(C,C|f,C)	(C,M|F, C)	(C,M|f, C)	Average
	Kv [m2]	8,6E-10	7,8E-10	6,9E-10	5,7E-10	7,3E-10	5,2E-10	8,4E-10	7,8E-10	5,6E-10	7,6E-10	5,3E-10	-
PM dry	grout mass (kg)	2,46	2,07	1,86	1,59	1,83	1,12	2,44	2,24	1,88	1,93	1,78	**1,93**
	grout vol. (cm^3)	1459	1227	1099	942	1087	663	1447	1329	1114	1144	1056	**1143**
	grout flow (cm^3/s)	42	37	24	13	26	-	39	27	32	23	26	**28,9**
PM wetted	grout mass (kg)	1,93	1,83	1,55	1,33	1,63	0,88	1,98	1,89	1,59	1,78	1,68	**1,64**
	grout vol. (cm^3)	1142	1087	919	787	963	523	1173	1120	944	1057	994	**974**
	grout flow (cm^3/s)	41	39	31	19	31	-	41	28	30	38	31	**32,8**
Water	water mass (kg)	1,30	1,48	1,27	1,35	1,54	1,20	1,31	1,24	1,18	1,29	1,20	**1,31**
	water vol. (cm^3)	1295	1485	1273	1353	1538	1196	1313	1235	1184	1285	1198	**1305**
	water flow (cm^3/s)	127	145	122	132	139	121	131	125	117	126	120	**127.7**

In general, permeability and voids size distribution are two of the most important properties with regard to the grout injectability (see Chapter 7). In fact, as observed in Fig. 9.6, both parameters revealed in general to be adequate to estimate the grout flow. Nevertheless, W_{nom} seems more suitable than permeability.

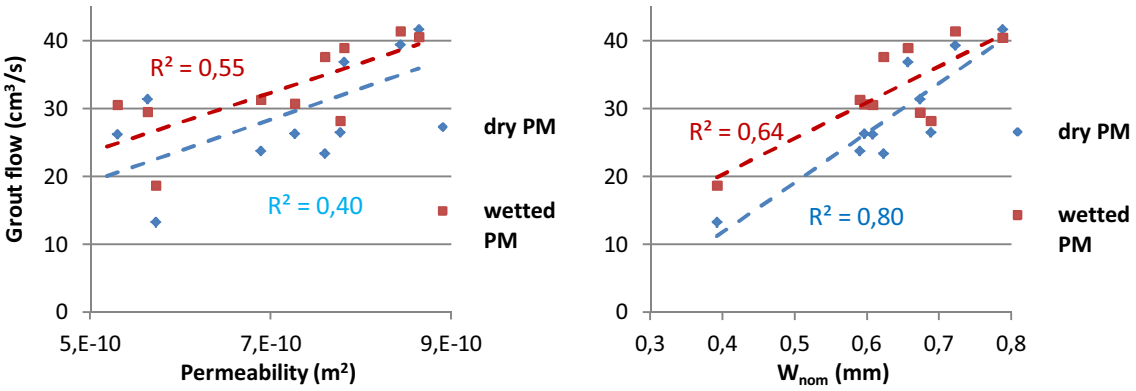

Fig. 9.6 - Influence of the permeability and W_{nom} on the grout flow

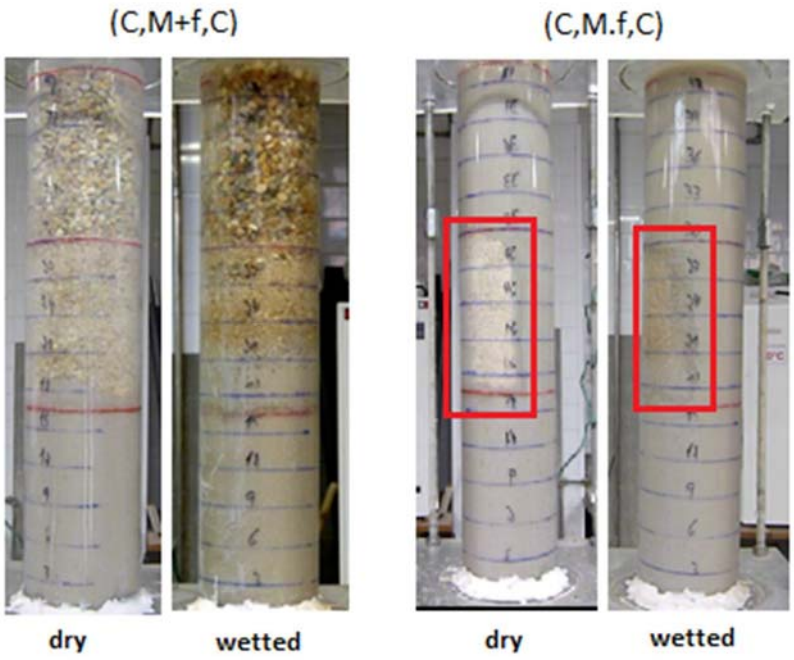

Fig. 9.7 – PM (C,M+f;C) and (C,M|f;C) after grout injection. As shown, the wetting procedure does not bring any advantage

9.4.1.3 Progress along the cylinder

From analysis of the video images of the test injections, the time to reach a certain height was recorded (Table 9.5), which allowed the analysis of the progress of the grout along the cylinder (PM). As already observed by Van Rickstal (Van Rickstal, 2000), there is a poor correlation (Table 9.5) between permeability and grout injection velocity (or grout injection time). Therefore, it can be concluded that the grout progress along the PM is not dependent only of the permeability of the PM. Other parameters such as the total volume to inject (reachable by the grout flow) are also important. Before a grout can progress inside a PM the voids need to be filled. In fact, the PM (C,C,C) and (C,C|M,C) have a higher permeability than (C,M,C), but in the latter, the time to reach the top of the cylinder is lower. As the PM (C,C,C) and (C,C|M,C) contain higher volume of voids (Table 9.5), more time is needed to fill the voids. As a result, the progress of the grout is affected because no pressure can be build up before the voids are filled (Van Rickstal, 2000). Another case where a PM with lower permeability requires less time to reach the top occurs in the PM with layout type 3 (where the middle layer was split vertically - Fig. 9.2). In fact, the injection time of the PM C,C|f,C (35.4s) is lower than C,C|M,C (36.7s) and C,C|F,C (50.1s). As the finest fraction f (with the smallest voids) creates a high resistance to grout to fill all voids, the grout chooses the easiest way, i.e., the grout proceed through fraction C (in the middle layer), leaving most of the voids of the fraction f empty (Fig. 9.5) because the resistance to fill these voids is too big for the grout suspension (see 9.4.1.4). Therefore, the injectability of the grout is dependent on the granulometry size and also the heterogeneity type of granulometry along the PM. In the present work the effectiveness of grout injection (the grout mass injected) is lower (Table 9.4) when the heterogeneity is perpendicular (C,M+F,C and C,M+f,C) to the grout flow direction than when the heterogeneity is parallel (C,M|F,C and C,M|f,C). However, in certain cases, when two fractions (that the grout can penetrate) with different permeability are in parallel, the reverse can occur. As the resistances offered to the grout are different, the grout chooses

the easiest way and not all the voids of the finer fraction are injected (Fig. 9.8), although this fraction (when isolated) may be injected. In fact, when the grout reaches large voids in the coarser fraction, no pressure can be built up in the neighbourhood of that voids, which means that the grout will enter the fine voids (of finer fraction) only over a short distance. When the heterogeneity is perpendicular to the grout flow direction (PM type 2 - Fig. 9.2), the layer is injected since the grout has no other way to flow (contrary to what occurs when heterogeneity is parallel).

Table 9.5 - Progress of the grout in the cylinders filled with dry PM

	Porous media internal arrangement										
height (cm)	**(C,C,C)**	**(C,M,C)**	**(C,F,C)**	**(F,C,F)**	**(C,M+F,C)**	**(C,M+f,C)**	**(C,C|M,C)**	**(C,C|F,C)**	**(C,C|f,C)**	**(C,M|F,C)**	**(C,M|f,C)**
3	0,0	0,0	0,0	0,0	0,0	0,0	0,0	0,0	0,0	0,0	0,0
6	2,2	2,0	2,2	3,5	2,2	2,0	2,0	2,1	1,6	3,0	1,5
9	4,7	4,7	4,6	6,5	4,9	3,9	4,6	4,5	3,9	4,8	4,0
12	6,4	6,4	6,6	10,1	7,4	5,9	7,4	6,6	6,3	7,2	6,4
15	8,7	8,5	8,8	14,0	9,2	8,7	9,4	9,0	8,5	9,0	8,7
16,5	9,8	9,5	9,5	18,4	10,0	9,4	10,3	9,8	9,6	10,1	10,3
18	11,6	11,3	10,7	19,8	11,2	10,8	12,2	11,1	10,6	11,2	11,1
21	13,6	13,3	13,9	21,9	13,6	**15,1**	14,0	15,7	12,0	13,5	12,8
24	16,2	15,8	17,1	24,5	16,1		16,8	17,8	13,4	15,8	14,1
27	19,0	18,4	21,1	28,3	19,7		20,1	21,0	15,5	19,7	15,8
30	22,0	21,4	24,9	30,6	23,2		23,6	26,1	16,8	24,8	17,3
33	24,6	23,9	29,2	35,7	26,4		25,6	30,4	19,5	29,5	22,1
36	27,3	25,2	33,7	45,7	29,9		28,8	34,8	23,1	33,8	26,6
39	29,8	28,1	37,4	53,8	33,6		33,1	39,5	27,4	37,9	31,5
42	32,5	31,2	41,4	62,7	36,8		34,5	44,8	32,0	43,4	36,0
43,5	**35,0**	**33,3**	**46,1**	**71,3**	**41,2**		**36,7**	**50,1**	**35,4**	**48,9**	**40,2**
Kv [m2]	8,6E-10	7,8E-10	6,9E-10	5,7E-10	7,3E-10	5,2E-10	8,4E-10	7,8E-10	5,6E-10	7,6E-10	5,3E-10

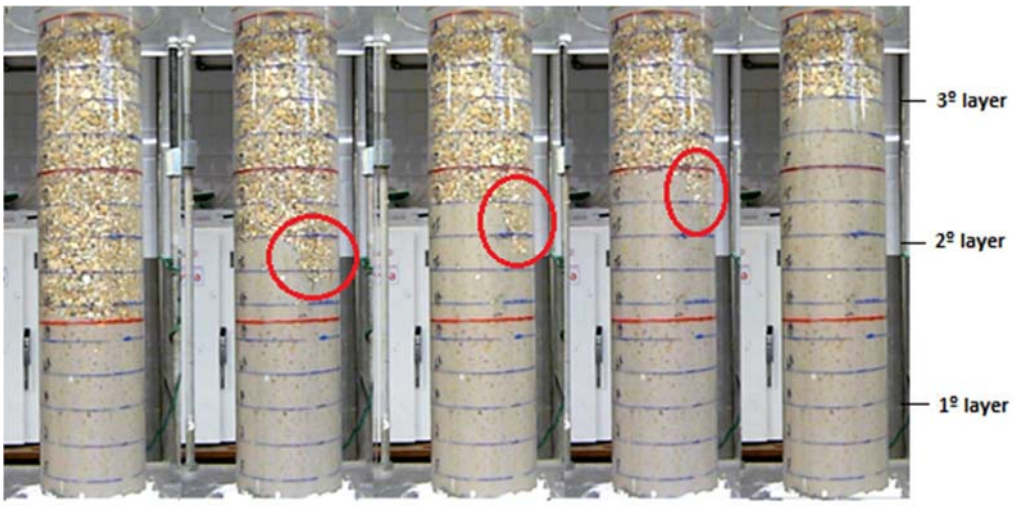

Fig. 9.8 – Cylinders filled with PM (C,C|F,C) during grout injection along a vertically splitted cylinder

From the analysis of Fig. 9.9 for dry and wetted PM considered in the present study, it was concluded that the W_{nom} is the main parameter of the PM that influences the evolution and distribution of the grout within the PM. Indeed, there is a reasonable correlation between the progress of the grout along the PM and W_{nom} (R^2 = 0.36 and 0.68). Regarding the permeability, the correlation is poor (R^2 = 0.13 and 0.21). Actually, the increase of both parameters leads to a reduction of the injection time, being higher the influence of W_{nom}.

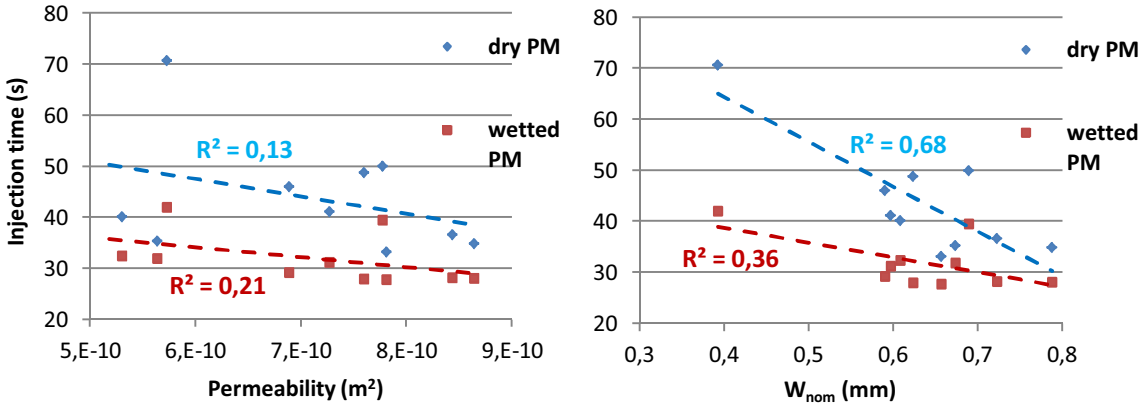

Fig. 9.9 – Influence of the permeability and W_{nom} on the injection time

9.4.1.4 Validation of Darcy's law and front resistance theory

The grout injection in a wetted PM was faster than on a dry PM. In fact, the average injection velocity along the cylinder was 24% higher. As already reported by Van Rickstal (Van Rickstal, 2000) and Bras (Bras & Henriques, 2012), the conductivity of a PM is dependent on the water content. Thus, through water injection there is an increase in the conductivity of the PM. Moreover, the grout wettability is reduced, i.e., the contact angle between grout (fluid) and the surface of the PM particles is increased (see 8.2.2.2), which also contributes to reduce the overall resistance to grout flow (from 2.77E+09 to 2.30E+09 Pa.s/m^3). Thus it not surprising that a pre-wetted media leads to an increase of the grout injection velocity (Table 9.6), in particular in the top layer (more than 50%). Nevertheless, it is much slower compared to water injection (Table 9.6), since the water is a Newtonian fluid (see 7.5.1.5).

As concluded in 8.2.2.2, the grout wettability depends on the water absorption capacity of the PM particles. As the water capacity of the PM particles has influence on the overall resistance to grout flow, it is possible to conclude that the overall resistance (especially the front resistance) can be estimated by grout wettability. Furthermore, as verified by 8.2.2.2 the grout wettability can be estimated by contact angle. A low contact angle indicates a grout with high affinity for the polar surface of the PM (high wetting). Therefore, a low contact angle leads an increase of the front resistance which is a drawback in grout flow capacity.

Table 9.6 – Velocity of each layer for different PM

	Velocity by layer (cm/s)											
	(C,C,C)	(C,M,C)	(C,F,C)	(F,C,F)	(C,M+F,C)	(C,M+f,C)	(C,C|M,C)	(C,C|F,C)	(C,C|f,C)	(C,M|F,C)	(C,M|f,C)	
Layers	**PM Dry**											**Average**
bottom	1,38	1,42	1,42	0,73	1,35	1,44	1,31	1,38	1,41	1,34	1,31	*1,32*
middle	1,10	1,13	0,88	1,11	1,02	-	1,02	0,83	1,87	0,92	1,93	*1,18*
top	1,04	1,11	0,64	0,33	0,75	-	1,03	0,56	0,73	0,56	0,59	*0,74*
$V_{bottom} \rightarrow V_{top}$	-24,5%	-21,8%	-55,2%	-54,8%	-44,4%	-	-21,4%	-59,2%	-48,5%	-58,1%	-55,0%	***-44,1%***
Layers	**PM wetted**											**Average**
bottom	1,52	1,61	1,78	1,63	1,46	1,73	1,50	0,99	1,65	1,69	1,23	*1,52*
middle	1,48	1,32	1,10	0,90	1,43	-	1,30	1,04	1,85	1,65	1,50	*1,36*
top	1,33	1,45	1,44	0,72	1,07	-	1,52	1,05	0,82	1,14	1,08	*1,16*
$V_{bottom} \rightarrow V_{top}$	-12,6%	-9,7%	-19,1%	-56,0%	-26,8%	-	1,1%	6,2%	-50,3%	-32,2%	-12,0%	***-21,1%***
Layers	**Water**											**Average**
bottom	4,3	4,2	4,1	4,2	4,1	4,3	4,4	4,4	4,4	4,2	4,2	*4,24*
middle	4,0	3,9	4,0	4,1	3,5	4,7	4,2	4,0	4,1	3,8	4,2	*4,04*
top	3,7	3,7	3,6	3,6	3,5	3,5	3,6	4,0	3,6	4,0	3,8	*3,69*
$V_{bottom} \rightarrow V_{top}$	-13,9%	-12,4%	-10,8%	-14,2%	-15,4%	-17,7%	-16,2%	-8,8%	-16,2%	-5,9%	-11,1%	***-13,0%***

As mentioned in 9.3.3.1, given the fluid and the PM used in injection tests, the Darcy resistance (given by Darcy's law) is lower than the total resistance. The results shown in Table 9.7 are in agreement. In fact, the Darcy resistance ($\boldsymbol{R_{Darcy}}$) is only 31% (on average) of the total resistance ($\boldsymbol{R_{total}}$). This inadequacy of Darcy's law to model grout injection is due to the several assumptions of this law that are not respected in the injection tests, namely:

- the laminar flow is not verified in the injection of coarse fractions, since the fluid velocity is too high (Table 9.2) ; thus, in these conditions turbulent flow and the inertia effects should be taken into account.
- the anisotropy is not taken into account in Darcy's law. Given the layouts of the PM studied and as the path of the grout during the injection is three-dimensional, the horizontal injectability is certainly different of the vertical injectability. So, the isotropy of the PM is not guaranteed.
- non-saturation of the PM voids prior to the test (for dry PM), which causes absorption of the water (especially by finer voids due to the higher capillary pressure) from the grout. Consequently, the fresh properties of the grout (viscosity and density) change throughout the PM.
- some bonds (chemical and physical) are established between grout and PM that are not considered by Darcy's law.

After checking the inadequacy of Darcy's law to model grout injection, Gil concluded that the main resistance to the grout flow is located at the injection front and the rest of resistance can almost be overlooked. Thus, after the complete injection of the PM cylinder the front resistance should disappear and the grout flow should increase immediately since there no front anymore. Nevertheless, such fact does not happen. The same was observed in (Van Rickstal, 2000). This author recorded the mass flow (during the injection tests) and observed that the grout flow gradually decreases when the cylinder is completely filled. The results in Table 9.6 also contradict that the main resistance is situated at the injection front. In layout type 2 (where the middle layer is finer than the first and the last layer - see Fig. 9.2 and Fig. 9.3), the velocity of grout injection decreases significantly when it reaches the denser zone – middle layer. In the last layer the penetration speeds up, however the injection velocity does

not increase again to the initial value of the first layer. Another example is the PM (F,C,F), where the low permeable zone is placed at the bottom and at the top. In this case, the grout injection velocity increases when it reaches the middle layer (which contains a higher permeability). In the last layer, since a low permeable zone is reached again, there is a decreasing of the grout penetration and the injection velocity is considerably lower than the first layer (decreasing of 54.8%). Regarding PM with the layout type 3 (split vertically in the middle layer) the slowing down of the grout penetration after the split zone is significant (reduction above 50% between the bottom and top layer). Hence, it is evident to the three types of PM that in the third layer the grout velocity does not recover the original velocity of the first layer, although both layers have the same fraction. Indeed, the evolution of the grout velocity decreases during the penetration of the PM because the resistance created by the part of the media already injected is constantly increasing. This can be explained by two phenomena that arise because the injection fluid (grout) is a suspension. The first phenomenon occurred throughout the injection where some water of the grout is absorbed by flow channels and the binder particles stick to the walls of the channels, thus reducing the aperture of the flow channels. Moreover, the grout viscosity increases because the w/b ratio of the grout decreases along the injection (filtration tendency). This phenomenon is more noticeable for PM filled with finer fractions (with low voids size and high specific surface). Due to the first phenomenon, the filtration tendency is amplified because it is related to the aperture of the voids and the w/b ratio of the grout suspension. Therefore the probability of filtration of the grout is higher for the voids with lower aperture (see 7.5.1.5) (Miltiadou-Fezans & Tassios, 2013a) and grouts with low w/b ratio (low w/b ratio implies a higher proportion of clogged binder grains) (Axelsson & Gustafson, 2010). Thus, it can be concluded that both phenomena contribute to increase the overall resistance to the grout flow. In addition, these phenomena enable the creation of a new additional resistance which is part of the overall resistance to the grout flow. As it is impossible to separately assess this new additional resistance and the front resistance, they are shown together in a single resistance – R_s – resistance of suspension (Table 9.7). Actually, the name of this resistance comes from the fact that the grout is a suspension. The increase along the PM depends on the fraction of the PM, as well as on the type of suspension (this variable was not studied since the grout is always the same). Similar results are found in literature (Gil, 1994; Van Rickstal, 2000) for the front resistance. However, in this work, a linear relation between the permeability and the R_s is not found. Actually, R_s depends mainly of the small apertures (W_{nom}) of the PM.

According to Table 9.7, the grout flow is essentially conditioned by the physical resistance given by R_s (on average 70% of the total resistance - R_{Total}) than by the injected media resistance, given by Darcy's law (on average 30% of the R_{Total}). In this way, the theory of R_s should be implemented in analytical models that attempt to estimate experimental injections with grouts suspension. The influence of R_s is even more significant for PM filled with finer fractions (e.g. PM F,C,F and C,M+f,C). In these cases, the percentage of R_s (relative to the total resistance- R_{Total}) is higher than 80% (Table 9.7). Furthermore, the range of the resistance calculated by Darcy's theory (0.4 - 0.98 Pa.s/m3) is lower than the range of the resistance calculated by R_s theory (1,07 – 4,39 Pa.s/m3), which means that the Darcy's theory is not as sensible to the physical change of the media granulometry compared to the R_s theory.

Table 9.7 – Darcy resistance (R_{darcy}) and Resistance of suspension (R_s) for PM studied

		Porous media internal arrangement											
		(C,C,C)	**(C,M, C)**	**(C,F,C)**	**(F,C,F)**	**(C,M+F, C)**	**(C,M+f, C)**	**(C,C|M, C)**	**(C,C|F, C)**	**(C,C|f, C)**	**(C,M|F, C)**	**(C,M|f, C)**	**Average**
Grout mass (kg)	dry PM	2,46	2,07	1,86	1,59	1,83	1,12	2,44	2,24	1,88	1,93	1,78	**1,93**
	wetted PM	1,93	1,83	1,55	1,33	1,63	0,88	1,98	1,89	1,71	1,78	1,68	**1,64**
Time injection (s)	dry PM	35,0	33,3	46,1	71,3	41,2	35,2	36,7	50,1	35,4	48,9	40,2	**43,7**
	wetted PM	28,2	27,9	29,3	42,1	31,3	23,6	28,3	39,6	29,7	28,0	32,5	**32,2**
Kv PM (m^2)		8,6E-10	7,8E-10	6,9E-10	5,7E-10	7,3E-10	5,2E-10	8,4E-10	7,8E-10	5,6E-10	7,6E-10	5,3E-10	-
q_{grout} (kg/s)	dry PM	0,070	0,062	0,040	0,022	0,045	0,032	0,067	0,045	0,053	0,040	0,044	**0,046**
	wetted PM	0,068	0,066	0,053	0,032	0,052	0,037	0,070	0,048	0,058	0,064	0,052	**0,054**
R_{Total} ($Pa.s/m^3$) x E+09	dry PM	1,68	1,90	2,94	5,30	2,65	3,72	1,78	2,64	2,22	2,99	2,67	**2,77**
	wetted PM	1,73	1,79	2,23	3,74	2,28	3,16	1,69	2,48	2,05	1,86	2,29	**2,30**
R_{darcy} ($Pa.s/m^3$) x E+09		0,60	0,67	0,76	0,91	0,72	0,45	0,62	0,67	0,93	0,69	0,98	-
R_s (Pa.s/m3) x E+09	dry PM	1,07	1,23	2,18	4,39	1,94	3,32	1,16	1,97	1,30	2,30	1,69	**2,05**
	wetted PM	1,12	1,13	1,48	2,83	1,56	2,71	1,07	1,81	1,13	1,17	1,31	**1,58**
R_{darcy} / R_{Total} (%)	dry PM	36	35	26	17	27	12	35	25	42	23	37	**29**
	wetted PM	35	37	34	24	31	13	37	27	45	37	43	**33**
R_s / R_{Total} (%)	dry PM	64	65	74	83	73	88	65	75	58	77	63	**71**
	wetted PM	65	63	66	76	69	87	63	73	55	63	57	**67**

According to Table 9.7, pre-wetting reduces 30% (on average) of the resistance suspension (**R_s**). Since the PM particles are saturated at the time of grout injection, the water absorption by these particles will be null, so the grout viscosity is not increased and the magnitude of filtration of the grout is reduced. This reduction of R_s is not more than 30%, because the finer capillaries are already filled with water (due to their high capillary pressure) when the grout injection is carried out, resulting in a lower grout mass injected (Table 9.4) which decreases the q (kg/s) and hence increases R_s.

The reduction of grout mass injected due to the pre-wetting operation can result in negative consequences, because the effectiveness of the injection is not so good compared to dry PM. Furthermore, as observed in the mechanical results of the chapter 8.4.2, the mechanical strength of these particular samples is very poor (as PM particles are previously saturated, they cannot absorb any water from the grout suspension, resulting in very low bond strength between grout and PM particles). In addition, after the injection the grout starts to drop towards the bottom of the cylinder, which also contributes to a very unsuccessful consolidation of the PM. So because of these negative factors, the mechanical tests were not performed for cylinders with wetted PM. The conclusions would be similar to other chapter (see 8.5) and other works of literature (Valluzzi, 2005).

9.4.2 Mechanical properties

9.4.2.1 Visual inspections after injection of the cylindrical models

After 45 days the cylinders were cut and an inspection of the degree of success of the injection in terms of penetration and diffusion of the grout was possible. A remark can be made regarding the presence of large amount of not injected zones for PM with finer fraction (f and F), as shown in Fig. 9.10 and Fig. 9.11. As the criteria to assess the grout injectability are not respected, the finest voids are not injected (Table 9.3). In contrast, when PM does not have any presence of finer fractions, a high effectiveness of grout injection is achieved (Fig. 9.10 and Fig. 9.11) which improves the cohesion of the PM injected and the adherence at the interfaces, as already reported in 8.4.1.

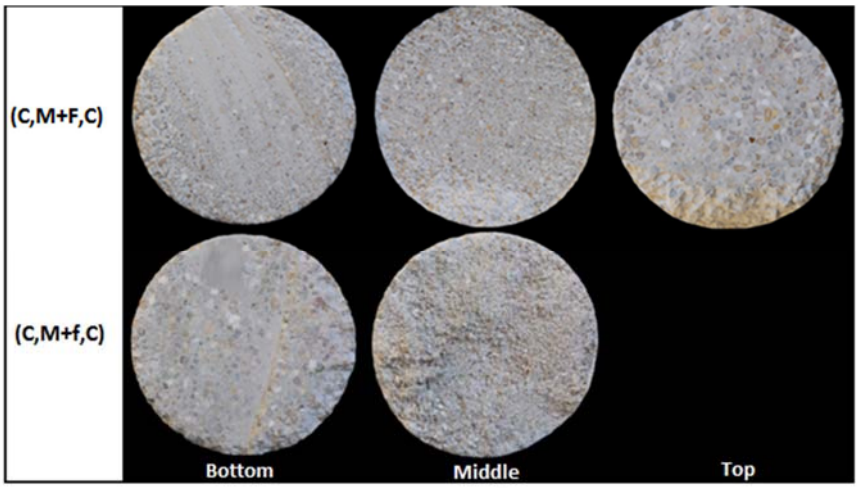

Fig. 9.10 - Inspection after cutting of the cylinders in different levels: bottom, middle and top

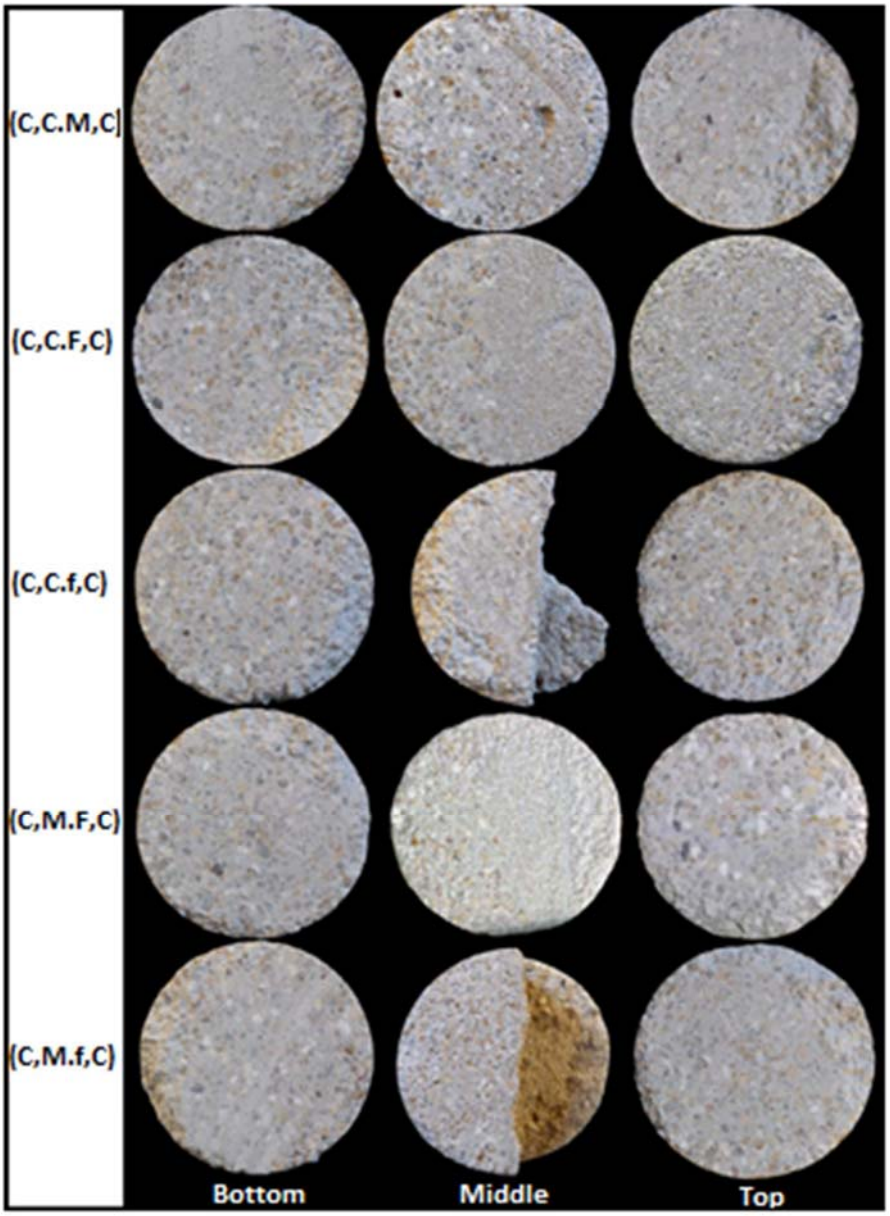

Fig. 9.11 – Inspection after cutting of the cylinders in different levels: bottom, middle and top

9.4.2.2 Tomographs

In this section the ultrasonic tomographs will be compared with the injection tests presented in section 9.4.1. Ultrasonic tomographs (Fig. 9.12 and Fig. 9.13) of horizontal sections for each level (bottom, middle and top) and 3D tomographs (Fig. 9.14, Fig. 9.15, Fig. 9.16 and Fig. 9.17) of the ultrasonic grid (Fig. 8.14) were obtained. According to chapter 8.4.5, the ultra-sonic velocities lower than 1200 m/s correspond to areas that were not injected, whereas areas with velocities higher than 1700 m/s indicate that this is a solid area of the PM, without voids, which shows that the voids had been successfully filled.

Some results from PM characterised by the presence of fine material (fraction f) are worthy of attention. It is the case of PM C,M+f,C (Fig. 9.12), C,M|f,C (Fig. 9.13) and C,C|f,C (Fig. 9.13) that show low velocities in zones that before the injection presented finer fraction. This trend is

systematically observed on the cylinders filled with this specific fraction (f), resulting in a non-homogeneous state after injection. Furthermore, the ultrasonic velocities decrease from bottom to top, indicating that the voids volume is higher in the top level (Fig. 9.12 and Fig. 9.13). Indeed, in the top horizontal tomograph appear some zones with low values of ultrasonic velocity (ultrasonic velocities lower than 1200 m/s). Regarding the PM type 3 with fraction f, the tomographs of the middle slice (Fig. 9.13) show a high area of voids concentrated in the section where the fraction f was placed before grout injection. As regards the other section (where fractions M or C were placed), the velocities higher than 2300 m/s indicate a good compactness. In fact, all layers filled with the fractions M or C exhibit a compact section characterized by the absence of large voids. Thus, no attenuation of the ultrasonic waves is verified since the ray-paths of the horizontal tomographies do not cross any large void. Therefore, a good effectiveness of grout injection for such fractions is revealed (Fig. 9.12 and Fig. 9.13) which confirms the findings of injection tests (see 9.4.1).

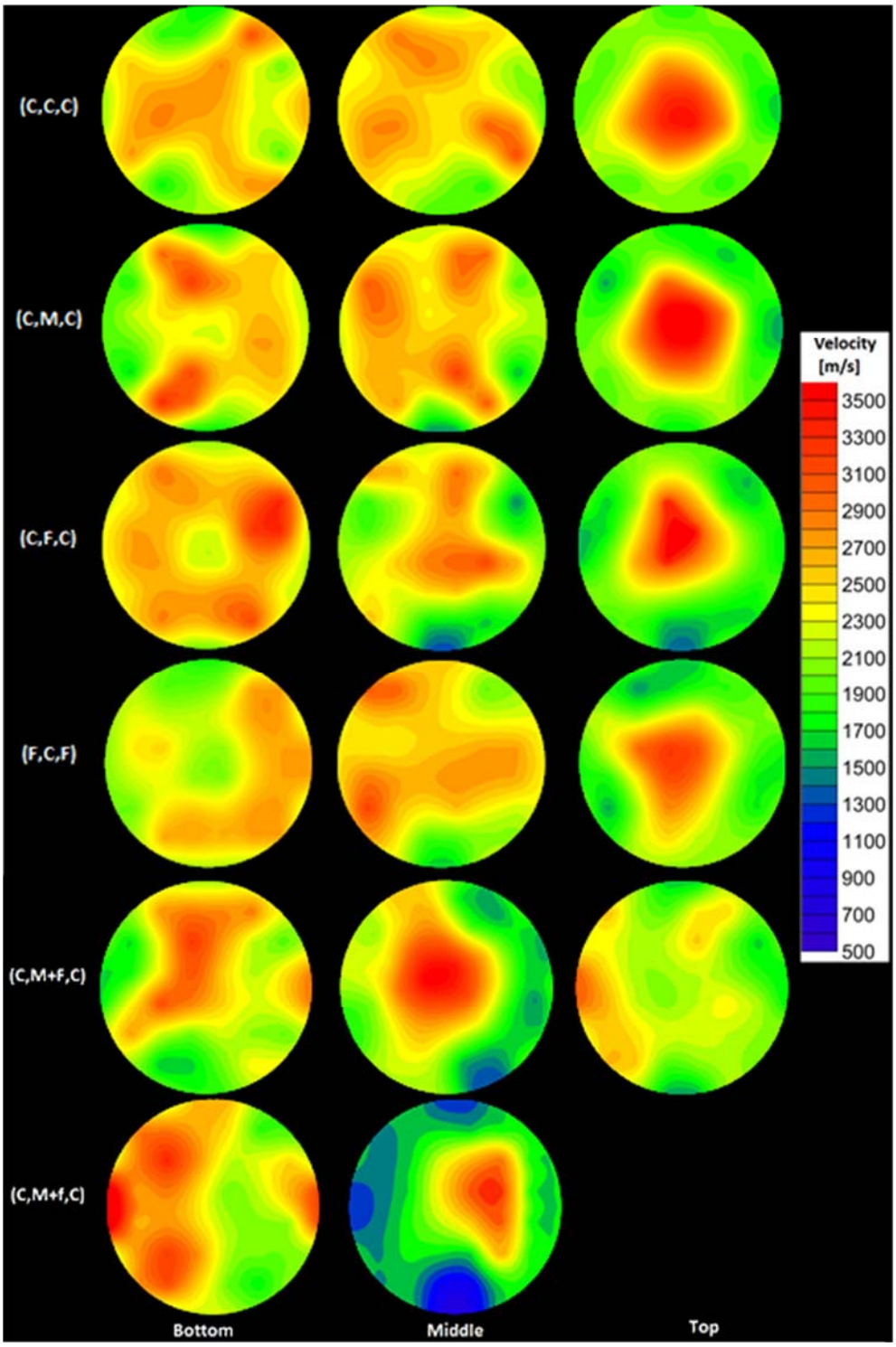

Fig. 9.12 - Ultrasonic horizontal tomography of PM type 1 and 2 (in levels: bottom, middle and Top of the cylinder)

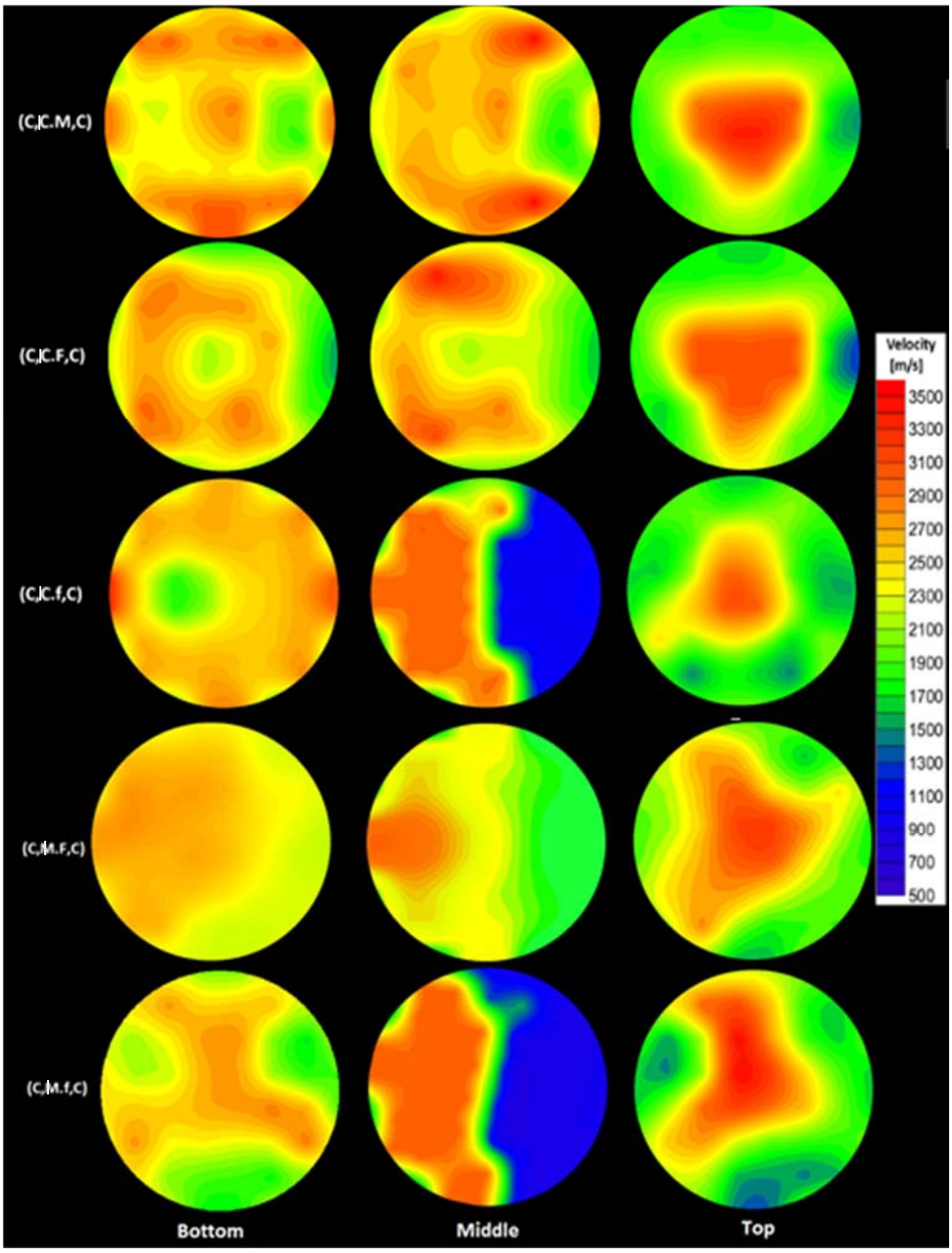

Fig. 9.13 - Ultrasonic horizontal tomography of PM type 3 (in levels: bottom, middle and Top of the cylinder)

The 3D tomographs from (Fig. 9.14 - Fig. 9.17) confirmed the results showed previously. In fact, PM with fractions f and F have a considerable area with an ultrasonic velocity lower than 1200 m/s. In contrast, in PM without finer fractions this area is almost non-existent, which proves that the voids present prior to injection were successfully filled by grout.

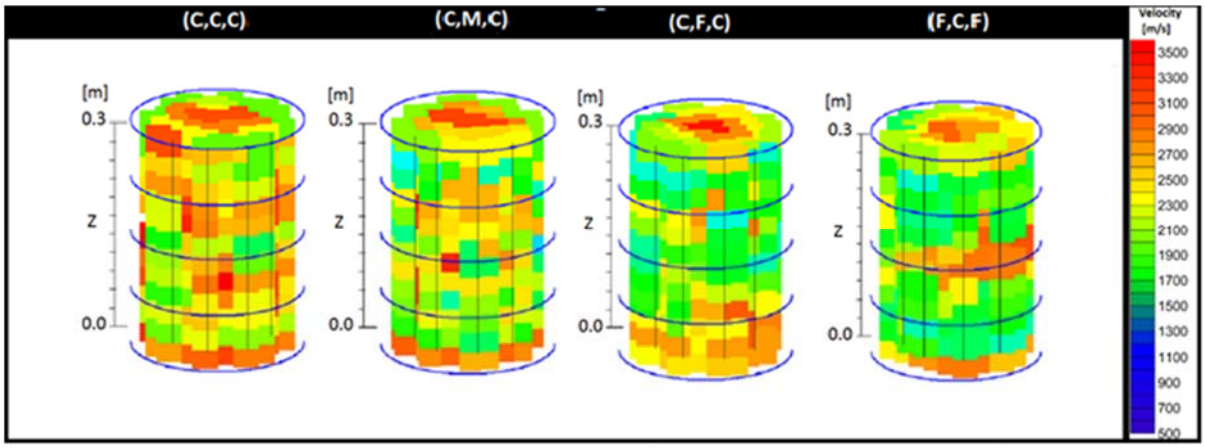

Fig. 9.14 – Results of the ultrasonic tomography (by Geotom CG) – 3D tomographies for cylinders of (C,C,C), (C,M,C), (C,F,C) and (F,C,F)

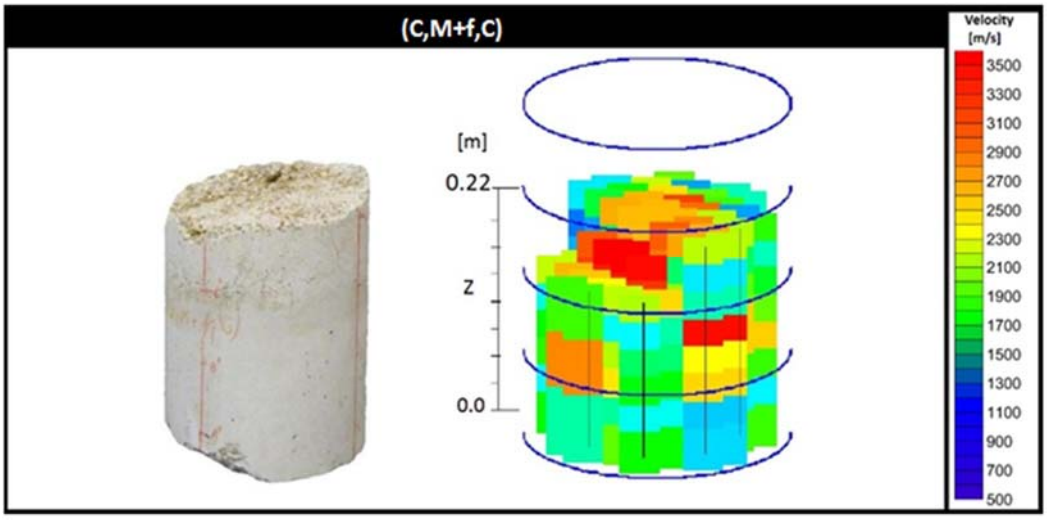

Fig. 9.15 - Inspecting of the cylinder (C,M+f,C) (left picture); 3D ultrasonic tomography by Geotom CG (right picture)

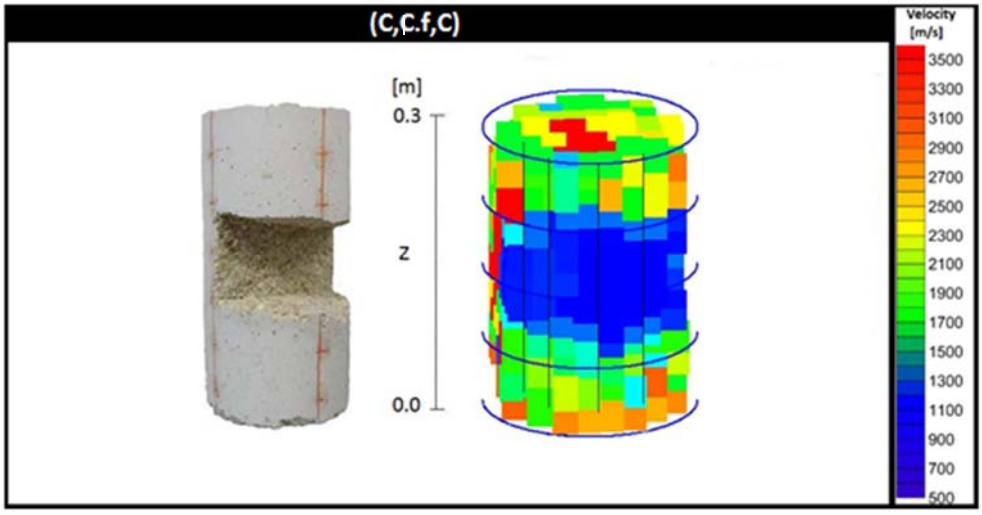

Fig. 9.16 - Inspecting of the cylinder (C,C|f,C)(left picture); 3D ultrasonic tomography by Geotom CG (right picture)

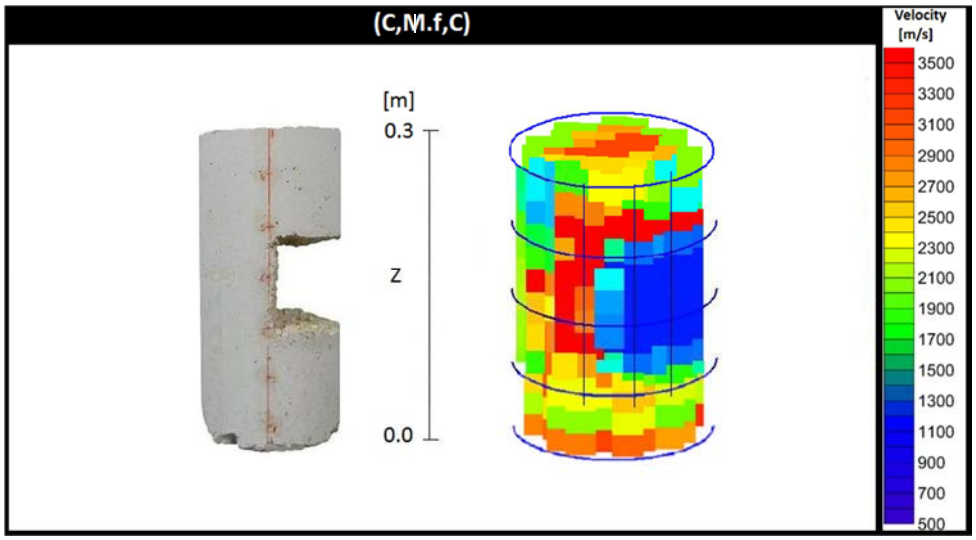

Fig. 9.17 - Inspecting of the cylinder (C,M|f,C)(left picture); 3D ultrasonic tomography by Geotom CG (right picture)

9.4.2.3 Splitting tests

In Table 9.8 is shown the splitting tensile strength values. It can be remarked that the strength values are ranging from 0.30 to 0.51 MPa. As observed in Fig. 9.12 and Fig. 9.13, the PM filled with the finer fractions show relevant voids after injection and a larger number of interfaces grout – PM particles compared to PM filled with the coarser fractions. Since the predominant failure mode in splitting test was through the interfaces (Vintzileou & Adami, 2009), it is expected that the mechanical results are higher for the PM without finer fractions (Table 9.8).

Compared to chapter 8.4.2, the lower values of tensile strength are higher, which can be related with the lower water absorption of sand particles. The low absorption is beneficial for grout fluidity and for reducing the filtration and blockages of the grout flow (see 7.5.1). Hence, a higher volume of injected material is verified. On the other hand, since the sand particles are non-porous aggregates, the bonding established between grout and PM particles is based on the simple deposition of constituents of grout hydrated (physical connection) – see 8.4.2. Therefore, the interfacial layer created between the binder grains and the channels walls is weak which contributes to low bond between both. Thus, the best result of these PM is lower than crushed brick PM (see 8.4.2), using the same grout and PM filled with similar fractions.

As verified in 9.4.1, the grout injectability of the first and third layer is not the same (though filled with the same fraction). Given the correlation between grout injectability and tensile strength value (already studied in 8.4.2 and 8.4.4), some variation in tensile strength values is verified from the first to the third layer (Table 9.8). For PM without finer fractions, there is a slightly positive variation, whereas for PM filled with finer fractions or vertically splitted in the middle level (PM type 3) there is a negative variation. There are several phenomena that explain this distinct strength variation. Regarding the positive variation, since the PM particles absorb some water of the grout there is an increase of the grout density, contributing to an increase of the interface cohesion. As regards the negative variation, the presence of fine voids (which contribute to higher resistance – Table 9.7) and the vertical heterogeneity in the middle layer (several phenomena occur producing obstruction of the grout injection) can be the reason. This variance on the tensile strength is not positive as regards the

risk of masonry failure after grout injection (see 8.4.5.3). Indeed, as concluded by Chaudhry (Chaudhry, 2007), the homogeneity (reduction of discontinuities and internal voids/cracks) of the masonry is an fundamental principle in order to reduce the differential stiffness in the walls and thus achieve the desired level of seismic resistance.

Table 9.8 - Splitting tensile strength [MPa] for different cylinder parts (bottom, middle and top) of PM type 1,2 and 3

Splitting Tensile Strength [MPa]					
Porous Medium	botto m	middle	top	Average	Δ bottom to top layer
C,C,C	0,46	0,51	0,48	0,50	+
C,M,C	0,45	0,49	0,46	0,47	+
C,F,C	0,46	0,36	0,39	0,40	-
F,C,F	0,34	0,40	0,33	0,36	-
C,M+F,C	0,47	0,39	0,43	0,43	-
C,M+f,C	0,45	0,30	-	0,38	-
C,C.M,C	0,46	0,43	0,42	0,44	-
C,C.F,C	0,43	0,37	0,41	0,40	-
C,C.f,C	0,40	-	0,35	0,38	-
C,M.F,C	0,42	0,36	0,40	0,39	-
C,M.f,C	0,43	-	0,34	0,39	

9.5 Conclusion

Based on the various findings, the conclusions and recommendations of this research are listed as follows:

- The void size distributions (aperture size and variability) of the PM and the grading of the solid grout particles are the main factors that affect the injectability of a grout suspension. When the several criteria (established in the literature) to assess the grout injectability are not respected (due to the presence of finer fractions), the reliability of the grout injection is jeopardized.

- The higher presence of fine particles causes an increase of the specific surface of PM, resulting in increased water absorption and hence the grout viscosity is increased. This effect is especially problematic in the case of grout injectability in dry PM.

- Through the pre-wetting the contact angle of the grout is increased as well as the grout filtration rate. Thus, the overall resistance to grout flow is reduced, leading to an increase in the grout injection velocity (cm/s) and the grout flow (cm^3/s).

- The grout progress along the PM is not dependent only on the permeability of the PM. Other parameters such as the volume (reachable by the grout flow - Bingham fluid) to inject are also important. Indeed, the progress of the grout is affected because no pressure can be build up before the voids are filled.

- The injection tests show that when the resistances offered to the grout flow (in a split vertically layer) are different, the grout chooses the easiest way and it does not penetrate in all the voids of the finest fraction, although the fraction (when isolated) can be injected. No pressure is built up in the neighbourhood of coarse voids. This result is particularly important as it emphasizes an important setback of the grout injectability, whenever there is just one flow direction and the heterogeneity is parallel to it.

With regard to the different resistances which arise during a grout injection, it was concluded:

- As the assumptions of Darcy's law are not respected in grout injection tests, this law showed inadequacy to model grout injection. The injection tests confirmed that the overall media resistance is underestimated by Darcy's law. Moreover, the injection tests contradict that the main resistance is situated at the injection front (as stated by certain authors). In fact, as the injection fluid is a suspension, the resistance to grout flow increases during the injection (regardless of the fraction injected), since the resistance created by the part of the media already injected is constantly increasing. So, it is created a new additional resistance called resistance of suspension (R_s) which should be implemented in analytical models that attempt to estimate grout injections. This additional resistance contains the part of the front resistance and is more significant for fractions with lower size, i.e., with lower voids aperture (W_{nom}).

- The size of the grout solid particles, the size of the voids of the front layer and the voids size distribution of the layers already injected are the main factors that influence the R_s value.

- The pre-wetting leads to a reduction of the R_s which contributes to reducing the overall resistance to the grout flow. However, the grout mass injected is lower. Thereby, this procedure should only be used in particular cases.

- As the predominant failure mode in splitting test was through the interfaces, it is expected that the mechanical results are higher for the PM without finer fractions.

- As the sand particles are non-porous aggregates, the interfacial layer created between the binder grains and the channels walls is weak (just a physical connection) which contributes to low bond between both. Thus, the best result of these PM is lower than crushed brick PM (see 8.4.2), using the same grout and PM filled with similar fractions.

– Tomography and mechanical tests showed density gradients that are originated from different grout injection capacities throughout the different fractions of each PM. For PM without finer fractions, there is a slightly positive variation, whereas for PM filled with finer fractions or vertically splitted in the middle level (PM type 3) there is a negative variation.

Chapter 10. Conclusions and recommendations

10.1 Conclusions

An evaluation regarding injectability of hydraulic lime grouts on old masonry consolidation has been conducted and it was concluded that the effectiveness of grout injection depends not only of the grout composition. In fact, besides composition there are other factors that can affect the performance of grout injection namely temperature, resting time, injection pressure and type of PM to be injected. The lack of information about the influence of the referred factors on the effectiveness of HL grouts consolidation justifies the present work.

The research was divided in five main chapters. Fig. 10.1 summarizes the different aspects studied and indicates the main reasons that motivated the study and the relationships that exist between the different chapters. Chapter 5 corresponds to the study of the combined effect of grout composition, temperature, resting time and injection pressure on hydraulic lime grout injectability. Chapter 6 continues the study of the previous chapter considering the phenomena after hardening of the grout within the PM. The main aim was to analyse the effect of the referred parameters in the filling process and in the bonding of the grout with the PM materials. Chapter 7 and Chapter 8 analyse the performance of consolidation of grout injection in different PM through injection tests on reduced models (cylinders). Several PM with different permeabilities and internal structures were injected in order to understand their influence in grout injectability. In Chapter 9 injectability of grouts in PM with different characteristics (porosity and void size distribution) along the height of injection was studied. From these injection tests a new concept of resistance to grout flow is proposed and the validity of Darcy law and front resistance is evaluated.

The conclusions that have been made in the different phases of the present work were presented at the end of each chapter. These conclusions are summarized in the next sections with the aim of providing a global picture of the fulfilment of the goals of this thesis.

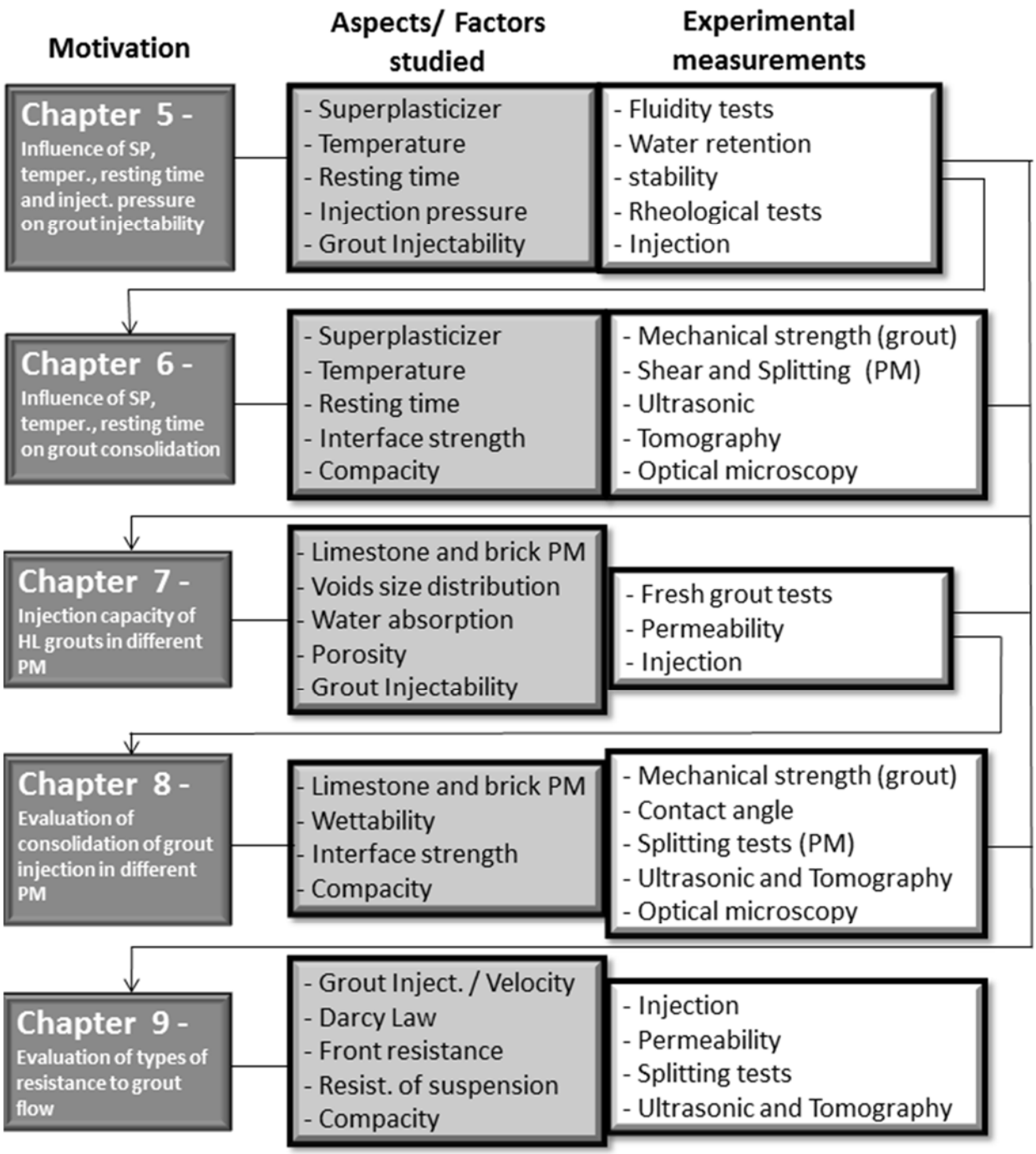

Fig. 10.1 - Scheme of the different studies performed in the present work

10.1.1 Influence of superplasticizer, temperature and resting time on fresh grout properties. Correlation between grout injectability and fresh grout parameters

For a successful injection it is necessary to ensure an adequate grout flow inside the masonry. This means that it is essential to ensure good fresh properties, such as good rheological behaviour, fluidity, water retention and stability in order to obtain a successful injection. In Chapter 5 the combined effect of temperature, resting time and grout composition on fresh grout performance was evaluated. The

results showed that the combined effect of these parameters is not negligible. The main achievements attained were:

- SP has a substantial role in the fresh grout properties of hydraulic lime based grouts. In general, the use of SP results in a higher fluidity factor, stability and water retention capability.

- SP contributes to a better grout performance, since it imposes repulsive forces (steric and electrostatic repulsions). This repulsion contributes to holding the particles far enough to prevent the solid particles to flocculate (deflocculating action).

- For low dosages of SP the intensity of interactions among solid particles is high resulting in strong attraction forces leading to high and quick flocculation phenomenon. For SP dosages higher than 1.2wt% (optimal dosage) some instability phenomena was observed.

- The injection tests showed that a lower yield stress and plastic viscosity means an easier injection process.

- The worse rheological behaviour was detected when the temperature increases from 20 to 40ºC. Thus, there is a reduction on grout injectability for this temperature range.

- For high temperatures (40 ºC) there is a faster evolution of hydration reactions and therefore flocculation occurs quicker (rapid change of grout microstructure). Some of the physical bonds formed start to be permanently connected between each other (permanent flocculation) causing a significance increase of the yield stress which leads to penetrability loss (PFI-theory).

- The injection tests confirmed that grouts with higher flocculation area (higher flocculation tendency) present lower injectability due to lower workability and penetrability.

- When the temperature decreases (below 20ºC) the fresh grout properties do not change much, suggesting that Brownian motion plays only a minor role.

- There is a correlation between the results of fresh grout parameters and those injection tests. The injectability parameter (dimensionless) depends mainly on yield stress and water retention, while for the injectability rate (s^{-1}), the plastic viscosity and fluidity factor (FFT) are the most influential parameters.

10.1.2 Influence of superplasticizer, temperature, resting time and injection pressure on hydraulic lime grout injectability

Considering the results of the grout fresh properties it seems that the study of the parameters (SP dosage, temperature and resting time) is inevitable when designing a grout for injection. The results showed that the effect of temperature and SP dosage are not negligible for fresh grout performance, meaning that during a real in situ injection a proper choice of environmental temperature (by choosing the correct season of the year) and grout composition (by choosing the correct SP dosage or other admixtures / additions) will allow an improvement of injection effectiveness. Moreover, the planning of a consolidation work with grouts should take into account that the influence of resting time varies over the day and mainly over the climatic seasons. The injection pressure is another parameter that influences grout consolidation.

In this context, the main achievements obtained are the following:

- The injection tests confirmed the relevance of SP on the fresh grout performance, since for higher SP dosages it was observed an increase on the injectability rate (s^{-1}) and injectability (dimensionless). The benefit of an adequate presence of SP (1.2 wt%) is highlighted when the grout is not injected immediately after the mixing process.

- The resting time should be taken into account during grout intervention, especially when the flow tends to stop enabling an increase of the particle flocculation phenomena (structural build-up) due to mutual attraction forces. Therefore, a low resting time is always recommended.

- The resting time is critical for warm weather. When the temperature is low (5 ºC), the influence of the resting time on grout injectability is significantly lower since the rheological behaviour does not change substantially over time. Furthermore, the hydration process (chemical formation of bonds between binder particles) is slower.

- A grout temperature around 5-20ºC leads to an adequate rheological behaviour, which should be ensured so that the grout may flow correctly inside the masonry core.

- The higher the injection pressure, the higher is the rate of grout injectability - Inj (s^{-1}). Nonetheless, regarding the percentage of voids filled there is not significant improvements on the effectiveness of grout injection when injection pressure is increased.

- There are two models of injection tests studied in this work. The French standard NF P 18-891 is not the most suitable because of two reasons: a) the diameter of the column (22.2mm) is too small for aggregate sizes studied in this work; b) due to geometric configuration of the column, the path of the grout during the injection is only one-dimensional, rather than three-dimensional, as in the case of the other model and the reality.

10.1.3 Combined effect of superplasticizer, temperature and resting time on hydraulic lime grout consolidation

In Chapter 6 the mechanical properties of the grout and the mechanical strength of the PM after injection was taken into account. The main goal was to study the influence of SP dosage, temperature (for injection and cure) and resting time on grout consolidation. For a successful consolidation, the grouts should have high injectability (analysed in Chapter 5), low or no shrinkage and good bond to masonry materials. Shrinkage has high influence on interfacial bond strength between grout and PM since additional stresses on the interface are created some cracks appear and hence there is a loss of adhesion between the grout and PM. The interfacial bond strength was evaluated by splitting and direct-shear test.

The following remarks are outlined:

- The mechanical properties of the grout (compressive and flexural strength) are not the main factors that control the mechanical strength of the PM injected. Grout injectability (with influence on the compactness / cohesion of the PM after injection) as well as the interfacial bond strength between grout and PM particles are more relevant.

- The grout with the best injectability (1.2 wt% of SP) shows the best interfacial bond strength because a stronger mechanical interlock with the PM particles along the failure surface is established.

- The PM in which there was no resting time (0 min) have interfacial bond strength on average 1.2 times higher (for splitting tensile strength and shear bond strength) than the PM injected with a resting time of 60min.

- The injection and curing temperature have influence on the compactness of the PM after injection, the best results being also dependent on the resting time. For a temperature of 20ºC the best performance was obtained for 0 min and for 5ºC the best was for 60min.

- Based on the deposition of hydration products (related to Arrhenius law) and shrinkage phenomenon, it can be stated that the interfacial bond strength is lower for higher curing temperatures (40ºC).

- The grout shrinkage level is one of the main factors that can affect the interfacial bond strength. The SP dosage and especially the curing temperature showed a significant influence on the grout shrinkage level. At 40ºC the loss of capillary water (due to the evaporation) is high, which contributes to the volume change of the material and thus increasing the degree of drying shrinkage.

- Regarding direct-shear test, the same failure mode (sliding shear failure) was observed in all tests. Nevertheless, the shear bond strength is significantly different, depending on the injectability of the grout and the interfacial bond strength.

10.1.4 Evaluation of consolidation of grout injection in different porous media

The flow of the grout through a PM depends on the fresh grout properties (studied in Chapter 5 and Chapter 6) and the characteristics of the PM to be injected. It is of utmost importance to know precisely the composition of the materials constituting the PM, the characteristics of the materials and the percentage and distribution of voids. The performance of the grout in different PM was evaluated (using different materials and grain size distributions) by controlling the grout injectability through injection tests on reduced models (cylinders). The injectability of the grout was analysed based on two equations. One expresses the percentage of voids volume that is filled after grout injection, and another takes into account the injection time and also the voids volume filled. Different grout injectability results were obtained for the various PM studied. The grout injection capacity was also evaluated based on appropriate criteria to express the penetrability of the grout in different PM.

The following conclusions can be drawn from the results obtained:

- The amount of water absorbed by the particles of PM during the injection process influences the grout fluidity, and hence the grout injection capacity.

- The permeability depends not only on the porosity of PM, but also of the specific surface and d(10). The finer particles size has a great influence on permeability, which fits well with Hazen equation.

- The porosity (voids volume) of each PM is not a representative measurement for the available volume for a grout suspension, since the available space in each PM that can be filled with water (Newtonian fluid) is not the same as the space that may be filled with the grout (Bingham fluid).

- The value of injectability of a grout in a given media is mainly affected by permeability, voids volume, size of the finer particles - d(10), rough surface and the water absorption capacity of the media particles. Depending on the grain size distribution and the type of material of PM, the parameters referred have different influence on injectability.

- For high amounts (over 33 wt%) of the finer material (0.15-2 mm) the reliability of the injection technique is jeopardized since during the injection process the finer particles tend to agglomerate causing a decrease of the voids diameter. Thus, the phenomenon of clogging up the finer channels is more visible, i.e., there is an increase of constrictions and resistance to the grout flow.

- The yield stress is more relevant in injectability of a fluid for finer PM, whereas for coarser PM viscosity and inertia have higher relevance.

- The pre-wetting of the PM cannot solve grout penetrability, since at the time of grout injection the finer capillaries are already filled with water (due to its high capillary pressure – Young-Laplace equation), hence hindering the penetration of the grout. The only advantage of pre-wetting is to increase the rate of injectability of grout, since the flow resistance is reduced by the water injection (PM with higher conductivity).

- The penetrability of a fluid is dependent on the aperture between the particles of PM and a function of the fluid type. Moreover, the variability in apertures and the magnitude of contact areas are also important PM features. As the finer PM present lower apertures and higher variability in apertures and magnitude of contact areas (i.e., higher specific surface), grout penetrability problems may arise.

- For a suspension (such as hydraulic lime grout) to be able to penetrate a certain PM, the grain size distribution of its solid phase should be compatible with the characteristic dimensions of the PM (apertures, voids, interfaces, etc.) to be injected. One "groutability ratio" criterion is not sufficient to ensure penetrability into very fine discontinuities. Indeed, the upper part of the entire grading curve of the binder must be taken into account, i.e., specific grading criteria should be verified in order to evaluate if the grout can be injected in a certain PM.

10.1.5 Evaluation of grout consolidation with tomography and mechanical tests

The performance of grout injection in different PM was studied in Chapter 7. In Chapter 8 the cylinders that resulted from injection tests were evaluated. In order to test the effectiveness of the filling process and the bonding of the grout to the PM materials, ultrasonic tests (NDTs) were conducted complemented with mechanical tests.

The ultrasonic velocities were used as raw data for the tomographs (using the software GeoTom CG) in order to control the penetration and diffusion of the grout during the injection tests on laboratory. It is worth noting that in real masonries the tomographs should be done based on sonic tests rather than ultrasonic results. The presence of large voids and discontinuities do not allow recording the signal of ultrasonic waves due to the high attenuation of waveform energy.

The main achievements attained were:

- Splitting tests show that the prevailing mode of failure occurs at the interface PM particles - grout. Thus, for PM (after injection) without relevant voids the PM with lower number of interfaces will have the higher mechanical results.

- The bond properties of the interfaces are affected by the characteristics of the particle surface (density, surface porosity, pore size, roughness and water content) and can be evaluated by the measurement of contact angle.

- Crushed brick PM with higher grout wettability (higher grout affinity with the particle polar surface – lower contact angle) promotes chemical reactions in the contact area between particles surface and the grout paste during the hydration process. Therefore, a better mechanical adhesion is established at the interface resulting in higher values in the splitting test. Regarding limestone PM only a physical connection is established on the PM particle surface.

- Ultrasonic and mechanical tests showed density and strength gradients that are originated from different penetration and diffusion capacity of the grout along the injected PM.

- The gravitational settling of the binder grains (instability phenomenon) contributes to the different binder concentration that may occur vertically (especially for higher heights), which means a negative strength gradient. Such result enables to conclude that besides the hydrostatic pressure also the strength gradient can limit the maximum injection height.

- Pre-wetting has deleterious effects on the mechanical strength and strength gradients of the injected PM. Indeed, the amount of water absorbed by the particles of PM during the injection process influences the mechanical bond between the grout - PM particles. When pre-wetting is made the absorption of the smaller pores – needed for a good adhesion between grout and PM particles – does not occur because they are saturated.

- Ultrasonic velocities can be successfully used to evaluate the quality of an injection. For this purpose, it is essential to choose a suitable frequency, as well as the format of the transducer in order to wrap conformably the material surface.

- The ultrasonic results also show that for heterogeneous materials the ultrasonic velocity depends not only on compactness but also on attenuation due to dispersion at the internal interfaces PM particles–grout, since when a propagating wave pulse impinges on an interface a portion of the wave energy is dissipated.

- The higher the presence of grout in a PM (i.e., a better quality of injection), the greater is the ultrasonic velocity measured since the presence of voids is lower (meaning lower attenuation).

- Given the heterogeneity of the samples (PM with different grout injections capacities) studied, the SIRT iterative method instead of RAYPT is more appropriate to perform the data inversion for the ultrasonic tomography. In what refers the ray tracing calculation, the curved-ray calculations are more accurate (especially for strong contrasts) to define more precisely the shape and size of the voids.

10.1.6 Non-validation of Darcy's law and front resistance and creation of a new resistance during grout injection

Since porosity and void size distribution are not constant within masonry, the efficiency of grouting varies along the injection. Thus, it is essential to study the injectability of grouts in PM with different characteristics along the height of injection. From the injection tests different resistances to grout penetration were detected, created by the PM to the flow. The knowledge of these resistances is crucial to estimate the grout penetration in the internal voids.

Regarding the different resistances which arise during a grout injection, it was concluded:

- When the resistances to grout flow (in a split vertically layer) are different, the grout chooses the easiest path and it does not penetrate all the voids of the finer fraction, although the fraction (when isolated) can be injected. Therefore, there is a particular concern when there is only one flow direction and the heterogeneity is parallel to it.

- The injection tests confirmed that the overall media resistance is underestimated by Darcy's law. Furthermore, the injection tests contradict that the main resistance is situated at the injection front (as stated by certain authors).

- The front resistance does not take into account that during the injection the resistance to grout flow increases. Thus, it was created a new additional resistance called resistance of suspension (R_s) containing the part of the front resistance

- The size of the grout solid particles, the size of the voids of the front layer and the voids size distribution of the layers already injected are the main factors that influence the R_s value. R_s is more significant for fractions with lower size, i.e., with lower voids aperture (W_{nom}).

- The pre-wetting leads to a reduction of the Rs which contributes to reducing the overall resistance to the grout flow. However, the grout mass injected is lower. Thereby, this procedure should only be used in particular cases.

10.1.7 Overall conclusions

This thesis correspond a larger study which analyses the performance of the grout consolidation, taking into account fresh and mechanical properties of the grout, grout injectability and the mechanical strength of the PM after injection. Fig. 10.2 shows the scientific approach followed in this thesis to evaluate grout consolidation in different PM. Such approach should be implemented in grout design to consolidate old masonries.

From this research, some overall conclusions can be outlined:

- Every old masonry has its specific properties, so conclusions taken from the evaluation of a particular masonry may not be generalized to other masonries.

- During conservation and retrofitting work not only the grout properties are important but also the characteristics of the masonry to be injected. Non-destructive testing (NDT) play an essential role especially in cultural heritage buildings with artistic value where the evaluation should be made with the minimal possible destruction.

- Given the irreversibility of injection grouting, attention needs to focus on the selection of injection grouts which should take into account the original materials of the old masonry.

- The effectiveness of grout consolidation can be evaluated based on the ability of the grout to fill the masonry voids and on the bonding established between grout and masonry materials after hardening.

- In grout design it is crucial to estimate the grout injectability and the grout capacity to increase the cohesion of the old masonry (consolidation effect).

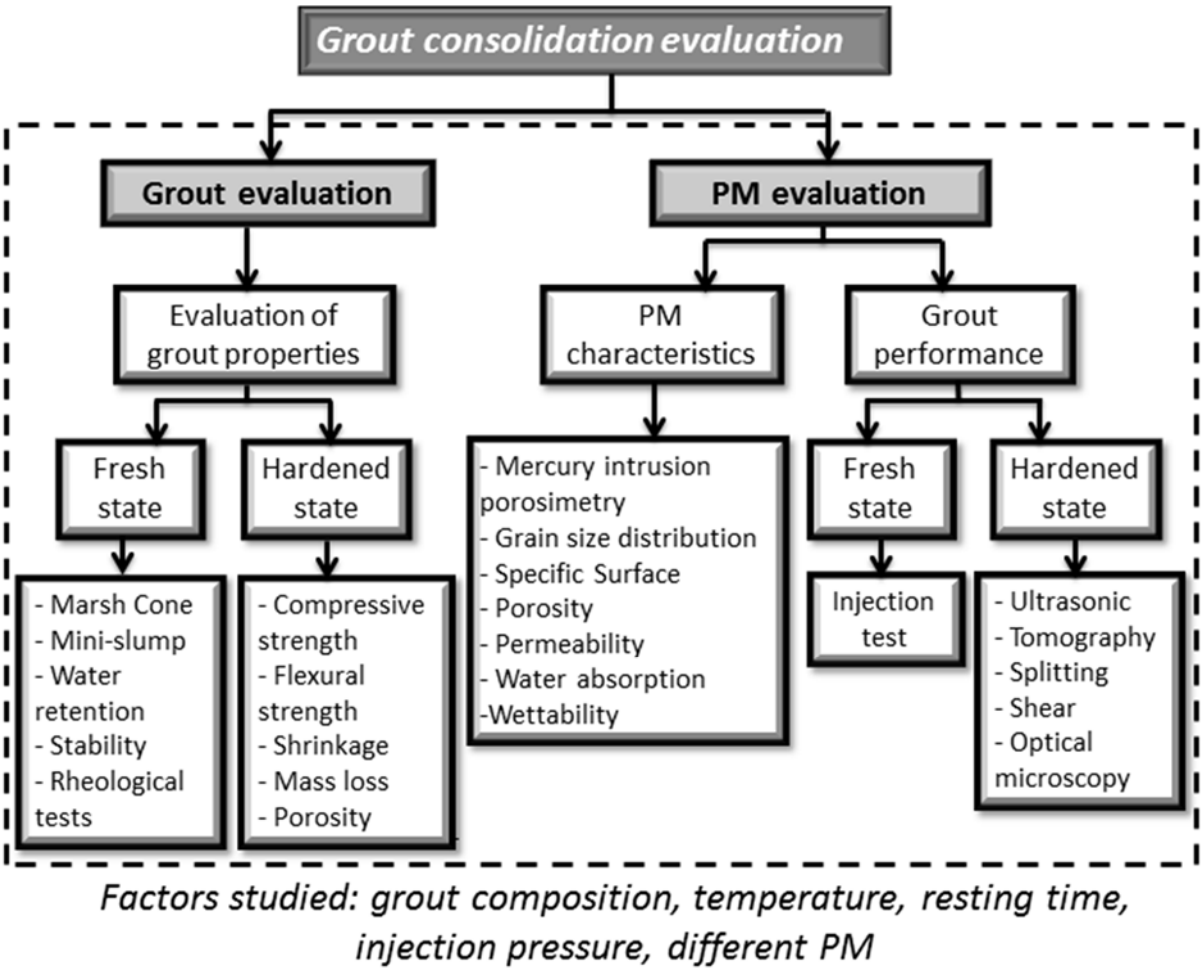

Fig. 10.2 - Scientific approach followed to evaluate grout consolidation

10.2 Recommendations for further research

During the development of this research work several aspects related to grout injection were studied, some of them deserving further investigation. In the following topics are presented some suggestions:

- Regarding the rheological measurements it became clear that controlling the rheological properties of grouts is crucial for successfully grouting process. Notwithstanding, during rheological measurements some issues can arise which may lead to test results having small relevance. Some authors (Banfill, 2011; Nehdi et al., 1997) have shown that wall slip can play a significant role during the rheological measurements of cementitious materials leading to an underestimation of the yield stress values and inaccurate viscosity results. Thus, it should be important to study the degree of wall slip effect during rheological measurements of NHL-based grouts in order to define an adequate measurement protocol.
- The presence of dry fine particles (with small size and high water absorption) prevents the penetration of the grout flux due to the high capillary pressure of those particles - Young-Laplace equation. In fact, while injecting the dry material segregation takes place between the water (absorbed by the finer pores) and the remaining phases of the grout. This effect should be further investigated in order to minimize its effects.

- The use of pozzolans (silica fume, fly ash, metakaolin) to improve fresh grout performance have been studied by several authors (Baltazar et al., 2014; Bras et al., 2010). The lack of information about the influence of these materials on grout injectability justifies further research work. Injection tests should be performed in order to analyse the penetrability of the grout, as well as the rate of grout injectability. Moreover, it should be evaluated the correlation between fresh grout properties and grout injectability, as it was done in this work with superplasticizer.

- As observed in injection tests the overall media resistance is underestimated by Darcy's law. In addition, the injection tests also show that the main resistance is not situated at the injection front. For that reason, it was created a new additional resistance - resistance of suspension (R_s) which should be implemented in analytical models that attempt to estimate grout injections. It is very important to accurately model the performance of grout injection in PM to avoid problematic situations that can occur in situ, when is not possible to check the injectability of grout.

- As concluded in this thesis, the effectiveness of the grout injection depends on the interfacial bond strength between the injected grout and the masonry materials. The bond strength was evaluated with splitting and shear tests. Nevertheless, other mechanical tests can be used as the pull-off test. In addition, other grouts formulations and other subtracts should be evaluated.

- The superplasticizers enable the development of repulsive forces due to the adsorption of the polymers on the surface of the grains. Nevertheless, as concluded by (Heikal et al., 2005), this adsorption capacity change with the temperature. Thus, it is recommended more detail in this study, since a particular grout composition can have different injectability values depending on temperature. In addition, the pH of water can be another parameter with influence on superplasticizer performance and consequently on fresh grout performance.
- As concluded by several authors (Toumbakari, 2002) (Van Gemert et al., 2015b), the grout needs to be adapted to the original material with regards to three aspects: chemical, mechanical/structural and physical compatibility. The aim is to avoid durability problems. This issue is of utmost importance since grout injection is an irreversible technique. So, a thorough study on this issue is crucial in order to choose suitable raw materials for the grout composition.

Chapter 11. References

Adami, C.-E.; Vintzileou, E. - *Interventions to historic masonries: Investigation of the bond mechanism between stones or bricks and grouts*. Materials and Structures, Volume 41, págs. 255–267, 2008.

Aiad, I. - *Influence of time addition of superplasticizers on the rheological properties of fresh cement pastes*. Cement and Concrete Research, Volume 33, págs. 1229–1234, 2003.

Aïtcin, P.C. - *High performance concrete*. London: E & FN Spon, 1998.

Alecci, V.; Fagone, M.; Rotunno, T.; De Stefano, M. - *Shear strength of brick masonry walls assembled with different types of mortar*. Construction and Building Materials, Volume 40, págs. 1038–1045, 2013.

Almeida, C.; Guedes, J.P.; Arêde, A.; Costa, C.Q.; Costa, A. - *Physical characterization and compression tests of one leaf stone masonry walls*. Construction and Building Materials, Volume 30, págs. 188–197, 2012.

Almeida, N.G.; Pinto, A.P.F.; Gomes, A. - *Caldas de cal hidraulica para cnsolidação de alvenarias antigas - Influência da relação a / l e do tipo de cura*. APFAC 2012, 2012.

Almeida, N.G.; Pinto, A.P.F.; Gomes, A.; Gonçalves, N. - *Caldas de injecção para alvenarias antigas fluidez versus capacidade de injecção*. Congresso Construção Coimbra 2012págs. 1–12, 2012.

Alsayed, S. - *Influence of superplasticizer, plasticizer, and silica fume on the drying shrinkage of high-strength concrete subjected to hot-dry field conditions*. Cement and Concrete Research, Volume 28, págs. 1405–1415, 1998.

Alterman, D.; Page, A.W.; Dean, L. - *The use of crushed brick as an aggregate replacement in concrete*, in: 9th International Masonry Conference 2014 in Guimarães, 2014.

Anzani, A.; Binda, L.; Carpinteri, A.; Lacidogna, G.; Manuello, A. - *Evaluation of the repair on multiple leaf stone masonry by acoustic emission*. Materials and Structures, Volume 41, págs. 1169–1189, 2007.

Anzani, A.; Binda, L.; Lualdi, M.; Tedeschi, C.; Zanzi, L.; Milano, D.I.S.P. - *Use of Sonic and GPR Tests to Control the Effectiveness of Grout Injections of Stone Masonry*. ECNDT 2006, Volume 3, págs. 1–7, 2006.

Artelt, C.; Garcia, E. - *Impact of superplasticizer concentration and of ultra-fine particles on the rheological behaviour of dense mortar suspensions*. Cement and Concrete Research, Volume 38, págs. 633–642, 2008.

Assaad, J.J.; Daou, Y. - *Cementitious grouts with adapted rheological properties for injection by vacuum techniques mixing procedure influence*. Cement and Concrete Research, Volume 59, págs. 43–54, 2014.

ASTM C957-02 - *Standard Test Method for Pulse Velocity Through Concrete*, 2002.

Axelsson, M.; Gustafson, G. - *Grouting with high water/solid-ratios –Literature and laboratory study*. Department of Civil and Environmental Engineering - Chalmers University of Technology, Göteborg, Sweden, 2007.

Axelsson, M.; Gustafson, G. - *The PenetraCone, a new robust field measurement device for determining the penetrability of cementitious grouts*. Tunnelling and Underground Space Technology, Volume 25, págs. 1–8, 2010.

Axelsson, M.; Gustafson, G.; Fransson, Å. - *Stop mechanism for cementitious grouts at different water-to-cement ratios*. Tunnelling and Underground Space Technology, Volume 24, págs. 390–397, 2009.

Baltazar, L.G.; Henriques, F.M.A. - *Rheology of Grouts for Masonry Injection*. Key Engineering Materials, Volume 624, págs. 283–290, 2014.

Baltazar, L.G.; Henriques, F.M.A.; Jorne, F.; Cidade, M.T. - *Performance improvement of hydraulic lime based grouts for masonry consolidation: an experimental study*. Structural Studies, Repairs and Maintenance of Heritage Architecture XIII, Volume 131, págs. 417–430, 2013.

Baltazar, L.G.; Henriques, F.M.A.; Jorne, F.; Cidade, M.T. - *The use of rheology in the study of the composition effects on the fresh behaviour of hydraulic lime grouts for injection of masonry walls*. Rheologica Acta, Volume 52, págs. 127–138, 2013.

Baltazar, L.G.; Henriques, F.M.A.; Jorne, F. - *Hydraulic lime grouts for masonry injection - effects of admixtures on the fresh grout properties*. Proc. of the 8th International Conference on Structural Analysis of Historical Constructions, 15th–17th October 2012, Wroclaw, Poland. ISBN 978-83-7125-216-7, 2012a.

Baltazar, L.G.; Henriques, F.M.A.; Jorne, F. - *Optimisation of flow behaviour and stability of superplasticized fresh hydraulic lime grouts through design of experiments*. Construction and Building Materials, Volume 35, págs. 838–845, 2012b.

Baltazar, L.G.; Henriques, F.M.A.; Jorne, F.; Cidade, M.T. - *Combined effect of superplasticizer, silica fume and temperature in the performance of natural hydraulic lime grouts*. Construction and Building Materials, Volume 50, págs. 584–597, 2014.

Banfill, P.F.G. - *Additivity effects in the rheology of fresh concrete containing water-reducing admixtures*. Construction and Building Materials, Volume 25, págs. 2955–2960, 2011.

Barbhuiya, S.A.; Gbagbo, J.K.; Russell, M.I. - *Properties of FA concrete modified with hydrated lime and SF*. Construction and Building Materials, 2009.

Baronio, G. et al - *Criteria and methods for the optimal choice of grouts according to the characteristics of masonries*. In: International workshop CNRGNDT, effectiveness of injection techniques for retrofitting of stone and brick masonry walls in seismic areas, Milan, March 30–31st; 1992., 1992.

Baronio, G.; Binda, L.; Tedeschi, C.; Tiraboschi, C. - *Characterisation of the materials used in the construction of the Noto Cathedral*. Construction and Building Materials, Volume 17, págs. 557–571, 2003.

Biçer-Simşir, B.; Griffin, I.; Palazzo-Bertholon, B.; Rainer, L. - *Lime-based injection grouts for the conservation of architectural surfaces*. Studies in Conservation (GETTY), Volume 55, págs. 3–17, 2009.

Binda, L.; Anzani, A. - *Structural behaviour and durability of stone masonry, saving our architectural heritage: the conservation of historic stone structures*. New York: Wiley, 1997:112-48, 1997.

Binda, L.; Baronio, G.; Tiraboschi, C.; Tedeschi, C. - *Experimental research for the choice of adequate materials for the reconstruction of the Cathedral of Noto*. Construction and Building Materials, Volume 17, págs. 629–639, 2003a.

Binda, L.; Cardani, G.; Saisi, A.; Valluzzi, M.R. - *Vulnerability analysis of the historical buildings in seismic area by a multilevel approach*. Asian Journal of Civil Engineering (Building and Housing), Volume 7, págs. 343–357, 2006.

Binda, L.; Modena, C.; Baronio, G.; Abbaneo, S. - *Repair and investigation techniques for stone masonry walls*. Construction and Building Materials, Volume 11, págs. 133–142, 1997.

Binda, L.; Saisi, A. - *State of the Art of Research on Historic Structures in Italy*. Dept. of Structural Engineering - Politecnico of Milan. Italy, 1996.

Binda, L.; Saisi, A.; Tiraboschi, C. - *Investigation procedures for the diagnosis of historic masonries*. Construction and Building Materials, Volume 14, págs. 199–233, 2000.

Binda, L.; Saisi, A.; Tiraboschi, C. - *Application of sonic tests to the diagnosis of damaged and repaired structures*. NDT & E International, Volume 34, págs. 123–138, 2001.

Binda, L.; Tiraboschi, C.; Baronio, G. - *On-site investigation on the remains of the Cathedral of Noto*. Construction and Building Materials, Volume 17, págs. 543–555, 2003b.

Bjornstrom, J.; Chandra, S. - *Effect of superplasticizers on the rheological properties of cements*. Materials and Structures, Volume 36, págs. 685–692, 2003.

Bliylikzt, O. - *Imaging of concrete structures*. NDT & E International, Volume 31, págs. 233–243,

1998.

Boineau, A. - *Injection des maçonneries*. Chapitre 3-2,STRRES GT N°4, Fascicule n°8, CEBTP, 1986.

Bombled, J.P. - *Rhéologie des mortiers et des bétons frais, étude de la pâte interstitielle de ciment*. Revue des matériaux de construction, Volume 688, págs. pp 137–155., 1974.

Borri, a.; Castori, G.; Corradi, M.; Speranzini, E. - *Shear behavior of unreinforced and reinforced masonry panels subjected to in situ diagonal compression tests*. Construction and Building Materials, Volume 25, págs. 4403–4414, 2011.

Bosiljkov, V.; Uranjek, M.; Žarnić, R.; Bokan-Bosiljkov, V. - *An integrated diagnostic approach for the assessment of historic masonry structures*. Journal of Cultural Heritage, Volume 11, págs. 239–249, 2010.

Bras, A. - *Grout optimization for masonry consolidation*. PhD Thesis, Faculdade de Ciências e Tecnologia da Universidade Nova de Lisboa, 2011.

Bras, A.; Gião, R.; Lúcio, V.; Chastre, C. - *Development of an injectable grout for concrete repair and strengthening*. Cement & Concrete Composites, Volume 37, págs. 185–195, 2013a.

Bras, A.; Henriques, F.M. a; Cidade, M.T. - *Rheological behaviour of hydraulic lime-based grouts. Shear-time and temperature dependence*. Mechanics of Time-Dependent Materials, Volume 17, págs. 223–242, 2013b.

Bras, A.; Henriques, F.M.A. - *The influence of the mixing procedures on the optimization of fresh grout properties*. Materials and Structures, Volume 42, págs. 1423–1432, 2009.

Bras, A.; Henriques, F.M.A. - *Natural hydraulic lime based grouts – The selection of grout injection parameters for masonry consolidation*. Construction and Building Materials, Volume 26, págs. 135–144, 2012.

Bras, A.; Henriques, F.M.A.; Cidade, M.T. - *Effect of environmental temperature and fly ash addition in hydraulic lime grout behaviour*. Construction and Building Materials, Volume 24, págs. 1511–1517, 2010.

BS EN 12504-4 - *Testing concrete. Determination of ultrasonic pulse velocity*. British Standards Institution, London, 2004.

Buyukozturk, O. - *Imaging of concrete structures*. NDT & E International, Volume 31, págs. 233–243, 1998.

Cachim, P.B. - *Mechanical properties of brick aggregate concrete*. Construction and Building Materials, Volume 23, págs. 1292–1297, 2009.

Caliskan, S. - *Aggregate/mortar interface: influence of silica fume at the micro- and macro-level*. Cement and Concrete Composites, Volume 25, págs. 557–564, 2003.

Cambefort, H. - *Principes et applications de l' injection*. Annales de l'ITBTP, Paris, Supp. no. 353, Série: Sols et fondations, no. 144, 23 pp, 1977.

Cantini, L. - *Sonic tomography applied to historic masonry structures: validation of the testing methodology and of the data elaboration by different computer codes*. SFR12, 2012.

Cantini, L.; Tedeschi, C.; Binda, L.; Rosa, R. La; Tringali, S.; Tests, S.; Techniques, B. - *Non destructive investigation as a tool for the diagnosis of masonry damaged by the earthquake and as a support for the right choice of repair techniques*. SFR12, 2012.

Carman, P.C. - *Flow of gases through porous media*. Butterworths Scientific Publications, London, UK., 1956.

Chaudhry, C. - *Evaluation of Grouting as a Strengthening Technique for Earthen Structures in Seismic Areas: Case Study Chiripa*. Theses (Historic Preservation), University of Pennsylvania, 2007.

Coias, V. - *Reabilitação Estrutural de Edifícios Antigos - Alvenaria, Madeira - Técnicas pouco intrusivas*. Ed. Argumentum & Gecorpa, Lisbon, Portugal (in Portuguese), 2007.

Collepardi, M. - *Degradation and restoration of masonry walls of historical buildings*. Materials and Structures, Volume 23, págs. 81–102, 1990.

Concu, G.; De Nicolo, B.; Piga, C.; Popescu, V. - *Non-Destructive Testing of Stone Masonry using Acoustic Attenuation Tomography Imaging*, 2009.

Concu, G.; De Nicolo, B.; Piga, C.; Popescu, V. - *Measurement system for non-destructive testing using ultrasonic tomography spectral attenuation*. 2010 12th International Conference on Optimization of Electrical and Electronic Equipmentpágs. 1016–1020, 2010.

Cotič, P.; Jagličić, Z.; Bosiljkov, V. - *Validation of non-destructive characterization of the structure and seismic damage propagation of plaster and texture in multi-leaf stone masonry walls of cultural-artistic value*. Journal of Cultural Heritage, 2013.

Da Porto, F.; Modena, C. - *Investigations for the knowledge of multi-leaf stone masonry walls*. Proceedings of the First International Congress on Construction History,2003págs. 713–722, 2003.

Da Porto, F.; Valluzzi, M.R.; Modena, C. - *Use of sonic tomography for the diagnosis and the control of intervention in historic masonry buildings*. International Symposium(NDT-CE 2003), 2003.

Dantu, P. - *Etude mécanique d'un milieu pulvérulent formé de sphères égales de compacité maxima*. 5ème Congrès International de Mécanique des sols et des Travaux de Fondations, Paris, Dunod, Publication 61-3, 10 pp, 1961.

David Carrier, W. - *Goodbye, Hazen; Hello, Kozeny-Carman*. Journal of Geotechnical and Geoenvironmental Engineering, Volume Vol. 129, págs. 1054–1056, 2003.

Demir, I.; Serhat Baspinar, M. - *Effect of silica fume and expanded perlite addition on the technical properties of the fly ash-lime-gypsum mixture*. Construction and Building Materials, Volume 22, págs. 1299–1304, 2008.

Diamond, S. - *Mercury porosimetry An inappropriate method for the measurement of pore size distributions in cement-based materials*. Cement and Concrete Research, Volume 30, págs. 1517–1525, 2000.

Domone, P. - *The slump flow test for high-workability concrete*. Cement and Concrete Research, Volume 28, págs. 177–182, 1998.

Eklund, D. - *Penetrability Due to Filtration Tendency of Cement Based Grouts*. Doctoral Thesis, Division of Soil and Rock Mechanics, Royal Institute of Technology,Stockholm, Sweden, 2005.

Eklund, D.; Stille, H. - *Penetrability due to filtration tendency of cement-based grouts*. Tunnelling and Underground Space Technology, Volume 23, págs. 389–398, 2008.

EN 1015-11 - *Methods of test for mortar for masonry - Part 11: Determination of flexural and compressive strength of hardened mortar*, 1999.

Epperson, G.S.; Abrams, D.P. - *Non destructive evaluation of masonry buildings*. Advanced Construction Technology Center, Doc. N. 89-26-03, October 1989, Urbana Illinois, United States, 208p, 1989.

Eriksson, M. - *Prediction of Grout Spread and Sealing Effect, a Probabilistic Approach*. Doctoral Thesis, Division of Soil and Rock Mechanics, Royal Institute of Technology, Stockholm, Sweden, 2002.

Eriksson, M.; Friedrich, M.; Vorschulze, C. - *Variations in the rheology and penetrability of cement-based grouts—an experimental study*. Cement and Concrete Research, Volume 34, págs. 1111–1119, 2004.

Faria, P.; Costa, J.; Lourenço, T.; Figueiredo, T.; Silva, V. - *Caracterização de rebocos de argamassas de cal aérea e de cal hidráulica natural com metacaulino e resíduos cerâmicos em exposição natural*. Argamassas 2014 - Simpósio de Argamassas e Soluções Térmicas de Revestimento, 2014.

Fernàndez-Altable, V.; Casanova, I. - *Influence of mixing sequence and superplasticiser dosage on the*

rheological response of cement pastes at different temperatures. Cement and Concrete Research, Volume 36, págs. 1222–1230, 2006.

Ferraro, C.C.; Boyd, A.J.; Consolazio, G.R. - *Evaluation of damage to bridge piers using pulse velocity tomography*. Construction and Building Materials, Volume 38, págs. 1303–1309, 2013.

Gil, N.P. - *Grouting as a repair and strengthening technique to historic masonry buildings*. Master thesis of Conservation of Historic Towns and Buildings. Katholieke Universiteit Leuven, 1994.

Heikal, M.; Morsy, M.S.; Aiad, I. - *Effect of treatment temperature on the early hydration characteristics of superplasticized silica fume blended cement pastes*. Cement and Concrete Research, Volume 35, págs. 680–687, 2005.

Hinks, J.; Cook, G. - *The technology of building defects*. E & FN SPON, 1997.

Hobbs, B. - *Development of a construction quality control procedure using ul trasonic testing*. IB2MAC - 9th International Brick and Block Masonry Conference, Berlin, Germany, 1991.

Hutchinson, M.T. - *Principles of grouting II*. Summary of a lecture given the 16-9-1981 in the Cement and Concrete Association Conference and Training Centre, UK, TDH 4710, p 6, 1981.

Ignoul, S.; Van Gemert, D.; Van Rickstal, F. - *Application of mineral grouts. case study and impact on structural behaviour: church of St. Catharina at Duisburg (b)*. Proceedings International Seminar IV "Structural Analysis of Historical Constructions", Padua, 10-12 November 2004, Balkema Publ., pp.719-726, 2004.

Jackson, M.J.; Tweeton, D.R. - *3DTOM: three dimensional geophysical tomography*. Reports of investigations 9617 – U.S. Geological Survey:, 1996.

Johnson, S.J. - *Cement and clay grouting of foundations:grouting with clay–cement grouts*. J Soil Mech Found Eng Div ASCE, Volume 84, págs. 1–12, 1958.

Jorne, F.; Henriques, F.M.A.; Baltazar, L.G. - *Análise das propriedades de grout endurecido - Influência da adição de sílica de fumo a grouts de cal hidráulica*, in: 4º Congreso de Patología Y Rehabilitación de Edificios. PATORREB 2012, 2012.

Jorne, F.; Henriques, F.M.A.; Silva, V.; Rosa, C. - *Caracterização de alvenarias de pedra antigas - Levantamento tipológico, análise das secções e caracterização dos materiais*. CONPAT 2015, 2015.

Kalagri, A.; Miltiadou-Fezans, A.; Vintzileou, E. - *Design and evaluation of hydraulic lime grouts for the strengthening of stone masonry historic structures*. Materials and Structures, Volume 43, págs. 1135–1146, 2010.

Kalali, A.; Kabir, M.Z. - *Experimental response of double-wythe masonry panels strengthened with glass fiber reinforced polymers subjected to diagonal compression tests*. Engineering Structures, Volume 39, págs. 24–37, 2012.

Kashif, S.; Rehman, U.; Ibrahim, Z.; Ali, S.; Jameel, M. - *Nondestructive test methods for concrete bridges : A review*. Construction and Building Materials, Volume 107, págs. 58–86, 2016.

Klein, N.S.; Bachmann, J.; Aguado, A.; Toralles-Carbonari, B. - *Evaluation of the wettability of mortar component granular materials through contact angle measurements*. Cement and Concrete Research, Volume 42, págs. 1611–1620, 2012.

Lehmann, B. - *Seismic Traveltime Tomography for Engineering and Exploration Applications*. EAGE Publications bv, DB Houton, the Netherlands, 2007.

León, C.A. - *New perspectives in mercury porosimetry*. Advances in Colloidal and Interface Sciencepágs. 341–372, 1998.

Léonard, Z.F. - *Grouting clay based and chemical*. The Engineer 26:864–866, 1961, 1961.

Leucci, G.; Vasanelli, E.; Calia, A.; Micelli, F.; Aiello, M.A. - *The use of ultrasonic pulse velocity tests for the diagnosis of ancient masonries : the influence of the applied load*. Geophysical Research, Volume 16, 2014.

Littlejohn, G.S. - *Chemical grouting*. South African Institution of Civil Engineers, University of Wetwatersrand Johannesburg, 4–6 July, 1983.

Lothenbach, B.; Winnefeld, F.; Alder, C.; Wieland, E.; Lunk, P. - *Effect of temperature on the pore solution, microstructure and hydration products of Portland cement pastes*. Cement and Concrete Research, Volume 37, págs. 483–491, 2007.

Luso, E.; Lourenço, P.B. - *Experimental characterization of commercial lime based grouts for stone masonry consolidation*. Construction and Building Materials, Volume 102, págs. 216–225, 2016.

Luso, E.C.P. - *Análise Experimental de Caldas à Base de Cal para Injeção de Alvenaria Antiga*. PhD Thesis, Universidade do Minho, 2012.

Mazzotti, C.; Sassoni, E.; Pagliai, G. - *Determination of shear strength of historic masonries by moderately destructive testing of masonry cores*. Construction and Building Materials, Volume 54, págs. 421–431, 2014.

Milosevic, J.; Gago, A.S.; Lopes, M.; Bento, R. - *Experimental assessment of shear strength parameters on rubble stone masonry specimens*. Construction and Building Materials, Volume 47, págs. 1372–1380, 2013.

Miltiadou-Fezans, A. - *Contribution à l'étude des coulis hydraulique pour la réparation et le renforcement des structures et des monuments historiques en maçonnerie*. PhD Thesis ENPC Paris, 1990.

Miltiadou-Fezans, A.; Tassios, T.P. - *Fluidity of hydraulic grouts for masonry strengthening*. Materials and Structures, Volume 45, págs. 1817–1828, 2012.

Miltiadou-Fezans, A.; Tassios, T.P. - *Penetrability of hydraulic grouts*. Materials and Structures, Volume 46, págs. 1653–1671, 2013a.

Miltiadou-Fezans, A.; Tassios, T.P. - *Stability of hydraulic grouts for masonry strengthening*. Materials and Structures, Volume 46, págs. 1631–1652, 2013b.

Miranda, L.; Rio, J.; Guedes, J.; Costa, A. - *Propagation of elastic waves on stone masonry walls*. 8th International Masonry Conference 2010 in Dresden págs. 555–562, 2010.

Mirza, J.; Mirza, M..; Lapointe, R. - *Laboratory and field performance of polymer-modified cement-based repair mortars in cold climates*. Construction and Building Materials, Volume 16, págs. 365–374, 2002a.

Mirza, J.; Mirza, M.S.; Roy, V.; Saleh, K. - *Basic rheological and mechanical properties of high-volume fly ash grouts*. Construction and Building Materials, Volume 16, págs. 353–363, 2002b.

Mirza, J.; Saleh, K.; Langevin, M.-A.; Mirza, S.; Bhutta, M.A.R.; Tahir, M.M. - *Properties of microfine cement grouts at 4°C, 10°C and 20°C*. Construction and Building Materials, Volume 47, págs. 1145–1153, 2013.

Mitchell, J.K. - *Soil improvement – state of the art*. Proceedings, 10th International Conference on Soil Mechanics and Foundation Engineering, vol. 4. Stockholm, Sweden págs. 509–566, 1982.

Mitchell, K.J. - *In-plane treatement of foundation soils*. Journal of the Soil Mechanics and Foundations Division,Proc. ASCE, SM1, pp. 73–110, 1970.

Mojmir, U.; Roko, Ž.; Violeta, B.-B.; Vlatko, B. - *Performance of NDT, MDT AND DT techniques in assessing the effectiveness of grouting*, in: Structural Analysis of Historical Constructions, 2012.

Moropoulou, A.; Labropoulos, K.C.; Delegou, E.T.; Karoglou, M.; Bakolas, A. - *Non-destructive techniques as a tool for the protection of built cultural heritage*. Construction and Building Materials, 2013.

Naik, T.R.; Malhotra, V.. .; Popovics, J.S. - *Structural assessment and residual bearing capacity - Handbook of NDT of Concrete*. Politecnico di Milano - Ingegneria Strutturale Corsi Felicetti, 2004.

Nehdi, M.; Mindess, S.; Aïtcin, P.C. - *Statistical modelling of the microfiller effect on the rheology of*

composite cement pastes. Adv. in Cem. Res., Volume 9, págs. 37–46, 1997.

Oktay, D.; Yuzer, N.; Ulukaya, S. - *Rheological properties of hydraulic grouts used in consolidation of brick masonry walls ,*. REHAB2015, Porto, Portugalpágs. 22–24, 2015.

Pagaimo, F. - *Caracterização Morfológica e Mecânica de Alvenarias Antigas; Caso de Estudo da Vila Histórica de Tentúgal*. Dissertação de Mestrado em engenharia civil pela FCT- UC, Coimbra, 2004.

Paillère, A.-M.; Guinez, R. - *Recherche d'une formulation de coulis a` base de liants hydrauliques pour l'injection dans les fines fissures et les cavite´s*. Bulletin de liaison des Laboratoires des Ponts et Chausse´es, Paris, no 130, pp 51–57, 1984.

Paillère, A.-M.; Rizoulières, Y. - *Réparation des structures en béton par injection de polymères*. Bulletin de Liaison des Laboratoires des Ponts et Chaussées 96:17–23, 1978.

Panzera, T.H.; Christoforo, A.L.; Cota, F.P.; Borges, P.H.R.; Bowen, C.R. - *Ultrasonic Pulse Velocity Evaluation of Cementitious Materials*. Advances in Composite Materials - Analysis of Natural and Man- Made Materials, Volume ISBN: 978-, 2011.

Papadakis, M. - *L' injectabilite´ des coulis et mortiers de ciments*. Revue des Materiaux de Construction. 531, publication technique nº. 11 CERILH, 48 pp, 1959.

Papayianni, I.; Pachta, V. - *Experimental study on the performance of lime-based grouts used in consolidating historic masonries*. Materials and Structurespágs. 2111–2121, 2014.

Park, D.C. - *Carbonation of concrete in relation to CO2 permeability and degradation of coatings*. Construction and Building Materials, Volume 22, págs. 2260–2268, 2008.

Petit, J.-Y.; Wirquin, E.; Helnan-Moussa, B. - *Effect of W/C and superplasticizer type on rheological parameters of SCC repair mortar for gravitational or light pressure injection*. Cement and Concrete Composites, Volume 33, págs. 1050–1056, 2011.

Petit, J.-Y.; Wirquin, E.; Khayat, K.H. - *Effect of temperature on the rheology of flowable mortars*. Cement and Concrete Composites, Volume 32, págs. 43–53, 2010.

Phan, T.H.; Chaouche, M.; Moranville, M. - *Influence of organic admixtures on the rheological behaviour of cement pastes*. Cement and Concrete Research, Volume 36, págs. 1807–1813, 2006.

Pichot, R.; Spyropoulos, F.; Norton, I.T. - *Competitive adsorption of surfactants and hydrophilic silica particles at the oil-water interface: interfacial tension and contact angle studies.*. Journal of colloid and interface science, Volume 377, págs. 396–405, 2012.

Pinho, F.F.S. - *Sistematização do estudo sobre paredes de edifícios antigos*. Ingenium, Volume 2° série, págs. pp. 49–59, 1997.

Pinho, F.F.S. - *Paredes de alvenaria ordinária – estudo experimental com modelos simples e reforçados*. Tese de doutoramento em Engenharia Civil, especialidade em Ciências da Construção. Universidade Nova de Lisboa – Faculdade de Ciências e Tecnologia, DEC, Lisboa, 2007.

Rao, G.A.; Prasad, B.K.R. - *Influence of the roughness of aggregate surface on the interface bond strength*. Cement and Concrete Research, Volume 32, págs. 253–257, 2002.

Reichel, A.; Hochberg, A.; Köpke, C. - *Plaster, Render, Paint and Coatings: Details, Products, Case Studies*. Birkhauser Edition Detail, 2005.

Riggio, M.; Sandak, A.; Sandak, J. - *In-situ assessment of structural timber using selected wave-based NDT methods*, in: Structural Analysis of Historical Constructions, 2012.

Riva, G.; Bettio, C.; Modena, C. - *The use of sonic wave technique for estimating the efficiency of masonry consolidation by injection*. IB2MAC - 11h International Brick and Block Masonry Conference, Shanghai, Chinapágs. 28–39, 1997.

Rojas, M.F.; Cabrera, J. - *The effect of temperature on the hydration rate and stability of the hydration phases of metakaolin–lime–water systems*. Cement and Concrete Research, Volume 32, págs.

133–138, 2002.

Rossignolo, J.A. - *Interfacial interactions in concretes with silica fume and SBR latex*. Construction and Building Materials, Volume 23, págs. 817–821, 2009.

Roussel, N.; Lemaître, A.; Flatt, R.J.; Coussot, P. - *Steady state flow of cement suspensions: A micromechanical state of the art*. Cement and Concrete Research, Volume 40, págs. 77–84, 2010.

Roussel, N.; Stefani, C.; Leroy, R. - *From mini-cone test to Abrams cone test: measurement of cement-based materials yield stress using slump tests*. Cement and Concrete Research, Volume 35, págs. 817–822, 2005.

Roy, D.M.; Asaga, K. - *Rheological properties of cement mixes: III. The effects of mixing procedures on viscometric properties of mixes containing superplasticizers*. Cement and Concrete Research, Volume 9, págs. 731–739, 1979.

Roy, R. Le; Roussel, N. - *The Marsh Cone as a viscometer : theoretical analysis and practical limits*. Materials and Structures, Volume 37, págs. 4–9, 2004.

Saisi, A.; Valle, S.; Zanzi, L.; Binda, L. - *Radar and sonic as complementary and / or alternative tests in the survey of structures*, 1999.

Scannell, S.; Lawrence, M.; Walker, P. - *A study of the impacts of calcitic aggregates on the properties of air lime mortar*, in: 9th International Masonry Conference 2014 in Guimarães, 2014.

Schuller, M.; Berra, M.; Fatticioni, A.; Atkinson, R.; Binda, L. - *Use of tomography for diagnosis and control of masonry repairs*. IB2MAC - 10h International Brick and Block Masonry Conference, Calgary, Canada págs. 1539–1550, 1994.

Schullerl, M.; Berra, M.; Binda, L. - *Acoustic tomography for evaluation of unreinforced masonry*. Construction and Building Materials, Volume 11, págs. 199–204, 1997.

Scrivener, K.L.; Crumbie, A.K.; Laugesen, P. - *The Interfacial Transition Zone (ITZ) Between Cement Paste and Aggregate in Concrete*. Interface Science, Volume 12, págs. 411–421, 2004.

Silva, B.; Dalla Benetta, M.; da Porto, F.; Modena, C. - *Experimental assessment of in-plane behaviour of three-leaf stone masonry walls*. Construction and Building Materials, Volume 53, págs. 149–161, 2014a.

Silva, B.; Pigouni, A.E.; Valluzzi, M.R.; Modena, C. - *Calibration of analytical formulations predicting compressive strength in consolidated three-leaf masonry walls*. Construction and Building Materials, Volume 64, págs. 28–38, 2014b.

Sonebi, M.; Lachemi, M.; Hossain, K.M. a. - *Optimisation of rheological parameters and mechanical properties of superplasticised cement grouts containing metakaolin and viscosity modifying admixture*. Construction and Building Materials, Volume 38, págs. 126–138, 2013.

Svermova, L.; Sonebi, M.; Bartos, P.J.M. - *Influence of mix proportions on rheology of cement grouts containing limestone powder*. Cement and Concrete Composites, Volume 25, págs. 737–749, 2003.

Toumbakari, E.-E. - *Lime-pozzolan-Cement grouts and their structural effects on composite masonry walls*. PhD Thesis, Katholieke Universiteit Leuven, 2002.

Toumbakari, E.-E.; Van Gemert, D.; Tassios, T.P. - *Methodology for the design of injection grouts for consolidation of ancient masonry*, in: International RILEM Workshop on Historic Mortars: Characteristics and Tests, 1999.

Toumbakari, E.-E.; Van Gemert, D.; Tassios, T.P.; Tenoutasse, N. - *Effect of mixing procedure on injectability of cementitious grouts*. Cement and Concrete Research, Volume 29, págs. 867–872, 1999.

Uranjek, M.; Bosiljkov, V. - *In situ tests and seismic assessment of a stone-masonry building*. Materials and Structures pags. 45:861–879, 2012.

Uranjek, M.; Žarnić, R.; Bokan-bosiljkov, V.; Bosiljkov, V. - *Seismic resistance of stone masonry*

building and effect of grouting. Journal of the Croatian Association of Civil Engineers, Volume 66, págs. 715–726, 2014.

Valluzzi, M.R. - *Requirements for the choice of mortar and grouts for consolidation of three-leaf stone masonry walls*. RILEM Workshop on Repair Mortars for Historic Masonry - Delft, 26th-28th January, 2005.

Valluzzi, M.R.; Da Porto, F.; Modena, C. - *Behavior and modeling of strengthened three-leaf stone masonry walls*. Materials and Structures, Volume 37, págs. 184–192, 2004.

Valluzzi, M.R.; Mazzon, N.; Munari, M.; Casarin, F.; Modena, C. - *Effectiveness of injections evaluated by sonic tests on reduced scale multi-leaf masonry building subjected to seismic actions Résumé*. NDTCE'09págs. 2–7, 2009.

Van Gemert, D.; Ignoul, S.; Brosens, K.; Toumbakari, E.-E. - *Consolidation and Strengthening of Historical Masonry by Means of Mineral Grouts: Grout Development*. Restoration of Buildings and Monuments, Volume 21, págs. 29–46, 2015a.

Van Gemert, D.; Toumbakari, E.-E.; Ignoul, S.; Brosens, K. - *Consolidation and Strengthening of Historical Masonry by Means of Mineral Grouts: Modeling Structural Behavior of Grouted Three-Leaf Masonry*. Restoration of Buildings and Monuments, Volume 21, págs. 47–54, 2015b.

Van Rickstal, F. - *Grout injection of masonry, scientific approach and modeling*. PhD Thesis. Katholieke Universiteit Leuven, 2000.

Van Rickstal, F.; Toumbakari, E.-E.; Ignoul, S.; Van Gemert, D. - *Development of mineral grouts for consolidation injection*. In Consolidation of Masonry, Ed. D. Van Gemert, Advances in Materials Science and Restoration, 2003, pp. 61-70, 2003.

Vikan, H. - *Rheology and reactivity of cementitious binders with plasticizers*. Doctoral Theses at Norwegian University of Science and Technology, 2005.

Vintzileou, E. - *Grounting of Three-Leaf Stone Masonry: Types of Grouts, Mechanical properties of Masonry before and after Grouting*. Proc. of the 5th International Conference on Structural Analysis of Historical Constructions, New Delhi, 2006., 2006.

Vintzileou, E. - *Three-Leaf Masonry in Compression, Before and After Grouting: A Review of Literature*. International Journal of Architectural Heritage, Volume 5, págs. 513–538, 2011.

Vintzileou, E.N.; Adami, C.-E.N. - *The Bond Mechanism in Stone- or Brick-to-Grout Interfaces*. Strain, Volume 45, págs. 400–409, 2009.

Wallevik, J.E. - *Thixotropic investigation on cement paste: Experimental and numerical approach*. Journal of Non-Newtonian Fluid Mechanics, Volume 132, págs. 86–99, 2005.

Wallevik, J.E. - *Rheological properties of cement paste: Thixotropic behavior and structural breakdown*. Cement and Concrete Research, Volume 39, págs. 14–29, 2009.

Webb, P.A.. - *An Introduction To The Physical Characterization of Materials by Mercury Intrusion Porosimetry with Emphasis On Reduction And Presentation of Experimental Data*. Norcross, Georgia : Micromeritics Instrument Corp, 2001.

Whittingham, T.A. - *Medical diagnostic applications and sources.*. Progress in biophysics and molecular biology, Volume 93, págs. 84–110, 2007.

Wongkeo, W.; Thongsanitgarn, P.; Chaipanich, A. - *Compressive strength and drying shrinkage of fly ash-bottom ash-silica fume multi-blended cement mortars*. Materials & Design, Volume 36, págs. 655–662, 2012.

Xuan, D.X.; Shui, Z.H.; Wu, S.P. - *Influence of silica fume on the interfacial bond between aggregate and matrix in near-surface layer of concrete*. Construction and Building Materials, Volume 23, págs. 2631–2635, 2009.

Yajun, J.; Cahyadi, J.H. - *Effects of densified silica fume on microstructure and compressive strength of blended cement pastes*. Cement and Concrete Research, Volume 33, págs. 1543–1548, 2003.

Yamada, K.; Takahashi, T.; Hanehara, S.; Matsuhisa, M. - *Effects of the chemical structure on the properties of polycarboxylate-type superplasticizer*. Cement and Concrete Research, Volume 30, págs. 197–207, 2000.

Yaman, O.; Inei, G.; Yesiller, N.; Aktan, H.M. - *Ultrasonic Pulse Velocity in Concrete Using Direct and Indirect Transmission*. ACI Materials Journalpágs. 450–457, 2002.

Zanzi, L.; Saisi, A.; Binda, L.; Cardarelli, E. - *Sonic tomography of the stone pillars of a 17th century church*. Transactions on the Built Environment, Volume 55, 2001.